

LIBRARY  
ROYAL AIRCRAFT ESTABLISHMENT  
BOWEN

R. & M. No. 3244



MINISTRY OF AVIATION

AERONAUTICAL RESEARCH COUNCIL  
REPORTS AND MEMORANDA

Pressure Distribution and Surface Flow on  
5% and 9% Thick Wings with Curved  
Tip and 60° Sweepback

By H. C. GARNER, M.A., A.F.R.Ae.S. and D. E. WALSH, B.Sc.  
OF THE AERODYNAMICS DIVISION, N.P.L.

LONDON: HER MAJESTY'S STATIONERY OFFICE

1962

PRICE £1 17s. 6d. NET

# Pressure Distribution and Surface Flow on 5% and 9% Thick Wings with Curved Tip and 60° Sweepback

By H. C. GARNER, M.A., A.F.R.Ae.S. and D. E. WALSH, B.Sc.

OF THE AERODYNAMICS DIVISION, N.P.L.

---

*Reports and Memoranda No. 3244\**

*January, 1960*

---

*Summary.* Extensive tables are given of pressure coefficients measured at Reynolds numbers from  $1.3 \times 10^6$  to  $3.9 \times 10^6$  on two half-models of identical planform with 5% RAE 101 and 9% RAE 101 streamwise sections. The planform of aspect ratio 3.899 has a straight trailing edge with 60° of sweepback, constant chord over most of the span and a parabolic outer portion of the leading edge curving to a pointed tip. The overall wing characteristics are obtained from integrated normal pressures and are compared with lifting-surface theory.

The low-speed experimental pressure distributions and surface oil-flow patterns are analysed and discussed in relation to the onset of separation and the distinct vortex flows that develop at high incidence. Series of contrasting upper-surface isobars illustrate some features of the different stalling processes of the two wings. The direct influence of the main vortex on local surface pressures is assessed in general terms. A fuller appraisal of secondary surface flow is obtained from the oil patterns, observations in water and measurements of high suction near the trailing edge.

Studies of the extent of leading-edge stall and location of part-span vortices, in particular two simultaneous leading-edge vortices on the thinner wing, follow from further analysis of local surface pressures. After a detailed discussion of the effect of Reynolds number and the distinct types of separated flow, a few results with leading-edge roughness are considered in relation to scale effect on separation and the extensive influence of part-span roughness.

---

1. *Introduction.* In order to examine the details of the unseparated flow over the curved tip of a swept wing, two large half-wing models of the same planform but different thickness have been pressure-plotted in the N.P.L. 13 ft  $\times$  9 ft Wind Tunnel. The wings differ only in their streamwise sections which are 5% RAE 101 and 9% RAE 101 aerofoils. The planform, shown in Fig. 1, has been chosen to have a high aspect ratio in relation to its basic sweepback of 60°, so that the curved outer portion of the wing is remote from root effects on the spanwise pressure distribution; the pressure holes are more concentrated near the tip. The models have also been used to investigate types of flow separation up to the highest Reynolds number attainable in the tunnel. The effect of wing thickness on the high-incidence behaviour of swept wings has been studied by means of surface oil-flow patterns.

---

\* Previously issued as A.R.C. 20,982 and 21,562.

Published with the permission of the Director, National Physical Laboratory.

The interest in curved-tip planforms centres on the basic idea that a swept wing can be so designed as to have uniform spanwise distributions of pressure near the leading edge over a range of incidence. Although this has not been fully attained in the present investigation, most of the surface isobars at low incidences retain high sweepback quite close to the curved tip; this is well illustrated in Fig. 2 for the 9% wing at  $\alpha = 6.24^\circ$  and  $R = 2.2 \times 10^6$ . At about this incidence, or rather lower in the case of the 5% wing, the effects of flow separation on the pressure distribution are apparent. Our main purpose is to consider the factors that influence the onset of separation accompanied by part-span vortices and the different types of flow that develop on the two models as incidence increases.

Because the extensive inner portion of the planform is of constant chord and  $60^\circ$  sweepback, it is instructive to consider first the flow over two-dimensional wings of the 5% RAE 101 and 9% RAE 101 streamwise sections yawed through  $\Lambda = 60^\circ$ . The ideal flow past the yawed wing is that of a two-dimensional unyawed aerofoil of thickness/chord ratio scaled up by the factor  $\sec \Lambda$  at incidence  $\sin^{-1}(\sin \alpha \sec \Lambda)$  in a mainstream of velocity  $V \cos \Lambda$  with a uniform spanwise flow of velocity  $V \sin \Lambda$  superposed. The resulting flows are those related to 10% RAE 101 and 18% RAE 101 aerofoils at an increased incidence of approximately  $\alpha \sec \Lambda$  which encourages flow separation. Whereas a 10% RAE 101 aerofoil will stall suddenly with the formation of a long bubble resulting from a forward laminar separation, the thicker 18% RAE 101 aerofoil will stall gradually as the turbulent separation spreads forward from the trailing edge. As sketched in Fig. 3, the flow separation over the curved-tip wings follows the same pattern; the thinner wing develops a part-span vortex with a well-defined origin close to the leading edge, while the flow over the thicker wing is characterized by a part-span vortex located nearer to the trailing edge and moving forward with increasing incidence.

After a description of the model and rig (Section 3), there are brief comments on the integrated normal pressures and longitudinal stability at incidences up to  $\alpha = 8.35^\circ$  (Section 4.2). In the remainder of Section 4 the measured pressures at the higher incidences are analysed with particular attention to chordwise pressure distributions, surface isobars and peak values near the trailing edge. Supplementary oil-flow patterns are presented in Section 5 and compared with the surface isobars. In Section 6 use is made of the method of selective pressure plotting, as described in Ref. 1 (Garner and Bryer, 1957), to locate the part-span vortex in plan view; it is thus possible to study the surface flow in detail. Sections 6.4 and 6.5 contain full descriptions of the respective types of flow over the 5% and 9% wings and discussion of wider implications. Finally Section 7 considers the effectiveness of limited surface roughness as a means of elucidating the effects of Reynolds number; these results tend to support the general conclusions to be drawn from the investigation (Section 8).

## 2. Notation

$A$	Aspect ratio of wing = $4s^2/S$
$c$	Local chord of wing [Eqn. (1)]
$\bar{c}$	Aerodynamic mean chord of wing [Eqn. (2)]
$c_r$	Root chord of wing
$C_D$	Drag coefficient = $\text{drag}/\frac{1}{2}\rho V^2 S$
$C_{D0}$	Drag coefficient at zero lift

$C_L$	Lift coefficient = lift/ $\frac{1}{2}\rho V^2 S$
$C_{LL}$	Local lift coefficient = lift per unit span/ $\frac{1}{2}\rho V^2 c$
$C_m$	Pitching-moment coefficient = pitching moment/ $\frac{1}{2}\rho V^2 S \bar{c}$ about aerodynamic mean quarter-chord axis defined in Eqn. (4)
$C_p$	Pressure coefficient = $(p - p_\infty)/\frac{1}{2}\rho V^2$
$(-C_p)_m$	Maximum suction coefficient (Section 6)
$(-C_p)_t$	Peak suction coefficient at 0.95 chord (Section 4.6)
$p$	Local pressure
$p_\infty$	Pressure of undisturbed stream
$R$	Reynolds number = $V\bar{c}/\nu$
$s$	Semi-span of wing
$S$	Area of planform of wing
$V$	Speed of undisturbed stream
$x$	Streamwise distance, measured from local leading edge
$X_{c.p.}$	Value of $x/c$ corresponding to local centre of pressure
$y$	Spanwise distance from centre-line of wing
$\alpha$	Angle of incidence of wing (deg)
$\alpha_m$	Value of $\alpha$ for which $-C_p = (-C_p)_m$
$\eta$	Non-dimensional spanwise distance = $y/s$
$\bar{\eta}$	Spanwise centre of pressure of half-wing
$\eta_R, \eta_S$	Outboard, inboard end of leading-edge roughness
$\eta_t$	Value of $\eta$ for which $-C_p = (-C_p)_t$
$\Lambda$	Angle of sweepback
$\nu$	Kinematic viscosity of fluid
$\rho$	Density of fluid

3. *Models and Rig.* The planform of the two wings and the positions of the pressure holes are identical; Fig. 1 gives some details of the planform and the nine streamwise pressure-plotting stations, each having 28 holes at the chordwise positions ( $x/c$ ) given in the tables of pressure coefficients. The wings differ only in the thickness of their streamwise sections which are 5% and 9% RAE 101 aerofoils (Ref. 2).

The models have a half-wing span  $s = 65.7$  in. and a root chord  $c_r = 36$  in. The wing chord  $c$  is given by

$$\left. \begin{aligned} c/c_r &= 1 && \text{for } 0 \leq y \text{ (in.)} \leq 40.5 \\ &= 1 - [1 - \{(s-y)/25.2\}^{1/2}]^2 && \text{for } 40.5 \leq y \text{ (in.)} \leq 65.7 \end{aligned} \right\} \quad (1)$$

where  $y$  is the perpendicular distance from the root chord. Eqn. (1) determines the aspect ratio  $A = (65.7)^2/1107 = 3.899$  and the aerodynamic mean chord  $\bar{c}$  by the equation

$$\bar{c}/c_r = \int_0^s (c/c_r)^2 dy / \int_0^s (c/c_r) dy = 58.98/61.5 = 0.959. \quad (2)$$

The trailing edge is of constant sweepback  $60^\circ$ ; the leading edge with its apex as origin is therefore defined by

$$\begin{aligned} x_l &= y\sqrt{3} && \text{for } 0 \leq y \text{ (in.)} \leq 40.5 \\ &= y\sqrt{3} + c_r[1 - \{(s-y)/25.2\}^{1/2}]^2 && \text{for } 40.5 \leq y \text{ (in.)} \leq 65.7. \end{aligned} \quad (3)$$

The outer portion curves to a pointed tip where the sweepback of the leading edge becomes  $90^\circ$ . Thus the inner three pressure-plotting stations in Fig. 1 have constant chord and the outer six lie on the curved tip of spanwise extent  $0.616 \leq \eta = y/s \leq 1$ .

Each aerofoil was constructed as a welded steel box-spar with wooden fairings and tufnol trailing edges. Pressure-plotting tubes were let into the surface along the 28 fixed chordwise positions ( $x/c$ ) and holes of diameter 0.015 in. were drilled at each of the selected values of  $\eta$  so that a complete chordwise pressure distribution could be displayed on a multi-tube manometer. To provide a check on incidence setting, additional pressure tubes at  $x/c = 0.001, 0.003$  and  $0.200$  were let into the reverse surface. The model of 5% RAE 101 section gave difficulty in fitting adequate pressure tubes to the outermost station owing to its small sectional area and the closeness of the forward pressure holes; this was partially overcome with the use of hyperdermic tubing of outer diameter 0.024 in. The half-wing models were mounted with span vertical in the N.P.L. 13 ft  $\times$  9 ft Wind Tunnel (Fig. 1) on a steel frame which was screened by a false floor faired to the tunnel. To avoid serious strut interference on the measuring surface, bracings from the models to the frame were fixed to the reverse surface. To allow a continuous variation in incidence with a minimum of displacement from the centre-line of the tunnel, the frame was free to rotate about a vertical axis situated 72 in. downstream of the root leading edge.

4. *Measured Pressure Distributions.* 4.1. *Tabulated Results.* Both models were tested over the speed range  $70 \leq V$  (ft/sec)  $\leq 210$ , which corresponds to Reynolds numbers  $1.3 \times 10^6 \leq R = V\bar{c}/\nu \leq 3.9 \times 10^6$ . In Table 1, the uncorrected incidences are listed for each model and Reynolds number. The model of 5% RAE 101 section was tested over the range of incidence up to  $11^\circ$  at the highest Reynolds number. However, the wing of 9% RAE 101 section required incidences up to  $16^\circ$  before separation approached the root; the main programme of pressure plotting was carried out at  $R = 2.2 \times 10^6$ , partly for structural reasons and partly because no large scale effect was apparent on the thicker model.

The pressure coefficient is calculated as  $C_p = (p - p_\infty)/\frac{1}{2}\rho V^2$ , where  $p$  is the measured surface pressure,  $p_\infty$  and  $\frac{1}{2}\rho V^2$  are respectively the undisturbed static and dynamic pressures corrected for tunnel blockage. The results for the 5% and 9% wings are given respectively in Tables 2 to 6 and Tables 7 to 9 in which  $\alpha$  is corrected for wall interference (Appendix I) but no residual corrections have been applied to  $C_p$ . The experiments on the 5% model at the station  $\eta = 0.981$  were hampered by blocked or slow hyperdermic tubes (Section 3), so that no results were obtainable for a few small values of  $x/c$  in the last column of Tables 2 to 6; in some cases measurements at this station were omitted altogether.

At incidences up to  $8^\circ$ , the lowest pressure coefficient on the 5% wing at  $R = 3.9 \times 10^6$  occurs close to the leading edge at  $\eta = 0.556$ , where  $C_p$  reaches  $-0.050\alpha^2$ ; as the incidence increases, the location of the lowest pressure coefficient moves inboard with the origin of the part-span vortex until  $C_p$  attains an absolute minimum value of about  $-5$  at  $\eta = 0.2$  and  $\alpha = 11.5^\circ$ . The tests at lower Reynolds numbers (Tables 4 and 5) show less negative pressure coefficients near the leading edge, since the vortex moves inboard at lower incidences. On the thicker wing the lowest

pressure coefficient still occurs at  $\eta = 0.556$ , but its value  $C_p = -0.020\alpha^2$  changes more slowly with increasing incidence. However, the breakdown of the peak suction is delayed to incidences much higher than  $11.5^\circ$  for all Reynolds numbers of test. At the highest incidence,  $\alpha = 16.6^\circ$ , a value  $C_p = -5$  is reached close to  $\eta = 0.383$  and its absolute minimum has not yet been attained.

Care was taken to set the models so that at  $\alpha = 0$  the pressures at 0.2 chord were as symmetrical as possible on the two wing surfaces; the measured coefficients  $C_p$  at negative incidences in Tables 2 to 9 therefore approximate to the values on the reverse surface at corresponding positive incidences. The complete pressure distributions are thus available for incidence settings up to  $8^\circ$ , and they are shown at this highest incidence in Fig. 4 for the 5% wing at  $R = 3.9 \times 10^6$  and the 9% wing at  $R = 2.2 \times 10^6$ . To give perspective, pressure is plotted on the planforms with respect to oblique axes through the leading edge; for each station, the scale of  $-C_p$  is normal to the trailing edge and the axis of  $x/c$  is along the chord. The distributions on the 5% wing illustrate the high peak suctions and consequent sharp adverse pressure gradients. A part-span vortex originates between  $\eta = 0.707$  and  $\eta = 0.831$ ; a reduced peak suction is seen to persist along the curved leading edge, and rearward humps in the upper-surface pressure indicate the path of the vortex. By contrast, the negative pressure coefficients on the 9% wing develop gradually and have only reached 40% of the peak values on the thinner wing. The chordwise distributions of the 9% wing do not vary greatly over much of the span. However, the pressures towards the rear of the curved tip indicate an increase in lift associated with a vortex lying parallel to the trailing edge.

4.2. *Integrated Normal Pressures.* The forces and moments at each section were evaluated from chordwise integrals on the basis that the pressures act normal to the aerofoil surface. Further spanwise integrations gave values of  $C_L$ ,  $C_D$ ,  $C_m$  and  $\bar{\eta}$ , the spanwise centre of pressure of the half-wing. The pitching moment is referred to the aerodynamic mean quarter-chord axis whose distance downstream of the leading apex of the wing is

$$x = \frac{\int_0^s c(x_i + \frac{1}{4}c)dy}{\int_0^s c dy} \quad (4)$$

$$= 1.8455\bar{c} \text{ by Eqns. (1), (2) and (3).}$$

The incidence of test and the integrated aerodynamic coefficients have been corrected for tunnel-wall interference by the formulae in Appendix I. The final results for incidences up to  $8.35^\circ$  are given in Tables 10 and 11 for the 5% and 9% wings respectively.

Multhopp's<sup>3</sup> (1950) lifting-surface theory with 15 spanwise and 4 chordwise terms gives the following values to compare with the corrected experimental quantities:

$$\left. \begin{aligned} C_L &= 0.0428\alpha \\ C_D &= 0.00016\alpha^2 \\ C_m &= 0.0012\alpha \\ -C_m/C_L &= -0.028 \\ \bar{\eta} &= 0.470 \\ C_D/C_L^2 &= 0.09 \end{aligned} \right\}, \quad (5)$$

where  $\alpha$  is measured in degrees.

The consistent theoretical and experimental values of  $\bar{\eta}$  and graphs of  $C_L$  against  $\alpha$  at the top of Fig. 5 suggest that the spanwise load distribution can be calculated satisfactorily. The discrepancy

in sign between the theoretical and experimental values of  $C_m$  is partly explained by the theoretical effect of aerofoil section; the differences, as they stand in the graphs of  $C_m$  against  $C_L$  in Fig. 5, amount to a displacement of  $0.06\bar{c}$  in the aerodynamic centre at low incidences. The stability characteristics of the curved-tip wing are seen to depend on aerofoil section and Reynolds number; the onset of flow separation is seen to be stabilizing ( $dC_m/dC_L$  decreasing) for the 5% wing and destabilizing ( $dC_m/dC_L$  increasing) for the 9% wing.

At the bottom of Fig. 5 it is seen that the drag from integrated normal pressures is always greater than its theoretical value. Nevertheless, for low incidences,  $(C_D - C_{D0})/C_L^2$ , where  $C_{D0}$  corresponds to  $\alpha = 0$ , has values of 0.12 for the 5% wing and 0.09<sub>5</sub> for the 9% wing to compare with the theoretical value 0.09 from Eqn. (5). By contrast, complete loss of leading-edge suction force would give

$$C_D = (\alpha/57.3)C_L,$$

i.e.,

$$C_D/C_L^2 = 0.41. \quad (6)$$

When there are extensive regions of separated flow, as on the 5% wing at  $\alpha = 8.35^\circ$ , the integrated drag is as much as three times the theoretical lift-dependent drag and lies about midway between the extremes of Eqns. (5) and (6).

**4.3. Chordwise Distributions.** As mentioned in Section 1 by analogy with the separated flow over two-dimensional yawed wings, the 5% wing exhibits a part-span vortex originating at the leading edge, while that on the 9% wing forms nearer to the trailing edge. The primary effects of these contrasting features are elucidated by means of Fig. 6, where the upper-surface pressures at  $\eta = 0.556$  are plotted for the 5% wing at  $R = 3.9 \times 10^6$  and for the 9% wing at  $R = 2.2 \times 10^6$  from the results given in Tables 6 and 8. These chordwise distributions over the untapered portions of the two wings show regions of low pressure where the influence of the part-span vortex is felt. At  $\alpha = 8.33^\circ$  the leading-edge suction on the 5% wing has begun to collapse: the stalled distributions for  $\alpha = 10.40^\circ$  and  $\alpha = 11.44^\circ$  in Fig. 6(a) show that the vortex has its greatest influence at 0.21 chord and 0.32 chord respectively. This rearward movement of the minimum pressure at  $\eta = 0.556$  with increasing incidence indicates an inward movement of the vortex sketched in the left-hand diagram of Fig. 3. By contrast, on the 9% wing in Fig. 6(b) peak suction at the leading edge persist while minima due to the part-span vortex, first evident at 0.88 chord when  $\alpha = 10.40^\circ$ , grow and progress smoothly forwards as follows:—

$\alpha$	$10.40^\circ$	$12.48^\circ$	$14.56^\circ$	$16.64^\circ$
$C_p$	- 0.3	- 0.7	- 1.2	- 1.6
$x/c$	0.88	0.67	0.55	0.43

This is analogous to a turbulent separation spreading from the rear of a thick aerofoil and corresponds to a forward movement of the vortex sketched in the right-hand diagram of Fig. 3.

The upper-surface pressures at  $\eta = 0.882$  are plotted similarly in Fig. 7. The sequence of minimum pressures in Fig. 7(a) resembles that at  $\eta = 0.556$  in Fig. 6(a) but occurs at lower incidence. When  $\alpha = 8.33^\circ$ , the leading-edge suction on the 5% wing has already collapsed and the vortex is prominent at 0.33 chord. It is seen that the minimum at 0.66 chord when  $\alpha = 9.36^\circ$  is less pronounced, being weaker and flatter because the vortex has spread further from the wing surface and lies in a more nearly chordwise direction. At  $\alpha = 10.40^\circ$  the increase in  $-C_p$  near the

trailing edge is evidence that the flow is energized by a secondary vortex whose axis coincides roughly with the trailing edge (*cf.* Fig. 18) and whose local influence masks that of the main vortex. Fig. 7(b) compares directly with Fig. 6(b), and on the 9% wing the vortex is again detected at the outer section at lower incidence. The minimum pressure appears at 0.89 chord when  $\alpha = 8.31^\circ$  and moves forward while the leading-edge suction persists until  $\alpha = 12.48^\circ$ . With further increase in  $\alpha$  the direct influence of the main vortex at  $\eta = 0.882$  disappears, but again there are high trailing-edge suction induced by the secondary vortex.

The greatest effect of Reynolds number on the pressure distributions occurs at the section  $\eta = 0.831$  and is shown for the two wings in Figs. 8 and 9. There is evidence of large scale effect on the 5% wing at  $\alpha = 8.35^\circ$  when the main vortex crosses the particular section. The vortex moves outwards as  $R$  is gradually increased from  $2.2 \times 10^6$  to  $3.9 \times 10^6$ , so that in Fig. 8 the position ( $x_v$ ) of the hump in upper-surface suction moves progressively forward from 0.78 chord to 0.21 chord; this is accompanied by a rapid growth in leading-edge suction and a forward movement of the local centre of pressure towards its low-incidence value  $X_{c.p.} = 0.245$ . The integrated local lift coefficients  $C_{LL}$  at  $\eta = 0.831$  for the four Reynolds numbers compare with an extrapolated experimental value  $C_{LL} = 0.330$  for unseparated flow over the 5% wing.

$R \times 10^{-6}$	2.2	2.8	3.3	3.9
$x_v/c$	0.78	0.62	0.27	0.21
$C_{LL}$	0.341	0.450	0.416	0.366
$X_{c.p.}$	0.466	0.458	0.365	0.249

From the tabulated values it is inferred that there are increases in local lift of 30% or more when the vortex lies over the central third of the chord. When the vortex lies over the rear half of the chord, the pressures on the lower surface begin to decrease, and at  $R = 2.2 \times 10^6$  the secondary vortex near the trailing edge exerts a marked influence on both surfaces.

The distributions for the 9% wing at the same incidence in Fig. 9(a) show much less dependence on Reynolds number; although at  $R = 1.3 \times 10^6$  the short separation bubble extending between 0.035 chord and 0.075 chord affects local pressures significantly, the only important scale effect from  $R = 2.2 \times 10^6$  to  $R = 3.9 \times 10^6$  is confined to the rear of the wing where the incipient main vortex is detectable. At the higher incidence  $\alpha = 12.5^\circ$  pressures on the lower surface are unknown, but the curves of upper-surface pressure in Fig. 9(b) show marked features which will be discussed later in relation to the corresponding isobars. Again the leading-edge flow at  $R = 1.3 \times 10^6$  is distinctive, but at the higher Reynolds numbers the scale effect is more significant away from the leading edge. As the minima in Fig. 9(b) are numerically similar to those shown for the 5% wing at lower incidence in Fig. 8, the two sets of curves can be used to illustrate some differences in the scale effect on the two wings between  $R = 2.2 \times 10^6$  and  $R = 3.9 \times 10^6$ . Apart from the low pressures near the trailing edge induced by the secondary vortex when  $R = 2.2 \times 10^6$ , the greatest local changes in  $C_p$  with Reynolds number on the 9% wing are of magnitude 0.2 which is less than half those occurring on the 5% wing at 0.2 chord and 0.7 chord. A related point of interest is that the mean pressure coefficient

$$\bar{C}_p = \int_0^1 C_p d(x/c)$$

for the upper surface of the 9% wing has practically the same value  $-0.64$  for the two Reynolds numbers while the above table shows quite important variations in  $C_{LL}$  and  $X_{c.p.}$  for the 5% wing.



Where the local pressures change fairly slowly with incidence, as on the 9% wing, the scale effect may be expected to be small. The major effect probably occurs at Reynolds numbers below  $2.2 \times 10^6$ ; above this, the scale effect is associated primarily with the rearward main vortex and, as already mentioned, is both smaller and more localized than on the 5% wing. By contrast, where the curves of  $-C_p$  against  $\alpha$  show peaks and steep gradients, as over most of the 5% wing, scale effect may be expected to be large. It will become increasingly clear that few precise deductions can be drawn concerning the 5% wing at full-scale Reynolds numbers.

4.4. *Surface Isobars.* The tabulated pressure distributions in Tables 2 to 9 are sufficient to enable contours of equal surface pressure to be plotted on the curved-tip planform, although these surface isobars cannot be drawn accurately in the region of strong vortices. Fig. 2 illustrates that at low incidences most of the isobars retain high sweepback quite close to the curved tip. This desirable configuration is distorted as incidence increases and the characteristic flows develop with separation. In Figs. 10 to 14 each surface isobar is labelled with its constant value of  $-C_p$ ; on each diagram any peak values of  $-C_p$  are indicated, and dashed lines are drawn to represent the sections  $\eta = 0.2, 0.4, 0.6, 0.7, 0.8$  and  $0.9$ .

Fig 10 shows the development of surface isobars on the 5% wing at the highest Reynolds number as the incidence is increased from  $8.33^\circ$  to  $11.44^\circ$ . The inward movement and lessening rate of increase in peak leading-edge suction are apparent, as are the rapid growth and slight inward movement of the low-pressure region associated with the secondary vortex along the outer part of the trailing edge. The swept isobars extend over less and less of the span, as given below:

$\alpha$	$8.33^\circ$	$9.36^\circ$	$10.40^\circ$	$11.44^\circ$
Extent	$\eta < 0.8_5$	$\eta < 0.6_5$	$\eta < 0.4_5$	$\eta < 0.3$

All these features stem from the inward movement and increasing strength of the part-span leading-edge vortex which roughly follows the low-pressure region where the isobars have maximum curvature. It should also be noted that a significant increase in pressure occurs inboard of the vortex; in Fig. 10 each of the contours of  $-C_p = 0.1$  over the inner portion of the wing curve away from the trailing edge. Fig. 10(a) is redrawn as Fig. 11(d) to show the effect of Reynolds number on the isobars of the 5% wing at  $\alpha = 8.3_5^\circ$ . In general appearance the isobars behave similarly with decreasing Reynolds number and with increasing incidence. This large scale effect has already been discussed in relation to the particular chordwise pressure distributions in Fig. 8. Fig. 11 illustrates more fully that an increase in Reynolds number reduces the inward spread of the part-span vortex. In consequence there is outward movement of and large increase in the peak leading-edge suction, discouragement of the secondary vortex, and swept isobars of greater spanwise extent:

$R \times 10^{-6}$	2.2	2.8	3.3	3.9
Extent	$\eta < 0.4$	$\eta < 0.5$	$\eta < 0.8$	$\eta < 0.8_5$

An increase in Reynolds number from  $2.2 \times 10^6$  to  $3.9 \times 10^6$  therefore delays the development of separated flow on the 5% wing by at least  $2^\circ$  of incidence.

Figs. 12(a) to 12(h) give the development of the surface isobars on the 9% wing at  $R = 2.2 \times 10^6$  as the incidence is increased from  $8.31^\circ$  to  $15.60^\circ$ . Because the basic stalling of the thicker wing is a turbulent separation spreading forward from the trailing edge, swept isobars persist along most of the leading edge and the maximum leading-edge suction grows steadily. The measured pressures

do not indicate the precise spanwise extent of the vortex, because it develops at some distance from the wing surface. As the vortex strengthens, its local influence grows until this is offset by the rapidly increasing displacement between vortex and wing. The magnitude and location of the peak suction directly below the vortex is given in the following table:

$\alpha$	8.3°	9.4°	10.4°	11.4°	12.5°	13.5°	14.6°	15.6°
$-C_p$	0.4	0.4	0.4	0.6	0.9	1.1	1.3	1.5
$x/c$	0.8 <sub>5</sub>	0.8	0.8 <sub>5</sub>	0.8	0.7 <sub>5</sub>	0.6 <sub>5</sub>	0.5 <sub>5</sub>	0.5
$\eta$	0.9	0.9	0.8	0.7	0.7	0.6 <sub>5</sub>	0.6	0.5 <sub>5</sub>

The beginnings of a similar development at  $R = 3.9 \times 10^6$  are apparent in Figs. 13(a) to 13(c). Characteristic of the 9% wing are the elongated isobars enclosing these tabulated peak suctions and indicating the course of the vortex. When the flow separation is largely confined to the curved tip, as in Figs. 10(b) and 12(f), the surface isobars on the two wings have few features in common. It is interesting that with a further increase in incidence of 2°, that is to say in Figs. 10(d) and 12(h), the configurations are noticeably more similar. This trend is likely to continue so that the completely stalled flow over the two wings would be basically the same.

The effect of Reynolds number on the 9% wing at  $\alpha = 12.5^\circ$  is shown in Figs. 14(a) to 14(c); as expected, the isobars near the leading edge are little changed where  $\eta < 0.8$ . The main and secondary peaks induced by the vortex are both greatest at the middle Reynolds number  $R = 2.2 \times 10^6$ . It is inferred that at  $R = 1.3 \times 10^6$  the separated boundary layers are thicker so that the vortex is more diffuse and remote from the wing surface, while at  $R = 3.9 \times 10^6$  the vortex is more compact but less strongly developed. At  $R = 1.3 \times 10^6$  the isobars suggest that there is a streamwise vortex in the region of  $\eta = 0.83$  originating well forward. The corresponding chordwise distributions of  $-C_p$  in Fig. 9b confirm this and reveal a similar feature at  $R = 3.9 \times 10^6$  but not at  $R = 2.2 \times 10^6$ . It seems that a weak vortex of this kind may be ancillary to the type of flow separation on the 9% wing, although it can seldom be detected from the pressure measurements.

**4.5. Influence of Main Vortex.** No precise information about the strength and displacement of the vortex can be deduced from the present investigation. But its influence over the rear half of the wing may be regarded as an incremental velocity  $v$  outwards normal to the line of the vortex which is inclined at 20°, say, to the local potential flow having a velocity  $1.1V$ , say. The resulting pressure coefficient is given by

$$-C_p = 0.21 - 2.2(v/V) \sin 20^\circ + (v/V)^2 \quad (7)$$

which has a minimum value of 0.07 when  $v = 1.1V \sin 20^\circ$ . Such a reduction in  $-C_p$  has already been noted well inboard of the vortex on the 5% wing in Fig. 10 where the isobars  $-C_p = 0.1$  curve away from the trailing edge initially. The same effect on the 9% wing is just discernible in Fig. 12(h). The peak value  $-C_p = 1.5$  in this diagram would imply a value  $v = 1.6V$  in Eqn. (7), that is to say a resultant flow of velocity  $1.6V$  inclined outwards at about 50° to the line of the vortex.

From the experiments it is possible to estimate approximate pressure distributions over the two wings, that would result if attached flow were postulated at any moderate incidence. By this means the local increments in  $-C_p$  associated with the main part-span vortex in separated flow can be deduced, and these increments will naturally be greatest immediately below the vortex. On the 5% wing the increment is very roughly constant over the forward part of the wing, as might be

expected on the basis of a superposed conical flow from the vortex origin. On the 9% wing, as already discussed, the increment rises to a flat maximum. The maximum increment  $\delta(-C_p)$  is dependent on the magnitude of the lift or circulation and on the spanwise extent of the separation. The approximate values of  $\delta(-C_p)$  in Table 12 show a measure of correlation between the two wings at  $R = 2.2 \times 10^6$  and  $R = 3.9 \times 10^6$  if  $\delta(-C_p)/\alpha$  is plotted against the value of  $\eta$  corresponding to the maximum increment. Hence the rough relationship

$$\delta(-C_p) = \alpha(0.15 - 0.12_5\eta) \quad (8)$$

$$= C_L(3.5 - 2.9\eta) \quad (9)$$

is derived to an accuracy of about  $\pm 0.1$ , as indicated by the last column of Table 12. For given values of  $\alpha$  and  $\eta$ ,  $\delta(-C_p)$  would decrease as aspect ratio or sweepback decreases; in fact only about half the increment from Eqn. (8) has been observed on the arrowhead wing in Ref. 1. The general order of magnitude of  $\delta(-C_p)$  appears to be  $0.8C_L \tan \Lambda_m$ , where  $\Lambda_m$  is the mid-chord sweepback.

4.6. *Trailing-Edge Pressures.* Some extra pressure holes were inserted in order to study the nature of the distributions near the secondary trailing-edge vortex. Fig. 15 gives in detail the chordwise behaviour at  $\eta = 0.831$  and the spanwise behaviour at  $x/c = 0.95$  on the 9% wing at various Reynolds numbers and two incidences. The upper diagram establishes that the peak suction occurs invariably at 0.96 or 0.97 chord and that the tabulated values at 0.95 chord do not seriously misrepresent the magnitude of the peak. Likewise, the curves of  $-C_p$  at 0.95 chord against  $\eta$  in the lower diagram show rounded maxima  $-C_p = (-C_p)_t$  which, it is found, can be deduced reasonably well from the tabulated pressures. The large scale effect is summarized by stating that at suitably high incidence there is a maximum in the curve of  $(-C_p)_t$  against  $R$  and that the corresponding value of  $R$  tends to increase with  $\alpha$ .

It is assumed that the pressure variation at 0.95 chord gives an equally good indication of secondary effects on the 5% wing. At  $\alpha = 8.35^\circ$  and  $\alpha = 11.45^\circ$ , increase in Reynolds number causes an outward movement of the origin of the main part-span vortex and in consequence in Fig. 16 a significant increase in the value of  $\eta = \eta_t$  corresponding to the maximum suction induced by the secondary vortex. The effect of incidence on the spanwise variation of  $-C_p$  at 0.95 chord is shown in Fig. 17 for the two wings in cases that correspond to the isobars in Figs. 10 and 12. The salient features are the progressive decrease in  $\eta_t$  and increase in  $(-C_p)_t$  as separated flow develops on the 5% wing, and the constant value of  $\eta_t$  and surprisingly large maximum in  $(-C_p)_t$  on the 9% wing. The lower diagram shows that this maximum value  $(-C_p)_t = 2.0$  occurs when  $\alpha$  is just below  $14^\circ$ . The subsequent decrease in  $(-C_p)_t$  is associated with the forward movement of the main vortex. It is noteworthy that the curves at the highest incidences are practically identical for the two wings and support an earlier remark that the two flows become increasingly similar as the stall is completed.

5. *Oil-Flow Patterns.* 5.1. *Visual Techniques.* Several visual methods, principally the oil-film technique, were used to study the flow; some preliminary observations on the 9% wing were made with tufts, with smoke and in water. A tuft traversed by hand revealed quite clearly the main part-span vortex which first appeared close and parallel to the trailing edge. There was further direct evidence from a smoke generator placed upstream of the wing, that at  $\alpha = 12.5^\circ$  and  $R = 0.5 \times 10^6$  two vortices streamed from the trailing edge inboard of the tip. A small model of the 9% wing was

tested in the water tunnel at  $R = 0.1 \times 10^6$  and photographs obtained at  $\alpha = 13^\circ$  are reproduced in Fig. 18. Air bubbles passing over the upper surface become entrained in the main vortex, and those passing close to the lower surface are seen to enter the secondary vortex along the trailing edge. The lower sketch and photograph illustrate that with careful positioning of a single jet of air bubbles the two vortices can be observed simultaneously when the model is viewed from the side. Owing to the low Reynolds number the fully separated flow in Fig. 18 is believed to be typical of the 5% and 9% wings at very high incidence.

In recent years, extensive use has been made of the oil-film technique for visualizing surface flow. As described in Ref. 1, the wing surface is coated with a suspension of titanium dioxide in a mixture of oleic acid and paraffin in such proportions that droplets form and move in the local flow direction leaving traces of titanium dioxide. At the lowest Reynolds number of  $1.3 \times 10^6$  ( $V = 70$  ft/sec), no satisfactory patterns were obtained, since the energy in the air stream was insufficient to produce droplets, but the quality of the patterns improved progressively with increasing speed. The more interesting cases were photographed using an Ilford 304 tricolour blue filter to accentuate the contrast between the white suspension and the wing surface which was of light wood with a clear phenoglaze finish.

*5.2. Interpretation of Oil Patterns.* Typical oil patterns of the curved tip are shown in Figs. 19 and 20; it may be helpful first to describe some of the features that can be deduced. In Fig. 19(b), the general flow direction close to the surface of the 5% wing at  $\alpha = 5.72^\circ$  is clearly shown by the striations. The dark region near  $\eta = 0.8$  indicates a local flow of high velocity which, together with the marked change in flow direction, shows the presence of a vortex. Immediately outboard of the vortex the suspension has been swept into a line where the outflowing boundary layer separates. Inboard of the vortex a short-bubble separation shows as a white line along the leading edge; this encloses dead air which has not disturbed the suspension accumulating from the high-velocity flow forward of the bubble. Care must therefore be taken to prevent the suspension from building to such a height that it alters the character of the flow.

Further general features are brought out in Fig. 20(d). The curved striations over the rear half of the 9% wing indicate a main vortex aligned parallel to the trailing edge which combines with another vortex originating well forward at a spanwise location  $\eta = 0.8$ . Very close to the trailing edge between  $\eta = 0.65$  and  $\eta = 0.85$  there lies a 'herring-bone' formation indicating an attachment line which divides air that is entrained beneath the vortex from the streamwise flow of air that has passed over the vortex; the secondary trailing-edge vortex observed near the tip in Fig. 18 can hardly be discerned from the oil patterns. Fig. 20(d) clearly shows an extensive dead-air region between the separation lines of the opposing high-velocity flows from the leading edge and from beneath the main vortex.

The progress of flow separation over the 5% wing with increase in incidence is recorded in Fig. 19. At the lower Reynolds number  $R = 2.2 \times 10^6$ , the part-span vortex with its origin close to the leading edge rapidly encompasses the curved tip, as the incidence rises from  $4.5^\circ$  to  $5.5^\circ$ . The oil pattern in Fig. 19(a) shows that at  $\alpha = 5.20^\circ$  the origin lies in the region of  $\eta = 0.75$ . Between there and  $\eta = 0.85$  there is evidence of both a leading-edge separation and a vortex-induced separation; that is to say, following a laminar separation due to adverse pressure gradient, the air is drawn over the vortex, reattaches in reverse flow beneath it and separates again. Whereas at  $R = 2.2 \times 10^6$  the vortex originates well inboard when  $\alpha = 5.72^\circ$ , the effect of increasing

Reynolds number to  $R = 3.9 \times 10^6$  in Fig. 19(b) is to delay the inward movement until  $\alpha = 6.25^\circ$  in Fig. 19(c).

Fig. 19(d) reveals the formation of another vortex at the extreme tip when  $\alpha = 6.77^\circ$ . At  $R = 2.2 \times 10^6$  there had been some evidence of multiple vortices at  $\alpha = 6.24^\circ$ , but the results were unrepeatable and inconclusive. At  $R = 3.9 \times 10^6$ , on the other hand, two vortices featured consistently in the range  $6.5^\circ < \alpha < 8.5^\circ$ . Figs. 19(e) and 19(f) show that the initial vortex moves further inboard and weakens while the other vortex appears to remain stationary near  $\eta = 0.96$  but strengthens and forces the initial separation line outwards. When  $\alpha = 8.33^\circ$ , the initial vortex has practically disappeared, and the oil pattern in Fig. 19(g) resembles that which would be obtained for an incidence of about  $6.0^\circ$ . Finally the second part-span vortex moves inwards; at  $\alpha = 9.36^\circ$  it extends well inboard of the curved leading edge. The phenomenon of multiple vortices is considered further in Section 6 in relation to pressure measurements.

A feature peculiar to the oil patterns of the 9% wing is the evidence of the main vortex lying parallel to the trailing edge and located between the extensive dead-air region and the trailing edge. Fig. 20 shows that there is no detectable scale effect on either the chordwise extent of the dead-air region or the chordwise location of the main vortex and of the 'herring-bone' attachment line near to the trailing edge. At  $R = 3.9 \times 10^6$  there is another vortex of the same sense as the main vortex terminating the dead-air region at  $\eta = 0.9$  and  $0.8$  for  $\alpha = 10.40^\circ$  and  $12.48^\circ$  respectively. It is noteworthy that this chordwise vortex originates at about 20% chord and soon coalesces with the main vortex. As further evidence of lack of scale effect, this phenomenon is already present at  $R = 2.2 \times 10^6$  and can just be detected in Fig. 20(b) where the main separation line is distorted in the region  $0.80 < \eta < 0.85$ . The effect of incidence can be studied in Figs. 20(a), 20(b) and the full-span oil patterns of Fig. 21. Over a considerable portion of the span at  $\alpha = 10.40^\circ$  there is a leading-edge bubble from 0.015 chord to 0.035 chord, then attached flow up to 0.30 chord, followed by the dead-air region bounded at 0.75 chord by the separation line from the main vortex. As incidence increases, the dead-air region moves forward and contracts, so that at  $\alpha = 14.56^\circ$  it lies much closer to the leading-edge bubble and there is attached flow induced by the vortex over the rear 60% of the chord.

*5.3. Isobars and Oil Patterns.* Some complementary features of the isobars in Figs. 10 to 14 and the oil patterns in Figs. 19 to 21 are now considered. Both presentations give a useful indication of the main vortex, as discussed earlier; the regions of abnormally low pressure and intense cross-flow are reasonably consistent. The spanwise extent of the unstalled leading-edge flow on the 5% wing is found to correspond to that of the isobar starting close to the root and terminating furthest outboard along the leading edge. The leading-edge pressures fall so sharply outboard of the vortex origin that its observed position lies close to the outer ends of the contours  $-C_p = 0.8$  in Fig. 10(a) and  $-C_p = 1.5$  in Fig. 10(b). The isobars inboard of the vortex indicate that the air entrained by the vortex is rapidly accelerated beneath the vortex and then encounters a positive pressure gradient causing separation outboard. There is some evidence that the pressure gradient falls suddenly at the separation lines deduced from the oil patterns in Figs. 19(g) and 19(h); it would then follow that the separation lines correspond to maximum curvature in the isobars though there is insufficient pressure-plotting to establish this result.

The dead-air region, observed on the 9% wing at incidences above  $9.36^\circ$  is seen in Figs. 12(b) to 12(h) to correspond to a region of roughly constant pressure coefficient which decreases from

$C_p = -0.2$  approaching  $C_p = -0.8$  as  $\alpha$  increases to  $15.60^\circ$ . Where the flow is dominated by the main vortex, the chordwise limits of this region  $x_1 < x < x_2$  vary roughly according to the following table:

$\alpha$	$9.36^\circ$	$11.44^\circ$	$13.52^\circ$	$15.60^\circ$
$x_1/c$	0.3	0.2 <sub>5</sub>	0.1 <sub>5</sub>	0.1
$x_2/c$	0.7	0.6	0.4 <sub>5</sub>	0.2 <sub>5</sub>

These values are reasonably consistent with the flow as interpreted from the oil patterns for  $R = 2.2 \times 10^6$  in Figs. 20 and 21. For  $R = 3.9 \times 10^6$  the constant-pressure or dead-air region at  $\alpha = 12.48^\circ$  is of chordwise extent  $0.2_5 < x/c < 0.5_5$  according to the isobars and oil pattern in Fig. 13; there is apparently no large scale effect. The forward separation line ahead of the dead-air region extends well outboard and eventually reaches the curved leading edge; this terminal point coincides with that of the isobar immediately forward of the dead-air region, as is well illustrated in Figs. 13(c) and 13(d). The condition, that the primary separation line reaches the leading edge, enables the chordwise vortex (Section 5.2) to be sustained slightly inboard of the terminal point.

6. Location of Vortices. 6.1. Selective Pressure Plotting. When the part-span vortex moves rapidly with change of incidence, the method of selective pressure plotting, as described in Ref. 1, gives a quick and accurate procedure for evaluating the plan view of the vortex. The method is illustrated by the sequence of graphs in Figs. 22 and 24(b) and the right-hand diagram of Fig. 26, which correspond to the 5% wing at  $R = 3.9 \times 10^6$ . First the pressure coefficients at fixed  $x/c$  are plotted against incidence for a series of positions  $\eta$ ; this is carried out for  $x/c = 0.001, 0.010, 0.05, 0.25$  and  $0.75$  in Figs. 22(a) to 22(e). Each curve determines an incidence  $\alpha = \alpha_m$  for which  $-C_p$  has a maximum value  $(-C_p)_m$ , though  $\alpha_m$  is less well defined for large  $x/c$ . Then in Fig. 24(b) the graphs of  $\alpha_m$  against  $\eta$  give the spanwise location of the vortex for the particular values of  $x/c$ . A cross-plot of Fig. 24(b) for fixed  $\alpha = \alpha_m$  gives pairs of values of  $x/c$  and  $\eta$  from which the plan view of the part-span vortex in Fig. 26 is prepared. Thus greater precision is obtained than from the chordwise pressure distributions or the isobars.

Many of the curves in Fig. 22 have two maxima which correspond to separate vortices. As discussed in Section 5.2, two vortices are detectable from the oil patterns in Fig. 19 for the 5% wing at  $R = 3.9 \times 10^6$  in the range of incidence  $6.5^\circ < \alpha < 8.5^\circ$ . Because of the greater sensitivity of the method of selective pressure plotting, these are now detectable over a larger range of incidence; the initial maxima in Fig. 22, occurring first near the leading edge when  $\alpha = 5.0^\circ$  and persisting at 0.05 chord until  $\alpha = 9.5^\circ$ , are recorded as curves of  $\alpha_m$  against  $\eta$  in Fig. 25(a). No such phenomenon at  $R = 2.2 \times 10^6$  is detectable from the curves for  $x = 0.001c$  in Fig. 23(a) or from corresponding curves for other values of  $x/c$ , which lead to the graphs of  $\alpha_m$  against  $\eta$  in Fig. 24(a). It is interesting to compare the location of the single vortex at  $R = 2.2 \times 10^6$  from Fig. 24(a) with the initial and final vortices at  $R = 3.9 \times 10^6$  from Figs. 25(a) and 24(b) respectively. Cross-plots of  $\eta$  against  $x/c$  for  $\alpha = 6.25^\circ$  and for  $\alpha = 8.33^\circ$  in Fig. 25(b) show how the single vortex at the lower Reynolds number is more closely related to the initial than to the final vortex. It is therefore helpful to consider the large scale effect on the 5% wing in two parts, namely a delay in the onset of vortex formation and a lengthening of the stalling process due to multiple vortices which appear at the highest Reynolds number only.

The plan views of the single vortex at  $R = 2.2 \times 10^6$  and the final vortex at  $R = 3.9 \times 10^6$  are presented in Fig. 26; in each case there is a rapid inward movement with increasing incidence. At  $R = 2.2 \times 10^6$  the origin of the vortex is seen to have traversed most of the curved tip when  $\alpha$  has reached  $5.2^\circ$  but at  $R = 3.9 \times 10^6$  this stage is delayed by as much as  $4^\circ$ . The more nearly chordwise attitude in the latter case is clearly attributable to the coalescence of the initial and final vortices. When the origin of the vortex moves off the curved tip, this influence disappears and the vortices at the two Reynolds numbers are then of consistent shape.

**6.2. Leading-Edge Stall.** A similar analysis for the 9% wing is of limited help since the location of the vortex changes slowly with incidence. Fortunately, however, the chordwise distributions or isobars are adequate to locate the vortex when it is rearward and sufficiently inclined to the chord. The method of selective pressure plotting at 0.001 chord is nevertheless useful to evaluate the inward spread of leading-edge stall. The curves of  $-C_p$  against  $\alpha$  for  $R = 2.2 \times 10^6$  in Fig. 23(b) show higher maxima and a much slower stall on the thicker wing. The quantities  $\alpha_m$  and  $(-C_p)_m$  are plotted against  $\eta$  in Fig. 27 for both wings and all Reynolds numbers. The displacement between the dashed curves for the 9% wing denotes some scale effect between  $R = 1.3 \times 10^6$  and  $R = 2.2 \times 10^6$ , but above this there is little systematic change in leading-edge stall. By contrast, the full curves in Fig. 27 for the 5% wing show large changes in  $\alpha_m$  and  $(-C_p)_m$  with Reynolds number; they also provide further evidence that the early onset of the stall at  $R = 2.2 \times 10^6$  is closely related to the temporary leading-edge stall associated with the initial vortex at  $R = 3.9 \times 10^6$ . It is the phenomenon of two part-span vortices that is primarily responsible for the large scale effect on the final leading-edge stall which occurs for values of  $(-C_p)_m$  similar to those for the 9% wing.

The significance of  $(-C_p)_m$  has been discussed at length in Ref. 1. For the arrowhead wing, having a leading-edge sweepback of  $49.4^\circ$ , the magnitude of  $(-C_p)_m$  was apparently related to the development of boundary-layer transition, and large changes in  $(-C_p)_m$  with Reynolds number and artificial turbulence were interpreted in that light. A higher sweepback of  $59.0^\circ$  was simulated by yawing the model through  $+10^\circ$ , and in this case it was argued that the vortex origin was located in a region of unseparated laminar flow. It would follow that there should be less scale effect on  $(-C_p)_m$  as sweepback is increased and that at sufficiently high Reynolds number  $(-C_p)_m$  should depend primarily on leading-edge sweepback when this is large. There is a striking resemblance between the curves of  $(-C_p)_m$  against  $\eta$  for the arrowhead wing with  $+10^\circ$  of yaw in the upper diagram of Fig. 19 in Ref. 1 and the curved-tip wing at the highest Reynolds number in the lower diagram of Fig. 27, both of which give  $(-C_p)_m = 4.7$  for  $60^\circ$  of sweepback in the region of mid-semi-span. Although no general conclusion can be drawn, it is plausible that this result could be typical of full-scale conditions, in which case the phenomenon of multiple vortices on the 5% curved-tip wing would only be expected for a limited range of Reynolds number.

**6.3. Surface-Flow Diagrams.** Maskell<sup>4</sup> (1955) has considered in general terms the concept of flow separation and the characteristic patterns formed on a wing surface by the limiting streamlines. In so far as these can be deduced from the oil-flow photographs the flow lines on the curved-tip wing have been sketched in Fig. 28 on the principles of Ref. 4. The limiting streamlines appear as arrowed dotted lines which start either at the leading edge or tangential to an attachment line indicated by dashes, and end at the trailing edge or tangential to a separation line. The main and

secondary vortices are superposed to complete the picture in four cases typical of the 5% and 9% wings with restricted and with extensive flow separations. It seems that the secondary vortex will generally originate at the intersection of the main attachment line and the trailing edge. Inboard of the attachment line the surface flow reaches the trailing edge smoothly, but outboard of it the main vortex entrains air from the lower surface, which separates from the sharp trailing edge and rolls up to form a trailing-edge vortex. The resulting flow is thus consistent with that observed in water in Fig. 18 which confirms also that the secondary vortex enters the wake outboard of the main vortex.

6.4. *Flow over 5% Wing.* Fig. 28(a) shows the essential features of the separated flow over the 5% wing. There is marked outflow of the tired air in the boundary layer originating ahead of the vortex. Immediately inboard of the vortex, mainstream air of high energy reattaches and retains a nearly chordwise direction. From outboard of the attachment line the air is entrained by the vortex and after a rapid outward acceleration separates from the surface because of the ensuing adverse pressure gradient. As soon as air from the lower surface is entrained, the secondary vortex of opposite sense develops and extends along the trailing edge to a position outboard of the main vortex. In this neighbourhood the air accelerated below the main vortex no longer separates but is diverted into the secondary vortex. Thus the separation line terminates and gives place to an outer attachment line bounding the surface air entrained in the secondary vortex.

All these features are present in the more extensive separated flow illustrated in Fig. 28(b); in addition there is a clear separation line at about  $\eta = 0.2$  where the outflowing boundary layer from the root gives way to the reattached chordwise flow.

We have discussed earlier the large scale effect on the 5% wing within the range of incidence for which part-span vortices occur. The picture is complicated by the observed multiple vortices at  $R = 3.9 \times 10^6$ , the highest Reynolds number of test, but these are likely to disappear at higher values of  $R$ . From the analogy with two-dimensional flow in Section 1, it is conceivable that at full-scale Reynolds numbers the flow patterns for even the 5% wing could be similar to those observed in the tests of the 9% wing, that is to say, a turbulent separation ahead of the trailing edge could then precede a leading-edge stall. Thus the flow, as sketched in Fig. 28(c), could be typical of both wings in flight.

6.5. *Flow over 9% Wing.* The flow over the 9% wing has greater complexity even for the case of restricted separation shown in Fig. 28(c). The dominating feature is a large shear layer springing from the foremost separation line and feeding the main vortex situated fairly close and parallel to the trailing edge. There can be no doubt that the vortex develops from a rearward turbulent separation typical of a thick two-dimensional aerofoil (Fig. 3), but the resulting stable three-dimensional flow has its own peculiar features. Although its precise location is unknown, the origin of the vortex is sketched downstream of the inboard end of the separation line. Inboard and ahead of the vortex the flow lines sweep outwards to the secondary separation line, while those from further out along the leading edge terminate at the foremost separation line. Between these separation lines there is little variation in surface pressure and the oil pattern in Fig. 13(d) shows an unmarked dead-air region. Downstream of the inner portion of the vortex the surface flow appears to indicate an attachment line along the trailing edge; as the shear layer becomes more tightly wrapped around the strengthening vortex, this attachment line moves closer to the vortex so that there is a chordwise flow of air between it and the trailing edge. Further along the trailing edge there is a weak secondary

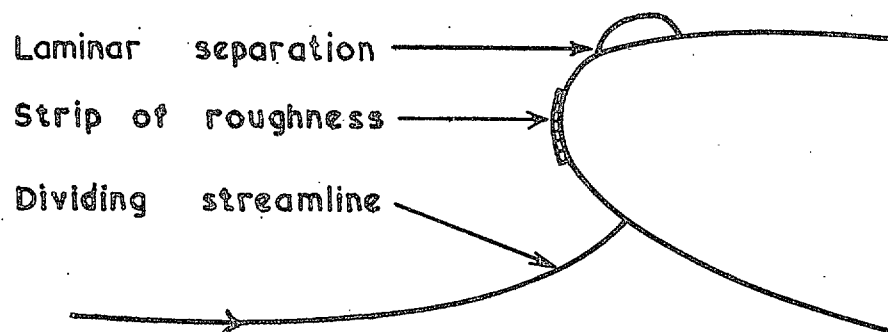


vortex of opposite sense and necessarily an attachment line between it and the main vortex. When the foremost separation line reaches the leading edge, the shear layer appears to feed another vortex which, being of the same sense and much weaker, soon merges with the main vortex. Although its spanwise location,  $\eta = 0.85$ , is consistent with the leading-edge stall determined by selective pressure plotting in Fig. 27, the real evidence for the chordwise vortex is the location of the outer separation line in Fig. 13(d) into which the flow beneath the main vortex is diverted. Outboard of  $\eta = 0.85$  the shear layer is bounded by a short attachment line fairly close to the leading edge; the outer separation line is thus defined by converging flow lines from the two sides, as Maskell<sup>4</sup> has formulated.

Fig. 28(d) shows how the flow over the 9% wing is affected by extensive separation. The dead-air region characteristic of the flows at  $R = 2.2 \times 10^6$  and incidences up to  $15.60^\circ$  now loses significance, since at  $\alpha = 16.64^\circ$  the chordwise vortex has moved rapidly inwards to an approximate position  $\eta = 0.4$ . The foremost separation line has moved much closer to the leading edge but still bends towards it in the region of the chordwise vortex and the leading-edge stall. The two vortices now merge inboard of the peak suction  $-C_p = 1.6$  in Fig. 21(d), and the feeding shear layer outboard of  $\eta = 0.4$  must have essential features in common with the 5% wing. The flow pattern between the two vortices in Fig. 21(c) has striking detail and is represented by separation and attachment lines converging towards the junction of the vortices. The main attachment line has moved from the trailing edge but still occurs on the rear half of the wing. Over the curved tip, however, the flows in Figs. 28(b) and 28(d) are remarkably similar and illustrate the diminishing effect of aerofoil section as the stalling process reaches its final stages.

It is probable that the type of flow observed on the thicker wing is not confined to such a restricted class of wing design. As discussed in Section 6.4, it may be typical of quite thin wings at very high Reynolds numbers. Moreover with any curved-tip planform, whatever the thickness/chord ratio, the flow pattern at supersonic speeds will ultimately include a shock wave lying over the rear part of the wing. When this shock wave is strong enough to induce a flow separation, it is likely that many features of the resulting flow pattern will bear some resemblance to those described above.

7. *Results with Roughened Leading Edge.* 7.1. *Limited Leading-Edge Roughness.* In an attempt to simulate the separated flow at higher Reynolds numbers, local roughness was applied to the wing so as to precipitate boundary-layer transition near the leading edge. It has been shown in Ref. 1 that an effective technique is to attach a full-span narrow strip of granulated carborundum close to the leading edge. Since too large a chordwise extent of roughness can excessively disturb the nature of the flow, the strip was limited to a region well within that bounded by the dividing streamline and the laminar separation, as shown in the diagram.



The position of the strip was chosen to be suitable for the larger angles of incidence. Height of roughness was varied between 0.006 in. and 0.012 in. and the width of the strip between 0.125 in. and 0.400 in. The effect of part-span roughness was also examined, and the results are described in Appendix II.

The quality of the oil patterns improved with the addition of roughness. To illustrate the effect of roughness on the 5% wing, Figs. 29(a) and 29(b) show that at  $R = 3.9 \times 10^6$  and  $\alpha = 8.33^\circ$  the part-span vortex is further inboard with roughness added. On the 9% wing at  $R = 2.2 \times 10^6$  and  $\alpha = 12.48^\circ$  no significant effect of roughness is apparent in Figs. 29(c) and 29(d) which support the earlier conclusion that scale effect on the oil patterns is small in this case. Whereas scale effect on the smooth 5% wing is large, the isobars on the roughened wing at  $\alpha = 10.40^\circ$  in Figs. 30(b) and 30(c) are practically indistinguishable at two different Reynolds numbers. Like the oil patterns on the curved tip in Figs. 29(a) and 29(b), Figs. 30(a) and 30(c) show an inward movement of the vortex at  $R = 3.9 \times 10^6$  when roughness is added. The corresponding full-span oil pattern in Fig. 30(d) has been analysed in Fig. 28(b) in conjunction with the isobars; particular features are the clearly defined 'herring-bone' formation inboard of the vortex, also seen in Fig. 29(b), and the extra separation line at about  $\eta = 0.2$  as discussed in Section 6.4.

*7.2. Roughness and Scale Effect.* The curves of Fig. 31 show the effect of a roughness strip of height 0.010 in. and width 0.25 in. on the low pressures due to the secondary vortex close to the trailing edge of the 5% wing. The magnitude  $(-C_p)_t$  and spanwise position  $\eta_t$  of the minimum pressure at 0.95 chord are influenced by roughness, though the curves against  $\alpha$  are similar in shape with and without roughness. At  $R = 2.2 \times 10^6$  the roughness produces lower values of  $(-C_p)_t$  at correspondingly higher values of  $\eta_t$ , which is consistent with the trend of the smooth wing with increase in Reynolds number; the effect on  $\eta_t$  is not so pronounced at the higher angles of incidence. It is less satisfactory that at  $R = 3.9 \times 10^6$  the effect of roughness is reversed so that  $(-C_p)_t$  is raised and  $\eta_t$  lowered. Although roughness appears to reduce scale effect, the sense with and without roughness is opposite. The equivalent curves of  $(-C_p)_t$  and  $\eta_t$  in Fig. 32 for the 9% wing with roughness of height 0.006 in. and width 0.19 in. at  $R = 1.3 \times 10^6$  are fairly consistent with results for the smooth wing at  $R = 2.2 \times 10^6$ . The curves of lowest pressure at 0.95 chord in the upper diagram of Fig. 32 suggest that the addition of roughness at  $R = 1.3 \times 10^6$  and an increase in Reynolds number affect the secondary vortex in much the same way.

The full curves and points ( $\square$ ) in Fig. 33 present the effect of roughness on the leading-edge stall of the 5% wing, as determined by the minima in curves of  $C_p$  against  $\alpha$  at 0.001 chord. Fig. 27 has already shown that on the smooth wing the values  $(-C_p)_m$  and  $\alpha_m$  corresponding to the minima are subject to large scale effect. The curves against  $\eta$  for the roughened wing at  $R = 2.2 \times 10^6$  resemble and lie between those for the smooth wing and by interpolation could well correspond to an equivalent Reynolds number of  $3.2 \times 10^6$ . If roughness were consistent in simulating an increase in Reynolds number, it would be expected at  $R = 3.9 \times 10^6$  that the curves for the roughened wing would lie above those for the smooth wing. However, the equivalent Reynolds number for the roughened wing in this case is only  $2.9 \times 10^6$ , which implies that roughness is ineffective at the higher Reynolds number. This result suggests that in the presence of roughness, turbulence is infused into the boundary layer in such a manner that the effect of  $R$  is reversed and greatly reduced in magnitude. Qualitatively similar effects were obtained for the leading-edge stall with different heights and widths of roughness and also for the low pressures near the trailing edge in Fig. 31, as described above.

Roughness on the 9% wing at  $R = 1.3 \times 10^6$  appears to simulate an increase in Reynolds number. This is not only true of the low pressures at 0.95 chord in Fig. 32, but according to Figs. 27 and 33 the leading-edge stall is similarly affected. The points ( $\diamond$ ) for the roughened wing at  $R = 1.3 \times 10^6$  lie very close to the dashed curves of  $\alpha_m$  and  $(-C_p)_m$  corresponding to the smooth 9% wing at  $R = 2.2 \times 10^6$ . Unfortunately, as for the 5% wing, an increase of  $R$  on the roughened wing reduces  $\alpha_m$ ; it is concluded that roughness is not producing the desired effect at the higher Reynolds numbers. The primary effect of roughness at the low Reynolds numbers is probably to reduce the chordwise extent of the leading-edge bubble, but at higher Reynolds numbers when the bubble is already small the artificial turbulence and local changes of pressure caused by the roughness may well have other significant reactions unrelated to scale effect. It was affirmed in Ref. 1 that an excessively roughened leading edge could precipitate irrelevant flow at any Reynolds number; it is now suggested that the amount of roughness to simulate higher Reynolds number on swept wings may decrease so rapidly with increasing  $R$  that it no longer remains a practical technique. At the same time there are likely to be important scale effects on many of the phenomena associated with separated flow and the occurrence of vortices.

8. *Concluding Remarks.* 1. The interest in curved-tip planforms centres on the basic idea that a swept wing can be so designed as to have uniform spanwise distributions of pressure near the leading edge over a range of incidence. Although this has not been fully attained in the present investigation, many of the effects of low-speed flow separation should be relevant to the optimum design.

2. Integrated normal pressures give experimental values of lift about 5 per cent below those calculated by lifting-surface theory. The spanwise centre of pressure is predicted within  $\pm 3$  per cent; the aerodynamic centre occurs about 0.06 aerodynamic mean chords downstream of its theoretical position. The stability characteristics of the curved-tip wing are found to depend on aerofoil section. The onset of leading-edge separation on the 5% wing improves longitudinal stability, while the rearward turbulent separation on the 9% wing has a destabilizing effect.

3. The higher the leading-edge suction and the higher the angle of sweepback, the more readily there develops a stable flow with a part-span leading-edge vortex. For the fairly thin 5% RAE 101 streamwise section the vortex forms near the curved tip at an incidence of about  $5^\circ$ ; then the peak suction coefficient is roughly  $-C_p = 1$ . The leading-edge suction develops more gradually in the case of the 9% thick section, so that the onset of flow separation is delayed until the incidence reaches about  $8^\circ$  when again the approximate peak value  $-C_p = 1$  is reached.

4. At moderate incidences the lowest pressure coefficients on both wings are proportional to the square of the incidence and occur close to the leading edge and inboard of its curved portion. At the highest Reynolds number,  $R = 3.9 \times 10^6$ , the pressure coefficient on the 5% wing attains an absolute minimum of about  $C_p = -5$  at  $\alpha = 11.5^\circ$ . By contrast, the lowest pressure on the 9% wing develops more gradually with increasing incidence, but for  $R = 2.2 \times 10^6$  it has reached the value  $C_p = -5$  and is still decreasing when  $\alpha = 16.6^\circ$ , the highest incidence of test.

5. On the 5% wing the origin of the vortex traverses the curved portion of the leading edge rapidly as incidence increases. At the top Reynolds number of  $3.9 \times 10^6$  a study of oil patterns and surface pressures (Section 6) leads to the conclusion that two part-span vortices traverse the curved

tip at an interval of  $3^\circ$  or  $4^\circ$  in incidence. The initial one weakens as the final one strengthens, and the stalling process over the inner portion of the wing is delayed until the peak leading-edge suction reaches a value  $-C_p = 4.7$  at an incidence of  $10.4^\circ$ . It is argued that such a value may be typical of full-scale Reynolds numbers, when the feature of multiple vortices may well have disappeared.

6. Although the initial separations on the two wings can be correlated, the subsequent development on the upper surface of the 9% wing is quite distinct. There soon forms a vortex situated fairly close and parallel to the trailing edge. This characteristic is undoubtedly linked to the rearward turbulent separation typical of the two-dimensional 18% RAE 101 section normal to the trailing edge (Section 1), but the resulting stable three-dimensional flow has its own peculiar and complex features (Section 6.5). The sketches in Figs. 28(a) and 28(c) and respective isobars in Figs. 10(b) and 13(c) illustrate the distinctive flows on the two wings.

7. Although these distinctive flows are believed to be typical of full scale, the effect of Reynolds number above  $3.9 \times 10^6$  on the 5% wing is paramount, while on the 9% wing it is probably small and localized near the rearward main vortex. Tests at much higher Reynolds number would be essential if a specific design of a thin round-nosed curved-tip wing were considered. The chief uncertainties lie in the occurrence of multiple vortices, in the location of part-span vortices over a critical range of incidence ( $5^\circ < \alpha < 10^\circ$  in the present case of the 5% wing), and in the possibility that the flow at high enough Reynolds number could become similar to that observed over the 9% wing.

8. As the complete stall is approached, the influence of aerofoil section diminishes. The progressive forward shift of the main vortex on the 9% wing and the eventual inward movement of the lesser chordwise vortex together lead to a flow over the curved tip ( $\eta > 0.616$ ) qualitatively similar to that on the 5% wing. The isobars in Figs. 10(d) and 21(d), whilst retaining the salient features of the individual wings, have much in common.

9. The maximum local increment in  $-C_p$  directly due to the part-span vortex increases with inward movement and with incidence but is found to be largely independent of wing thickness and Reynolds number. The general order of magnitude appears to be  $\delta(-C_p) = 0.8 C_L \tan \Lambda_m$ , where  $\Lambda_m$  is the mid-chord sweepback.

10. As soon as the main vortex entrains air from the lower surface, the secondary flow separates from the sharp edge and induces a vortex of the opposite sense along the trailing edge. It is observed in water that this secondary vortex enters the wake outboard of the main vortex. Figs. 15 to 17 show that in a limited region the secondary vortex has an effect on surface pressures greater than the maximum increment due to the main vortex; values as high as  $-C_p = 2$  are recorded when the main vortex lies rearward on the 9% wing.

11. Limited leading-edge roughness has been used to study the possibility of a large scale effect associated with a rapid transition to turbulence in the boundary layer (Section 7). Roughness is only found to have a large effect when the smooth wing is sensitive to Reynolds number; in all such cases oil patterns, isobars, leading-edge stalls and trailing-edge peak suction show less scale effect with roughness than without it. Therefore the results with roughness bring confidence in the general conclusions drawn from the rest of the investigation. However, when scale effect on the smooth wing is small, the addition of roughness usually reverses the sign of this. It is considered that the use of roughness to simulate an increase in Reynolds number is then no longer practicable.

9. *Acknowledgements.* The experiments were planned in collaboration with Mr. D. W. Bryer. Mr. N. G. Marcus of the Aerodynamics Division, N.P.L. was responsible for the design of the models which were constructed under contract to the Ministry of Supply by Messrs. Short Bros. & Harland, Ltd. Acknowledgements are also due to Mr. D. Ferriss, who carried out a considerable part of the experimental work, and to Mrs. S. Lucas, who helped to prepare the tables and figures.

---

REFERENCES

<i>No.</i>	<i>Author</i>	<i>Title, etc.</i>
1	H. C. Garner and D. W. Bryer ..	Experimental study of surface flow and part-span vortex layers on a cropped arrowhead wing. A.R.C. R. & M. 3107. April, 1957.
2	R. C. Pankhurst and H. B. Squire	Calculated pressure distributions for the RAE 100-104 aerofoil sections. (With Addendum.) A.R.C. C.P. 80. March, 1950.
3	H. Multhopp .. ..	Methods for calculating the lift distribution of wings. (Subsonic lifting surface theory.) A.R.C. R. & M. 2884. January, 1950.
4	E. C. Maskell .. ..	Flow separation in three dimensions. A.R.C. 18,063. November, 1955.

---

## APPENDIX I

### *Tunnel Interference Corrections*

The flow in the empty tunnel fitted with the false floor showed no significant pressure gradients over the region to be occupied by the model, so that the static and dynamic pressures measured well upstream of the model were easily related to datum values  $p_0$  and  $\frac{1}{2}\rho V_0^2$  at the model.

A small correction to the speed of test for solid and wake blockage has been applied, so that

$$V = V_0 + (\Delta V),$$

where

$$\left. \begin{aligned} (\Delta V) &= V_0(0.0006 + 0.037 C_D) \text{ for the } 5\% \text{ wing} \\ (\Delta V) &= V_0(0.0012 + 0.037 C_D) \text{ for the } 9\% \text{ wing} \end{aligned} \right\}, \quad (\text{A.1})$$

where the value  $C_D = 0.01$  has been used throughout. The increment  $(\Delta V)$  implies a drop in the datum static pressure at the working section and hence an increment  $2(\Delta V)/V_0$  to the measured pressure coefficient, so that the tabulated quantity is

$$\left. \begin{aligned} C_p &= 0.002 + 0.998 (p - p_0)/\frac{1}{2}\rho V_0^2 \text{ for the } 5\% \text{ wing} \\ C_p &= 0.003 + 0.997 (p - p_0)/\frac{1}{2}\rho V_0^2 \text{ for the } 9\% \text{ wing} \end{aligned} \right\}. \quad (\text{A.2})$$

The correction  $(\Delta\alpha)$  to be applied to the incidence setting has been calculated for a complete model in a rectangular tunnel 18 ft  $\times$  13 ft, *i.e.*, of twice the spanwise dimension. With the aid of lifting-surface theory (Ref. 3), the interference upwash is averaged over the planform to give

$$(\Delta\alpha) = 0.96 C_L \text{ deg}, \quad (\text{A.3})$$

such that there is no residual correction to lift for induced curvature of flow. No allowance was made for the corner fillets of the N.P.L. 13 ft  $\times$  9 ft Wind Tunnel, since they produce negligible interference in the region of the curved tip. In cases of high incidence, when  $C_L$  could not be calculated, a correction  $\Delta\alpha = 0.04\alpha$  deg was applied.

After the corrections for blockage and lift effect on incidence in Eqns. (A.2) and (A.3) have been applied, there remain residual corrections to the pitching moment and spanwise centre of pressure, which have been evaluated by lifting-surface theory. The pitching-moment coefficient ( $C_m$ ) is subject to an increment

$$(\Delta C_m) = 0.0105 C_L, \quad (\text{A.4})$$

which is independent of pitching axis. The spanwise centre of pressure ( $\bar{\eta}$ ) requires a residual correction

$$(\Delta\bar{\eta}) = -0.0025. \quad (\text{A.5})$$

As described in Eqns. (4) and (5) of Ref. 1, wall interference due to lift introduces rotation of the wind axes by an amount

$$\epsilon = 0.0149 C_L \text{ radians} \quad (\text{A.6})$$

which leads to corrections to the lift and drag coefficients

$$\left. \begin{aligned} (\Delta C_L) &= C_L (\cos \epsilon - 1) - C_D \sin \epsilon \\ (\Delta C_D) &= C_L \sin \epsilon + C_D (\cos \epsilon - 1) \end{aligned} \right\}. \quad (\text{A.7})$$

Since  $C_L$  never exceeds 0.4,  $\epsilon < 0.006$  radians,  $(\Delta C_L)$  is negligible and it is sufficient to take

$$(\Delta C_D) = 0.0149 C_L^2. \quad (\text{A.8})$$

## APPENDIX II

### *Results with Part-Span Roughness*

A limited study of the effect of part-span roughness has revealed some points of interest. Although the roughness on the 5% wing was of smaller height than that used to investigate the effect of Reynolds number in Section 7, the curves of the local angle of stall  $\alpha_m$  against  $\eta$  are essentially independent of the height of roughness. The curves in Fig. 34 labelled  $\eta_R = 0$ , for the smooth wing, are reproduced from Fig. 27, no account being taken of the initial vortex for  $R = 3.9 \times 10^6$ . At this Reynolds number the effect of roughness is to reduce  $\alpha_m$ , and with roughness of part-span  $0 < \eta < \eta_R$  the vortex origin changes suddenly as the roughness takes effect; this is indicated in the lower diagram of Fig. 34 by the horizontal dashed lines from the curve  $\eta_R = 0$  to the curve  $\eta_R = 1$ . This implies that roughness inboard of  $\eta = \eta_R$  exerts an influence beyond  $\eta = \frac{1}{2}(1 + \eta_R)$ , that is more than half way from its outboard end to the wing tip. For  $R = 2.2 \times 10^6$ , moreover, when the effect of roughness is to increase  $\alpha_m$ , part-span roughness appears to delay the tip stall slightly, even for  $\eta_R = 0.38$ . The upper diagram of Fig. 34 shows that with increase in incidence the tip stall spreads very rapidly inboard to a position  $\eta = \eta_1$ , say, but it is uncertain whether a part-span vortex forms during this stage. The values  $\eta = \eta_1$ , indicated by the vertical dashed lines, are as follows:

$\eta_R =$	0.38	0.56	0.71	0.88
$\eta_1 =$	0.62	0.71	0.77	0.83

After a renewed decrease in leading-edge pressure with further increase in incidence the origin of the vortex becomes detectable from surface pressures in the region of  $\eta = \eta_1$ . When separated flow extends inboard of this, the part-span vortex behaves as if there were full-span roughness.

The effect of roughness on the 9% wing is exemplified by changes in the pressure distribution at  $\eta = 0.831$ . The following table shows that at  $R = 1.3 \times 10^6$  the addition of full-span roughness tends to simulate an increase in Reynolds number:

$-C_p$ at $\eta = 0.831$ on 9% wing at $\alpha = 12.5^\circ$			
$x/c$	$R = 1.3 \times 10^6$ Smooth wing	$R = 1.3 \times 10^6$ Full-span roughness	$R = 2.2 \times 10^6$ Smooth wing
0.015	1.08	1.68	1.92
0.250	0.86	0.46	0.45
0.800	0.43	0.58	0.64
0.950	0.57	1.38	1.51

The variation in these pressure coefficients with part-span roughness is shown in Fig. 35. The removal of roughness from the outer third of the leading edge has negligible effect, but the pressures at each of the four chordwise positions depends critically on the span of roughness  $0 < \eta < \eta_R$  as  $\eta_R$  is decreased from 0.67 to 0.59. This result is consistent with the earlier statement for the 5% wing, that part-span roughness exerts an influence rather beyond  $\eta = \frac{1}{2}(1 + \eta_R)$ . Radically different

chordwise pressure distributions at  $\eta = 0.831$  occur for  $\eta_R = 0.67$  and  $\eta_R = 0.59$ , while only trivial changes occur as  $\eta_R$  is decreased either from 1 to 0.67 or from 0.59 to 0.05. It is noteworthy that there is still a marked effect of roughness of part-span  $0 < \eta < 0.05$ , particularly at 0.95 chord. It seems likely that the formation of the secondary vortex along the trailing edge can be influenced by the degree of turbulence in the out-flowing boundary layer originating close to the root leading edge. With reference to Fig. 28(c), for small values of  $\eta_R$  roughness affects mainly the rearward attachment line, but for  $\eta_R = 0.6$  there is also a direct effect of roughness on the forward separation line. A few results for roughness of extent  $\eta_S < \eta < 0.831$  are shown on the right-hand side of Fig. 35; by contrast with the curves against  $\eta_R$ , the pressure coefficients vary gradually throughout the range of  $\eta_S$ . It is concluded that with roughness of part-span  $\eta_S < \eta < \eta_R$ , the outboard end  $\eta = \eta_R$  is the more significant.

On both wings special cases of large scale effect have been studied with varying spans of leading-edge roughness. Roughness over an inner portion of the wing is found to influence the leading-edge stall midway between the pointed tip and the outer limit of roughness. On the 9% wing a small strip of roughness over the innermost 5% of the leading edge can have a marked effect on the peak suction near the secondary trailing-edge vortex (Fig. 35).



TABLE 1

*Scope of Pressure Plotting*

$V$ (ft/sec)	$R \times 10^{-6}$	Uncorrected incidences of test		Tables
		5% RAE 101	9% RAE 101	
70	1.3	$0^\circ, \pm 2^\circ, \pm 5^\circ$	$0^\circ, \pm 2^\circ, \pm 8^\circ, 12^\circ$	2, 7
120	2.2	$0^\circ, \pm 2^\circ, \pm 4^\circ, \pm 5^\circ$ $\pm 5\frac{1}{2}^\circ, \pm 6^\circ, \pm 8^\circ$	$0^\circ, \pm 1^\circ, \pm 2^\circ, \pm 4^\circ$ $\pm 6^\circ, 7^\circ, \pm 8^\circ, 9^\circ$ $10^\circ, 11^\circ, 12^\circ, 13^\circ$ $14^\circ, 15^\circ, 16^\circ$	3, 8
150	2.8	$\pm 8^\circ$	—	4
180	3.3	$\pm 8^\circ$	—	5
210	3.9	$0^\circ, \pm \frac{1}{2}^\circ, \pm 1^\circ, \pm 2^\circ$ $\pm 4^\circ, \pm 5^\circ, \pm 6^\circ, \pm 7^\circ$ $\pm 8^\circ, 9^\circ, 10^\circ, 11^\circ$	$0^\circ, \pm 2^\circ, \pm 8^\circ$ $10^\circ, 12^\circ$	6, 9

TABLE 2

Pressure Distributions on 5% Wing at  $R = 1.3 \times 10^6$

5% RAE 101. Values of  $C_p$  for  $R = 1.3 \times 10^6$  and  $\alpha = -5.20^\circ$

$x/c$	$\eta$	0.195	0.383	0.556	0.707	0.831	0.882	0.924	0.957	0.981
0.001		-0.11	-0.18	-0.13	-0.16	-0.26	-0.25	-0.28	-0.25	
0.003		0.04	0.05	0.07	0.01	-0.15	-0.15	-0.22	-0.22	
0.006		0.18	0.17	0.18	0.12	-0.03	-0.10	-0.14	-0.18	
0.010		0.23	0.24	0.25	0.18	0.06	-0.02	-0.05	-0.16	
0.015		0.25	0.25	0.25	0.20	0.10	0.03	-0.04	-0.12	
0.025		0.23	0.25	0.23	0.20	0.13	0.08	0.01	-0.06	
0.035		0.21	0.22	0.22	0.19	0.13	0.09	0.04	-0.03	
0.050		0.18	0.20	0.19	0.16	0.12	0.09	0.06	-0.01	
0.075		0.15	0.16	0.16	0.13	0.11	0.09	0.06	0.02	
0.100		0.13	0.14	0.15	0.11	0.09	0.08	0.06	0.02	
0.125		0.11	0.12	0.11	0.09	0.08	0.07	0.05	0.03	
0.150		0.09	0.10	0.09	0.08	0.07	0.06	0.05	0.03	
0.200		0.07	0.07	0.06	0.05	0.05	0.04	0.04	0.03	
0.250		0.06	0.06	0.04	0.04	0.03	0.03	0.03	0.03	
0.300		0.04	0.04	0.02	0.01	0.02	0.02	0.02	0.02	
0.350		0.04	0.03	0.02	0.01	0.02	0.02	0.02	0.02	
0.400		0.03	0.03	0.01	0.01	0.01	0.01	0.02	0.02	
0.450		0.03	0.03	0.01	0.00	0.01	0.01	0.02	0.01	
0.500		0.03	0.02	0.01	0.00	0.01	0.01	0.02	0.01	
0.550		0.03	0.02	0.01	0.00	0.01	0.01	0.01	0.01	
0.600		0.03	0.01	0.01	0.00	0.01	0.01	0.01	0.01	
0.650		0.03	0.01	0.00	0.00	0.01	0.01	0.01	0.01	
0.700		0.03	0.01	0.00	0.00	0.01	0.01	0.01	0.00	
0.750		0.03	0.01	0.00	0.00	0.01	0.01	0.01	-0.01	
0.800		0.03	0.01	0.00	0.00	0.01	0.01	0.01	-0.01	
0.850		0.03	0.00	-0.01	0.00	0.01	0.01	0.01	-0.03	
0.900		0.03	0.00	-0.01	0.00	0.01	0.01	0.01	-0.05	
0.950		0.02	-0.01	-0.02	0.00	0.02	0.01	-0.02	-0.10	

5% RAE 101. Values of  $C_p$  for  $R = 1.3 \times 10^6$  and  $\alpha = -2.08^\circ$

$x/c$	$\eta$	0.195	0.383	0.556	0.707	0.831	0.882	0.924	0.957	0.981
0.001		0.22	0.22	0.23	0.17	0.09	-0.01	-0.04	-0.11	
0.003		0.24	0.25	0.25	0.20	0.12	0.05	-0.01	-0.06	
0.006		0.23	0.23	0.23	0.18	0.12	0.06	0.02	-0.05	
0.010		0.20	0.20	0.20	0.17	0.11	0.08	0.05	-0.03	
0.015		0.17	0.17	0.16	0.15	0.09	0.08	0.06	-0.01	
0.025		0.13	0.13	0.12	0.11	0.07	0.07	0.06	0.01	
0.035		0.10	0.11	0.09	0.08	0.05	0.06	0.05	0.02	
0.050		0.07	0.08	0.06	0.05	0.03	0.04	0.04	0.02	
0.075		0.05	0.05	0.03	0.03	0.01	0.03	0.03	0.01	
0.100		0.02	0.03	0.01	0.01	0.00	0.01	0.01	0.01	
0.125		0.01	0.01	0.00	0.00	-0.01	0.00	0.01	0.00	
0.150		0.00	0.00	-0.01	-0.01	-0.01	-0.01	0.00	0.00	
0.200		-0.02	-0.02	-0.02	-0.02	-0.02	-0.02	-0.01	-0.01	
0.250		-0.02	-0.02	-0.04	-0.04	-0.04	-0.03	-0.02	-0.01	
0.300		-0.04	-0.03	-0.05	-0.05	-0.04	-0.04	-0.02	-0.02	
0.350		-0.03	-0.03	-0.04	-0.04	-0.03	-0.04	-0.02	-0.01	
0.400		-0.03	-0.03	-0.04	-0.04	-0.03	-0.04	-0.02	-0.01	
0.450		-0.02	-0.03	-0.04	-0.04	-0.03	-0.03	-0.02	-0.01	
0.500		-0.02	-0.02	-0.03	-0.03	-0.02	-0.02	-0.01	-0.01	
0.550		-0.02	-0.02	-0.03	-0.03	-0.02	-0.02	-0.01	-0.01	
0.600		-0.01	-0.02	-0.03	-0.03	-0.02	-0.02	-0.01	-0.01	
0.650		-0.01	-0.02	-0.03	-0.03	-0.02	-0.02	-0.01	-0.01	
0.700		0.00	-0.02	-0.02	-0.02	-0.01	-0.01	0.00	0.00	
0.750		0.00	-0.01	-0.02	-0.02	-0.01	-0.01	0.01	0.00	
0.800		0.01	-0.01	-0.01	-0.01	0.00	0.00	0.01	0.01	
0.850		0.01	-0.01	-0.01	-0.01	0.00	0.00	0.01	0.01	
0.900		0.01	-0.01	-0.02	-0.01	0.01	0.01	0.01	0.01	
0.950		0.02	0.00	-0.01	0.00	0.01	0.01	0.01	0.01	

TABLE 2—continued

5% RAE 101. Values of  $C_p$  for  $R = 1.3 \times 10^6$  and  $\alpha = 0^\circ$ 

$x/c$ $\eta$	0.195	0.383	0.556	0.707	0.831	0.882	0.924	0.957	0.981
0.001	0.21	0.21	0.18	0.15	0.12	0.08	0.05	0.06	
0.003	0.17	0.14	0.11	0.10	0.06	0.06	0.03	0.01	
0.006	0.10	0.07	0.05	0.02	0.03	0.01	0.01	0.00	
0.010	0.05	0.03	0.01	-0.01	0.01	0.01	-0.01	-0.01	
0.015	0.03	0.01	-0.03	-0.02	-0.02	-0.02	-0.01	-0.02	
0.025	0.00	-0.02	-0.04	-0.04	-0.03	-0.04	-0.03	-0.03	
0.035	-0.02	-0.03	-0.06	-0.05	-0.05	-0.04	-0.04	-0.04	
0.050	-0.04	-0.05	-0.07	-0.07	-0.07	-0.06	-0.05	-0.04	
0.075	-0.05	-0.06	-0.08	-0.08	-0.07	-0.06	-0.06	-0.05	
0.100	-0.06	-0.07	-0.08	-0.08	-0.08	-0.07	-0.07	-0.06	
0.125	-0.07	-0.07	-0.08	-0.08	-0.08	-0.07	-0.07	-0.06	
0.150	-0.07	-0.07	-0.08	-0.09	-0.09	-0.08	-0.07	-0.06	
0.200	-0.08	-0.08	-0.09	-0.09	-0.09	-0.08	-0.07	-0.06	
0.250	-0.08	-0.08	-0.09	-0.09	-0.09	-0.08	-0.07	-0.06	
0.300	-0.08	-0.08	-0.10	-0.10	-0.09	-0.08	-0.07	-0.06	
0.350	-0.07	-0.07	-0.09	-0.08	-0.08	-0.07	-0.06	-0.05	
0.400	-0.06	-0.07	-0.08	-0.08	-0.07	-0.07	-0.06	-0.05	
0.450	-0.06	-0.06	-0.08	-0.07	-0.07	-0.06	-0.05	-0.04	
0.500	-0.05	-0.05	-0.06	-0.06	-0.05	-0.05	-0.04	-0.03	
0.550	-0.04	-0.05	-0.06	-0.06	-0.05	-0.04	-0.04	-0.03	
0.600	-0.04	-0.05	-0.06	-0.05	-0.04	-0.04	-0.04	-0.03	
0.650	-0.03	-0.04	-0.05	-0.04	-0.04	-0.04	-0.03	-0.03	
0.700	-0.03	-0.03	-0.04	-0.04	-0.03	-0.03	-0.02	-0.02	
0.750	-0.01	-0.02	-0.04	-0.03	-0.02	-0.02	-0.01	-0.01	
0.800	0.00	-0.01	-0.02	-0.02	-0.01	-0.01	0.01	0.01	
0.850	0.01	-0.01	-0.02	-0.01	0.00	0.01	0.01	0.01	
0.900	0.01	-0.01	-0.02	0.00	0.01	0.01	0.01	0.02	
0.950	0.02	0.00	-0.01	0.00	0.01	0.02	0.02	0.03	

5% RAE 101. Values of  $C_p$  for  $R = 1.3 \times 10^6$  and  $\alpha = 2.08^\circ$ 

$x/c$ $\eta$	0.195	0.383	0.556	0.707	0.831	0.882	0.924	0.957	0.981
0.001	-0.02	-0.13	-0.20	-0.18	-0.10	-0.13	-0.20	-0.16	
0.003	-0.09	-0.21	-0.29	-0.25	-0.25	-0.20	-0.22	-0.22	
0.006	-0.16	-0.27	-0.32	-0.34	-0.29	-0.28	-0.25	-0.23	
0.010	-0.19	-0.28	-0.33	-0.32	-0.29	-0.28	-0.26	-0.24	
0.015	-0.19	-0.25	-0.32	-0.29	-0.27	-0.28	-0.26	-0.24	
0.025	-0.18	-0.22	-0.27	-0.26	-0.25	-0.25	-0.25	-0.25	
0.035	-0.17	-0.21	-0.25	-0.24	-0.23	-0.23	-0.24	-0.24	
0.050	-0.17	-0.20	-0.24	-0.23	-0.23	-0.23	-0.22	-0.22	
0.075	-0.16	-0.18	-0.21	-0.21	-0.20	-0.20	-0.20	-0.20	
0.100	-0.16	-0.17	-0.20	-0.19	-0.19	-0.18	-0.19	-0.20	
0.125	-0.15	-0.17	-0.18	-0.18	-0.18	-0.18	-0.19	-0.19	
0.150	-0.14	-0.16	-0.18	-0.18	-0.17	-0.17	-0.17	-0.18	
0.200	-0.14	-0.15	-0.17	-0.17	-0.16	-0.15	-0.16	-0.15	
0.250	-0.13	-0.14	-0.15	-0.15	-0.15	-0.14	-0.14	-0.13	
0.300	-0.13	-0.13	-0.15	-0.15	-0.14	-0.13	-0.13	-0.13	
0.350	-0.12	-0.12	-0.13	-0.14	-0.13	-0.12	-0.11	-0.10	
0.400	-0.10	-0.11	-0.13	-0.12	-0.12	-0.10	-0.09	-0.09	
0.450	-0.09	-0.10	-0.11	-0.11	-0.09	-0.08	-0.09	-0.08	
0.500	-0.09	-0.07	-0.08	-0.08	-0.07	-0.07	-0.07	-0.06	
0.550	-0.07	-0.06	-0.08	-0.07	-0.07	-0.06	-0.06	-0.06	
0.600	-0.05	-0.06	-0.07	-0.07	-0.05	-0.06	-0.06	-0.05	
0.650	-0.04	-0.05	-0.06	-0.06	-0.05	-0.04	-0.04	-0.04	
0.700	-0.03	-0.04	-0.05	-0.04	-0.04	-0.04	-0.03	-0.03	
0.750	-0.02	-0.04	-0.04	-0.04	-0.03	-0.03	-0.02	-0.02	
0.800	-0.02	-0.03	-0.04	-0.03	-0.02	-0.02	-0.01	-0.01	
0.850	0.00	-0.02	-0.03	-0.05	-0.01	-0.01	0.00	-0.01	
0.900	0.01	-0.01	-0.03	-0.04	-0.01	0.00	0.00	0.00	
0.950	0.01	0.00	-0.02	0.00	0.01	0.01	0.01	0.01	

TABLE 2—continued

5% RAE 101. Values of  $C_p$  for  $R = 1.3 \times 10^6$  and  $\alpha = 5.20^\circ$

$x/c$	$\eta$	0.195	0.383	0.556	0.707	0.831	0.882	0.924	0.957	0.981
0.001		-0.74	-1.05	-1.00	-0.84	-0.57	-0.49	-0.37	-0.30	-0.17
0.003		-0.76	-0.97	-0.90	-0.76	-0.59	-0.45	-0.35	-0.27	
0.006		-0.71	-0.86	-0.87	-0.70	-0.54	-0.44	-0.35	-0.27	
0.010		-0.65	-0.84	-0.86	-0.70	-0.54	-0.43	-0.34	-0.27	-0.17
0.015		-0.60	-0.83	-0.86	-0.70	-0.53	-0.43	-0.35	-0.27	
0.025		-0.59	-0.85	-0.87	-0.71	-0.53	-0.43	-0.34	-0.27	
0.035		-0.62	-0.60	-0.79	-0.69	-0.53	-0.43	-0.34	-0.26	
0.050		-0.33	-0.44	-0.63	-0.61	-0.53	-0.43	-0.34	-0.26	-0.17
0.075		-0.31	-0.38	-0.46	-0.49	-0.51	-0.42	-0.33	-0.25	-0.16
0.100		-0.30	-0.34	-0.38	-0.41	-0.50	-0.42	-0.33	-0.25	-0.16
0.125		-0.27	-0.31	-0.33	-0.35	-0.49	-0.41	-0.32	-0.24	-0.16
0.150		-0.26	-0.29	-0.30	-0.32	-0.48	-0.41	-0.32	-0.24	-0.15
0.200		-0.23	-0.26	-0.27	-0.27	-0.45	-0.41	-0.32	-0.23	-0.15
0.250		-0.21	-0.23	-0.24	-0.24	-0.36	-0.42	-0.31	-0.22	-0.13
0.300		-0.20	-0.21	-0.22	-0.22	-0.28	-0.43	-0.32	-0.22	-0.13
0.350		-0.17	-0.18	-0.20	-0.19	-0.20	-0.40	-0.32	-0.22	-0.12
0.400		-0.15	-0.16	-0.17	-0.17	-0.16	-0.35	-0.35	-0.20	-0.11
0.450		-0.13	-0.14	-0.15	-0.15	-0.12	-0.28	-0.38	-0.19	-0.11
0.500		-0.11	-0.12	-0.13	-0.12	-0.10	-0.21	-0.39	-0.19	-0.09
0.550		-0.10	-0.11	-0.11	-0.11	-0.09	-0.15	-0.39	-0.19	-0.09
0.600		-0.09	-0.10	-0.10	-0.09	-0.07	-0.10	-0.37	-0.21	-0.08
0.650		-0.07	-0.08	-0.08	-0.08	-0.06	-0.06	-0.32	-0.22	-0.07
0.700		-0.06	-0.07	-0.07	-0.07	-0.06	-0.05	-0.27	-0.23	-0.06
0.750		-0.04	-0.06	-0.06	-0.06	-0.04	-0.04	-0.22	-0.24	-0.06
0.800		-0.03	-0.05	-0.05	-0.04	-0.02	-0.02	-0.17	-0.24	-0.05
0.850		-0.02	-0.04	-0.04	-0.04	-0.02	-0.02	-0.12	-0.24	-0.06
0.900		-0.01	-0.03	-0.04	-0.03	-0.01	-0.01	-0.09	-0.22	-0.07
0.950		0.01	-0.02	-0.03	-0.02	0.00	0.01	-0.06	-0.20	-0.11

TABLE 3

Pressure Distributions on 5% Wing at  $R = 2.2 \times 10^6$ 

5% RAE 101. Values of  $C_p$  for  $R = 2.2 \times 10^6$  and  $\alpha = -8.37^\circ$

$x/c$ $\eta$	0.195	0.383	0.556	0.707	0.831	0.882	0.924	0.957	0.981
0.001	-0.72	-0.48	-0.24	-0.26	-0.25	-0.20	-0.18	-0.16	
0.003	-0.44	-0.19	-0.04	-0.10	-0.18	-0.15	-0.15	-0.12	
0.006	-0.08	0.03	0.11	0.04	-0.07	-0.11	-0.10	-0.10	
0.010	0.11	0.16	0.21	0.13	0.02	-0.04	-0.04	-0.09	
0.015	0.20	0.24	0.25	0.19	0.08	0.02	-0.02	-0.06	
0.025	0.26	0.27	0.27	0.21	0.12	0.07	0.02	-0.04	
0.035	0.26	0.28	0.27	0.21	0.14	0.09	0.04	-0.01	
0.050	0.26	0.27	0.25	0.21	0.15	0.11	0.07	0.01	
0.075	0.24	0.25	0.23	0.19	0.14	0.11	0.07	0.02	
0.100	0.21	0.22	0.20	0.17	0.13	0.10	0.07	0.02	
0.125	0.20	0.20	0.18	0.16	0.12	0.09	0.07	0.03	
0.150	0.18	0.18	0.17	0.14	0.11	0.09	0.06	0.03	
0.200	0.15	0.15	0.13	0.11	0.09	0.07	0.05	0.02	
0.250	0.13	0.13	0.11	0.09	0.07	0.05	0.04	0.01	
0.300	0.11	0.11	0.09	0.07	0.06	0.04	0.03	0.00	
0.350	0.10	0.10	0.07	0.06	0.04	0.03	0.01	0.00	
0.400	0.09	0.08	0.06	0.05	0.04	0.01	-0.01	-0.01	
0.450	0.09	0.08	0.05	0.04	0.03	0.01	-0.01	-0.01	
0.500	0.08	0.07	0.05	0.04	0.01	-0.01	-0.01	-0.02	
0.550	0.07	0.06	0.05	0.03	0.01	-0.02	-0.02	-0.02	
0.600	0.07	0.05	0.04	0.02	-0.01	-0.03	-0.04	-0.03	
0.650	0.06	0.05	0.03	0.02	-0.01	-0.04	-0.03	-0.03	
0.700	0.06	0.04	0.03	0.02	-0.03	-0.05	-0.04	-0.04	
0.750	0.05	0.03	0.03	0.01	-0.04	-0.06	-0.05	-0.04	
0.800	0.05	0.03	0.02	0.00	-0.06	-0.07	-0.06	-0.05	
0.850	0.04	0.02	0.01	-0.01	-0.08	-0.10	-0.06	-0.06	
0.900	0.03	0.02	0.00	-0.03	-0.12	-0.12	-0.08	-0.07	
0.950	0.02	0.01	-0.01	-0.06	-0.18	-0.16	-0.10	-0.07	

5% RAE 101. Values of  $C_p$  for  $R = 2.2 \times 10^6$  and  $\alpha = -6.25^\circ$ 

$x/c$ $\eta$	0.195	0.383	0.556	0.707	0.831	0.882	0.924	0.957	0.981
0.001	-0.33	-0.27	-0.18	-0.18	-0.26	-0.24	-0.25	-0.22	
0.003	-0.12	-0.01	0.03	-0.02	-0.16	-0.17	-0.20	-0.19	
0.006	0.11	0.14	0.16	0.10	-0.05	-0.11	-0.14	-0.17	
0.010	0.21	0.22	0.23	0.17	0.04	-0.04	-0.06	-0.15	
0.015	0.24	0.26	0.26	0.20	0.09	0.02	-0.04	-0.11	
0.025	0.25	0.26	0.25	0.20	0.12	0.07	0.01	-0.07	
0.035	0.24	0.25	0.24	0.20	0.14	0.09	0.03	-0.04	
0.050	0.22	0.23	0.21	0.18	0.13	0.09	0.06	-0.01	
0.075	0.19	0.19	0.18	0.15	0.12	0.09	0.07	0.01	
0.100	0.16	0.17	0.15	0.13	0.11	0.08	0.06	0.02	
0.125	0.14	0.14	0.13	0.12	0.10	0.07	0.06	0.02	
0.150	0.13	0.13	0.12	0.10	0.09	0.07	0.06	0.03	
0.200	0.10	0.10	0.09	0.07	0.07	0.05	0.05	0.03	
0.250	0.09	0.08	0.07	0.06	0.05	0.04	0.04	0.03	
0.300	0.07	0.07	0.05	0.04	0.04	0.03	0.03	0.02	
0.350	0.06	0.05	0.04	0.03	0.03	0.02	0.03	0.01	
0.400	0.06	0.05	0.03	0.03	0.03	0.02	0.03	0.01	
0.450	0.05	0.05	0.03	0.02	0.03	0.02	0.02	0.01	
0.500	0.05	0.04	0.03	0.02	0.02	0.01	0.02	0.00	
0.550	0.05	0.04	0.02	0.02	0.02	0.01	0.02	0.00	
0.600	0.04	0.03	0.02	0.01	0.02	0.01	0.01	-0.01	
0.650	0.04	0.03	0.01	0.01	0.02	0.01	0.01	-0.02	
0.700	0.04	0.03	0.01	0.01	0.02	0.00	0.01	-0.03	
0.750	0.04	0.02	0.01	0.01	0.02	0.00	-0.01	-0.05	
0.800	0.03	0.02	0.01	0.01	0.01	0.00	-0.02	-0.06	
0.850	0.03	0.01	0.01	0.01	0.01	-0.01	-0.04	-0.08	
0.900	0.03	0.01	0.01	0.01	0.01	-0.03	-0.07	-0.10	
0.950	0.03	0.00	0.01	0.01	0.01	-0.05	-0.14	-0.12	

TABLE 3—continued

5% RAE 101. Values of  $C_p$  for  $R = 2.2 \times 10^6$  and  $\alpha = -5.73^\circ$ 

$x/c$ $\eta$	0.195	0.383	0.556	0.707	0.831	0.882	0.924	0.957	0.981
0.001	-0.21	-0.32	-0.24	-0.26	-0.32	-0.28	-0.31	-0.28	
0.003	-0.03	-0.04	0.01	-0.06	-0.20	-0.19	-0.25	-0.24	
0.006	0.15	0.13	0.15	0.08	-0.07	-0.13	-0.17	-0.20	
0.010	0.22	0.22	0.23	0.18	0.03	-0.05	-0.08	-0.14	
0.015	0.25	0.25	0.25	0.20	0.09	0.02	-0.06	-0.12	
0.025	0.24	0.25	0.25	0.20	0.12	0.07	0.00	-0.09	
0.035	0.23	0.24	0.23	0.20	0.13	0.09	0.03	-0.05	
0.050	0.20	0.21	0.21	0.17	0.13	0.09	0.06	-0.04	
0.075	0.17	0.18	0.17	0.15	0.12	0.09	0.07	0.01	
0.100	0.15	0.15	0.15	0.12	0.10	0.08	0.06	0.02	
0.125	0.13	0.13	0.13	0.11	0.09	0.07	0.06	0.02	
0.150	0.11	0.12	0.11	0.09	0.08	0.07	0.05	0.03	
0.200	0.09	0.09	0.08	0.07	0.06	0.06	0.05	0.03	
0.250	0.07	0.07	0.06	0.05	0.05	0.04	0.04	0.02	
0.300	0.05	0.05	0.04	0.03	0.03	0.03	0.03	0.02	
0.350	0.05	0.05	0.03	0.03	0.03	0.02	0.03	0.02	
0.400	0.05	0.04	0.03	0.02	0.02	0.02	0.03	0.02	
0.450	0.04	0.04	0.03	0.01	0.02	0.02	0.02	0.02	
0.500	0.04	0.04	0.02	0.01	0.02	0.02	0.03	0.01	
0.550	0.04	0.03	0.02	0.01	0.02	0.01	0.02	0.01	
0.600	0.04	0.02	0.01	0.01	0.01	0.01	0.01	0.01	
0.650	0.03	0.02	0.01	0.01	0.01	0.01	0.02	0.01	
0.700	0.04	0.02	0.01	0.01	0.01	0.01	0.02	0.00	
0.750	0.03	0.01	0.01	0.01	0.01	0.01	0.01	-0.01	
0.800	0.03	0.01	0.01	0.01	0.01	0.01	0.01	-0.02	
0.850	0.03	0.01	0.00	0.01	0.01	0.01	0.01	-0.05	
0.900	0.03	0.00	-0.01	0.01	0.01	0.01	-0.01	-0.07	
0.950	0.03	-0.01	-0.02	0.00	0.01	0.01	-0.04	-0.11	

5% RAE 101. Values of  $C_p$  for  $R = 2.2 \times 10^6$  and  $\alpha = -5.20^\circ$ 

$x/c$ $\eta$	0.195	0.383	0.556	0.707	0.831	0.882	0.924	0.957	0.981
0.001	-0.11	-0.25	-0.25	-0.32	-0.42	-0.37	-0.39	-0.35	
0.003	0.03	0.01	0.01	-0.09	-0.27	-0.25	-0.31	-0.29	
0.006	0.18	0.16	0.15	0.07	-0.10	-0.17	-0.21	-0.26	
0.010	0.24	0.23	0.23	0.16	0.01	-0.06	-0.10	-0.22	
0.015	0.24	0.26	0.25	0.19	0.08	0.00	-0.07	-0.18	
0.025	0.23	0.25	0.24	0.20	0.12	0.06	-0.01	-0.11	
0.035	0.21	0.23	0.22	0.19	0.13	0.09	0.02	-0.06	
0.050	0.19	0.20	0.19	0.16	0.12	0.09	0.05	-0.03	
0.075	0.16	0.16	0.16	0.14	0.11	0.09	0.06	0.00	
0.100	0.13	0.14	0.13	0.12	0.10	0.08	0.06	0.01	
0.125	0.11	0.12	0.11	0.10	0.09	0.07	0.05	0.02	
0.150	0.09	0.10	0.09	0.08	0.07	0.06	0.05	0.02	
0.200	0.07	0.07	0.07	0.06	0.06	0.05	0.04	0.02	
0.250	0.06	0.06	0.05	0.04	0.04	0.03	0.03	0.02	
0.300	0.04	0.04	0.03	0.03	0.03	0.03	0.03	0.02	
0.350	0.04	0.04	0.03	0.02	0.02	0.03	0.02	0.01	
0.400	0.03	0.03	0.02	0.01	0.02	0.02	0.02	0.01	
0.450	0.03	0.03	0.02	0.01	0.02	0.01	0.02	0.01	
0.500	0.03	0.03	0.02	0.01	0.01	0.01	0.02	0.01	
0.550	0.03	0.03	0.01	0.01	0.01	0.01	0.01	0.01	
0.600	0.03	0.02	0.01	0.01	0.01	0.01	0.01	0.01	
0.650	0.03	0.02	0.01	0.01	0.01	0.01	0.02	0.01	
0.700	0.03	0.02	0.01	0.01	0.01	0.01	0.02	0.01	
0.750	0.03	0.01	0.01	0.01	0.01	0.01	0.02	0.01	
0.800	0.03	0.01	0.01	0.01	0.01	0.01	0.02	0.00	
0.850	0.03	0.01	0.00	0.01	0.01	0.01	0.02	-0.01	
0.900	0.03	0.01	-0.01	0.01	0.01	0.01	0.01	-0.02	
0.950	0.03	0.00	-0.01	0.01	0.01	0.01	0.01	-0.04	

TABLE 3—continued

5% RAE 101. Values of  $C_p$  for  $R = 2.2 \times 10^6$  and  $\alpha = -4.16^\circ$ 

$x/c$ $\eta$	0.195	0.383	0.556	0.707	0.831	0.882	0.924	0.957	0.981
0.001	0.04	-0.03	-0.04	-0.12	-0.31	-0.36	-0.44	-0.44	
0.003	0.14	0.14	0.13	0.05	-0.16	-0.21	-0.33	-0.37	
0.006	0.22	0.23	0.22	0.14	-0.03	-0.13	-0.21	-0.33	
0.010	0.24	0.25	0.25	0.19	0.05	-0.03	-0.10	-0.27	
0.015	0.24	0.25	0.24	0.20	0.10	0.03	-0.06	-0.20	
0.025	0.21	0.22	0.21	0.18	0.12	0.07	0.00	-0.12	
0.035	0.18	0.20	0.19	0.17	0.12	0.09	0.03	-0.07	
0.050	0.15	0.17	0.16	0.14	0.11	0.09	0.05	-0.03	
0.075	0.12	0.13	0.13	0.11	0.09	0.08	0.05	0.00	
0.100	0.10	0.11	0.10	0.09	0.07	0.07	0.05	0.01	
0.125	0.08	0.09	0.08	0.07	0.06	0.06	0.04	0.01	
0.150	0.07	0.07	0.06	0.06	0.05	0.05	0.04	0.01	
0.200	0.05	0.05	0.04	0.04	0.04	0.03	0.03	0.01	
0.250	0.03	0.03	0.02	0.01	0.02	0.02	0.02	0.01	
0.300	0.02	0.02	0.01	0.00	0.01	0.01	0.01	0.01	
0.350	0.02	0.01	0.00	0.00	0.01	0.01	0.01	0.01	
0.400	0.02	0.01	0.00	0.00	0.00	0.00	0.01	0.01	
0.450	0.01	0.01	0.00	0.00	0.00	0.00	0.01	0.01	
0.500	0.01	0.01	0.00	0.00	0.00	0.00	0.01	0.01	
0.550	0.01	0.01	0.00	0.00	0.00	0.00	0.01	0.01	
0.600	0.02	0.01	0.00	0.00	0.00	0.00	0.00	0.01	
0.650	0.01	0.01	0.00	0.00	0.00	0.01	0.01	0.01	
0.700	0.02	0.01	0.00	0.00	0.01	0.01	0.01	0.01	
0.750	0.02	0.01	0.00	0.01	0.01	0.01	0.01	0.00	
0.800	0.02	0.01	0.00	0.01	0.01	0.01	0.01	0.00	
0.850	0.02	0.00	-0.01	0.01	0.01	0.01	0.02	0.00	
0.900	0.03	0.00	-0.01	0.01	0.01	0.01	0.01	-0.01	
0.950	0.03	0.00	-0.01	0.01	0.01	0.01	0.01	-0.01	

5% RAE 101. Values of  $C_p$  for  $R = 2.2 \times 10^6$  and  $\alpha = -2.08^\circ$ 

$x/c$ $\eta$	0.195	0.383	0.556	0.707	0.831	0.882	0.924	0.957	0.981
0.001	0.22	0.23	0.23	0.17	0.05	0.01	-0.04	-0.11	
0.003	0.24	0.25	0.24	0.20	0.10	0.05	-0.01	-0.06	
0.006	0.23	0.23	0.22	0.18	0.12	0.07	0.03	-0.04	
0.010	0.19	0.20	0.19	0.16	0.12	0.09	0.05	-0.02	
0.015	0.16	0.17	0.15	0.14	0.11	0.09	0.05	-0.01	
0.025	0.12	0.13	0.11	0.11	0.09	0.07	0.05	0.01	
0.035	0.09	0.10	0.09	0.08	0.07	0.06	0.05	0.01	
0.050	0.07	0.07	0.06	0.05	0.05	0.04	0.04	0.01	
0.075	0.04	0.04	0.03	0.03	0.03	0.03	0.02	0.01	
0.100	0.02	0.02	0.01	0.01	0.01	0.01	0.01	0.00	
0.125	0.01	0.01	0.00	0.00	0.00	0.00	0.00	0.00	
0.150	0.00	0.00	-0.01	-0.01	-0.01	-0.01	0.00	0.00	
0.200	-0.01	-0.01	-0.02	-0.02	-0.02	-0.02	-0.01	-0.01	
0.250	-0.02	-0.02	-0.03	-0.03	-0.03	-0.02	-0.02	-0.01	
0.300	-0.03	-0.03	-0.04	-0.03	-0.03	-0.03	-0.02	-0.02	
0.350	-0.02	-0.03	-0.04	-0.04	-0.03	-0.03	-0.02	-0.02	
0.400	-0.02	-0.03	-0.04	-0.04	-0.03	-0.03	-0.02	-0.02	
0.450	-0.02	-0.03	-0.04	-0.04	-0.03	-0.03	-0.02	-0.02	
0.500	-0.02	-0.02	-0.04	-0.04	-0.03	-0.03	-0.02	-0.01	
0.550	-0.02	-0.02	-0.03	-0.03	-0.02	-0.02	-0.01	-0.01	
0.600	-0.01	-0.02	-0.03	-0.03	-0.02	-0.01	-0.01	-0.01	
0.650	-0.01	-0.02	-0.03	-0.02	-0.01	-0.01	-0.01	-0.01	
0.700	0.00	-0.02	-0.02	-0.02	-0.01	-0.01	0.00	-0.01	
0.750	0.01	-0.01	-0.01	-0.01	-0.01	-0.01	0.00	0.00	
0.800	0.01	-0.01	-0.01	-0.01	0.00	-0.01	0.00	0.00	
0.850	0.02	0.00	-0.01	0.00	0.01	0.01	0.01	0.00	
0.900	0.02	0.00	-0.01	0.00	0.01	0.01	0.01	0.00	
0.950	0.03	0.01	-0.01	0.00	0.01	0.02	0.02	0.01	

TABLE 3—continued

5% RAE 101. Values of  $C_p$  for  $R = 2.2 \times 10^6$  and  $\alpha = 0^\circ$

$x/c$ $\eta$	0.195	0.383	0.556	0.707	0.831	0.882	0.924	0.957	0.981
0.001	0.21	0.20	0.17	0.15	0.12	0.08	0.05	0.05	
0.003	0.17	0.13	0.10	0.09	0.07	0.05	0.03	0.00	
0.006	0.10	0.06	0.04	0.01	0.04	0.02	0.02	0.00	
0.010	0.05	0.02	0.00	-0.01	0.01	0.01	-0.01	-0.01	
0.015	0.02	-0.01	-0.03	-0.03	-0.01	-0.01	-0.01	-0.01	
0.025	-0.01	-0.02	-0.04	-0.04	-0.03	-0.04	-0.03	-0.03	
0.035	-0.02	-0.04	-0.06	-0.05	-0.05	-0.05	-0.04	-0.04	
0.050	-0.04	-0.05	-0.07	-0.07	-0.06	-0.06	-0.05	-0.05	
0.075	-0.05	-0.07	-0.08	-0.08	-0.07	-0.07	-0.06	-0.05	
0.100	-0.06	-0.07	-0.08	-0.08	-0.07	-0.07	-0.06	-0.06	
0.125	-0.06	-0.07	-0.08	-0.08	-0.08	-0.07	-0.07	-0.06	
0.150	-0.07	-0.08	-0.09	-0.09	-0.08	-0.08	-0.07	-0.06	
0.200	-0.08	-0.08	-0.09	-0.09	-0.08	-0.08	-0.07	-0.06	
0.250	-0.08	-0.08	-0.09	-0.09	-0.08	-0.08	-0.07	-0.06	
0.300	-0.08	-0.08	-0.09	-0.09	-0.08	-0.07	-0.07	-0.06	
0.350	-0.07	-0.08	-0.08	-0.08	-0.08	-0.07	-0.06	-0.06	
0.400	-0.06	-0.07	-0.08	-0.08	-0.07	-0.06	-0.06	-0.05	
0.450	-0.06	-0.06	-0.07	-0.07	-0.06	-0.06	-0.05	-0.05	
0.500	-0.05	-0.06	-0.06	-0.07	-0.05	-0.05	-0.04	-0.04	
0.550	-0.04	-0.05	-0.06	-0.06	-0.05	-0.05	-0.04	-0.04	
0.600	-0.03	-0.04	-0.05	-0.05	-0.04	-0.04	-0.03	-0.03	
0.650	-0.02	-0.03	-0.04	-0.03	-0.03	-0.03	-0.02	-0.02	
0.700	-0.01	-0.02	-0.03	-0.03	-0.02	-0.02	-0.01	-0.01	
0.750	-0.01	-0.02	-0.02	-0.02	-0.01	-0.01	-0.01	0.00	
0.800	0.00	-0.02	-0.02	-0.02	-0.01	0.00	0.00	0.00	
0.850	0.01	-0.01	-0.02	-0.01	0.00	0.00	0.01	0.00	
0.900	0.01	-0.01	-0.02	-0.01	0.00	0.01	0.01	0.01	
0.950	0.02	0.00	-0.01	0.00	0.01	0.02	0.02	0.02	

5% RAE 101. Values of  $C_p$  for  $R = 2.2 \times 10^6$  and  $\alpha = 2.08^\circ$

$x/c$ $\eta$	0.195	0.383	0.556	0.707	0.831	0.882	0.924	0.957	0.981
0.001	-0.03	-0.15	-0.21	-0.19	-0.10	-0.14	-0.20	-0.16	-0.35
0.003	-0.10	-0.24	-0.30	-0.27	-0.26	-0.22	-0.23	-0.22	-0.34
0.006	-0.16	-0.29	-0.33	-0.35	-0.30	-0.30	-0.23	-0.23	
0.010	-0.20	-0.29	-0.34	-0.34	-0.29	-0.28	-0.27	-0.24	-0.33
0.015	-0.19	-0.27	-0.32	-0.30	-0.27	-0.28	-0.26	-0.24	
0.025	-0.18	-0.24	-0.27	-0.26	-0.25	-0.26	-0.25	-0.25	
0.035	-0.17	-0.22	-0.25	-0.24	-0.24	-0.24	-0.24	-0.24	
0.050	-0.17	-0.21	-0.23	-0.23	-0.22	-0.22	-0.22	-0.22	-0.33
0.075	-0.16	-0.19	-0.21	-0.21	-0.20	-0.20	-0.20	-0.20	-0.32
0.100	-0.16	-0.18	-0.19	-0.19	-0.19	-0.18	-0.19	-0.20	-0.32
0.125	-0.15	-0.17	-0.18	-0.18	-0.18	-0.18	-0.18	-0.18	-0.31
0.150	-0.15	-0.16	-0.17	-0.17	-0.17	-0.17	-0.17	-0.16	-0.29
0.200	-0.14	-0.15	-0.16	-0.16	-0.16	-0.15	-0.15	-0.14	-0.29
0.250	-0.13	-0.14	-0.15	-0.15	-0.15	-0.14	-0.14	-0.12	-0.28
0.300	-0.13	-0.13	-0.14	-0.15	-0.14	-0.12	-0.12	-0.12	-0.27
0.350	-0.12	-0.12	-0.13	-0.13	-0.12	-0.11	-0.11	-0.10	-0.29
0.400	-0.10	-0.10	-0.11	-0.11	-0.10	-0.10	-0.09	-0.10	-0.27
0.450	-0.09	-0.09	-0.10	-0.10	-0.09	-0.08	-0.08	-0.08	-0.29
0.500	-0.06	-0.08	-0.09	-0.09	-0.08	-0.08	-0.07	-0.06	-0.31
0.550	-0.06	-0.07	-0.08	-0.08	-0.07	-0.07	-0.06	-0.05	-0.32
0.600	-0.05	-0.06	-0.07	-0.07	-0.06	-0.05	-0.06	-0.04	-0.31
0.650	-0.05	-0.05	-0.06	-0.05	-0.05	-0.05	-0.04	-0.03	-0.29
0.700	-0.03	-0.05	-0.05	-0.05	-0.04	-0.04	-0.03	-0.02	-0.27
0.750	-0.02	-0.04	-0.04	-0.04	-0.03	-0.03	-0.02	-0.02	-0.23
0.800	-0.02	-0.03	-0.03	-0.03	-0.02	-0.01	-0.01	-0.01	-0.21
0.850	0.00	-0.02	-0.03	-0.02	-0.01	-0.01	0.00	0.00	-0.18
0.900	0.01	-0.01	-0.02	-0.01	-0.01	0.00	0.00	0.00	-0.16
0.950	0.02	0.00	-0.01	0.00	0.01	0.01	0.01	0.01	-0.14



TABLE 3—continued

5% RAE 101. Values of  $C_p$  for  $R = 2.2 \times 10^6$  and  $\alpha = 4.16^\circ$

$x/c$ $\eta$	0.195	0.383	0.556	0.707	0.831	0.882	0.924	0.957	0.981
0.001	-0.50	-0.81	-0.92	-0.83	-0.61	-0.66	-0.75	-0.61	-0.22
0.003	-0.55	-0.81	-0.93	-0.85	-0.82	-0.71	-0.72	-0.56	-0.22
0.006	-0.56	-0.77	-0.84	-0.82	-0.77	-0.77	-0.69	-0.55	
0.010	-0.53	-0.69	-0.77	-0.75	-0.70	-0.69	-0.64	-0.52	-0.22
0.015	-0.48	-0.66	-0.74	-0.73	-0.69	-0.66	-0.62	-0.51	
0.025	-0.42	-0.65	-0.71	-0.67	-0.69	-0.67	-0.62	-0.51	
0.035	-0.39	-0.38	-0.42	-0.41	-0.44	-0.64	-0.62	-0.51	
0.050	-0.32	-0.37	-0.40	-0.40	-0.39	-0.38	-0.60	-0.51	-0.23
0.075	-0.27	-0.33	-0.35	-0.35	-0.35	-0.35	-0.35	-0.49	-0.20
0.100	-0.25	-0.29	-0.31	-0.31	-0.31	-0.31	-0.31	-0.47	-0.20
0.125	-0.23	-0.27	-0.28	-0.28	-0.28	-0.28	-0.29	-0.46	-0.19
0.150	-0.22	-0.25	-0.26	-0.27	-0.26	-0.27	-0.27	-0.45	-0.18
0.200	-0.19	-0.22	-0.24	-0.24	-0.23	-0.23	-0.24	-0.41	-0.18
0.250	-0.19	-0.20	-0.21	-0.21	-0.21	-0.21	-0.21	-0.35	-0.18
0.300	-0.18	-0.18	-0.20	-0.20	-0.19	-0.18	-0.18	-0.28	-0.15
0.350	-0.16	-0.16	-0.17	-0.17	-0.17	-0.17	-0.16	-0.20	-0.10
0.400	-0.14	-0.14	-0.15	-0.15	-0.14	-0.14	-0.14	-0.14	-0.09
0.450	-0.12	-0.13	-0.13	-0.13	-0.12	-0.12	-0.12	-0.09	-0.08
0.500	-0.10	-0.11	-0.11	-0.11	-0.11	-0.11	-0.10	-0.08	-0.06
0.550	-0.09	-0.10	-0.10	-0.10	-0.09	-0.09	-0.09	-0.06	-0.06
0.600	-0.08	-0.08	-0.09	-0.09	-0.08	-0.08	-0.08	-0.06	-0.04
0.650	-0.06	-0.07	-0.07	-0.07	-0.07	-0.07	-0.06	-0.05	
0.700	-0.05	-0.06	-0.06	-0.06	-0.06	-0.05	-0.04	-0.04	
0.750	-0.04	-0.05	-0.05	-0.05	-0.04	-0.04	-0.04	-0.03	
0.800	-0.03	-0.04	-0.04	-0.04	-0.03	-0.03	-0.03	-0.03	
0.850	-0.02	-0.03	-0.03	-0.03	-0.03	-0.02	-0.02	-0.03	
0.900	0.00	-0.02	-0.03	-0.01	-0.01	-0.01	-0.02	-0.03	
0.950	0.01	-0.01	-0.01	-0.01	0.00	0.00	-0.01	-0.03	

5% RAE 101. Values of  $C_p$  for  $R = 2.2 \times 10^6$  and  $\alpha = 5.20^\circ$

$x/c$ $\eta$	0.195	0.383	0.556	0.707	0.831	0.882	0.924	0.957	0.981
0.001	-0.78	-1.19	-1.26	-1.02	-0.67	-0.57	-0.41	-0.41	-0.19
0.003	-0.80	-1.12	-1.16	-0.93	-0.69	-0.53	-0.41	-0.35	-0.19
0.006	-0.75	-1.00	-1.09	-0.87	-0.64	-0.52	-0.41	-0.35	
0.010	-0.69	-0.96	-1.07	-0.88	-0.64	-0.51	-0.41	-0.35	-0.21
0.015	-0.65	-0.96	-1.10	-0.89	-0.64	-0.52	-0.41	-0.35	
0.025	-0.65	-0.60	-0.68	-0.76	-0.63	-0.51	-0.41	-0.35	
0.035	-0.39	-0.52	-0.57	-0.64	-0.61	-0.51	-0.40	-0.35	
0.050	-0.38	-0.47	-0.50	-0.53	-0.58	-0.49	-0.39	-0.34	-0.18
0.075	-0.33	-0.40	-0.42	-0.43	-0.53	-0.48	-0.38	-0.34	-0.18
0.100	-0.30	-0.35	-0.37	-0.37	-0.49	-0.47	-0.37	-0.34	-0.18
0.125	-0.27	-0.32	-0.33	-0.33	-0.45	-0.47	-0.36	-0.34	-0.17
0.150	-0.26	-0.29	-0.31	-0.31	-0.39	-0.47	-0.35	-0.34	-0.17
0.200	-0.23	-0.26	-0.27	-0.27	-0.34	-0.46	-0.33	-0.33	-0.16
0.250	-0.21	-0.23	-0.24	-0.24	-0.25	-0.40	-0.32	-0.33	-0.15
0.300	-0.20	-0.21	-0.22	-0.22	-0.21	-0.33	-0.32	-0.31	-0.15
0.350	-0.17	-0.18	-0.19	-0.19	-0.18	-0.24	-0.32	-0.28	-0.14
0.400	-0.15	-0.16	-0.17	-0.17	-0.16	-0.18	-0.32	-0.27	-0.14
0.450	-0.13	-0.14	-0.15	-0.15	-0.14	-0.13	-0.31	-0.25	-0.12
0.500	-0.10	-0.12	-0.13	-0.13	-0.12	-0.10	-0.28	-0.25	-0.11
0.550	-0.09	-0.11	-0.11	-0.11	-0.10	-0.08	-0.25	-0.25	-0.10
0.600	-0.08	-0.09	-0.10	-0.09	-0.08	-0.07	-0.23	-0.26	-0.08
0.650	-0.07	-0.08	-0.09	-0.08	-0.07	-0.06	-0.18	-0.25	-0.08
0.700	-0.06	-0.07	-0.07	-0.06	-0.06	-0.05	-0.14	-0.24	-0.07
0.750	-0.04	-0.06	-0.06	-0.05	-0.05	-0.05	-0.12	-0.24	-0.06
0.800	-0.03	-0.05	-0.05	-0.04	-0.04	-0.03	-0.10	-0.22	-0.06
0.850	-0.02	-0.04	-0.04	-0.03	-0.03	-0.03	-0.07	-0.20	-0.06
0.900	-0.01	-0.03	-0.03	-0.02	-0.02	-0.02	-0.07	-0.19	-0.08
0.950	0.01	-0.02	-0.02	-0.01	-0.01	-0.01	-0.05	-0.16	-0.10

TABLE 3—continued

5% RAE 101. Values of  $C_p$  for  $R = 2.2 \times 10^6$  and  $\alpha = 5.73^\circ$

$x/c$	$\eta$	0.195	0.383	0.556	0.707	0.831	0.882	0.924	0.957	0.981
0.001		-0.93	-1.37	-1.15	-0.79	-0.56	-0.42	-0.33	-0.30	-0.15
0.003		-0.95	-1.24	-1.11	-0.74	-0.51	-0.41	-0.33	-0.26	
0.006		-0.86	-1.15	-1.10	-0.74	-0.50	-0.41	-0.33	-0.26	
0.010		-0.79	-1.13	-1.10	-0.74	-0.51	-0.41	-0.33	-0.26	-0.15
0.015		-0.77	-1.17	-1.09	-0.74	-0.51	-0.41	-0.33	-0.26	
0.025		-0.69	-0.67	-0.98	-0.74	-0.51	-0.41	-0.33	-0.26	
0.035		-0.44	-0.59	-0.89	-0.72	-0.50	-0.41	-0.32	-0.26	
0.050		-0.42	-0.52	-0.72	-0.71	-0.50	-0.40	-0.31	-0.25	-0.14
0.075		-0.36	-0.45	-0.51	-0.69	-0.48	-0.39	-0.30	-0.25	-0.13
0.100		-0.33	-0.39	-0.41	-0.64	-0.48	-0.39	-0.30	-0.24	-0.13
0.125		-0.30	-0.35	-0.36	-0.55	-0.47	-0.39	-0.29	-0.24	-0.12
0.150		-0.27	-0.32	-0.33	-0.31	-0.46	-0.39	-0.29	-0.23	-0.12
0.200		-0.25	-0.28	-0.29	-0.29	-0.46	-0.39	-0.28	-0.23	-0.12
0.250		-0.23	-0.25	-0.25	-0.24	-0.44	-0.41	-0.27	-0.22	-0.11
0.300		-0.21	-0.22	-0.23	-0.21	-0.41	-0.41	-0.26	-0.21	-0.11
0.350		-0.18	-0.20	-0.20	-0.18	-0.36	-0.43	-0.25	-0.20	-0.10
0.400		-0.16	-0.17	-0.17	-0.16	-0.30	-0.43	-0.25	-0.19	-0.09
0.450		-0.14	-0.15	-0.15	-0.14	-0.24	-0.41	-0.25	-0.18	-0.08
0.500		-0.12	-0.13	-0.13	-0.12	-0.19	-0.39	-0.26	-0.17	-0.07
0.550		-0.11	-0.12	-0.11	-0.11	-0.14	-0.35	-0.29	-0.16	-0.06
0.600		-0.09	-0.10	-0.10	-0.09	-0.10	-0.30	-0.31	-0.15	-0.06
0.650		-0.08	-0.09	-0.08	-0.08	-0.07	-0.25	-0.31	-0.15	-0.05
0.700		-0.06	-0.08	-0.07	-0.06	-0.06	-0.20	-0.31	-0.15	-0.05
0.750		-0.04	-0.07	-0.06	-0.05	-0.03	-0.14	-0.30	-0.16	-0.04
0.800		-0.03	-0.05	-0.05	-0.04	-0.02	-0.10	-0.28	-0.16	-0.05
0.850		-0.02	-0.04	-0.05	-0.03	-0.01	-0.07	-0.24	-0.18	-0.06
0.900		-0.01	-0.03	-0.04	-0.02	-0.01	-0.05	-0.22	-0.19	-0.09
0.950		0.01	-0.02	-0.03	-0.01	0.01	-0.02	-0.19	-0.21	-0.12

5% RAE 101. Values of  $C_p$  for  $R = 2.2 \times 10^6$  and  $\alpha = 6.25^\circ$

$x/c$	$\eta$	0.195	0.383	0.556	0.707	0.831	0.882	0.924	0.957	0.981
0.001		-1.11	-1.18	-0.99	-0.65	-0.48	-0.36	-0.28	-0.24	-0.12
0.003		-1.09	-1.15	-0.98	-0.64	-0.46	-0.35	-0.28	-0.21	
0.006		-0.97	-1.15	-0.98	-0.64	-0.46	-0.35	-0.28	-0.21	
0.010		-0.92	-1.15	-0.97	-0.64	-0.47	-0.35	-0.29	-0.22	-0.12
0.015		-0.93	-1.09	-0.97	-0.64	-0.47	-0.35	-0.28	-0.22	
0.025		-0.63	-0.97	-0.96	-0.63	-0.46	-0.35	-0.28	-0.21	
0.035		-0.50	-0.87	-0.96	-0.63	-0.46	-0.34	-0.27	-0.20	
0.050		-0.46	-0.72	-0.94	-0.62	-0.46	-0.34	-0.27	-0.19	-0.11
0.075		-0.40	-0.54	-0.83	-0.62	-0.45	-0.34	-0.26	-0.19	-0.10
0.100		-0.36	-0.45	-0.67	-0.63	-0.44	-0.33	-0.26	-0.19	-0.10
0.125		-0.32	-0.40	-0.55	-0.64	-0.44	-0.33	-0.26	-0.18	-0.10
0.150		-0.30	-0.36	-0.45	-0.65	-0.44	-0.33	-0.25	-0.18	-0.10
0.200		-0.27	-0.31	-0.31	-0.61	-0.45	-0.32	-0.25	-0.17	-0.09
0.250		-0.24	-0.27	-0.23	-0.51	-0.46	-0.32	-0.25	-0.17	-0.08
0.300		-0.22	-0.24	-0.21	-0.39	-0.46	-0.32	-0.25	-0.17	-0.08
0.350		-0.20	-0.21	-0.18	-0.27	-0.47	-0.33	-0.24	-0.16	-0.08
0.400		-0.17	-0.18	-0.16	-0.18	-0.47	-0.34	-0.23	-0.15	-0.07
0.450		-0.15	-0.16	-0.14	-0.13	-0.46	-0.36	-0.23	-0.14	-0.06
0.500		-0.13	-0.14	-0.12	-0.10	-0.43	-0.39	-0.22	-0.12	-0.06
0.550		-0.12	-0.12	-0.10	-0.08	-0.38	-0.41	-0.23	-0.11	-0.06
0.600		-0.10	-0.10	-0.09	-0.07	-0.31	-0.42	-0.25	-0.10	-0.05
0.650		-0.08	-0.09	-0.08	-0.06	-0.24	-0.41	-0.27	-0.10	-0.06
0.700		-0.06	-0.08	-0.06	-0.04	-0.19	-0.39	-0.28	-0.09	-0.06
0.750		-0.04	-0.07	-0.05	-0.04	-0.10	-0.36	-0.31	-0.09	-0.06
0.800		-0.04	-0.05	-0.04	-0.03	-0.06	-0.31	-0.31	-0.10	-0.08
0.850		-0.02	-0.05	-0.03	-0.02	-0.03	-0.26	-0.29	-0.12	-0.10
0.900		-0.01	-0.04	-0.03	-0.01	-0.01	-0.21	-0.29	-0.16	-0.12
0.950		0.01	-0.03	-0.02	0.00	0.01	-0.15	-0.28	-0.23	-0.14

TABLE 3—continued

5% RAE 101. Values of  $C_p$  for  $R = 2.2 \times 10^6$  and  $\alpha = 8.37^\circ$

$x/c$ $\eta$	0.195	0.383	0.556	0.707	0.831	0.882	0.924	0.957	0.981
0.001	-1.40	-0.84	-0.63	-0.47	-0.32	-0.24	-0.16	-0.10	-0.08
0.003	-1.39	-0.84	-0.63	-0.47	-0.32	-0.24	-0.16	-0.10	
0.006	-1.39	-0.84	-0.63	-0.47	-0.32	-0.24	-0.16	-0.10	
0.010	-1.37	-0.84	-0.63	-0.47	-0.32	-0.24	-0.16	-0.10	-0.08
0.015	-1.29	-0.83	-0.63	-0.47	-0.31	-0.23	-0.16	-0.10	
0.025	-1.22	-0.83	-0.62	-0.47	-0.31	-0.23	-0.15	-0.09	
0.035	-1.15	-0.83	-0.63	-0.47	-0.31	-0.22	-0.15	-0.09	
0.050	-1.00	-0.82	-0.63	-0.47	-0.31	-0.22	-0.14	-0.09	-0.08
0.075	-0.70	-0.83	-0.63	-0.46	-0.30	-0.22	-0.14	-0.09	-0.08
0.100	-0.52	-0.84	-0.64	-0.47	-0.30	-0.22	-0.14	-0.09	-0.08
0.125	-0.40	-0.86	-0.64	-0.47	-0.30	-0.22	-0.14	-0.09	-0.08
0.150	-0.36	-0.88	-0.65	-0.47	-0.30	-0.22	-0.14	-0.09	-0.08
0.200	-0.33	-0.87	-0.67	-0.48	-0.32	-0.22	-0.14	-0.09	-0.08
0.250	-0.31	-0.77	-0.71	-0.48	-0.31	-0.22	-0.14	-0.09	-0.09
0.300	-0.29	-0.59	-0.74	-0.50	-0.31	-0.22	-0.14	-0.10	-0.09
0.350	-0.25	-0.39	-0.74	-0.53	-0.30	-0.21	-0.14	-0.10	-0.10
0.400	-0.22	-0.24	-0.72	-0.56	-0.29	-0.20	-0.13	-0.10	-0.10
0.450	-0.20	-0.16	-0.65	-0.58	-0.28	-0.18	-0.12	-0.10	-0.10
0.500	-0.17	-0.11	-0.56	-0.59	-0.29	-0.17	-0.12	-0.10	-0.11
0.550	-0.15	-0.09	-0.44	-0.59	-0.30	-0.16	-0.12	-0.10	-0.11
0.600	-0.13	-0.08	-0.31	-0.56	-0.33	-0.16	-0.12	-0.11	-0.11
0.650	-0.12	-0.08	-0.19	-0.52	-0.36	-0.16	-0.12	-0.12	-0.12
0.700	-0.10	-0.07	-0.09	-0.46	-0.39	-0.17	-0.12	-0.13	-0.12
0.750	-0.08	-0.06	-0.04	-0.39	-0.41	-0.20	-0.14	-0.14	-0.12
0.800	-0.06	-0.05	-0.01	-0.31	-0.41	-0.23	-0.16	-0.15	-0.12
0.850	-0.05	-0.04	0.00	-0.23	-0.40	-0.26	-0.19	-0.16	-0.12
0.900	-0.04	-0.03	0.01	-0.17	-0.36	-0.33	-0.22	-0.16	-0.11
0.950	-0.03	-0.02	0.01	-0.11	-0.54	-0.51	-0.24	-0.15	-0.10

TABLE 4

Pressure Distributions on 5% Wing at  $R = 2.8 \times 10^6$ 5% RAE 101. Values of  $C_p$  for  $R = 2.8 \times 10^6$  and  $\alpha = -8.35^\circ$ 

$x/c$	$\eta$	0.195	0.383	0.556	0.707	0.831	0.882	0.924	0.957	0.981
0.001		-0.88	-1.06	-0.59	-0.50	-0.51	-0.37	-0.29	-0.28	
0.003		-0.54	-0.56	-0.31	-0.27	-0.39	-0.30	-0.26	-0.22	
0.006		-0.12	-0.16	-0.06	-0.08	-0.22	-0.24	-0.20	-0.20	
0.010		0.09	0.06	0.11	0.07	-0.08	-0.13	-0.12	-0.18	
0.015		0.19	0.19	0.20	0.16	0.01	-0.04	-0.08	-0.14	
0.025		0.26	0.26	0.26	0.20	0.10	0.04	-0.02	-0.10	
0.035		0.26	0.27	0.26	0.21	0.13	0.08	0.01	-0.06	
0.050		0.25	0.26	0.26	0.21	0.14	0.10	0.05	-0.02	
0.075		0.24	0.25	0.24	0.20	0.15	0.11	0.07	0.01	
0.100		0.21	0.22	0.20	0.18	0.14	0.11	0.07	0.02	
0.125		0.19	0.20	0.19	0.16	0.13	0.10	0.07	0.03	
0.150		0.18	0.19	0.17	0.14	0.12	0.10	0.07	0.03	
0.200		0.15	0.15	0.15	0.12	0.10	0.09	0.07	0.03	
0.250		0.14	0.13	0.12	0.10	0.09	0.07	0.06	0.03	
0.300		0.11	0.11	0.09	0.08	0.07	0.06	0.05	0.02	
0.350		0.10	0.10	0.07	0.07	0.06	0.05	0.03	0.02	
0.400		0.09	0.09	0.07	0.06	0.05	0.04	0.03	0.01	
0.450		0.09	0.08	0.07	0.05	0.05	0.04	0.02	0.01	
0.500		0.08	0.07	0.05	0.05	0.04	0.03	0.01	0.00	
0.550		0.08	0.07	0.05	0.04	0.04	0.02	0.01	0.00	
0.600		0.07	0.06	0.04	0.03	0.03	0.01	0.00	-0.01	
0.650		0.07	0.05	0.03	0.03	0.02	0.00	-0.01	-0.02	
0.700		0.07	0.05	0.03	0.03	0.02	-0.01	-0.02	-0.02	
0.750		0.07	0.04	0.03	0.03	0.01	-0.01	-0.03	-0.03	
0.800		0.06	0.04	0.03	0.03	0.00	-0.03	-0.04	-0.04	
0.850		0.06	0.03	0.01	0.02	-0.02	-0.06	-0.06	-0.06	
0.900		0.05	0.02	0.01	0.01	-0.04	-0.09	-0.09	-0.08	
0.950		0.04	0.01	-0.01	0.00	-0.08	-0.14	-0.15	-0.09	

5% RAE 101. Values of  $C_p$  for  $R = 2.8 \times 10^6$  and  $\alpha = 8.35^\circ$ 

$x/c$	$\eta$	0.195	0.383	0.556	0.707	0.831	0.882	0.924	0.957	0.981
0.001		-2.04	-1.14	-0.93	-0.62	-0.48	-0.32	-0.22	-0.21	
0.003		-1.91	-1.11	-0.92	-0.61	-0.45	-0.31	-0.22	-0.14	
0.006		-1.81	-1.05	-0.90	-0.60	-0.42	-0.31	-0.22	-0.14	
0.010		-1.57	-1.00	-0.88	-0.59	-0.41	-0.30	-0.22	-0.14	
0.015		-1.11	-0.94	-0.87	-0.58	-0.40	-0.29	-0.22	-0.14	
0.025		-0.88	-0.88	-0.86	-0.56	-0.40	-0.29	-0.21	-0.13	
0.035		-0.78	-0.83	-0.87	-0.57	-0.41	-0.29	-0.22	-0.14	
0.050		-0.67	-0.77	-0.88	-0.57	-0.41	-0.29	-0.21	-0.14	
0.075		-0.54	-0.69	-0.88	-0.56	-0.40	-0.28	-0.20	-0.13	
0.100		-0.48	-0.64	-0.90	-0.57	-0.40	-0.29	-0.21	-0.13	
0.125		-0.43	-0.59	-0.92	-0.56	-0.40	-0.29	-0.21	-0.13	
0.150		-0.39	-0.54	-0.95	-0.58	-0.39	-0.29	-0.20	-0.12	
0.200		-0.35	-0.49	-0.88	-0.60	-0.39	-0.29	-0.20	-0.12	
0.250		-0.30	-0.43	-0.77	-0.62	-0.40	-0.29	-0.20	-0.12	
0.300		-0.28	-0.37	-0.53	-0.67	-0.40	-0.29	-0.20	-0.12	
0.350		-0.24	-0.32	-0.29	-0.71	-0.40	-0.29	-0.19	-0.10	
0.400		-0.22	-0.27	-0.12	-0.68	-0.41	-0.28	-0.18	-0.10	
0.450		-0.18	-0.23	-0.08	-0.65	-0.44	-0.26	-0.16	-0.09	
0.500		-0.17	-0.20	-0.07	-0.57	-0.49	-0.27	-0.15	-0.09	
0.550		-0.14	-0.17	-0.06	-0.46	-0.52	-0.27	-0.14	-0.08	
0.600		-0.12	-0.15	-0.06	-0.34	-0.54	-0.29	-0.13	-0.09	
0.650		-0.11	-0.13	-0.05	-0.24	-0.53	-0.31	-0.12	-0.09	
0.700		-0.09	-0.11	-0.04	-0.14	-0.52	-0.33	-0.13	-0.10	
0.750		-0.07	-0.09	-0.03	-0.08	-0.47	-0.35	-0.14	-0.11	
0.800		-0.05	-0.07	-0.03	-0.04	-0.42	-0.35	-0.16	-0.14	
0.850		-0.04	-0.06	-0.03	-0.02	-0.37	-0.35	-0.20	-0.19	
0.900		-0.02	-0.05	-0.03	-0.00	-0.31	-0.34	-0.28	-0.23	
0.950		-0.01	-0.04	-0.02	-0.01	-0.26	-0.40	-0.41	-0.25	

TABLE 5

Pressure Distributions on 5% Wing at  $R = 3.3 \times 10^6$ 

5% RAE 101. Values of  $C_p$  for  $R = 3.3 \times 10^6$  and  $\alpha = -8.34^\circ$

$x/c$ $\eta$	0.195	0.383	0.556	0.707	0.831	0.882	0.924	0.957	0.981
0.001	-0.86	-1.35	-1.30	-1.23	-1.45	-1.26	-0.71	-0.64	
0.003	-0.53	-0.68	-0.67	-0.74	-1.16	-0.98	-0.64	-0.47	
0.006	-0.11	-0.26	-0.27	-0.37	-0.73	-0.82	-0.52	-0.45	
0.010	0.10	0.10	0.00	-0.09	-0.41	-0.53	-0.36	-0.41	
0.015	0.20	0.17	0.14	0.07	-0.18	-0.31	-0.29	-0.36	
0.025	0.26	0.25	0.24	0.17	-0.01	-0.10	-0.16	-0.26	
0.035	0.26	0.26	0.26	0.20	0.06	-0.01	-0.08	-0.18	
0.050	0.25	0.26	0.26	0.21	0.11	0.05	0.00	-0.11	
0.075	0.24	0.25	0.24	0.20	0.13	0.10	0.05	-0.04	
0.100	0.21	0.22	0.21	0.18	0.13	0.10	0.06	-0.01	
0.125	0.19	0.20	0.20	0.17	0.13	0.10	0.07	0.01	
0.150	0.18	0.18	0.18	0.15	0.12	0.10	0.07	0.01	
0.200	0.14	0.15	0.15	0.13	0.11	0.10	0.08	0.03	
0.250	0.13	0.13	0.12	0.11	0.09	0.09	0.07	0.04	
0.300	0.11	0.11	0.10	0.09	0.08	0.07	0.06	0.03	
0.350	0.10	0.10	0.08	0.07	0.07	0.06	0.05	0.03	
0.400	0.09	0.09	0.07	0.06	0.06	0.05	0.05	0.03	
0.450	0.09	0.08	0.07	0.06	0.06	0.05	0.05	0.03	
0.500	0.08	0.07	0.06	0.05	0.05	0.04	0.04	0.03	
0.550	0.08	0.07	0.05	0.04	0.05	0.04	0.04	0.03	
0.600	0.07	0.06	0.04	0.04	0.04	0.03	0.03	0.01	
0.650	0.06	0.05	0.04	0.04	0.04	0.03	0.02	0.01	
0.700	0.07	0.05	0.04	0.03	0.04	0.02	0.02	0.00	
0.750	0.07	0.04	0.04	0.03	0.03	0.02	0.01	0.00	
0.800	0.06	0.04	0.03	0.03	0.03	0.01	0.00	-0.01	
0.850	0.06	0.03	0.02	0.02	0.02	0.00	0.00	-0.04	
0.900	0.05	0.02	0.01	0.02	0.01	-0.01	-0.03	-0.07	
0.950	0.04	0.01	0.00	-0.01	-0.01	-0.03	-0.06	-0.09	

5% RAE 101. Values of  $C_p$  for  $R = 3.3 \times 10^6$  and  $\alpha = 8.34^\circ$ 

$x/c$ $\eta$	0.195	0.383	0.556	0.707	0.831	0.882	0.924	0.957	0.981
0.001	-2.10	-2.29	-2.22	-1.55	-0.98	-0.53	-0.35	-0.33	
0.003	-1.98	-2.02	-1.91	-1.45	-0.82	-0.51	-0.35	-0.25	
0.006	-1.82	-1.74	-1.68	-1.30	-0.70	-0.50	-0.34	-0.23	
0.010	-1.59	-1.51	-1.49	-1.11	-0.65	-0.49	-0.34	-0.24	
0.015	-1.15	-1.29	-1.34	-0.96	-0.63	-0.48	-0.33	-0.22	
0.025	-0.90	-1.09	-1.14	-0.85	-0.62	-0.47	-0.33	-0.23	
0.035	-0.78	-0.97	-1.06	-0.79	-0.62	-0.47	-0.33	-0.24	
0.050	-0.65	-0.85	-0.97	-0.74	-0.62	-0.47	-0.33	-0.23	
0.075	-0.54	-0.71	-0.86	-0.68	-0.60	-0.47	-0.32	-0.23	
0.100	-0.48	-0.62	-0.80	-0.64	-0.60	-0.47	-0.32	-0.23	
0.125	-0.43	-0.55	-0.72	-0.61	-0.60	-0.47	-0.32	-0.22	
0.150	-0.39	-0.49	-0.66	-0.59	-0.60	-0.47	-0.31	-0.22	
0.200	-0.34	-0.41	-0.45	-0.56	-0.59	-0.48	-0.30	-0.22	
0.250	-0.30	-0.35	-0.42	-0.52	-0.59	-0.48	-0.30	-0.21	
0.300	-0.28	-0.32	-0.33	-0.50	-0.55	-0.51	-0.29	-0.20	
0.350	-0.24	-0.26	-0.26	-0.46	-0.49	-0.50	-0.29	-0.19	
0.400	-0.21	-0.23	-0.20	-0.42	-0.42	-0.48	-0.29	-0.17	
0.450	-0.18	-0.19	-0.16	-0.38	-0.37	-0.46	-0.29	-0.16	
0.500	-0.16	-0.17	-0.14	-0.32	-0.35	-0.44	-0.30	-0.15	
0.550	-0.14	-0.15	-0.11	-0.27	-0.32	-0.41	-0.30	-0.13	
0.600	-0.11	-0.13	-0.10	-0.22	-0.30	-0.38	-0.30	-0.13	
0.650	-0.10	-0.11	-0.09	-0.17	-0.28	-0.34	-0.29	-0.13	
0.700	-0.08	-0.09	-0.07	-0.13	-0.25	-0.31	-0.28	-0.14	
0.750	-0.06	-0.08	-0.06	-0.09	-0.22	-0.29	-0.28	-0.15	
0.800	-0.05	-0.07	-0.06	-0.07	-0.19	-0.26	-0.27	-0.15	
0.850	-0.03	-0.06	-0.05	-0.05	-0.16	-0.23	-0.26	-0.17	
0.900	-0.02	-0.05	-0.05	-0.05	-0.13	-0.21	-0.27	-0.20	
0.950	0.00	-0.04	-0.04	-0.02	-0.11	-0.19	-0.30	-0.22	

TABLE 6

Pressure Distributions on 5% Wing at  $R = 3.9 \times 10^6$ 

5% RAE 101. Values of  $C_p$  for  $R = 3.9 \times 10^6$  and  $\alpha = -8.33^\circ$

$x/c$	$\eta$	0.195	0.383	0.556	0.707	0.831	0.882	0.924	0.957	0.981
0.001		-0.86	-1.37	-1.40	-1.46	-1.74	-1.69	-0.98	-0.80	-0.32
0.003		-0.52	-0.70	-0.73	-0.88	-1.37	-1.30	-0.86	-0.62	-0.34
0.006		-0.11	-0.26	-0.30	-0.45	-0.87	-1.08	-0.70	-0.57	
0.010	0.10	0.00	0.00	-0.02	-0.13	-0.50	-0.71	-0.48	-0.52	-0.36
0.015	0.20	0.16	0.14	0.06	0.06	-0.23	-0.42	-0.41	-0.46	
0.025	0.26	0.25	0.24	0.16	0.16	-0.04	-0.16	-0.24	-0.33	
0.035	0.26	0.25	0.26	0.19	0.19	0.04	-0.05	-0.14	-0.23	
0.050	0.25	0.25	0.26	0.20	0.20	0.09	0.03	-0.04	-0.14	-0.23
0.075	0.23	0.25	0.24	0.20	0.20	0.13	0.09	0.03	-0.06	-0.16
0.100	0.21	0.22	0.22	0.18	0.18	0.13	0.10	0.05	-0.03	-0.15
0.125	0.19	0.20	0.20	0.17	0.17	0.12	0.11	0.06	0.00	-0.10
0.150	0.18	0.19	0.18	0.15	0.15	0.12	0.11	0.07	0.01	-0.07
0.200	0.15	0.15	0.15	0.13	0.13	0.11	0.10	0.07	0.02	-0.04
0.250	0.13	0.13	0.12	0.11	0.11	0.09	0.09	0.07	0.04	-0.02
0.300	0.11	0.11	0.10	0.08	0.08	0.08	0.08	0.06	0.03	-0.01
0.350	0.10	0.10	0.08	0.07	0.06	0.06	0.07	0.05	0.03	0.00
0.400	0.09	0.09	0.08	0.06	0.06	0.06	0.06	0.05	0.03	0.00
0.450	0.09	0.08	0.07	0.05	0.05	0.06	0.06	0.04	0.04	0.01
0.500	0.08	0.07	0.06	0.05	0.05	0.05	0.05	0.04	0.03	0.01
0.550	0.08	0.06	0.06	0.04	0.04	0.04	0.04	0.03	0.03	0.01
0.600	0.07	0.06	0.05	0.04	0.04	0.04	0.04	0.03	0.02	0.00
0.650	0.06	0.05	0.04	0.03	0.03	0.03	0.03	0.03	0.02	-0.01
0.700	0.07	0.05	0.04	0.03	0.03	0.03	0.02	0.02	0.01	-0.01
0.750	0.06	0.04	0.04	0.03	0.03	0.03	0.02	0.01	0.00	-0.02
0.800	0.06	0.04	0.03	0.03	0.03	0.02	0.02	0.01	-0.01	-0.03
0.850	0.06	0.03	0.02	0.03	0.03	0.01	0.01	0.01	-0.03	-0.04
0.900	0.05	0.02	0.01	0.02	0.02	0.01	0.00	-0.01	-0.05	-0.06
0.950	0.04	0.00	0.00	0.01	0.01	-0.01	0.00	-0.03	-0.09	-0.10

5% RAE 101. Values of  $C_p$  for  $R = 3.9 \times 10^6$  and  $\alpha = -7.29^\circ$ 

$x/c$	$\eta$	0.195	0.383	0.556	0.707	0.831	0.882	0.924	0.957	0.981
0.001		-0.54	-0.92	-0.96	-1.05	-1.34	-1.37	-1.53	-1.00	
0.003		-0.28	-0.40	-0.43	-0.58	-1.03	-1.01	-1.25	-0.77	
0.006		0.03	-0.08	-0.11	-0.25	-0.62	-0.83	-0.93	-0.70	
0.010	0.17	0.11	0.10	0.10	-0.01	-0.33	-0.52	-0.61	-0.61	
0.015	0.24	0.22	0.20	0.12	0.12	-0.12	-0.30	-0.30	-0.51	
0.025	0.26	0.26	0.25	0.19	0.19	0.02	-0.09	-0.28	-0.35	
0.035	0.26	0.26	0.26	0.20	0.20	0.08	-0.01	-0.17	-0.23	
0.050	0.24	0.25	0.24	0.20	0.20	0.11	0.05	-0.06	-0.14	
0.075	0.21	0.23	0.22	0.19	0.13	0.13	0.08	0.02	-0.06	
0.100	0.19	0.20	0.19	0.16	0.12	0.12	0.09	0.04	-0.02	
0.125	0.17	0.18	0.17	0.15	0.11	0.11	0.09	0.05	0.00	
0.150	0.15	0.16	0.16	0.13	0.11	0.11	0.09	0.06	0.01	
0.200	0.13	0.13	0.13	0.11	0.09	0.09	0.08	0.06	0.02	
0.250	0.11	0.11	0.10	0.09	0.07	0.07	0.07	0.06	0.04	
0.300	0.09	0.09	0.08	0.07	0.06	0.06	0.06	0.06	0.03	
0.350	0.08	0.08	0.06	0.05	0.05	0.05	0.05	0.04	0.03	
0.400	0.08	0.07	0.06	0.05	0.05	0.05	0.04	0.05	0.03	
0.450	0.07	0.06	0.05	0.04	0.04	0.04	0.04	0.04	0.04	
0.500	0.07	0.05	0.04	0.03	0.03	0.03	0.03	0.04	0.03	
0.550	0.06	0.05	0.04	0.03	0.03	0.03	0.03	0.03	0.03	
0.600	0.06	0.04	0.03	0.03	0.03	0.03	0.03	0.02	0.02	
0.650	0.05	0.04	0.03	0.03	0.03	0.03	0.02	0.03	0.02	
0.700	0.06	0.04	0.03	0.03	0.03	0.03	0.02	0.03	0.02	
0.750	0.06	0.03	0.03	0.03	0.03	0.03	0.02	0.02	0.01	
0.800	0.05	0.03	0.02	0.02	0.02	0.02	0.02	0.02	0.01	
0.850	0.05	0.02	0.02	0.02	0.02	0.01	0.01	0.02	-0.01	
0.900	0.05	0.01	0.01	0.02	0.02	0.01	0.00	0.00	-0.02	
0.950	0.04	0.00	-0.01	0.01	0.01	0.00	-0.01	-0.01	-0.04	

TABLE 6—continued

5% RAE 101. Values of  $C_p$  for  $R = 3.9 \times 10^6$  and  $\alpha = -6.25^\circ$

$x/c$	$\eta$	0.195	0.383	0.556	0.707	0.831	0.882	0.924	0.957	0.981
0.001		-0.31	-0.57	-0.60	-0.70	-0.96	-0.99	-1.17	-1.19	
0.003		-0.11	-0.18	-0.20	-0.34	-0.70	-0.71	-0.94	-0.96	
0.006		0.12	0.06	0.03	-0.09	-0.39	-0.55	-0.68	-0.86	
0.010		0.21	0.18	0.17	0.08	-0.17	-0.33	-0.43	-0.73	
0.015		0.25	0.25	0.23	0.16	-0.03	-0.16	-0.35	-0.59	
0.025		0.25	0.27	0.26	0.20	0.07	-0.02	-0.18	-0.40	
0.035		0.24	0.25	0.25	0.20	0.10	0.04	-0.10	-0.27	
0.050		0.21	0.23	0.23	0.19	0.12	0.07	-0.01	-0.17	
0.075		0.19	0.20	0.19	0.17	0.12	0.09	0.03	-0.08	
0.100		0.16	0.17	0.17	0.14	0.11	0.09	0.04	-0.04	
0.125		0.14	0.15	0.15	0.13	0.10	0.08	0.05	-0.01	
0.150		0.13	0.13	0.13	0.11	0.09	0.08	0.05	0.00	
0.200		0.10	0.11	0.10	0.09	0.08	0.07	0.05	0.02	
0.250		0.08	0.09	0.08	0.07	0.06	0.06	0.05	0.03	
0.300		0.06	0.07	0.06	0.05	0.04	0.05	0.04	0.03	
0.350		0.06	0.06	0.05	0.04	0.03	0.04	0.03	0.03	
0.400		0.05	0.05	0.04	0.03	0.03	0.03	0.03	0.03	
0.450		0.05	0.05	0.04	0.03	0.03	0.03	0.03	0.03	
0.500		0.05	0.04	0.03	0.02	0.02	0.02	0.03	0.02	
0.550		0.05	0.04	0.03	0.02	0.02	0.02	0.03	0.03	
0.600		0.04	0.03	0.02	0.02	0.02	0.02	0.02	0.02	
0.650		0.04	0.03	0.02	0.02	0.02	0.02	0.02	0.02	
0.700		0.04	0.03	0.02	0.02	0.02	0.02	0.02	0.02	
0.750		0.04	0.02	0.02	0.02	0.02	0.02	0.02	0.02	
0.800		0.04	0.02	0.02	0.02	0.02	0.02	0.02	0.02	
0.850		0.04	0.02	0.01	0.02	0.01	0.02	0.02	0.01	
0.900		0.04	0.01	0.00	0.01	0.01	0.01	0.01	0.00	
0.950		0.03	0.00	-0.01	0.01	0.00	0.01	0.00	-0.01	

5% RAE 101. Values of  $C_p$  for  $R = 3.9 \times 10^6$  and  $\alpha = -5.20^\circ$

$x/c$	$\eta$	0.195	0.383	0.556	0.707	0.831	0.882	0.924	0.957	0.981
0.001		-0.10	-0.26	-0.27	-0.36	-0.55	-0.58	-0.61	-0.67	
0.003		0.04	0.01	0.00	-0.11	-0.36	-0.40	-0.48	-0.54	
0.006		0.19	0.16	0.15	0.06	-0.16	-0.28	-0.33	-0.46	
0.010		0.24	0.23	0.23	0.16	-0.03	-0.14	-0.19	-0.40	
0.015		0.25	0.26	0.25	0.20	0.06	-0.04	-0.14	-0.33	
0.025		0.24	0.25	0.25	0.20	0.11	0.04	-0.05	-0.21	
0.035		0.21	0.23	0.22	0.19	0.12	0.07	-0.01	-0.13	
0.050		0.18	0.20	0.19	0.17	0.12	0.08	0.03	-0.07	
0.075		0.15	0.16	0.16	0.14	0.11	0.09	0.05	-0.03	
0.100		0.12	0.14	0.13	0.12	0.10	0.08	0.05	-0.01	
0.125		0.11	0.12	0.11	0.10	0.08	0.07	0.05	0.01	
0.150		0.10	0.10	0.10	0.08	0.07	0.06	0.05	0.02	
0.200		0.07	0.07	0.08	0.06	0.05	0.05	0.04	0.02	
0.250		0.06	0.06	0.06	0.05	0.04	0.04	0.03	0.02	
0.300		0.04	0.04	0.03	0.03	0.03	0.03	0.02	0.02	
0.350		0.04	0.03	0.03	0.02	0.02	0.02	0.02	0.02	
0.400		0.04	0.03	0.02	0.01	0.02	0.02	0.02	0.02	
0.450		0.04	0.03	0.02	0.01	0.02	0.02	0.01	0.02	
0.500		0.03	0.02	0.01	0.01	0.01	0.01	0.01	0.01	
0.550		0.03	0.02	0.01	0.01	0.01	0.01	0.01	0.02	
0.600		0.03	0.02	0.01	0.01	0.01	0.01	0.01	0.01	
0.650		0.03	0.01	0.01	0.01	0.01	0.01	0.01	0.01	
0.700		0.03	0.01	0.01	0.01	0.01	0.01	0.01	0.01	
0.750		0.03	0.01	0.01	0.01	0.01	0.01	0.01	0.01	
0.800		0.03	0.01	0.01	0.01	0.01	0.01	0.01	0.01	
0.850		0.03	0.01	0.00	0.01	0.01	0.01	0.02	0.00	
0.900		0.03	0.01	0.00	0.01	0.01	0.01	0.01	-0.01	
0.950		0.03	-0.01	-0.02	0.01	0.00	0.00	0.00	-0.02	

TABLE 6—continued

5% RAE 101. Values of  $C_p$  for  $R = 3.9 \times 10^6$  and  $\alpha = -4.16^\circ$

$x/c$	$\eta$	0.195	0.383	0.556	0.707	0.831	0.882	0.924	0.957	0.981
0.001	0.05		-0.04	-0.04	-0.13	-0.33	-0.38	-0.48	-0.52	-0.68
0.003	0.15		0.14	0.14	0.04	-0.17	-0.23	-0.36	-0.47	-0.56
0.006	0.23		0.22	0.22	0.15	-0.03	-0.13	-0.23	-0.37	
0.010	0.25		0.25	0.25	0.19	0.05	-0.04	-0.11	-0.30	-0.46
0.015	0.24		0.25	0.24	0.20	0.10	0.02	-0.07	-0.23	
0.025	0.21		0.23	0.22	0.19	0.12	0.07	-0.01	-0.13	
0.035	0.18		0.20	0.19	0.17	0.12	0.08	0.02	-0.08	
0.050	0.15		0.16	0.16	0.14	0.11	0.08	0.05	-0.04	-0.20
0.075	0.12		0.13	0.13	0.11	0.09	0.07	0.05	-0.01	-0.13
0.100	0.10		0.10	0.10	0.09	0.07	0.06	0.05	0.00	-0.12
0.125	0.08		0.08	0.08	0.07	0.06	0.05	0.04	0.01	-0.07
0.150	0.07		0.07	0.07	0.06	0.05	0.05	0.04	0.02	-0.05
0.200	0.04		0.04	0.05	0.04	0.04	0.03	0.03	0.01	-0.03
0.250	0.04		0.04	0.03	0.02	0.02	0.02	0.03	0.02	-0.01
0.300	0.02		0.02	0.01	0.01	0.01	0.01	0.02	0.01	-0.01
0.350	0.02		0.01	0.00	0.00	0.00	0.00	0.01	0.01	0.00
0.400	0.02		0.01	0.00	0.00	0.00	0.00	0.01	0.01	0.00
0.450	0.02		0.01	0.00	0.00	0.00	0.01	0.01	0.01	0.01
0.500	0.02		0.01	0.00	0.00	0.00	0.00	0.01	0.01	0.01
0.550	0.02		0.01	0.00	0.00	0.00	0.00	0.01	0.01	0.01
0.600	0.02		0.01	0.00	0.00	0.00	0.00	0.01	0.01	0.01
0.650	0.02		0.01	0.00	0.00	0.00	0.00	0.01	0.01	0.01
0.700	0.02		0.01	0.00	0.00	0.00	0.00	0.01	0.01	0.01
0.750	0.03		0.01	0.00	0.00	0.00	0.01	0.01	0.01	0.02
0.800	0.03		0.01	0.00	0.01	0.00	0.01	0.01	0.01	0.02
0.850	0.03		0.01	0.00	0.01	0.00	0.01	0.02	0.01	0.02
0.900	0.03		0.00	-0.01	0.01	0.01	0.01	0.01	0.01	0.01
0.950	0.03		0.00	-0.01	0.00	0.01	0.01	0.01	0.01	-0.01

5% RAE 101. Values of  $C_p$  for  $R = 3.9 \times 10^6$  and  $\alpha = -2.08^\circ$

$x/c$	$\eta$	0.195	0.383	0.556	0.707	0.831	0.882	0.924	0.957	0.981
0.001	0.23		0.23	0.23	0.17	0.05	0.00	-0.05	-0.07	-0.17
0.003	0.24		0.25	0.25	0.20	0.10	0.05	-0.01	-0.06	-0.16
0.006	0.23		0.23	0.23	0.18	0.12	0.06	0.03	-0.04	
0.010	0.19		0.20	0.20	0.17	0.12	0.09	0.05	-0.03	-0.10
0.015	0.16		0.17	0.16	0.14	0.11	0.08	0.06	-0.01	
0.025	0.12		0.13	0.12	0.11	0.09	0.07	0.05	0.01	
0.035	0.09		0.09	0.09	0.08	0.07	0.06	0.05	0.02	
0.050	0.06		0.07	0.06	0.05	0.05	0.04	0.04	0.02	-0.03
0.075	0.04		0.04	0.03	0.03	0.03	0.02	0.03	0.01	-0.01
0.100	0.02		0.02	0.02	0.01	0.01	0.01	0.01	0.01	-0.01
0.125	0.01		0.01	0.00	0.00	0.00	0.00	0.00	0.00	0.00
0.150	0.00		0.00	-0.01	-0.01	-0.01	-0.01	0.00	0.00	0.00
0.200	-0.02		-0.02	-0.02	-0.02	-0.02	-0.01	-0.01	0.00	0.00
0.250	-0.02		-0.02	-0.03	-0.03	-0.03	-0.02	-0.02	-0.01	0.00
0.300	-0.03		-0.03	-0.04	-0.04	-0.04	-0.03	-0.02	-0.01	0.00
0.350	-0.03		-0.03	-0.04	-0.04	-0.04	-0.03	-0.02	-0.01	0.00
0.400	-0.02		-0.03	-0.04	-0.04	-0.03	-0.03	-0.02	-0.01	0.00
0.450	-0.02		-0.02	-0.03	-0.04	-0.03	-0.02	-0.02	0.00	0.00
0.500	-0.02		-0.02	-0.03	-0.03	-0.03	-0.02	-0.01	-0.01	0.01
0.550	-0.01		-0.02	-0.03	-0.03	-0.02	-0.02	-0.01	0.00	0.00
0.600	-0.01		-0.02	-0.02	-0.02	-0.02	-0.01	-0.01	0.00	0.01
0.650	-0.01		-0.02	-0.02	-0.02	-0.02	-0.01	0.00	0.01	0.00
0.700	0.00		-0.01	-0.02	-0.01	-0.01	-0.01	0.00	0.01	0.01
0.750	0.01		-0.01	-0.01	-0.01	-0.01	0.00	0.00	0.01	0.01
0.800	0.01		-0.01	-0.01	-0.01	0.00	0.01	0.01	0.01	0.02
0.850	0.02		-0.01	-0.01	0.00	0.00	0.01	0.02	0.01	0.02
0.900	0.02		0.00	-0.01	0.00	0.00	0.01	0.01	0.01	0.02
0.950	0.03		-0.01	-0.01	0.00	0.01	0.02	0.02	0.02	0.02



TABLE 6—*continued*

5% RAE 101. Values of  $C_p$  for  $R = 3.9 \times 10^6$  and  $\alpha = -1.04^\circ$

$x/c$ $\eta$	0.195	0.383	0.556	0.707	0.831	0.882	0.924	0.957	0.981
0.001	0.24	0.25	0.24	0.20	0.12	0.08	0.05	0.03	-0.04
0.003	0.23	0.22	0.21	0.18	0.12	0.08	0.05	0.01	-0.03
0.006	0.18	0.17	0.16	0.13	0.11	0.08	0.06	0.01	
0.010	0.13	0.12	0.12	0.10	0.09	0.07	0.05	0.02	-0.02
0.015	0.10	0.09	0.08	0.07	0.06	0.05	0.05	0.02	
0.025	0.07	0.06	0.05	0.04	0.04	0.03	0.03	0.02	
0.035	0.04	0.03	0.02	0.02	0.01	0.01	0.02	0.01	
0.050	0.01	0.01	0.00	-0.01	0.00	0.00	0.01	0.00	0.00
0.075	0.00	-0.01	-0.02	-0.02	-0.02	-0.02	-0.01	-0.01	0.00
0.100	-0.02	-0.02	-0.03	-0.03	-0.03	-0.03	-0.02	-0.01	-0.01
0.125	-0.03	-0.03	-0.04	-0.04	-0.04	-0.03	-0.03	-0.02	-0.01
0.150	-0.03	-0.04	-0.05	-0.05	-0.04	-0.04	-0.03	-0.02	-0.01
0.200	-0.04	-0.05	-0.05	-0.05	-0.05	-0.04	-0.04	-0.03	-0.01
0.250	-0.05	-0.05	-0.06	-0.06	-0.05	-0.05	-0.04	-0.03	-0.01
0.300	-0.06	-0.06	-0.07	-0.06	-0.06	-0.05	-0.04	-0.03	-0.02
0.350	-0.05	-0.05	-0.06	-0.06	-0.05	-0.05	-0.04	-0.03	-0.02
0.400	-0.04	-0.05	-0.06	-0.06	-0.05	-0.05	-0.04	-0.03	-0.02
0.450	-0.03	-0.04	-0.05	-0.05	-0.04	-0.03	-0.03	-0.02	-0.01
0.500	-0.03	-0.04	-0.05	-0.05	-0.04	-0.03	-0.03	-0.02	-0.01
0.550	-0.02	-0.03	-0.04	-0.04	-0.03	-0.03	-0.02	-0.02	-0.01
0.600	-0.02	-0.03	-0.03	-0.04	-0.03	-0.02	-0.02	-0.01	0.00
0.650	-0.02	-0.03	-0.03	-0.03	-0.03	-0.02	-0.02	-0.01	0.00
0.700	-0.01	-0.02	-0.02	-0.02	-0.02	-0.02	-0.01	0.00	0.00
0.750	0.00	-0.02	-0.02	-0.02	-0.01	-0.01	0.00	0.01	0.01
0.800	0.00	-0.01	-0.02	-0.01	-0.01	0.00	0.01	0.01	0.03
0.850	0.01	-0.01	-0.02	-0.01	0.00	0.00	0.02	0.01	0.02
0.900	0.03	-0.01	-0.01	0.00	0.00	0.01	0.01	0.01	0.02
0.950	0.03	-0.01	-0.01	0.00	0.01	0.01	0.02	0.02	0.02

5% RAE 101. Values of  $C_p$  for  $R = 3.9 \times 10^6$  and  $\alpha = -0.52^\circ$

$x/c$ $\eta$	0.195	0.383	0.556	0.707	0.831	0.882	0.924	0.957	0.981
0.001	0.23	0.23	0.22	0.19	0.14	0.09	0.06	0.05	0.00
0.003	0.21	0.18	0.16	0.15	0.11	0.07	0.06	0.02	0.01
0.006	0.14	0.12	0.11	0.07	0.08	0.06	0.05	0.02	
0.010	0.09	0.07	0.06	0.05	0.05	0.04	0.03	0.02	0.00
0.015	0.06	0.04	0.03	0.03	0.03	0.02	0.03	0.01	
0.025	0.03	0.02	0.00	0.00	0.01	0.00	0.01	0.00	
0.035	0.01	-0.01	-0.02	-0.02	-0.02	-0.01	-0.01	-0.01	
0.050	-0.02	-0.02	-0.04	-0.04	-0.03	-0.04	-0.02	-0.02	-0.01
0.075	-0.03	-0.04	-0.05	-0.05	-0.04	-0.04	-0.03	-0.02	-0.01
0.100	-0.04	-0.05	-0.06	-0.06	-0.05	-0.05	-0.04	-0.03	-0.02
0.125	-0.05	-0.05	-0.06	-0.06	-0.06	-0.05	-0.05	-0.04	-0.02
0.150	-0.05	-0.06	-0.06	-0.06	-0.06	-0.06	-0.05	-0.04	-0.02
0.200	-0.06	-0.06	-0.07	-0.07	-0.06	-0.06	-0.05	-0.04	-0.02
0.250	-0.06	-0.06	-0.08	-0.08	-0.07	-0.06	-0.06	-0.04	-0.02
0.300	-0.07	-0.07	-0.08	-0.08	-0.06	-0.06	-0.06	-0.04	-0.03
0.350	-0.06	-0.06	-0.08	-0.08	-0.06	-0.06	-0.05	-0.04	-0.02
0.400	-0.06	-0.06	-0.07	-0.07	-0.06	-0.06	-0.05	-0.04	-0.02
0.450	-0.05	-0.05	-0.06	-0.06	-0.05	-0.05	-0.04	-0.03	-0.02
0.500	-0.04	-0.04	-0.05	-0.05	-0.04	-0.04	-0.04	-0.03	-0.02
0.550	-0.03	-0.04	-0.04	-0.04	-0.04	-0.03	-0.03	-0.02	-0.01
0.600	-0.02	-0.04	-0.04	-0.04	-0.03	-0.03	-0.02	-0.01	-0.01
0.650	-0.02	-0.03	-0.04	-0.04	-0.03	-0.02	-0.01	0.00	0.00
0.700	-0.01	-0.02	-0.03	-0.03	-0.02	-0.02	0.00	0.00	0.01
0.750	0.00	-0.02	-0.02	-0.02	-0.02	-0.01	0.00	0.01	0.02
0.800	0.00	-0.02	-0.02	-0.01	-0.01	0.00	0.02	0.01	0.03
0.850	0.01	-0.01	-0.02	-0.01	0.00	0.01	0.01	0.01	0.03
0.900	0.02	-0.01	-0.01	0.00	0.00	0.01	0.01	0.01	0.03
0.950	0.02	-0.01	-0.01	0.00	0.01	0.02	0.02	0.03	0.02

TABLE 6—*continued*

5% RAE 101. Values of  $C_p$  for  $R = 3.9 \times 10^6$  and  $\alpha = 0^\circ$

$x/c$	$\eta$	0·195	0·383	0·556	0·707	0·831	0·882	0·924	0·957	0·981
0·001		0·20	0·19	0·17	0·15	0·13	0·08	0·05	0·05	0·01
0·003		0·17	0·13	0·10	0·09	0·07	0·05	0·04	0·01	0·01
0·006		0·09	0·06	0·04	0·01	0·03	0·02	0·02	0·00	
0·010		0·04	0·01	0·00	-0·01	0·00	0·01	0·00	0·00	0·00
0·015		0·02	-0·01	-0·03	-0·03	-0·02	-0·01	-0·01	-0·01	
0·025		-0·01	-0·02	-0·05	-0·04	-0·03	-0·03	-0·03	-0·02	
0·035		-0·03	-0·04	-0·06	-0·06	-0·05	-0·04	-0·04	-0·04	
0·050		-0·05	-0·05	-0·07	-0·07	-0·06	-0·06	-0·05	-0·04	-0·02
0·075		-0·05	-0·06	-0·08	-0·08	-0·07	-0·06	-0·06	-0·05	-0·03
0·100		-0·07	-0·07	-0·08	-0·08	-0·08	-0·07	-0·07	-0·05	-0·04
0·125		-0·07	-0·08	-0·09	-0·08	-0·08	-0·07	-0·07	-0·06	-0·04
0·150		-0·07	-0·08	-0·09	-0·09	-0·08	-0·08	-0·07	-0·06	-0·04
0·200		-0·08	-0·08	-0·09	-0·09	-0·08	-0·08	-0·07	-0·06	-0·04
0·250		-0·08	-0·08	-0·09	-0·09	-0·08	-0·08	-0·07	-0·06	-0·04
0·300		-0·08	-0·08	-0·09	-0·09	-0·08	-0·08	-0·07	-0·06	-0·04
0·350		-0·08	-0·08	-0·09	-0·09	-0·08	-0·07	-0·07	-0·05	-0·04
0·400		-0·07	-0·07	-0·08	-0·08	-0·07	-0·07	-0·06	-0·05	-0·04
0·450		-0·05	-0·06	-0·07	-0·07	-0·06	-0·06	-0·05	-0·04	-0·03
0·500		-0·04	-0·05	-0·06	-0·06	-0·05	-0·05	-0·04	-0·03	-0·02
0·550		-0·04	-0·05	-0·05	-0·05	-0·04	-0·04	-0·03	-0·02	-0·02
0·600		-0·03	-0·04	-0·05	-0·04	-0·04	-0·03	-0·03	-0·01	-0·01
0·650		-0·03	-0·04	-0·04	-0·04	-0·03	-0·02	-0·01	0·00	0·00
0·700		-0·02	-0·03	-0·03	-0·03	-0·02	-0·02	-0·01	0·00	0·01
0·750		-0·01	-0·02	-0·02	-0·02	-0·02	-0·01	-0·01	0·00	0·01
0·800		0·00	-0·02	-0·02	-0·02	-0·01	0·00	0·00	0·01	0·02
0·850		0·00	-0·01	-0·02	-0·01	0·00	0·00	0·02	0·01	0·03
0·900		0·01	-0·01	-0·01	0·00	0·00	0·01	0·01	0·01	0·03
0·950		0·02	-0·01	-0·01	0·00	0·01	0·02	0·02	0·03	0·03

5% RAE 101. Values of  $C_p$  for  $R = 3.9 \times 10^6$  and  $\alpha = 0.52^\circ$

$x/c$	$\eta$	0·195	0·383	0·556	0·707	0·831	0·882	0·924	0·957	0·981
0·001		0·16	0·13	0·10	0·10	0·10	0·05	0·02	0·03	-0·01
0·003		0·12	0·06	0·02	0·03	0·02	0·00	0·00	-0·02	0·00
0·006		0·04	-0·01	-0·04	-0·06	-0·03	-0·04	-0·02	-0·03	
0·010		-0·01	-0·06	-0·08	-0·08	-0·05	-0·05	-0·05	-0·04	-0·02
0·015		-0·03	-0·06	-0·10	-0·08	-0·07	-0·07	-0·05	-0·05	
0·025		-0·05	-0·07	-0·10	-0·09	-0·07	-0·08	-0·07	-0·06	
0·035		-0·06	-0·08	-0·11	-0·10	-0·09	-0·09	-0·08	-0·07	
0·050		-0·08	-0·09	-0·11	-0·10	-0·10	-0·10	-0·08	-0·08	-0·06
0·075		-0·08	-0·09	-0·11	-0·11	-0·10	-0·10	-0·08	-0·08	-0·06
0·100		-0·09	-0·10	-0·11	-0·11	-0·10	-0·10	-0·09	-0·08	-0·07
0·125		-0·09	-0·10	-0·11	-0·10	-0·10	-0·10	-0·09	-0·08	-0·06
0·150		-0·09	-0·10	-0·11	-0·10	-0·10	-0·10	-0·09	-0·08	-0·06
0·200		-0·09	-0·10	-0·11	-0·10	-0·10	-0·09	-0·09	-0·08	-0·07
0·250		-0·09	-0·09	-0·11	-0·10	-0·10	-0·09	-0·08	-0·07	-0·06
0·300		-0·09	-0·09	-0·11	-0·10	-0·10	-0·09	-0·08	-0·07	-0·06
0·350		-0·08	-0·09	-0·10	-0·10	-0·09	-0·08	-0·08	-0·06	-0·05
0·400		-0·07	-0·08	-0·09	-0·09	-0·08	-0·07	-0·06	-0·06	-0·04
0·450		-0·06	-0·06	-0·07	-0·07	-0·07	-0·06	-0·06	-0·05	-0·04
0·500		-0·05	-0·06	-0·06	-0·06	-0·06	-0·05	-0·05	-0·04	-0·03
0·550		-0·04	-0·05	-0·06	-0·06	-0·06	-0·04	-0·04	-0·02	-0·02
0·600		-0·04	-0·05	-0·05	-0·05	-0·05	-0·04	-0·03	-0·02	-0·01
0·650		-0·03	-0·04	-0·05	-0·04	-0·04	-0·03	-0·02	0·00	-0·01
0·700		-0·02	-0·03	-0·04	-0·03	-0·02	-0·02	-0·01	0·00	0·01
0·750		-0·02	-0·03	-0·03	-0·02	-0·02	-0·01	-0·01	0·00	0·01
0·800		-0·01	-0·02	-0·02	-0·02	-0·01	0·00	0·00	0·01	0·01
0·850		0·01	-0·02	-0·02	-0·01	-0·01	0·00	0·01	0·01	0·02
0·900		0·01	-0·01	-0·02	0·00	0·00	0·00	0·01	0·01	0·03
0·950		0·02	-0·01	-0·01	0·00	0·01	0·02	0·02	0·03	0·03

TABLE 6—*continued*

5% RAE 101. Values of  $C_p$  for  $R = 3.9 \times 10^6$  and  $\alpha = 1.04^\circ$

$x/c$	$\eta$	0.195	0.383	0.556	0.707	0.831	0.882	0.924	0.957	0.981
0.001		0.11	0.05	0.02	0.02	-0.06	0.00	-0.03	-0.02	-0.05
0.003		0.05	-0.03	-0.07	-0.06	-0.06	-0.06	-0.06	-0.07	-0.05
0.006		-0.02	-0.10	-0.12	-0.15	-0.10	-0.11	-0.09	-0.08	
0.010		-0.07	-0.13	-0.15	-0.16	-0.12	-0.12	-0.11	-0.09	-0.07
0.015		-0.08	-0.13	-0.17	-0.15	-0.13	-0.13	-0.11	-0.10	
0.025		-0.09	-0.12	-0.15	-0.14	-0.13	-0.13	-0.13	-0.12	
0.035		-0.10	-0.13	-0.15	-0.14	-0.14	-0.14	-0.13	-0.12	
0.050		-0.11	-0.13	-0.15	-0.14	-0.14	-0.14	-0.13	-0.12	-0.10
0.075		-0.11	-0.12	-0.14	-0.14	-0.13	-0.12	-0.12	-0.11	-0.10
0.100		-0.11	-0.12	-0.13	-0.13	-0.13	-0.12	-0.12	-0.11	-0.11
0.125		-0.11	-0.12	-0.13	-0.13	-0.13	-0.12	-0.12	-0.11	-0.10
0.150		-0.11	-0.12	-0.13	-0.13	-0.12	-0.12	-0.11	-0.10	-0.09
0.200		-0.11	-0.12	-0.13	-0.12	-0.12	-0.12	-0.11	-0.10	-0.09
0.250		-0.10	-0.11	-0.12	-0.12	-0.11	-0.11	-0.10	-0.09	-0.08
0.300		-0.10	-0.11	-0.12	-0.12	-0.11	-0.10	-0.09	-0.09	-0.08
0.350		-0.09	-0.10	-0.11	-0.11	-0.10	-0.09	-0.09	-0.08	-0.07
0.400		-0.08	-0.09	-0.09	-0.09	-0.09	-0.09	-0.07	-0.07	-0.06
0.450		-0.06	-0.07	-0.08	-0.08	-0.07	-0.07	-0.07	-0.05	-0.05
0.500		-0.06	-0.06	-0.07	-0.07	-0.07	-0.06	-0.05	-0.04	-0.04
0.550		-0.05	-0.06	-0.06	-0.06	-0.05	-0.05	-0.04	-0.03	-0.03
0.600		-0.04	-0.05	-0.06	-0.06	-0.05	-0.04	-0.04	-0.03	-0.02
0.650		-0.04	-0.05	-0.05	-0.05	-0.04	-0.03	-0.03	-0.01	-0.02
0.700		-0.02	-0.04	-0.04	-0.04	-0.02	-0.03	-0.02	-0.01	-0.01
0.750		-0.01	-0.03	-0.03	-0.03	-0.02	-0.02	-0.01	0.00	0.00
0.800		-0.01	-0.02	-0.02	-0.02	-0.01	-0.01	0.00	0.00	0.01
0.850		0.00	-0.02	-0.02	-0.01	-0.01	0.00	0.01	0.01	0.02
0.900		0.01	-0.01	-0.02	-0.01	0.00	0.00	0.01	0.01	0.02
0.950		0.02	-0.01	-0.01	0.00	0.01	0.02	0.02	0.03	0.02

5% RAE 101. Values of  $C_p$  for  $R = 3.9 \times 10^6$  and  $\alpha = 2.08^\circ$

$x/c$	$\eta$	0.195	0.383	0.556	0.707	0.831	0.882	0.924	0.957	0.981
0.001		-0.04	-0.16	-0.22	-0.20	-0.09	-0.15	-0.21	-0.18	-0.22
0.003		-0.11	-0.24	-0.31	-0.27	-0.26	-0.22	-0.23	-0.23	-0.20
0.006		-0.17	-0.30	-0.34	-0.36	-0.30	-0.30	-0.26	-0.24	
0.010		-0.21	-0.30	-0.34	-0.34	-0.30	-0.29	-0.27	-0.25	-0.22
0.015		-0.20	-0.27	-0.32	-0.30	-0.27	-0.28	-0.26	-0.25	
0.025		-0.18	-0.23	-0.28	-0.26	-0.24	-0.26	-0.26	-0.25	
0.035		-0.18	-0.23	-0.26	-0.24	-0.24	-0.24	-0.24	-0.24	
0.050		-0.18	-0.21	-0.25	-0.22	-0.22	-0.22	-0.23	-0.23	-0.23
0.075		-0.16	-0.19	-0.21	-0.21	-0.20	-0.20	-0.21	-0.21	-0.20
0.100		-0.16	-0.17	-0.19	-0.19	-0.19	-0.19	-0.19	-0.20	-0.20
0.125		-0.15	-0.17	-0.18	-0.18	-0.17	-0.17	-0.18	-0.18	-0.19
0.150		-0.15	-0.16	-0.17	-0.17	-0.16	-0.15	-0.16	-0.16	-0.19
0.200		-0.14	-0.14	-0.16	-0.15	-0.15	-0.14	-0.14	-0.14	-0.18
0.250		-0.13	-0.14	-0.15	-0.14	-0.14	-0.13	-0.13	-0.13	-0.14
0.300		-0.13	-0.13	-0.14	-0.14	-0.13	-0.12	-0.13	-0.13	-0.11
0.350		-0.11	-0.12	-0.13	-0.13	-0.12	-0.11	-0.12	-0.11	-0.10
0.400		-0.10	-0.10	-0.11	-0.11	-0.10	-0.10	-0.10	-0.10	-0.09
0.450		-0.08	-0.09	-0.10	-0.10	-0.09	-0.08	-0.09	-0.08	-0.07
0.500		-0.07	-0.08	-0.09	-0.09	-0.08	-0.07	-0.07	-0.07	-0.06
0.550		-0.06	-0.07	-0.08	-0.08	-0.07	-0.06	-0.06	-0.05	-0.05
0.600		-0.05	-0.06	-0.07	-0.06	-0.06	-0.05	-0.05	-0.05	-0.04
0.650		-0.05	-0.06	-0.06	-0.05	-0.05	-0.04	-0.04	-0.03	-0.04
0.700		-0.03	-0.05	-0.05	-0.04	-0.04	-0.03	-0.03	-0.02	-0.03
0.750		-0.02	-0.04	-0.04	-0.03	-0.03	-0.02	-0.02	-0.01	-0.02
0.800		-0.02	-0.03	-0.03	-0.03	-0.02	-0.01	-0.01	-0.01	-0.01
0.850		0.00	-0.02	-0.03	-0.02	-0.01	-0.01	0.00	0.00	0.00
0.900		0.01	-0.01	-0.02	-0.01	0.00	0.00	0.00	0.00	0.00
0.950		0.02	-0.01	-0.01	0.00	0.00	0.01	0.01	0.02	0.01









TABLE 7

Pressure Distributions on 9% Wing at  $R = 1.3 \times 10^6$ 

9% RAE 101. Values of  $C_p$  for  $R = 1.3 \times 10^6$  and  $\alpha = -8.31^\circ$

$x/c$ $\eta$	0.195	0.383	0.556	0.707	0.831	0.882	0.924	0.957	0.981
0.001	-0.38	-0.56	-0.58	-0.58	-0.84	-0.83	-0.87	-0.81	-0.38
0.003	-0.15	-0.27	-0.30	-0.35	-0.52	-0.68	-0.77	-0.74	-0.38
0.006	0.06	-0.07	-0.08	-0.16	-0.34	-0.53	-0.66	-0.67	-0.37
0.010	0.14	0.09	0.08	-0.03	-0.20	-0.38	-0.53	-0.61	-0.35
0.015	0.20	0.18	0.17	0.08	-0.12	-0.26	-0.42	-0.54	-0.34
0.025	0.25	0.24	0.24	0.17	0.01	-0.12	-0.28	-0.45	-0.31
0.035	0.26	0.27	0.26	0.20	0.06	-0.03	-0.19	-0.37	-0.28
0.050	0.25	0.26	0.25	0.20	0.10	0.02	-0.10	-0.27	-0.24
0.075	0.22	0.24	0.23	0.19	0.12	0.06	-0.03	-0.17	-0.20
0.100	0.20	0.21	0.20	0.17	0.11	0.08	0.01	-0.11	-0.16
0.125	0.17	0.18	0.18	0.15	0.11	0.08	0.03	-0.07	-0.13
0.150	0.15	0.15	0.15	0.13	0.10	0.08	0.04	-0.04	-0.09
0.200	0.11	0.12	0.11	0.09	0.08	0.08	0.04	-0.01	-0.06
0.250	0.09	0.09	0.08	0.07	0.06	0.06	0.04	0.01	-0.03
0.300	0.06	0.06	0.05	0.04	0.04	0.04	0.03	0.01	-0.02
0.350	0.06	0.06	0.04	0.03	0.04	0.04	0.03	0.02	-0.01
0.400	0.06	0.04	0.03	0.03	0.03	0.04	0.03	0.02	0.00
0.450	0.05	0.04	0.02	0.02	0.02	0.03	0.02	0.02	0.01
0.500	0.05	0.04	0.02	0.01	0.02	0.02	0.02	0.02	0.01
0.550	0.05	0.03	0.02	0.01	0.02	0.02	0.01	0.01	0.00
0.600	0.04	0.03	0.02	0.01	0.02	0.01	0.01	0.00	-0.01
0.650	0.05	0.03	0.02	0.01	0.02	0.01	0.01	-0.01	-0.01
0.700	0.05	0.02	0.02	0.01	0.02	0.01	0.01	-0.01	-0.01
0.750	0.05	0.02	0.02	0.02	0.02	0.01	0.00	-0.02	-0.02
0.800	0.05	0.02	0.02	0.02	0.01	0.01	-0.01	-0.03	-0.03
0.850	0.05	0.01	0.02	0.02	0.01	-0.01	-0.03	-0.06	-0.04
0.900	0.05	0.01	0.01	0.03	0.00	-0.01	-0.05	-0.08	-0.06
0.950	0.04	0.01	0.01	0.03	-0.01	-0.04	-0.10	-0.14	-0.09

9% RAE 101. Values of  $C_p$  for  $R = 1.3 \times 10^6$  and  $\alpha = -2.08^\circ$ 

$x/c$ $\eta$	0.195	0.383	0.556	0.707	0.831	0.882	0.924	0.957	0.981
0.001	0.22	0.23	0.22	0.18	0.07	0.03	-0.01	-0.06	-0.08
0.003	0.23	0.25	0.24	0.19	0.11	0.06	0.01	-0.03	-0.07
0.006	0.24	0.24	0.22	0.19	0.11	0.06	0.02	-0.03	-0.06
0.010	0.20	0.21	0.20	0.17	0.11	0.07	0.04	-0.01	-0.05
0.015	0.17	0.18	0.16	0.14	0.10	0.07	0.04	-0.01	-0.04
0.025	0.13	0.13	0.12	0.11	0.08	0.06	0.04	0.00	-0.03
0.035	0.09	0.10	0.08	0.08	0.06	0.04	0.03	0.00	-0.02
0.050	0.06	0.06	0.04	0.04	0.04	0.02	0.02	0.00	-0.01
0.075	0.02	0.02	0.00	0.00	0.00	0.00	0.01	0.00	-0.01
0.100	-0.01	-0.01	-0.03	-0.03	-0.02	-0.02	-0.01	-0.01	-0.01
0.125	-0.03	-0.03	-0.04	-0.05	-0.03	-0.03	-0.02	-0.01	-0.01
0.150	-0.05	-0.05	-0.06	-0.06	-0.05	-0.04	-0.03	-0.02	-0.01
0.200	-0.07	-0.07	-0.08	-0.08	-0.07	-0.05	-0.05	-0.03	-0.01
0.250	-0.08	-0.08	-0.10	-0.10	-0.08	-0.07	-0.06	-0.03	-0.01
0.300	-0.09	-0.09	-0.10	-0.10	-0.09	-0.08	-0.06	-0.04	-0.02
0.350	-0.08	-0.08	-0.10	-0.10	-0.08	-0.07	-0.06	-0.04	-0.02
0.400	-0.07	-0.07	-0.09	-0.09	-0.07	-0.06	-0.05	-0.03	-0.01
0.450	-0.06	-0.06	-0.08	-0.08	-0.06	-0.05	-0.04	-0.02	-0.01
0.500	-0.05	-0.06	-0.07	-0.07	-0.05	-0.05	-0.04	-0.02	0.00
0.550	-0.04	-0.05	-0.06	-0.06	-0.05	-0.04	-0.03	-0.01	0.00
0.600	-0.03	-0.05	-0.06	-0.05	-0.04	-0.03	-0.03	-0.01	0.00
0.650	-0.03	-0.04	-0.05	-0.04	-0.03	-0.03	-0.02	-0.01	0.00
0.700	-0.01	-0.03	-0.03	-0.03	-0.02	-0.02	-0.01	0.00	0.01
0.750	0.01	-0.01	-0.01	-0.01	0.00	0.01	0.01	0.01	0.02
0.800	0.01	0.00	-0.01	0.01	0.01	0.01	0.02	0.03	0.03
0.850	0.02	0.00	0.00	0.00	0.01	0.02	0.02	0.03	0.04
0.900	0.03	0.01	0.00	0.01	0.02	0.03	0.03	0.03	0.04
0.950	0.04	0.02	0.00	0.02	0.04	0.04	0.04	0.04	0.04



TABLE 7—continued

9% RAE 101. Values of  $C_p$  for  $R = 1.3 \times 10^6$  and  $\alpha = 0^\circ$ 

$x/c$	$\eta$	0.195	0.383	0.556	0.707	0.831	0.882	0.924	0.957	0.981
0.001		0.22	0.23	0.22	0.17	0.10	0.07	0.04	0.00	-0.01
0.003		0.18	0.18	0.17	0.14	0.08	0.06	0.03	0.00	-0.01
0.006		0.16	0.14	0.12	0.10	0.06	0.04	0.02	-0.01	-0.01
0.010		0.11	0.09	0.07	0.06	0.04	0.02	0.01	-0.01	-0.01
0.015		0.06	0.04	0.02	0.01	0.02	0.00	0.00	-0.01	-0.01
0.025		0.01	-0.01	-0.03	-0.03	-0.02	-0.03	-0.02	-0.02	-0.02
0.035		-0.03	-0.03	-0.06	-0.05	-0.04	-0.05	-0.04	-0.03	-0.02
0.050		-0.06	-0.07	-0.09	-0.09	-0.07	-0.07	-0.06	-0.05	-0.02
0.075		-0.08	-0.09	-0.11	-0.12	-0.10	-0.09	-0.08	-0.06	-0.03
0.100		-0.10	-0.11	-0.12	-0.13	-0.12	-0.11	-0.09	-0.07	-0.04
0.125		-0.11	-0.12	-0.13	-0.14	-0.12	-0.11	-0.10	-0.08	-0.06
0.150		-0.12	-0.13	-0.14	-0.14	-0.13	-0.12	-0.11	-0.09	-0.06
0.200		-0.14	-0.14	-0.15	-0.15	-0.14	-0.12	-0.12	-0.10	-0.07
0.250		-0.14	-0.15	-0.15	-0.15	-0.14	-0.13	-0.12	-0.10	-0.07
0.300		-0.15	-0.15	-0.16	-0.16	-0.14	-0.14	-0.12	-0.10	-0.08
0.350		-0.13	-0.13	-0.15	-0.14	-0.12	-0.12	-0.11	-0.09	-0.07
0.400		-0.11	-0.12	-0.13	-0.12	-0.11	-0.10	-0.10	-0.08	-0.06
0.450		-0.10	-0.10	-0.11	-0.11	-0.10	-0.09	-0.08	-0.06	-0.05
0.500		-0.09	-0.10	-0.10	-0.10	-0.09	-0.09	-0.08	-0.06	-0.04
0.550		-0.08	-0.08	-0.09	-0.09	-0.07	-0.05	-0.06	-0.05	-0.04
0.600		-0.06	-0.05	-0.06	-0.05	-0.04	-0.04	-0.03	-0.03	-0.02
0.650		-0.05	-0.04	-0.05	-0.04	-0.03	-0.03	-0.02	-0.01	0.00
0.700		-0.02	-0.03	-0.04	-0.03	-0.02	-0.02	-0.01	0.00	0.01
0.750		-0.01	-0.03	-0.03	-0.02	-0.01	-0.01	0.01	0.01	0.02
0.800		0.00	-0.01	-0.01	-0.01	0.00	0.00	0.01	0.02	0.03
0.850		0.01	-0.01	-0.01	0.00	0.01	0.01	0.02	0.02	0.04
0.900		0.03	0.01	0.00	0.01	0.02	0.02	0.03	0.03	0.04
0.950		0.04	0.02	0.01	0.02	0.04	0.04	0.04	0.04	0.05

9% RAE 101. Values of  $C_p$  for  $R = 1.3 \times 10^6$  and  $\alpha = 2.08^\circ$ 

$x/c$	$\eta$	0.195	0.383	0.556	0.707	0.831	0.882	0.924	0.957	0.981
0.001		0.13	0.08	0.05	0.01	-0.03	-0.04	-0.06	-0.08	-0.09
0.003		0.05	0.00	-0.03	-0.05	-0.07	-0.07	-0.08	-0.10	-0.10
0.006		0.00	-0.06	-0.10	-0.10	-0.12	-0.12	-0.12	-0.12	-0.11
0.010		-0.07	-0.12	-0.15	-0.17	-0.15	-0.14	-0.13	-0.13	-0.10
0.015		-0.11	-0.15	-0.20	-0.21	-0.16	-0.16	-0.15	-0.10	-0.12
0.025		-0.15	-0.19	-0.23	-0.22	-0.19	-0.19	-0.17	-0.16	-0.13
0.035		-0.17	-0.21	-0.24	-0.24	-0.21	-0.21	-0.19	-0.18	-0.14
0.050		-0.19	-0.23	-0.25	-0.26	-0.23	-0.22	-0.21	-0.20	-0.15
0.075		-0.20	-0.22	-0.25	-0.26	-0.23	-0.22	-0.22	-0.20	-0.16
0.100		-0.20	-0.22	-0.25	-0.26	-0.24	-0.23	-0.22	-0.20	-0.18
0.125		-0.20	-0.22	-0.24	-0.25	-0.24	-0.22	-0.22	-0.20	-0.18
0.150		-0.20	-0.22	-0.24	-0.24	-0.23	-0.22	-0.22	-0.21	-0.19
0.200		-0.21	-0.22	-0.23	-0.24	-0.23	-0.21	-0.21	-0.20	-0.19
0.250		-0.20	-0.21	-0.22	-0.23	-0.21	-0.20	-0.20	-0.19	-0.18
0.300		-0.19	-0.20	-0.22	-0.21	-0.20	-0.20	-0.19	-0.19	-0.18
0.350		-0.17	-0.18	-0.20	-0.19	-0.19	-0.18	-0.17	-0.17	-0.16
0.400		-0.16	-0.17	-0.18	-0.18	-0.17	-0.17	-0.17	-0.16	-0.16
0.450		-0.15	-0.15	-0.17	-0.16	-0.16	-0.15	-0.15	-0.15	-0.15
0.500		-0.11	-0.10	-0.12	-0.11	-0.10	-0.09	-0.08	-0.10	-0.15
0.550		-0.08	-0.09	-0.10	-0.10	-0.08	-0.07	-0.06	-0.06	-0.13
0.600		-0.07	-0.07	-0.08	-0.08	-0.07	-0.06	-0.05	-0.05	-0.08
0.650		-0.05	-0.06	-0.06	-0.06	-0.05	-0.04	-0.03	-0.03	-0.05
0.700		-0.04	-0.05	-0.05	-0.05	-0.03	-0.03	-0.02	-0.02	-0.03
0.750		-0.02	-0.03	-0.03	-0.03	-0.02	-0.01	-0.01	-0.01	-0.02
0.800		-0.01	-0.02	-0.02	-0.01	-0.01	0.00	0.01	0.01	-0.01
0.850		0.01	-0.01	-0.01	-0.01	0.00	0.01	0.01	0.01	-0.01
0.900		0.02	0.00	0.00	0.01	0.02	0.03	0.03	0.02	0.01
0.950		0.04	0.01	0.01	0.02	0.04	0.04	0.04	0.04	0.02

TABLE 7—continued

9% RAE 101. Values of  $C_p$  for  $R = 1.3 \times 10^6$  and  $\alpha = 8.31^\circ$

$x/c$ $\eta$	0.195	0.383	0.556	0.707	0.831	0.882	0.924	0.957	0.981
0.001	-0.78	-1.16	-1.28	-1.20	-1.14	-1.02	-0.92	-0.71	-0.20
0.003	-0.89	-1.24	-1.36	-1.24	-1.16	-1.09	-0.96	-0.71	-0.20
0.006	-0.90	-1.23	-1.34	-1.24	-1.14	-1.09	-0.99	-0.71	-0.20
0.010	-0.92	-1.18	-1.28	-1.24	-1.10	-1.08	-0.97	-0.70	-0.20
0.015	-0.89	-1.12	-1.20	-1.17	-1.05	-1.04	-0.92	-0.67	-0.19
0.025	-0.81	-1.01	-1.35	-1.09	-0.96	-0.96	-0.87	-0.63	-0.19
0.035	-0.76	-0.98	-1.34	-1.07	-0.94	-0.93	-0.85	-0.60	-0.19
0.050	-0.73	-0.95	-1.03	-1.03	-0.92	-0.94	-0.84	-0.58	-0.18
0.075	-0.67	-0.62	-0.71	-0.69	-0.85	-0.88	-0.82	-0.56	-0.17
0.100	-0.52	-0.60	-0.64	-0.62	-0.57	-0.55	-0.80	-0.54	-0.16
0.125	-0.49	-0.56	-0.59	-0.57	-0.54	-0.52	-0.52	-0.52	-0.15
0.150	-0.47	-0.52	-0.54	-0.51	-0.50	-0.49	-0.42	-0.47	-0.13
0.200	-0.43	-0.46	-0.46	-0.45	-0.42	-0.40	-0.33	-0.40	-0.11
0.250	-0.38	-0.41	-0.41	-0.39	-0.35	-0.31	-0.25	-0.39	-0.10
0.300	-0.35	-0.36	-0.36	-0.33	-0.28	-0.25	-0.19	-0.40	-0.10
0.350	-0.30	-0.29	-0.29	-0.26	-0.20	-0.18	-0.17	-0.39	-0.08
0.400	-0.26	-0.25	-0.24	-0.20	-0.16	-0.15	-0.16	-0.36	-0.08
0.450	-0.22	-0.20	-0.19	-0.16	-0.14	-0.14	-0.15	-0.32	-0.07
0.500	-0.18	-0.17	-0.15	-0.13	-0.12	-0.14	-0.15	-0.27	-0.06
0.550	-0.15	-0.14	-0.13	-0.12	-0.12	-0.14	-0.14	-0.23	-0.06
0.600	-0.13	-0.12	-0.12	-0.10	-0.12	-0.15	-0.13	-0.20	-0.04
0.650	-0.10	-0.10	-0.10	-0.10	-0.12	-0.16	-0.12	-0.18	-0.04
0.700	-0.08	-0.09	-0.10	-0.10	-0.13	-0.16	-0.12	-0.18	-0.04
0.750	-0.06	-0.08	-0.08	-0.10	-0.14	-0.16	-0.13	-0.18	-0.04
0.800	-0.03	-0.07	-0.08	-0.10	-0.16	-0.18	-0.15	-0.18	-0.04
0.850	-0.02	-0.06	-0.08	-0.11	-0.19	-0.20	-0.17	-0.18	-0.05
0.900	-0.01	-0.06	-0.09	-0.12	-0.20	-0.20	-0.18	-0.18	-0.06
0.950	0.01	-0.06	-0.09	-0.12	-0.18	-0.16	-0.16	-0.16	-0.06

9% RAE 101. Values of  $C_p$  for  $R = 1.3 \times 10^6$  and  $\alpha = 12.48^\circ$

$x/c$ $\eta$	0.195	0.383	0.556	0.707	0.831	0.882	0.924	0.957	0.981
0.001	-1.98	-2.88	-2.94	-2.43	-1.03	-0.48	-0.28	-0.19	-0.10
0.003	-2.01	-2.83	-2.88	-2.34	-1.00	-0.47	-0.26	-0.18	-0.10
0.006	-1.91	-2.68	-2.70	-2.23	-0.99	-0.47	-0.26	-0.17	-0.09
0.010	-1.80	-2.49	-2.53	-2.14	-0.97	-0.46	-0.24	-0.16	-0.08
0.015	-1.71	-2.43	-2.46	-2.06	-0.93	-0.44	-0.23	-0.14	-0.08
0.025	-1.69	-2.08	-2.05	-1.93	-0.86	-0.42	-0.22	-0.14	-0.08
0.035	-1.52	-1.60	-1.53	-1.32	-0.82	-0.41	-0.21	-0.13	-0.08
0.050	-1.06	-1.43	-1.35	-1.19	-0.77	-0.40	-0.21	-0.13	-0.08
0.075	-0.95	-1.16	-1.08	-0.95	-0.74	-0.38	-0.21	-0.12	-0.08
0.100	-0.84	-1.00	-0.90	-0.77	-0.73	-0.36	-0.21	-0.13	-0.08
0.125	-0.77	-0.89	-0.76	-0.65	-0.74	-0.35	-0.20	-0.12	-0.08
0.150	-0.70	-0.79	-0.66	-0.56	-0.76	-0.34	-0.20	-0.12	-0.08
0.200	-0.61	-0.64	-0.51	-0.51	-0.80	-0.33	-0.20	-0.12	-0.08
0.250	-0.54	-0.53	-0.44	-0.47	-0.81	-0.32	-0.20	-0.11	-0.08
0.300	-0.47	-0.45	-0.42	-0.44	-0.76	-0.33	-0.19	-0.12	-0.09
0.350	-0.40	-0.40	-0.41	-0.42	-0.64	-0.32	-0.18	-0.11	-0.09
0.400	-0.35	-0.37	-0.42	-0.42	-0.55	-0.31	-0.17	-0.11	-0.10
0.450	-0.31	-0.36	-0.42	-0.42	-0.49	-0.31	-0.16	-0.11	-0.10
0.500	-0.27	-0.37	-0.44	-0.42	-0.48	-0.30	-0.16	-0.11	-0.10
0.550	-0.25	-0.39	-0.48	-0.43	-0.48	-0.31	-0.17	-0.11	-0.10
0.600	-0.21	-0.43	-0.56	-0.47	-0.49	-0.33	-0.18	-0.12	-0.11
0.650	-0.19	-0.47	-0.69	-0.53	-0.50	-0.33	-0.18	-0.13	-0.11
0.700	-0.16	-0.47	-0.74	-0.58	-0.49	-0.33	-0.19	-0.13	-0.11
0.750	-0.14	-0.43	-0.73	-0.60	-0.45	-0.31	-0.20	-0.14	-0.10
0.800	-0.11	-0.35	-0.61	-0.58	-0.40	-0.30	-0.21	-0.14	-0.10
0.850	-0.08	-0.22	-0.42	-0.51	-0.34	-0.29	-0.21	-0.14	-0.11
0.900	-0.05	-0.08	-0.23	-0.36	-0.38	-0.31	-0.22	-0.13	-0.10
0.950	-0.02	0.01	-0.06	-0.50	-0.55	-0.33	-0.21	-0.13	-0.09

TABLE 8

Pressure Distributions on 9% Wing at  $R = 2.2 \times 10^6$ 

9% RAE 101. Values of  $C_p$  for  $R = 2.2 \times 10^6$  and  $\alpha = -8.31^\circ$

$x/c$ $\eta$	0.195	0.383	0.556	0.707	0.831	0.882	0.924	0.957	0.981
0.001	-0.40	-0.57	-0.59	-0.60	-0.92	-0.88	-0.92	-0.92	-0.79
0.003	-0.16	-0.28	-0.31	-0.34	-0.55	-0.72	-0.81	-0.84	-0.74
0.006	0.06	-0.08	-0.09	-0.17	-0.36	-0.56	-0.70	-0.76	-0.70
0.010	0.13	0.09	0.07	-0.04	-0.22	-0.50	-0.57	-0.69	-0.64
0.015	0.20	0.17	0.16	0.08	-0.14	-0.19	-0.45	-0.61	-0.62
0.025	0.25	0.24	0.24	0.16	0.00	-0.13	-0.30	-0.51	-0.55
0.035	0.26	0.26	0.26	0.20	0.05	-0.05	-0.21	-0.43	-0.49
0.050	0.24	0.26	0.26	0.20	0.10	0.01	-0.11	-0.32	-0.41
0.075	0.22	0.24	0.23	0.19	0.12	0.06	-0.04	-0.21	-0.34
0.100	0.19	0.21	0.20	0.17	0.12	0.07	0.01	-0.14	-0.27
0.125	0.17	0.18	0.18	0.15	0.11	0.08	0.03	-0.10	-0.23
0.150	0.15	0.16	0.15	0.14	0.11	0.08	0.04	-0.08	-0.18
0.200	0.11	0.14	0.12	0.10	0.09	0.07	0.04	-0.03	-0.12
0.250	0.09	0.09	0.08	0.07	0.07	0.06	0.04	0.00	-0.07
0.300	0.07	0.07	0.06	0.05	0.05	0.05	0.04	0.01	-0.05
0.350	0.06	0.06	0.04	0.03	0.04	0.04	0.03	0.01	-0.03
0.400	0.05	0.05	0.03	0.03	0.03	0.04	0.03	0.02	-0.02
0.450	0.05	0.04	0.02	0.02	0.03	0.03	0.03	0.03	-0.01
0.500	0.04	0.03	0.02	0.02	0.03	0.02	0.03	0.03	0.00
0.550	0.05	0.03	0.02	0.01	0.03	0.03	0.02	0.02	0.00
0.600	0.05	0.03	0.02	0.02	0.02	0.02	0.02	0.02	0.00
0.650	0.05	0.03	0.02	0.02	0.02	0.02	0.02	0.02	-0.01
0.700	0.04	0.03	0.02	0.02	0.02	0.02	0.02	0.01	-0.01
0.750	0.05	0.02	0.02	0.02	0.02	0.02	0.02	0.01	-0.02
0.800	0.05	0.03	0.02	0.03	0.02	0.01	0.02	0.00	-0.04
0.850	0.05	0.02	0.02	0.03	0.01	0.01	0.01	-0.02	-0.05
0.900	0.05	0.02	0.02	0.03	0.01	0.01	0.01	-0.05	-0.07
0.950	0.04	0.01	0.01	0.03	0.00	0.00	-0.01	-0.13	-0.11

9% RAE 101. Values of  $C_p$  for  $R = 2.2 \times 10^6$  and  $\alpha = -6.24^\circ$ 

$x/c$ $\eta$	0.195	0.383	0.556	0.707	0.831	0.882	0.924	0.957	0.981
0.001	-0.10	-0.17	-0.18	-0.21	-0.46	-0.45	-0.50	-0.54	-0.59
0.003	0.06	0.01	0.00	-0.05	-0.22	-0.35	-0.43	-0.48	-0.54
0.006	0.19	0.13	0.13	0.05	-0.11	-0.24	-0.35	-0.43	-0.50
0.010	0.22	0.20	0.20	0.12	-0.05	-0.15	-0.27	-0.38	-0.46
0.015	0.24	0.24	0.24	0.17	0.02	-0.08	-0.19	-0.32	-0.43
0.025	0.24	0.25	0.25	0.20	0.09	0.00	-0.11	-0.26	-0.38
0.035	0.23	0.24	0.24	0.20	0.11	0.05	-0.06	-0.21	-0.33
0.050	0.20	0.22	0.21	0.18	0.12	0.06	-0.01	-0.15	-0.27
0.075	0.16	0.18	0.18	0.15	0.11	0.08	0.02	-0.08	-0.22
0.100	0.13	0.15	0.14	0.12	0.10	0.07	0.04	-0.05	-0.18
0.125	0.11	0.12	0.12	0.10	0.08	0.07	0.04	-0.03	-0.15
0.150	0.09	0.09	0.09	0.08	0.07	0.06	0.04	-0.03	-0.11
0.200	0.05	0.07	0.06	0.05	0.05	0.05	0.03	0.00	-0.07
0.250	0.03	0.03	0.03	0.02	0.03	0.03	0.03	0.01	-0.05
0.300	0.01	0.01	0.00	0.01	0.01	0.01	0.01	0.01	-0.03
0.350	0.01	0.01	0.00	-0.01	0.00	0.01	0.01	0.01	-0.02
0.400	0.01	0.01	-0.01	-0.01	0.00	0.01	0.00	0.01	-0.01
0.450	0.01	0.00	-0.01	-0.01	0.00	0.01	0.00	0.01	0.00
0.500	0.01	0.00	-0.01	-0.01	0.00	0.00	0.00	0.01	0.00
0.550	0.01	0.00	-0.01	-0.01	0.00	0.00	0.00	0.01	0.00
0.600	0.01	0.01	0.00	0.00	0.00	0.01	0.00	0.01	0.00
0.650	0.02	0.00	0.00	0.00	0.00	0.01	0.01	0.01	0.00
0.700	0.02	0.01	0.00	0.01	0.00	0.01	0.01	0.01	0.00
0.750	0.03	0.01	0.01	0.01	0.01	0.01	0.01	0.01	0.00
0.800	0.03	0.01	0.01	0.02	0.01	0.01	0.01	0.01	-0.01
0.850	0.04	0.01	0.01	0.02	0.01	0.01	0.01	0.01	-0.02
0.900	0.04	0.01	0.00	0.02	0.01	0.01	0.01	0.00	-0.05
0.950	0.04	0.01	0.00	0.03	0.01	0.01	0.00	-0.01	-0.09

TABLE 8—continued

9% RAE 101. Values of  $C_p$  for  $R = 2.2 \times 10^6$  and  $\alpha = -4.16^\circ$

$x/c$ $\eta$	0.195	0.383	0.556	0.707	0.831	0.882	0.924	0.957	0.981
0.001	0.11	0.09	0.09	0.04	-0.12	-0.15	-0.20	-0.26	-0.32
0.003	0.19	0.18	0.18	0.12	0.01	-0.09	-0.15	-0.22	-0.29
0.006	0.25	0.23	0.23	0.17	0.06	-0.03	-0.11	-0.19	-0.26
0.010	0.24	0.25	0.25	0.19	0.09	0.01	-0.07	-0.16	-0.23
0.015	0.23	0.24	0.24	0.19	0.11	0.04	-0.03	-0.13	-0.22
0.025	0.20	0.21	0.21	0.16	0.12	0.06	0.01	-0.10	-0.18
0.035	0.17	0.19	0.18	0.16	0.12	0.07	0.03	-0.07	-0.15
0.050	0.14	0.15	0.15	0.13	0.11	0.07	0.04	-0.04	-0.12
0.075	0.10	0.11	0.10	0.09	0.08	0.06	0.04	-0.02	-0.09
0.100	0.07	0.07	0.07	0.06	0.05	0.05	0.04	-0.01	-0.07
0.125	0.05	0.05	0.05	0.03	0.03	0.04	0.03	0.00	-0.06
0.150	0.03	0.03	0.02	0.02	0.02	0.02	0.02	-0.01	-0.04
0.200	0.00	0.00	-0.01	-0.01	0.00	0.00	0.01	0.00	-0.03
0.250	-0.02	-0.02	-0.03	-0.03	-0.02	-0.01	0.00	0.00	-0.02
0.300	-0.04	-0.04	-0.05	-0.04	-0.03	-0.02	-0.01	-0.01	-0.02
0.350	-0.04	-0.04	-0.05	-0.05	-0.03	-0.02	-0.02	-0.01	-0.02
0.400	-0.03	-0.03	-0.04	-0.04	-0.03	-0.02	-0.02	-0.01	-0.01
0.450	-0.02	-0.03	-0.04	-0.04	-0.03	-0.02	-0.01	0.00	0.00
0.500	-0.02	-0.02	-0.03	-0.02	-0.02	-0.02	-0.01	0.00	0.00
0.550	-0.02	-0.02	-0.03	-0.03	-0.02	-0.02	-0.01	0.00	0.00
0.600	-0.01	-0.01	-0.02	-0.02	-0.01	-0.01	0.00	0.00	0.00
0.650	0.00	-0.01	-0.01	-0.01	-0.01	0.00	0.00	0.00	0.01
0.700	0.01	-0.01	-0.01	0.00	-0.01	0.00	0.01	0.01	0.01
0.750	0.01	-0.01	-0.01	0.00	0.01	0.01	0.02	0.01	0.01
0.800	0.02	0.00	0.00	0.01	0.01	0.01	0.03	0.02	0.01
0.850	0.03	0.00	0.01	0.01	0.01	0.02	0.03	0.01	0.01
0.900	0.03	0.01	0.00	0.02	0.02	0.03	0.03	0.01	0.01
0.950	0.04	0.02	0.00	0.03	0.03	0.04	0.03	0.01	0.00

9% RAE 101. Values of  $C_p$  for  $R = 2.2 \times 10^6$  and  $\alpha = -2.08^\circ$

$x/c$ $\eta$	0.195	0.383	0.556	0.707	0.831	0.882	0.924	0.957	0.981
0.001	0.22	0.23	0.23	0.18	0.07	0.03	-0.01	-0.06	-0.09
0.003	0.24	0.25	0.24	0.20	0.11	0.06	0.01	-0.03	-0.07
0.006	0.24	0.23	0.23	0.19	0.12	0.07	0.03	-0.02	-0.06
0.010	0.20	0.20	0.20	0.17	0.12	0.08	0.04	-0.01	-0.05
0.015	0.17	0.18	0.17	0.16	0.11	0.07	0.04	0.00	-0.04
0.025	0.13	0.12	0.12	0.10	0.09	0.06	0.04	0.00	-0.04
0.035	0.09	0.09	0.08	0.07	0.07	0.05	0.04	0.00	-0.02
0.050	0.05	0.05	0.04	0.03	0.04	0.03	0.03	0.00	-0.01
0.075	0.01	0.01	0.00	0.00	0.00	0.00	0.01	0.00	-0.01
0.100	-0.02	-0.02	-0.02	-0.03	-0.02	-0.01	0.00	0.00	-0.01
0.125	-0.03	-0.04	-0.04	-0.05	-0.04	-0.03	-0.02	-0.01	-0.01
0.150	-0.05	-0.05	-0.06	-0.06	-0.05	-0.04	-0.03	-0.02	-0.01
0.200	-0.07	-0.07	-0.08	-0.08	-0.07	-0.05	-0.04	-0.02	-0.01
0.250	-0.08	-0.09	-0.10	-0.10	-0.08	-0.06	-0.05	-0.03	-0.01
0.300	-0.09	-0.09	-0.10	-0.10	-0.09	-0.07	-0.06	-0.04	-0.02
0.350	-0.08	-0.09	-0.10	-0.10	-0.08	-0.07	-0.06	-0.04	-0.02
0.400	-0.07	-0.08	-0.09	-0.10	-0.08	-0.06	-0.05	-0.03	-0.02
0.450	-0.06	-0.07	-0.08	-0.08	-0.06	-0.06	-0.04	-0.02	-0.01
0.500	-0.06	-0.06	-0.07	-0.07	-0.05	-0.05	-0.04	-0.02	-0.01
0.550	-0.04	-0.04	-0.06	-0.06	-0.04	-0.04	-0.03	-0.02	0.00
0.600	-0.03	-0.04	-0.05	-0.04	-0.04	-0.03	-0.02	-0.01	0.00
0.650	-0.02	-0.04	-0.03	-0.03	-0.03	-0.01	-0.01	0.00	0.01
0.700	-0.01	-0.02	-0.03	-0.02	0.02	0.00	0.01	0.01	0.02
0.750	0.00	-0.02	-0.01	-0.01	0.00	0.00	0.02	0.02	0.02
0.800	0.01	-0.01	-0.01	0.00	0.01	0.01	0.02	0.03	0.03
0.850	0.02	0.00	0.00	0.00	0.01	0.02	0.03	0.03	0.03
0.900	0.03	0.01	0.00	0.01	0.02	0.03	0.03	0.03	0.03
0.950	0.04	0.01	0.01	0.02	0.03	0.04	0.04	0.04	0.04

TABLE 8—continued

9% RAE 101. Values of  $C_p$  for  $R = 2.2 \times 10^6$  and  $\alpha = -1.04^\circ$

$x/c$	$\eta$	0.195	0.383	0.556	0.707	0.831	0.882	0.924	0.957	0.981
0.001		0.23	0.24	0.24	0.20	0.10	0.07	0.03	-0.01	-0.01
0.003		0.22	0.23	0.22	0.18	0.12	0.07	0.04	0.00	-0.01
0.006		0.21	0.20	0.19	0.16	0.11	0.07	0.04	0.00	-0.01
0.010		0.16	0.15	0.15	0.12	0.09	0.07	0.04	0.01	0.00
0.015		0.12	0.12	0.10	0.08	0.08	0.05	0.04	0.01	0.00
0.025		0.07	0.06	0.05	0.04	0.04	0.03	0.03	0.01	-0.01
0.035		0.03	0.03	0.02	0.01	0.02	0.01	0.01	0.00	-0.01
0.050		0.00	-0.01	-0.02	-0.02	-0.01	-0.02	-0.01	-0.01	-0.01
0.075		-0.04	-0.04	-0.05	-0.06	-0.04	-0.04	-0.03	-0.02	-0.02
0.100		-0.06	-0.06	-0.07	-0.08	-0.07	-0.06	-0.04	-0.03	-0.02
0.125		-0.08	-0.08	-0.09	-0.09	-0.08	-0.07	-0.05	-0.04	-0.03
0.150		-0.09	-0.09	-0.10	-0.10	-0.09	-0.08	-0.06	-0.05	-0.04
0.200		-0.11	-0.11	-0.11	-0.12	-0.10	-0.09	-0.08	-0.06	-0.05
0.250		-0.12	-0.11	-0.13	-0.13	-0.11	-0.10	-0.09	-0.06	-0.05
0.300		-0.13	-0.12	-0.13	-0.13	-0.11	-0.10	-0.09	-0.07	-0.06
0.350		-0.11	-0.11	-0.12	-0.12	-0.10	-0.10	-0.08	-0.06	-0.06
0.400		-0.10	-0.10	-0.11	-0.11	-0.09	-0.08	-0.07	-0.05	-0.05
0.450		-0.09	-0.09	-0.10	-0.10	-0.08	-0.07	-0.06	-0.04	-0.04
0.500		-0.08	-0.08	-0.09	-0.09	-0.07	-0.07	-0.05	-0.04	-0.03
0.550		-0.06	-0.06	-0.07	-0.07	-0.05	-0.05	-0.05	-0.04	-0.02
0.600		-0.05	-0.04	-0.05	-0.05	-0.04	-0.03	-0.03	-0.02	0.00
0.650		-0.04	-0.04	-0.04	-0.04	-0.03	-0.02	-0.01	0.00	0.01
0.700		-0.02	-0.03	-0.03	-0.02	-0.03	-0.01	0.00	0.00	0.02
0.750		-0.01	-0.02	-0.02	-0.02	-0.01	0.00	0.01	0.01	0.02
0.800		0.00	-0.01	-0.01	-0.01	0.00	0.01	0.02	0.02	0.03
0.850		0.01	-0.01	0.00	0.00	0.01	0.02	0.02	0.03	0.04
0.900		0.02	0.00	0.00	0.01	0.02	0.03	0.03	0.03	0.05
0.950		0.03	0.02	0.01	0.02	0.03	0.04	0.04	0.04	0.06

9% RAE 101. Values of  $C_p$  for  $R = 2.2 \times 10^6$  and  $\alpha = 0^\circ$ 

$x/c$	$\eta$	0.195	0.383	0.556	0.707	0.831	0.882	0.924	0.957	0.981
0.001		0.23	0.22	0.22	0.17	0.10	0.07	0.04	0.00	-0.01
0.003		0.19	0.18	0.17	0.14	0.09	0.06	0.04	0.00	-0.01
0.006		0.13	0.14	0.12	0.10	0.06	0.04	0.03	0.00	-0.01
0.010		0.10	0.08	0.07	0.05	0.03	0.02	0.01	-0.01	-0.01
0.015		0.05	0.04	0.02	0.00	0.02	0.00	0.00	-0.01	-0.01
0.025		0.01	-0.02	-0.03	-0.04	-0.02	-0.03	-0.02	-0.02	-0.01
0.035		-0.03	-0.04	-0.06	-0.06	-0.05	-0.05	-0.04	-0.04	-0.02
0.050		-0.06	-0.08	-0.09	-0.09	-0.07	-0.07	-0.05	-0.05	-0.02
0.075		-0.09	-0.10	-0.11	-0.12	-0.10	-0.09	-0.08	-0.06	-0.03
0.100		-0.11	-0.11	-0.13	-0.13	-0.12	-0.11	-0.09	-0.07	-0.04
0.125		-0.12	-0.13	-0.14	-0.14	-0.13	-0.11	-0.10	-0.08	-0.05
0.150		-0.13	-0.13	-0.14	-0.14	-0.13	-0.12	-0.11	-0.09	-0.06
0.200		-0.14	-0.14	-0.15	-0.15	-0.14	-0.12	-0.12	-0.10	-0.07
0.250		-0.15	-0.15	-0.16	-0.16	-0.15	-0.13	-0.12	-0.10	-0.07
0.300		-0.15	-0.15	-0.16	-0.16	-0.15	-0.13	-0.12	-0.10	-0.07
0.350		-0.13	-0.13	-0.14	-0.15	-0.13	-0.12	-0.11	-0.09	-0.07
0.400		-0.12	-0.12	-0.13	-0.13	-0.12	-0.11	-0.10	-0.08	-0.06
0.450		-0.11	-0.11	-0.12	-0.12	-0.11	-0.10	-0.09	-0.07	-0.05
0.500		-0.09	-0.09	-0.10	-0.10	-0.09	-0.08	-0.06	-0.05	-0.04
0.550		-0.06	-0.07	-0.08	-0.08	-0.06	-0.06	-0.04	-0.03	-0.02
0.600		-0.05	-0.06	-0.06	-0.06	-0.05	-0.04	-0.03	-0.02	-0.01
0.650		-0.04	-0.05	-0.05	-0.04	-0.04	-0.03	-0.02	-0.01	0.00
0.700		-0.03	-0.04	-0.04	-0.03	-0.03	-0.02	-0.01	0.00	0.01
0.750		-0.01	-0.03	-0.03	-0.02	-0.02	-0.01	0.00	0.01	0.02
0.800		0.00	-0.02	-0.01	-0.01	0.00	0.00	0.01	0.02	0.03
0.850		0.01	-0.01	-0.01	0.00	0.00	0.01	0.02	0.03	0.04
0.900		0.03	0.00	0.00	0.01	0.02	0.03	0.03	0.04	0.05
0.950		0.04	0.01	0.01	0.02	0.03	0.04	0.05	0.05	0.06

TABLE 8—continued

9% RAE 101. Values of  $C_p$  for  $R = 2.2 \times 10^6$  and  $\alpha = 1.04^\circ$

$x/c$ $\eta$	0.195	0.383	0.556	0.707	0.831	0.882	0.924	0.957	0.981
0.001	0.18	0.18	0.15	0.11	0.06	0.03	0.01	-0.02	-0.03
0.003	0.13	0.11	0.08	0.06	0.03	0.01	-0.01	-0.03	-0.03
0.006	0.09	0.05	0.02	0.01	-0.01	-0.02	-0.02	-0.04	-0.04
0.010	0.02	-0.02	-0.04	-0.04	-0.04	-0.05	-0.04	-0.05	-0.04
0.015	-0.03	-0.06	-0.09	-0.10	-0.06	-0.07	-0.06	-0.06	-0.05
0.025	-0.07	-0.10	-0.13	-0.12	-0.10	-0.10	-0.08	-0.08	-0.06
0.035	-0.10	-0.12	-0.15	-0.14	-0.12	-0.12	-0.10	-0.10	-0.07
0.050	-0.12	-0.15	-0.17	-0.17	-0.14	-0.14	-0.12	-0.11	-0.07
0.075	-0.15	-0.16	-0.18	-0.19	-0.16	-0.16	-0.14	-0.12	-0.09
0.100	-0.16	-0.17	-0.19	-0.19	-0.17	-0.16	-0.15	-0.13	-0.10
0.125	-0.17	-0.18	-0.20	-0.19	-0.18	-0.16	-0.15	-0.14	-0.11
0.150	-0.17	-0.18	-0.20	-0.19	-0.18	-0.17	-0.16	-0.15	-0.12
0.200	-0.18	-0.18	-0.20	-0.19	-0.18	-0.17	-0.16	-0.15	-0.13
0.250	-0.18	-0.18	-0.20	-0.19	-0.18	-0.17	-0.16	-0.15	-0.13
0.300	-0.18	-0.18	-0.19	-0.19	-0.17	-0.17	-0.15	-0.14	-0.12
0.350	-0.16	-0.16	-0.17	-0.17	-0.16	-0.15	-0.14	-0.13	-0.11
0.400	-0.15	-0.15	-0.16	-0.15	-0.14	-0.13	-0.13	-0.11	-0.10
0.450	-0.13	-0.12	-0.14	-0.14	-0.13	-0.11	-0.11	-0.10	-0.10
0.500	-0.10	-0.10	-0.10	-0.10	-0.09	-0.09	-0.07	-0.06	-0.08
0.550	-0.08	-0.08	-0.09	-0.09	-0.07	-0.07	-0.06	-0.05	-0.04
0.600	-0.06	-0.06	-0.07	-0.07	-0.06	-0.06	-0.05	-0.04	-0.02
0.650	-0.05	-0.06	-0.06	-0.06	-0.05	-0.04	-0.03	-0.02	-0.01
0.700	-0.04	-0.04	-0.05	-0.04	-0.04	-0.02	-0.01	-0.01	0.00
0.750	-0.02	-0.04	-0.03	-0.03	-0.02	-0.01	0.00	0.00	0.01
0.800	-0.01	-0.02	-0.02	-0.02	0.00	0.00	0.01	0.02	0.02
0.850	0.01	-0.02	-0.01	-0.01	0.00	0.02	0.02	0.02	0.03
0.900	0.02	0.00	0.00	0.01	0.02	0.03	0.03	0.04	0.04
0.950	0.03	0.01	0.01	0.02	0.03	0.04	0.04	0.05	0.05

9% RAE 101. Values of  $C_p$  for  $R = 2.2 \times 10^6$  and  $\alpha = 2.08^\circ$

$x/c$ $\eta$	0.195	0.383	0.556	0.707	0.831	0.882	0.924	0.957	0.981
0.001	0.13	0.07	0.05	0.01	-0.03	-0.04	-0.06	-0.09	-0.10
0.003	0.05	-0.01	-0.04	-0.05	-0.07	-0.08	-0.08	-0.10	-0.10
0.006	0.01	-0.07	-0.11	-0.11	-0.11	-0.11	-0.11	-0.11	-0.11
0.010	-0.06	-0.13	-0.17	-0.17	-0.15	-0.15	-0.13	-0.13	-0.12
0.015	-0.10	-0.17	-0.21	-0.21	-0.16	-0.17	-0.15	-0.15	-0.12
0.025	-0.15	-0.20	-0.24	-0.23	-0.20	-0.20	-0.17	-0.16	-0.14
0.035	-0.17	-0.22	-0.24	-0.24	-0.22	-0.22	-0.19	-0.19	-0.15
0.050	-0.19	-0.24	-0.25	-0.26	-0.23	-0.23	-0.21	-0.20	-0.15
0.075	-0.21	-0.23	-0.25	-0.26	-0.24	-0.23	-0.22	-0.20	-0.17
0.100	-0.21	-0.23	-0.25	-0.26	-0.24	-0.23	-0.22	-0.20	-0.18
0.125	-0.21	-0.23	-0.25	-0.25	-0.24	-0.22	-0.22	-0.21	-0.19
0.150	-0.21	-0.22	-0.24	-0.25	-0.23	-0.22	-0.22	-0.21	-0.20
0.200	-0.21	-0.22	-0.23	-0.24	-0.23	-0.22	-0.21	-0.20	-0.20
0.250	-0.21	-0.22	-0.23	-0.23	-0.22	-0.21	-0.21	-0.20	-0.20
0.300	-0.20	-0.21	-0.22	-0.21	-0.20	-0.20	-0.19	-0.19	-0.19
0.350	-0.18	-0.19	-0.20	-0.20	-0.19	-0.18	-0.17	-0.17	-0.18
0.400	-0.17	-0.17	-0.18	-0.17	-0.17	-0.17	-0.16	-0.16	-0.17
0.450	-0.13	-0.13	-0.14	-0.14	-0.14	-0.12	-0.12	-0.13	-0.17
0.500	-0.11	-0.11	-0.12	-0.11	-0.10	-0.11	-0.10	-0.07	-0.16
0.550	-0.09	-0.09	-0.10	-0.10	-0.09	-0.08	-0.07	-0.06	-0.07
0.600	-0.07	-0.08	-0.08	-0.08	-0.08	-0.07	-0.06	-0.05	-0.05
0.650	-0.05	-0.07	-0.06	-0.06	-0.06	-0.05	-0.04	-0.03	-0.03
0.700	-0.04	-0.05	-0.05	-0.04	-0.05	-0.03	-0.02	-0.02	-0.02
0.750	-0.02	-0.04	-0.03	-0.03	-0.02	-0.02	-0.01	0.00	-0.01
0.800	-0.01	-0.02	-0.02	-0.02	-0.01	-0.01	0.01	0.01	0.00
0.850	0.01	-0.02	-0.01	-0.01	0.00	0.01	0.02	0.02	0.01
0.900	0.02	0.00	0.00	0.01	0.02	0.03	0.03	0.03	0.02
0.950	0.04	0.01	0.01	0.02	0.04	0.04	0.05	0.04	0.03

TABLE 8—continued

9% RAE 101. Values of  $C_p$  for  $R = 2.2 \times 10^6$  and  $\alpha = 4.16^\circ$

$x/c$	$\eta$	0.195	0.383	0.556	0.707	0.831	0.882	0.924	0.957	0.981
0.001		-0.09	-0.22	-0.29	-0.30	-0.32	-0.30	-0.31	-0.32	-0.34
0.003		-0.19	-0.33	-0.40	-0.37	-0.37	-0.37	-0.35	-0.34	-0.34
0.006		-0.24	-0.39	-0.46	-0.43	-0.41	-0.40	-0.39	-0.37	-0.36
0.010		-0.31	-0.43	-0.50	-0.50	-0.43	-0.43	-0.41	-0.39	-0.37
0.015		-0.34	-0.45	-0.53	-0.52	-0.44	-0.45	-0.42	-0.41	-0.38
0.025		-0.35	-0.45	-0.50	-0.49	-0.45	-0.45	-0.43	-0.43	-0.40
0.035		-0.36	-0.44	-0.47	-0.47	-0.45	-0.45	-0.43	-0.43	-0.41
0.050		-0.35	-0.42	-0.45	-0.46	-0.43	-0.44	-0.43	-0.44	-0.41
0.075		-0.34	-0.39	-0.42	-0.42	-0.41	-0.41	-0.42	-0.42	-0.42
0.100		-0.32	-0.36	-0.39	-0.39	-0.38	-0.39	-0.40	-0.41	-0.41
0.125		-0.31	-0.35	-0.37	-0.37	-0.37	-0.36	-0.38	-0.40	-0.41
0.150		-0.30	-0.33	-0.35	-0.35	-0.35	-0.35	-0.37	-0.39	-0.41
0.200		-0.29	-0.31	-0.32	-0.33	-0.32	-0.32	-0.34	-0.36	-0.39
0.250		-0.27	-0.29	-0.30	-0.30	-0.30	-0.31	-0.32	-0.35	-0.38
0.300		-0.26	-0.26	-0.27	-0.25	-0.26	-0.28	-0.27	-0.35	-0.38
0.350		-0.24	-0.22	-0.24	-0.23	-0.22	-0.23	-0.23	-0.29	-0.38
0.400		-0.18	-0.21	-0.21	-0.20	-0.20	-0.19	-0.20	-0.19	-0.39
0.450		-0.16	-0.17	-0.18	-0.18	-0.16	-0.16	-0.16	-0.16	-0.33
0.500		-0.14	-0.14	-0.15	-0.14	-0.13	-0.14	-0.13	-0.13	-0.25
0.550		-0.13	-0.12	-0.13	-0.12	-0.11	-0.11	-0.11	-0.11	-0.22
0.600		-0.10	-0.10	-0.10	-0.10	-0.09	-0.08	-0.08	-0.09	-0.21
0.650		-0.07	-0.08	-0.08	-0.07	-0.07	-0.06	-0.06	-0.06	-0.19
0.700		-0.06	-0.06	-0.06	-0.05	-0.05	-0.04	-0.04	-0.04	-0.16
0.750		-0.03	-0.05	-0.04	-0.04	-0.03	-0.02	-0.02	-0.03	-0.09
0.800		-0.02	-0.03	-0.03	-0.02	-0.01	-0.01	-0.01	-0.01	-0.04
0.850		0.00	-0.02	-0.01	0.00	0.01	0.01	0.01	0.00	-0.02
0.900		0.02	0.00	0.00	0.01	0.02	0.02	0.02	0.01	-0.02
0.950		0.04	0.01	0.01	0.03	0.04	0.04	0.03	0.02	-0.02

9% RAE 101. Values of  $C_p$  for  $R = 2.2 \times 10^6$  and  $\alpha = 6.24^\circ$

$x/c$	$\eta$	0.195	0.383	0.556	0.707	0.831	0.882	0.924	0.957	0.981
0.001		-0.39	-0.64	-0.74	-0.72	-0.71	-0.65	-0.63	-0.61	-0.62
0.003		-0.50	-0.75	-0.84	-0.78	-0.75	-0.73	-0.68	-0.63	-0.61
0.006		-0.54	-0.79	-0.88	-0.82	-0.77	-0.76	-0.73	-0.67	-0.62
0.010		-0.60	-0.79	-0.88	-0.87	-0.77	-0.77	-0.74	-0.69	-0.63
0.015		-0.61	-0.77	-0.87	-0.86	-0.76	-0.77	-0.72	-0.70	-0.63
0.025		-0.57	-0.73	-0.79	-0.77	-0.73	-0.73	-0.71	-0.70	-0.64
0.035		-0.55	-0.67	-0.73	-0.72	-0.70	-0.69	-0.68	-0.70	-0.64
0.050		-0.51	-0.63	-0.68	-0.67	-0.65	-0.65	-0.66	-0.67	-0.62
0.075		-0.48	-0.57	-0.60	-0.60	-0.60	-0.61	-0.62	-0.64	-0.60
0.100		-0.44	-0.50	-0.51	-0.52	-0.56	-0.57	-0.60	-0.61	-0.57
0.125		-0.42	-0.44	-0.47	-0.47	-0.48	-0.46	-0.59	-0.60	-0.55
0.150		-0.40	-0.42	-0.44	-0.43	-0.44	-0.44	-0.48	-0.59	-0.54
0.200		-0.35	-0.37	-0.39	-0.39	-0.40	-0.40	-0.41	-0.46	-0.52
0.250		-0.33	-0.35	-0.36	-0.36	-0.36	-0.36	-0.36	-0.37	-0.52
0.300		-0.30	-0.32	-0.32	-0.31	-0.32	-0.32	-0.32	-0.33	-0.52
0.350		-0.27	-0.27	-0.28	-0.28	-0.27	-0.27	-0.26	-0.25	-0.44
0.400		-0.22	-0.22	-0.23	-0.23	-0.22	-0.21	-0.21	-0.18	-0.40
0.450		-0.19	-0.19	-0.20	-0.20	-0.18	-0.17	-0.16	-0.13	-0.42
0.500		-0.17	-0.16	-0.16	-0.16	-0.14	-0.14	-0.12	-0.10	-0.45
0.550		-0.14	-0.13	-0.13	-0.13	-0.11	-0.11	-0.10	-0.09	-0.43
0.600		-0.11	-0.11	-0.10	-0.10	-0.09	-0.08	-0.08	-0.09	-0.36
0.650		-0.08	-0.09	-0.08	-0.08	-0.06	-0.06	-0.07	-0.08	-0.29
0.700		-0.06	-0.07	-0.06	-0.06	-0.05	-0.05	-0.06	-0.08	-0.23
0.750		-0.04	-0.05	-0.04	-0.04	-0.04	-0.04	-0.06	-0.08	-0.20
0.800		-0.02	-0.04	-0.03	-0.03	-0.02	-0.04	-0.06	-0.08	-0.18
0.850		-0.01	-0.02	-0.02	-0.02	-0.02	-0.04	-0.07	-0.08	-0.18
0.900		0.01	-0.02	-0.01	-0.01	-0.01	-0.03	-0.07	-0.10	-0.17
0.950		0.03	-0.01	-0.01	0.00	0.00	-0.03	-0.08	-0.11	-0.15

TABLE 8—continued

9% RAE 101. Values of  $C_p$  for  $R = 2.2 \times 10^6$  and  $\alpha = 7.28^\circ$ 

$x/c$	$\eta$	0.195	0.383	0.556	0.707	0.831	0.882	0.924	0.957	0.981
0.001		-0.59	-0.90	-1.03	-0.97	-0.94	-0.87	-0.81	-0.75	-0.64
0.003		-0.70	-1.00	-1.12	-1.02	-0.98	-0.94	-0.87	-0.77	-0.63
0.006		-0.73	-1.02	-1.14	-1.04	-0.98	-0.96	-0.91	-0.81	-0.63
0.010		-0.77	-0.99	-1.11	-1.08	-0.97	-0.97	-0.91	-0.82	-0.62
0.015		-0.76	-0.96	-1.07	-1.04	-0.94	-0.95	-0.89	-0.82	-0.62
0.025		-0.70	-0.88	-0.96	-0.93	-0.87	-0.89	-0.85	-0.82	-0.60
0.035		-0.66	-0.82	-0.91	-0.89	-0.84	-0.84	-0.81	-0.80	-0.57
0.050		-0.61	-0.76	-0.82	-0.81	-0.78	-0.79	-0.78	-0.76	-0.53
0.075		-0.57	-0.63	-0.65	-0.65	-0.71	-0.71	-0.73	-0.71	-0.50
0.100		-0.52	-0.54	-0.59	-0.58	-0.57	-0.57	-0.68	-0.67	-0.44
0.125		-0.45	-0.51	-0.54	-0.53	-0.54	-0.53	-0.56	-0.65	-0.40
0.150		-0.43	-0.49	-0.50	-0.48	-0.50	-0.51	-0.49	-0.60	-0.34
0.200		-0.40	-0.42	-0.43	-0.43	-0.43	-0.43	-0.43	-0.39	-0.27
0.250		-0.37	-0.38	-0.39	-0.38	-0.38	-0.37	-0.36	-0.30	-0.22
0.300		-0.33	-0.34	-0.34	-0.33	-0.33	-0.32	-0.29	-0.21	-0.20
0.350		-0.29	-0.29	-0.29	-0.28	-0.27	-0.25	-0.21	-0.16	-0.18
0.400		-0.25	-0.24	-0.24	-0.23	-0.21	-0.19	-0.17	-0.14	-0.17
0.450		-0.21	-0.20	-0.20	-0.19	-0.16	-0.15	-0.14	-0.14	-0.16
0.500		-0.18	-0.17	-0.16	-0.15	-0.13	-0.13	-0.13	-0.15	-0.15
0.550		-0.15	-0.13	-0.13	-0.12	-0.10	-0.11	-0.14	-0.16	-0.14
0.600		-0.12	-0.11	-0.10	-0.10	-0.09	-0.11	-0.15	-0.17	-0.12
0.650		-0.11	-0.09	-0.08	-0.08	-0.08	-0.11	-0.16	-0.18	-0.10
0.700		-0.07	-0.07	-0.07	-0.06	-0.07	-0.11	-0.17	-0.19	-0.08
0.750		-0.05	-0.06	-0.05	-0.06	-0.07	-0.12	-0.19	-0.21	-0.07
0.800		-0.03	-0.04	-0.04	-0.05	-0.07	-0.13	-0.21	-0.23	-0.08
0.850		-0.01	-0.04	-0.04	-0.05	-0.07	-0.13	-0.23	-0.27	-0.09
0.900		0.01	-0.03	-0.03	-0.04	-0.07	-0.13	-0.24	-0.27	-0.11
0.950		0.02	-0.02	-0.03	-0.04	-0.08	-0.11	-0.19	-0.21	-0.15

9% RAE 101. Values of  $C_p$  for  $R = 2.2 \times 10^6$  and  $\alpha = 8.31^\circ$ 

$x/c$	$\eta$	0.195	0.383	0.556	0.707	0.831	0.882	0.924	0.957	0.981
0.001		-0.81	-1.19	-1.34	-1.25	-1.20	-1.08	-0.98	-0.82	-0.43
0.003		-0.92	-1.29	-1.42	-1.29	-1.22	-1.16	-1.03	-0.84	-0.41
0.006		-0.93	-1.28	-1.41	-1.30	-1.21	-1.17	-1.07	-0.86	-0.39
0.010		-0.95	-1.23	-1.36	-1.31	-1.18	-1.16	-1.06	-0.87	-0.36
0.015		-0.93	-1.17	-1.29	-1.25	-1.14	-1.13	-1.03	-0.86	-0.34
0.025		-0.85	-1.06	-1.17	-1.13	-1.04	-1.04	-0.98	-0.84	-0.29
0.035		-0.79	-0.99	-1.04	-1.02	-0.99	-0.96	-0.92	-0.82	-0.24
0.050		-0.72	-0.83	-0.88	-0.86	-0.87	-0.87	-0.86	-0.75	-0.18
0.075		-0.62	-0.70	-0.75	-0.75	-0.75	-0.73	-0.76	-0.63	-0.14
0.100		-0.55	-0.63	-0.67	-0.66	-0.66	-0.64	-0.64	-0.49	-0.13
0.125		-0.51	-0.58	-0.60	-0.60	-0.59	-0.57	-0.56	-0.40	-0.11
0.150		-0.49	-0.53	-0.55	-0.53	-0.54	-0.53	-0.49	-0.32	-0.11
0.200		-0.44	-0.46	-0.47	-0.46	-0.45	-0.43	-0.37	-0.20	-0.09
0.250		-0.40	-0.41	-0.42	-0.40	-0.38	-0.34	-0.25	-0.18	-0.09
0.300		-0.36	-0.36	-0.36	-0.34	-0.30	-0.25	-0.19	-0.17	-0.09
0.350		-0.31	-0.30	-0.30	-0.27	-0.23	-0.18	-0.17	-0.16	-0.09
0.400		-0.27	-0.25	-0.24	-0.22	-0.18	-0.16	-0.17	-0.16	-0.09
0.450		-0.23	-0.20	-0.20	-0.17	-0.15	-0.15	-0.18	-0.15	-0.09
0.500		-0.19	-0.17	-0.16	-0.14	-0.14	-0.15	-0.19	-0.15	-0.08
0.550		-0.16	-0.14	-0.13	-0.12	-0.14	-0.16	-0.20	-0.15	-0.07
0.600		-0.13	-0.11	-0.11	-0.11	-0.14	-0.17	-0.21	-0.14	-0.07
0.650		-0.10	-0.10	-0.10	-0.10	-0.14	-0.18	-0.23	-0.13	-0.06
0.700		-0.08	-0.09	-0.09	-0.10	-0.14	-0.20	-0.25	-0.12	-0.07
0.750		-0.06	-0.08	-0.08	-0.10	-0.15	-0.23	-0.28	-0.11	-0.07
0.800		-0.04	-0.07	-0.08	-0.10	-0.16	-0.26	-0.32	-0.13	-0.10
0.850		-0.02	-0.06	-0.07	-0.11	-0.17	-0.29	-0.37	-0.16	-0.11
0.900		-0.01	-0.06	-0.08	-0.11	-0.18	-0.30	-0.35	-0.22	-0.15
0.950		0.02	-0.05	-0.08	-0.11	-0.15	-0.23	-0.34	-0.34	-0.14



TABLE 8—continued

9% RAE 101. Values of  $C_p$  for  $R = 2.2 \times 10^6$  and  $\alpha = 9.36^\circ$

$x/c$ $\eta$	0.195	0.383	0.556	0.707	0.831	0.882	0.924	0.957	0.981
0.001	-1.06	-1.54	-1.70	-1.57	-1.47	-1.28	-1.09	-0.75	-0.21
0.003	-1.17	-1.61	-1.77	-1.59	-1.47	-1.35	-1.13	-0.75	-0.18
0.006	-1.16	-1.58	-1.72	-1.57	-1.43	-1.35	-1.16	-0.75	-0.16
0.010	-1.16	-1.49	-1.63	-1.56	-1.37	-1.33	-1.14	-0.74	-0.13
0.015	-1.11	-1.41	-1.54	-1.47	-1.32	-1.28	-1.09	-0.71	-0.12
0.025	-1.01	-1.28	-1.43	-1.36	-1.20	-1.17	-1.02	-0.66	-0.10
0.035	-0.95	-1.11	-1.07	-1.07	-1.12	-1.06	-0.95	-0.59	-0.09
0.050	-0.78	-0.95	-1.01	-0.98	-0.94	-0.92	-0.84	-0.48	-0.08
0.075	-0.70	-0.79	-0.85	-0.84	-0.80	-0.76	-0.70	-0.31	-0.08
0.100	-0.63	-0.71	-0.74	-0.72	-0.69	-0.64	-0.54	-0.22	-0.07
0.125	-0.57	-0.64	-0.66	-0.64	-0.61	-0.55	-0.42	-0.20	-0.07
0.150	-0.54	-0.59	-0.60	-0.57	-0.54	-0.48	-0.32	-0.18	-0.07
0.200	-0.48	-0.50	-0.50	-0.48	-0.42	-0.32	-0.22	-0.16	-0.07
0.250	-0.43	-0.44	-0.44	-0.40	-0.32	-0.23	-0.19	-0.15	-0.07
0.300	-0.39	-0.39	-0.36	-0.32	-0.24	-0.19	-0.19	-0.14	-0.07
0.350	-0.33	-0.32	-0.29	-0.24	-0.20	-0.18	-0.19	-0.13	-0.06
0.400	-0.28	-0.26	-0.23	-0.19	-0.19	-0.18	-0.20	-0.13	-0.06
0.450	-0.24	-0.22	-0.19	-0.17	-0.19	-0.18	-0.20	-0.13	-0.06
0.500	-0.21	-0.18	-0.16	-0.16	-0.19	-0.19	-0.20	-0.11	-0.06
0.550	-0.17	-0.15	-0.15	-0.15	-0.20	-0.20	-0.21	-0.11	-0.05
0.600	-0.14	-0.13	-0.14	-0.16	-0.20	-0.21	-0.21	-0.10	-0.05
0.650	-0.11	-0.13	-0.14	-0.16	-0.21	-0.23	-0.20	-0.09	-0.06
0.700	-0.09	-0.12	-0.13	-0.16	-0.23	-0.26	-0.21	-0.08	-0.06
0.750	-0.07	-0.11	-0.13	-0.18	-0.24	-0.31	-0.23	-0.08	-0.07
0.800	-0.05	-0.11	-0.14	-0.20	-0.28	-0.36	-0.26	-0.10	-0.09
0.850	-0.03	-0.11	-0.15	-0.22	-0.29	-0.37	-0.27	-0.13	-0.10
0.900	-0.02	-0.10	-0.16	-0.23	-0.26	-0.34	-0.27	-0.17	-0.11
0.950	0.00	-0.09	-0.14	-0.19	-0.19	-0.27	-0.34	-0.21	-0.10

9% RAE 101. Values of  $C_p$  for  $R = 2.2 \times 10^6$  and  $\alpha = 10.40^\circ$ 

$x/c$ $\eta$	0.195	0.383	0.556	0.707	0.831	0.882	0.924	0.957	0.981
0.001	-1.34	-1.92	-2.13	-1.94	-1.74	-1.43	-1.06	-0.44	-0.13
0.003	-1.43	-1.98	-2.16	-1.92	-1.71	-1.49	-1.08	-0.41	-0.11
0.006	-1.41	-1.91	-2.08	-1.88	-1.65	-1.47	-1.09	-0.38	-0.09
0.010	-1.38	-1.78	-1.95	-1.84	-1.56	-1.42	-1.04	-0.34	-0.08
0.015	-1.31	-1.67	-1.83	-1.73	-1.50	-1.35	-0.95	-0.29	-0.07
0.025	-1.20	-1.54	-1.69	-1.62	-1.36	-1.24	-0.89	-0.22	-0.07
0.035	-1.07	-1.20	-1.25	-1.18	-1.19	-1.03	-0.75	-0.18	-0.07
0.050	-0.89	-1.09	-1.15	-1.10	-1.00	-0.88	-0.57	-0.15	-0.06
0.075	-0.78	-0.90	-0.96	-0.92	-0.82	-0.68	-0.38	-0.13	-0.06
0.100	-0.70	-0.79	-0.82	-0.78	-0.69	-0.52	-0.26	-0.12	-0.06
0.125	-0.63	-0.72	-0.73	-0.68	-0.57	-0.38	-0.22	-0.12	-0.06
0.150	-0.59	-0.65	-0.65	-0.59	-0.48	-0.29	-0.21	-0.11	-0.06
0.200	-0.52	-0.54	-0.54	-0.47	-0.32	-0.23	-0.20	-0.11	-0.06
0.250	-0.47	-0.48	-0.45	-0.36	-0.26	-0.22	-0.19	-0.11	-0.06
0.300	-0.41	-0.41	-0.36	-0.27	-0.25	-0.21	-0.19	-0.11	-0.06
0.350	-0.35	-0.33	-0.29	-0.23	-0.25	-0.21	-0.18	-0.11	-0.05
0.400	-0.30	-0.27	-0.24	-0.21	-0.26	-0.22	-0.19	-0.10	-0.05
0.450	-0.25	-0.23	-0.22	-0.21	-0.27	-0.22	-0.18	-0.09	-0.05
0.500	-0.22	-0.20	-0.21	-0.21	-0.28	-0.23	-0.17	-0.09	-0.05
0.550	-0.18	-0.19	-0.20	-0.21	-0.28	-0.24	-0.16	-0.08	-0.05
0.600	-0.15	-0.17	-0.20	-0.23	-0.29	-0.25	-0.16	-0.08	-0.05
0.650	-0.12	-0.17	-0.21	-0.24	-0.31	-0.29	-0.16	-0.08	-0.06
0.700	-0.10	-0.17	-0.22	-0.27	-0.34	-0.31	-0.17	-0.08	-0.06
0.750	-0.08	-0.17	-0.25	-0.31	-0.36	-0.34	-0.18	-0.08	-0.06
0.800	-0.06	-0.17	-0.28	-0.35	-0.39	-0.36	-0.19	-0.09	-0.07
0.850	-0.04	-0.17	-0.30	-0.37	-0.36	-0.32	-0.20	-0.10	-0.07
0.900	-0.03	-0.15	-0.29	-0.32	-0.30	-0.29	-0.20	-0.11	-0.07
0.950	-0.01	-0.11	-0.19	-0.22	-0.29	-0.30	-0.22	-0.12	-0.07

TABLE 8—continued

9% RAE 101. Values of  $C_p$  for  $R = 2.2 \times 10^6$  and  $\alpha = 11.44^\circ$ 

$x/c$	$\eta$	0.195	0.383	0.556	0.707	0.831	0.882	0.924	0.957	0.981
0.001		-1.66	-2.34	-2.60	-2.36	-2.05	-1.52	-0.86	-0.25	-0.11
0.003		-1.74	-2.37	-2.59	-2.31	-1.98	-1.56	-0.84	-0.22	-0.09
0.006		-1.69	-2.26	-2.47	-2.22	-1.89	-1.50	-0.80	-0.18	-0.08
0.010		-1.62	-2.09	-2.30	-2.16	-1.78	-1.42	-0.75	-0.16	-0.07
0.015		-1.53	-1.99	-2.17	-2.03	-1.72	-1.35	-0.68	-0.13	-0.07
0.025		-1.42	-1.66	-1.73	-1.77	-1.44	-1.21	-0.50	-0.11	-0.06
0.035		-1.11	-1.39	-1.44	-1.36	-1.25	-0.86	-0.36	-0.11	-0.06
0.050		-1.01	-1.24	-1.30	-1.23	-1.04	-0.69	-0.27	-0.11	-0.06
0.075		-0.88	-1.01	-0.96	-1.00	-0.80	-0.43	-0.22	-0.11	-0.06
0.100		-0.77	-0.88	-0.90	-0.83	-0.61	-0.30	-0.22	-0.10	-0.06
0.125		-0.70	-0.79	-0.78	-0.71	-0.46	-0.27	-0.21	-0.10	-0.06
0.150		-0.65	-0.70	-0.69	-0.60	-0.37	-0.25	-0.20	-0.11	-0.06
0.200		-0.56	-0.59	-0.55	-0.44	-0.32	-0.24	-0.19	-0.10	-0.05
0.250		-0.50	-0.50	-0.44	-0.34	-0.32	-0.24	-0.18	-0.10	-0.05
0.300		-0.44	-0.42	-0.35	-0.30	-0.34	-0.25	-0.18	-0.10	-0.05
0.350		-0.37	-0.34	-0.31	-0.29	-0.36	-0.25	-0.18	-0.10	-0.05
0.400		-0.32	-0.29	-0.29	-0.29	-0.37	-0.26	-0.17	-0.09	-0.05
0.450		-0.27	-0.26	-0.29	-0.29	-0.38	-0.26	-0.16	-0.08	-0.05
0.500		-0.24	-0.24	-0.29	-0.29	-0.38	-0.25	-0.15	-0.08	-0.05
0.550		-0.20	-0.24	-0.29	-0.31	-0.38	-0.26	-0.15	-0.08	-0.06
0.600		-0.17	-0.24	-0.31	-0.33	-0.40	-0.28	-0.15	-0.08	-0.06
0.650		-0.14	-0.26	-0.35	-0.37	-0.44	-0.32	-0.15	-0.08	-0.06
0.700		-0.13	-0.26	-0.41	-0.45	-0.47	-0.34	-0.16	-0.09	-0.06
0.750		-0.10	-0.26	-0.47	-0.51	-0.47	-0.33	-0.17	-0.09	-0.06
0.800		-0.08	-0.24	-0.51	-0.54	-0.44	-0.31	-0.17	-0.10	-0.07
0.850		-0.06	-0.21	-0.49	-0.50	-0.35	-0.27	-0.18	-0.10	-0.07
0.900		-0.03	-0.15	-0.39	-0.35	-0.30	-0.26	-0.18	-0.11	-0.07
0.950		-0.01	-0.08	-0.18	-0.34	-0.35	-0.27	-0.17	-0.11	-0.06

9% RAE 101. Values of  $C_p$  for  $R = 2.2 \times 10^6$  and  $\alpha = 12.48^\circ$ 

$x/c$	$\eta$	0.195	0.383	0.556	0.707	0.831	0.883	0.924	0.957	0.981
0.001		-1.98	-2.81	-3.09	-2.78	-2.36	-1.57	-0.56	-0.25	-0.11
0.003		-2.04	-2.80	-3.04	-2.68	-2.23	-1.56	-0.52	-0.21	-0.11
0.006		-1.96	-2.64	-2.87	-2.57	-2.10	-1.48	-0.46	-0.18	-0.09
0.010		-1.87	-2.45	-2.68	-2.47	-1.99	-1.40	-0.40	-0.16	-0.09
0.015		-1.76	-2.35	-2.55	-2.33	-1.92	-1.34	-0.34	-0.15	-0.08
0.025		-1.64	-1.79	-1.88	-1.75	-1.41	-0.92	-0.29	-0.14	-0.08
0.035		-1.24	-1.58	-1.63	-1.51	-1.25	-0.65	-0.26	-0.14	-0.08
0.050		-1.13	-1.39	-1.43	-1.31	-0.98	-0.47	-0.24	-0.13	-0.08
0.075		-0.97	-1.12	-1.15	-1.03	-0.66	-0.36	-0.23	-0.13	-0.08
0.100		-0.84	-0.97	-0.96	-0.81	-0.49	-0.33	-0.22	-0.13	-0.08
0.125		-0.76	-0.86	-0.82	-0.65	-0.44	-0.32	-0.21	-0.13	-0.08
0.150		-0.70	-0.76	-0.71	-0.52	-0.43	-0.32	-0.21	-0.13	-0.09
0.200		-0.60	-0.63	-0.53	-0.43	-0.43	-0.31	-0.21	-0.14	-0.09
0.250		-0.53	-0.52	-0.43	-0.41	-0.45	-0.32	-0.21	-0.13	-0.09
0.300		-0.47	-0.43	-0.39	-0.41	-0.46	-0.32	-0.22	-0.13	-0.10
0.350		-0.40	-0.37	-0.38	-0.41	-0.46	-0.32	-0.22	-0.12	-0.11
0.400		-0.34	-0.33	-0.39	-0.41	-0.47	-0.32	-0.21	-0.11	-0.13
0.450		-0.30	-0.32	-0.41	-0.42	-0.47	-0.32	-0.20	-0.11	-0.13
0.500		-0.26	-0.33	-0.45	-0.45	-0.48	-0.31	-0.18	-0.12	-0.15
0.550		-0.22	-0.33	-0.53	-0.51	-0.47	-0.30	-0.16	-0.13	-0.16
0.600		-0.20	-0.35	-0.64	-0.60	-0.51	-0.29	-0.16	-0.14	-0.18
0.650		-0.18	-0.39	-0.72	-0.74	-0.60	-0.29	-0.17	-0.16	-0.19
0.700		-0.16	-0.39	-0.71	-0.85	-0.69	-0.34	-0.18	-0.19	-0.20
0.750		-0.12	-0.34	-0.59	-0.89	-0.69	-0.37	-0.21	-0.22	-0.21
0.800		-0.10	-0.27	-0.35	-0.85	-0.64	-0.38	-0.25	-0.25	-0.21
0.850		-0.06	-0.16	-0.14	-0.70	-0.58	-0.37	-0.31	-0.27	-0.21
0.900		-0.04	-0.06	0.01	-0.47	-0.59	-0.41	-0.40	-0.28	-0.20
0.950		-0.01	0.01	0.01	-0.30	-1.50	-0.73	-0.49	-0.27	-0.18
							-1.04	-0.46	-0.23	-0.16

TABLE 8—continued

9% RAE 101. Values of  $C_p$  for  $R = 2.2 \times 10^6$  and  $\alpha = 13.5^\circ$

$x/c$	$\eta$	0.195	0.383	0.556	0.707	0.831	0.882	0.924	0.957	0.981
0.001		-2.34	-3.28	-3.54	-3.00	-2.21	-1.15	-0.40	-0.26	-0.11
0.003		-2.37	-3.22	-3.44	-2.87	-2.06	-1.12	-0.35	-0.23	-0.09
0.006		-2.27	-3.02	-3.23	-2.72	-1.94	-1.05	-0.31	-0.20	-0.09
0.010		-2.14	-2.82	-3.03	-2.59	-1.83	-0.96	-0.27	-0.18	-0.08
0.015		-2.03	-2.72	-2.87	-2.45	-1.66	-0.84	-0.25	-0.16	-0.08
0.025		-1.71	-2.01	-2.08	-1.72	-1.09	-0.60	-0.24	-0.15	-0.07
0.035		-1.40	-1.76	-1.76	-1.47	-0.88	-0.51	-0.23	-0.15	-0.07
0.050		-1.26	-1.50	-1.51	-1.22	-0.64	-0.46	-0.22	-0.15	-0.07
0.075		-1.06	-1.21	-1.17	-0.85	-0.50	-0.43	-0.22	-0.15	-0.08
0.100		-0.92	-1.03	-0.94	-0.62	-0.47	-0.41	-0.22	-0.15	-0.08
0.125		-0.82	-0.91	-0.77	-0.52	-0.46	-0.41	-0.22	-0.15	-0.08
0.150		-0.75	-0.80	-0.64	-0.51	-0.46	-0.40	-0.22	-0.15	-0.08
0.200		-0.65	-0.64	-0.53	-0.50	-0.47	-0.38	-0.22	-0.14	-0.09
0.250		-0.57	-0.53	-0.50	-0.50	-0.48	-0.37	-0.22	-0.13	-0.10
0.300		-0.49	-0.45	-0.50	-0.51	-0.49	-0.36	-0.22	-0.12	-0.11
0.350		-0.42	-0.42	-0.51	-0.53	-0.49	-0.35	-0.20	-0.11	-0.13
0.400		-0.36	-0.41	-0.54	-0.57	-0.49	-0.33	-0.18	-0.11	-0.14
0.450		-0.32	-0.42	-0.59	-0.60	-0.48	-0.31	-0.16	-0.11	-0.16
0.500		-0.29	-0.44	-0.68	-0.64	-0.46	-0.29	-0.14	-0.13	-0.18
0.550		-0.26	-0.49	-0.85	-0.77	-0.45	-0.26	-0.13	-0.15	-0.20
0.600		-0.23	-0.53	-0.95	-0.96	-0.47	-0.24	-0.14	-0.18	-0.22
0.650		-0.20	-0.55	-0.94	-1.07	-0.55	-0.24	-0.15	-0.21	-0.24
0.700		-0.18	-0.46	-0.79	-1.03	-0.62	-0.27	-0.18	-0.26	-0.25
0.750		-0.15	-0.29	-0.52	-0.91	-0.64	-0.22	-0.24	-0.31	-0.26
0.800		-0.10	-0.10	-0.22	-0.75	-0.60	-0.33	-0.36	-0.34	-0.25
0.850		-0.06	0.02	-0.03	-0.57	-0.48	-0.47	-0.54	-0.35	-0.23
0.900		-0.02	0.05	0.04	-0.40	-0.67	-1.02	-0.66	-0.32	-0.22
0.950		0.01	0.05	0.06	-0.26	-1.97	-1.39	-0.58	-0.26	-0.18

9% RAE 101. Values of  $C_p$  for  $R = 2.2 \times 10^6$  and  $\alpha = 14.55^\circ$

$x/c$	$\eta$	0.195	0.383	0.556	0.707	0.831	0.882	0.924	0.957	0.981
0.001		-2.73	-3.86	-3.92	-3.05	-1.61	-0.68	-0.37	-0.22	-0.11
0.003		-2.72	-3.67	-3.73	-2.87	-1.54	-0.63	-0.31	-0.20	-0.09
0.006		-2.59	-3.46	-3.57	-2.72	-1.36	-0.55	-0.27	-0.17	-0.09
0.010		-2.44	-3.23	-3.35	-2.58	-1.12	-0.49	-0.25	-0.15	-0.08
0.015		-2.33	-3.05	-2.85	-2.39	-0.96	-0.44	-0.24	-0.13	-0.08
0.025		-1.72	-2.24	-2.22	-1.60	-0.74	-0.41	-0.23	-0.13	-0.08
0.035		-1.58	-1.96	-1.83	-1.29	-0.66	-0.39	-0.22	-0.13	-0.08
0.050		-1.39	-1.66	-1.51	-0.97	-0.59	-0.38	-0.22	-0.12	-0.08
0.075		-1.15	-1.30	-1.10	-0.66	-0.56	-0.36	-0.22	-0.12	-0.08
0.100		-0.98	-1.11	-0.83	-0.60	-0.55	-0.35	-0.21	-0.12	-0.08
0.125		-0.89	-0.96	-0.70	-0.60	-0.54	-0.35	-0.21	-0.13	-0.09
0.150		-0.80	-0.83	-0.66	-0.60	-0.54	-0.34	-0.21	-0.13	-0.09
0.200		-0.69	-0.67	-0.64	-0.61	-0.54	-0.34	-0.21	-0.12	-0.10
0.250		-0.59	-0.55	-0.66	-0.62	-0.53	-0.33	-0.20	-0.12	-0.11
0.300		-0.52	-0.51	-0.70	-0.62	-0.53	-0.32	-0.20	-0.11	-0.12
0.350		-0.45	-0.51	-0.75	-0.66	-0.50	-0.31	-0.18	-0.11	-0.14
0.400		-0.39	-0.51	-0.85	-0.68	-0.48	-0.28	-0.17	-0.11	-0.16
0.450		-0.34	-0.54	-1.03	-0.71	-0.45	-0.25	-0.15	-0.11	-0.18
0.500		-0.32	-0.62	-1.16	-0.82	-0.42	-0.23	-0.14	-0.13	-0.20
0.550		-0.29	-0.65	-1.21	-0.99	-0.41	-0.21	-0.14	-0.16	-0.23
0.600		-0.27	-0.67	-1.09	-1.08	-0.45	-0.20	-0.14	-0.19	-0.25
0.650		-0.23	-0.56	-0.79	-1.07	-0.52	-0.21	-0.16	-0.23	-0.26
0.700		-0.18	-0.33	-0.44	-0.99	-0.56	-0.24	-0.20	-0.28	-0.27
0.750		-0.13	-0.08	-0.20	-0.86	-0.56	-0.27	-0.28	-0.32	-0.28
0.800		-0.08	0.04	-0.06	-0.71	-0.51	-0.34	-0.40	-0.36	-0.27
0.850		-0.05	0.05	0.00	-0.55	-0.46	-0.56	-0.55	-0.36	-0.26
0.900		-0.01	0.05	0.01	-0.42	-0.87	-1.05	-0.63	-0.32	-0.23
0.950		0.01	0.04	0.02	-0.30	-1.81	-1.20	-0.54	-0.26	-0.20

TABLE 8—continued

9% RAE 101. Values of  $C_p$  for  $R = 2.2 \times 10^6$  and  $\alpha = 15.6^\circ$ 

$x/c$	$\eta$	0.195	0.383	0.556	0.707	0.831	0.882	0.924	0.957	0.981
0.001		-3.13	-4.38	-4.15	-2.64	-1.01	-0.52	-0.32	-0.18	-0.11
0.003		-3.09	-4.14	-3.91	-2.49	-0.92	-0.47	-0.28	-0.16	-0.09
0.006		-2.92	-3.89	-3.71	-2.34	-0.78	-0.40	-0.24	-0.14	-0.10
0.010		-2.76	-3.66	-3.48	-2.11	-0.69	-0.37	-0.22	-0.12	-0.10
0.015		-2.64	-3.12	-2.70	-1.66	-0.64	-0.35	-0.21	-0.11	-0.10
0.025		-1.91	-2.46	-2.10	-1.17	-0.58	-0.33	-0.20	-0.11	
0.035		-1.74	-2.12	-1.63	-0.96	-0.56	-0.32	-0.20	-0.11	-0.09
0.050		-1.51	-1.78	-1.23	-0.83	-0.54	-0.32	-0.20	-0.11	-0.09
0.075		-1.24	-1.37	-0.86	-0.77	-0.53	-0.31	-0.20	-0.11	-0.09
0.100		-1.06	-1.15	-0.79	-0.76	-0.52	-0.30	-0.20	-0.12	-0.10
0.125		-0.95	-0.97	-0.77	-0.76	-0.51	-0.30	-0.20	-0.12	-0.10
0.150		-0.86	-0.83	-0.77	-0.76	-0.50	-0.30	-0.20	-0.12	-0.10
0.200		-0.73	-0.70	-0.79	-0.76	-0.49	-0.30	-0.20	-0.11	-0.11
0.250		-0.62	-0.65	-0.84	-0.75	-0.48	-0.30	-0.18	-0.12	-0.13
0.300		-0.55	-0.65	-0.92	-0.74	-0.47	-0.28	-0.18	-0.12	-0.14
0.350		-0.48	-0.67	-1.03	-0.75	-0.44	-0.26	-0.17	-0.12	-0.16
0.400		-0.43	-0.73	-1.29	-0.77	-0.41	-0.24	-0.16	-0.12	-0.18
0.450		-0.39	-0.80	-1.48	-0.84	-0.37	-0.22	-0.15	-0.13	-0.20
0.500		-0.37	-0.84	-1.43	-0.96	-0.35	-0.20	-0.14	-0.15	-0.21
0.550		-0.34	-0.77	-1.18	-1.06	-0.35	-0.19	-0.15	-0.18	-0.23
0.600		-0.30	-0.58	-0.80	-1.08	-0.38	-0.18	-0.16	-0.21	-0.24
0.650		-0.25	-0.27	-0.52	-1.02	-0.43	-0.20	-0.19	-0.24	-0.25
0.700		-0.18	-0.05	-0.31	-0.92	-0.46	-0.23	-0.24	-0.26	-0.26
0.750		-0.11	0.03	-0.18	-0.80	-0.47	-0.28	-0.32	-0.31	-0.26
0.800		-0.06	0.03	-0.11	-0.67	-0.45	-0.39	-0.41	-0.33	-0.25
0.850		-0.03	0.02	-0.07	-0.54	-0.40	-0.62	-0.50	-0.32	-0.24
0.900		0.00	0.02	-0.05	-0.43	-0.91	-0.92	-0.52	-0.28	-0.22
0.950		0.01	0.02	-0.03	-0.34	-1.42	-0.92	-0.44	-0.23	-0.20

9% RAE 101. Values of  $C_p$  for  $R = 2.2 \times 10^6$  and  $\alpha = 16.6^\circ$ 

$x/c$	$\eta$	0.195	0.383	0.556	0.707	0.831	0.882	0.924	0.957	0.981
0.001		-3.59	-4.91	-4.11	-1.52	-0.79	-0.43	-0.28	-0.16	-0.14
0.003		-3.51	-4.62	-3.84	-1.41	-0.69	-0.38	-0.23	-0.14	-0.12
0.006		-3.31	-4.34	-3.65	-1.25	-0.60	-0.32	-0.21	-0.12	-0.12
0.010		-3.12	-4.12	-3.07	-1.13	-0.55	-0.30	-0.20	-0.11	-0.12
0.015		-2.99	-3.16	-2.41	-1.06	-0.52	-0.29	-0.19	-0.10	-0.11
0.025		-2.14	-2.68	-1.69	-0.99	-0.49	-0.28	-0.18	-0.10	
0.035		-1.92	-2.28	-1.21	-0.97	-0.48	-0.27	-0.18	-0.10	-0.11
0.050		-1.65	-1.88	-0.99	-0.94	-0.47	-0.27	-0.18	-0.10	-0.11
0.075		-1.35	-1.40	-0.93	-0.92	-0.47	-0.27	-0.18	-0.10	-0.12
0.100		-1.15	-1.13	-0.92	-0.89	-0.47	-0.28	-0.18	-0.10	-0.12
0.125		-1.02	-0.96	-0.93	-0.88	-0.46	-0.28	-0.18	-0.11	-0.12
0.150		-0.92	-0.88	-0.95	-0.87	-0.45	-0.28	-0.18	-0.11	-0.13
0.200		-0.77	-0.86	-1.00	-0.86	-0.44	-0.27	-0.17	-0.11	-0.14
0.250		-0.67	-0.86	-1.05	-0.85	-0.43	-0.25	-0.16	-0.12	-0.15
0.300		-0.59	-0.94	-1.11	-0.82	-0.41	-0.23	-0.16	-0.14	-0.16
0.350		-0.53	-1.06	-1.31	-0.84	-0.38	-0.21	-0.16	-0.14	-0.18
0.400		-0.49	-1.15	-1.56	-0.89	-0.34	-0.20	-0.16	-0.15	-0.20
0.450		-0.45	-1.09	-1.57	-1.00	-0.31	-0.18	-0.16	-0.16	-0.21
0.500		-0.43	-0.80	-1.37	-1.07	-0.29	-0.18	-0.17	-0.18	-0.22
0.550		-0.39	-0.38	-1.10	-1.11	-0.30	-0.18	-0.18	-0.21	-0.24
0.600		-0.32	-0.14	-0.78	-1.09	-0.34	-0.20	-0.20	-0.23	-0.24
0.650		-0.25	-0.06	-0.54	-1.01	-0.38	-0.22	-0.23	-0.26	-0.24
0.700		-0.17	-0.05	-0.37	-0.89	-0.40	-0.26	-0.28	-0.28	-0.25
0.750		-0.09	-0.04	-0.25	-0.76	-0.42	-0.32	-0.33	-0.28	-0.25
0.800		-0.05	-0.03	-0.18	-0.62	-0.44	-0.42	-0.39	-0.29	-0.24
0.850		-0.02	-0.03	-0.13	-0.51	-0.51	-0.56	-0.43	-0.27	-0.23
0.900		0.00	-0.02	-0.11	-0.42	-0.76	-0.70	-0.42	-0.24	-0.21
0.950		0.01	-0.02	-0.08	-0.36	-1.01	-0.66	-0.35	-0.20	-0.19

TABLE 9

Pressure Distributions on 9% Wing at  $R = 3.9 \times 10^6$ 

9% RAE 101. Values of  $C_p$  for  $R = 3.9 \times 10^6$  and  $\alpha = -8.32^\circ$

$x/c$	$\eta$	0.195	0.383	0.556	0.707	0.831	0.882	0.924	0.957	0.981
0.001		-0.38	-0.58	-0.62	-0.63	-0.95	-0.91	-0.95	-0.95	-0.70
0.003		-0.14	-0.28	-0.32	-0.35	-0.56	-0.74	-0.83	-0.86	-0.65
0.006		0.07	-0.07	-0.10	-0.17	-0.38	-0.58	-0.71	-0.78	-0.62
0.010		0.15	0.09	0.07	-0.04	-0.23	-0.42	-0.58	-0.71	-0.58
0.015		0.21	0.17	0.16	0.08	-0.14	-0.29	-0.46	-0.62	-0.55
0.025		0.26	0.24	0.24	0.16	-0.01	-0.14	-0.30	-0.52	-0.50
0.035		0.26	0.26	0.26	0.20	0.05	-0.05	-0.20	-0.44	-0.45
0.050		0.25	0.26	0.25	0.21	0.10	0.01	-0.10	-0.33	-0.38
0.075		0.22	0.24	0.23	0.20	0.12	0.06	-0.03	-0.21	-0.32
0.100		0.19	0.21	0.20	0.18	0.12	0.07	0.00	-0.14	-0.26
0.125		0.17	0.18	0.18	0.15	0.11	0.08	0.03	-0.10	-0.22
0.150		0.15	0.16	0.15	0.14	0.11	0.08	0.04	-0.08	-0.17
0.200		0.11	0.12	0.11	0.10	0.09	0.07	0.04	-0.02	-0.12
0.250		0.09	0.09	0.08	0.08	0.07	0.06	0.05	0.01	-0.09
0.300		0.07	0.07	0.05	0.06	0.05	0.05	0.04	0.01	-0.06
0.350		0.06	0.06	0.04	0.04	0.04	0.04	0.03	0.02	-0.04
0.400		0.05	0.05	0.03	0.03	0.03	0.04	0.03	0.03	-0.03
0.450		0.05	0.04	0.03	0.02	0.03	0.03	0.03	0.03	-0.01
0.500		0.04	0.03	0.02	0.02	0.02	0.02	0.03	0.03	-0.01
0.550		0.05	0.03	0.02	0.02	0.03	0.03	0.03	0.02	-0.01
0.600		0.05	0.03	0.02	0.02	0.03	0.03	0.03	0.02	-0.01
0.650		0.05	0.02	0.02	0.02	0.03	0.03	0.03	0.02	-0.01
0.700		0.04	0.03	0.02	0.03	0.03	0.03	0.03	0.01	-0.01
0.750		0.05	0.02	0.02	0.03	0.03	0.03	0.03	0.01	-0.02
0.800		0.05	0.03	0.02	0.03	0.03	0.02	0.03	0.01	-0.04
0.850		0.05	0.02	0.02	0.03	0.02	0.02	0.02	-0.02	-0.05
0.900		0.05	0.02	0.01	0.04	0.02	0.03	0.02	-0.05	-0.07
0.950		0.04	0.01	0.01	0.04	0.02	0.03	0.01	-0.12	-0.10

9% RAE 101. Values of  $C_p$  for  $R = 3.9 \times 10^6$  and  $\alpha = -2.08^\circ$ 

$x/c$	$\eta$	0.195	0.383	0.556	0.707	0.831	0.882	0.924	0.957	0.981
0.001		0.23	0.23	0.23	0.18	0.05	0.03	-0.01	-0.06	-0.10
0.003		0.24	0.25	0.25	0.20	0.11	0.06	0.01	-0.04	-0.08
0.006		0.24	0.24	0.23	0.19	0.11	0.07	0.02	-0.03	-0.06
0.010		0.21	0.21	0.21	0.17	0.11	0.08	0.03	-0.02	-0.05
0.015		0.17	0.18	0.17	0.14	0.11	0.07	0.04	-0.01	-0.04
0.025		0.13	0.12	0.12	0.10	0.08	0.06	0.05	0.00	-0.03
0.035		0.08	0.09	0.08	0.07	0.06	0.04	0.04	0.00	-0.03
0.050		0.05	0.05	0.04	0.03	0.03	0.02	0.03	0.00	-0.02
0.075		0.01	0.01	0.00	-0.01	0.00	0.01	0.01	0.00	-0.01
0.100		-0.02	-0.02	-0.02	-0.03	-0.02	-0.01	-0.01	-0.01	-0.01
0.125		-0.03	-0.04	-0.04	-0.05	-0.03	-0.02	-0.02	-0.02	-0.01
0.150		-0.05	-0.05	-0.06	-0.06	-0.05	-0.04	-0.03	-0.03	-0.01
0.200		-0.07	-0.07	-0.07	-0.07	-0.06	-0.05	-0.04	-0.03	-0.01
0.250		-0.09	-0.08	-0.09	-0.09	-0.08	-0.06	-0.05	-0.03	-0.01
0.300		-0.09	-0.09	-0.10	-0.09	-0.08	-0.07	-0.06	-0.04	-0.02
0.350		-0.08	-0.09	-0.10	-0.10	-0.08	-0.07	-0.06	-0.04	-0.02
0.400		-0.07	-0.08	-0.09	-0.09	-0.07	-0.06	-0.05	-0.03	-0.02
0.450		-0.06	-0.07	-0.08	-0.08	-0.06	-0.05	-0.04	-0.02	-0.01
0.500		-0.06	-0.06	-0.07	-0.07	-0.05	-0.05	-0.03	-0.01	-0.01
0.550		-0.04	-0.05	-0.06	-0.06	-0.04	-0.04	-0.02	-0.01	0.00
0.600		-0.03	-0.04	-0.05	-0.04	-0.03	-0.03	-0.02	-0.01	0.01
0.650		-0.02	-0.04	-0.04	-0.03	-0.02	-0.02	-0.01	0.00	0.01
0.700		-0.02	-0.03	-0.03	-0.02	-0.01	-0.01	0.00	0.00	0.01
0.750		0.00	-0.02	-0.02	-0.01	-0.01	0.00	0.01	0.01	0.02
0.800		0.01	-0.01	-0.01	0.00	0.01	0.01	0.02	0.02	0.03
0.850		0.01	-0.01	-0.01	0.00	0.01	0.02	0.02	0.02	0.03
0.900		0.03	0.00	-0.01	0.01	0.02	0.03	0.03	0.03	0.03
0.950		0.04	0.02	0.00	0.02	0.03	0.04	0.04	0.04	0.04

TABLE 9—continued

9% RAE 101. Values of  $C_p$  for  $R = 3.9 \times 10^6$  and  $\alpha = 0^\circ$

$x/c$	$\eta$	0.195	0.383	0.556	0.707	0.831	0.882	0.924	0.957	0.981
0.001		0.23	0.23	0.22	0.17	0.09	0.07	0.04	0.00	-0.02
0.003		0.19	0.18	0.17	0.14	0.09	0.06	0.04	0.00	-0.01
0.006		0.16	0.14	0.12	0.10	0.06	0.04	0.02	-0.01	-0.01
0.010		0.10	0.08	0.06	0.05	0.04	0.02	0.01	-0.01	-0.01
0.015		0.05	0.04	0.01	0.00	0.02	0.00	0.00	-0.01	-0.01
0.025		0.00	-0.02	-0.03	-0.03	-0.02	-0.03	-0.01	-0.02	-0.01
0.035		-0.04	-0.05	-0.07	-0.06	-0.04	-0.05	-0.04	-0.04	-0.02
0.050		-0.06	-0.08	-0.10	-0.09	-0.06	-0.07	-0.06	-0.05	-0.03
0.075		-0.09	-0.10	-0.12	-0.12	-0.10	-0.09	-0.07	-0.06	-0.04
0.100		-0.11	-0.12	-0.13	-0.13	-0.11	-0.10	-0.08	-0.08	-0.05
0.125		-0.11	-0.13	-0.13	-0.14	-0.12	-0.10	-0.09	-0.09	-0.06
0.150		-0.13	-0.14	-0.15	-0.14	-0.13	-0.11	-0.10	-0.10	-0.06
0.200		-0.13	-0.14	-0.15	-0.15	-0.13	-0.12	-0.11	-0.09	-0.07
0.250		-0.15	-0.15	-0.16	-0.16	-0.14	-0.13	-0.11	-0.10	-0.08
0.300		-0.15	-0.15	-0.17	-0.16	-0.14	-0.13	-0.11	-0.11	-0.08
0.350		-0.13	-0.14	-0.15	-0.14	-0.12	-0.12	-0.11	-0.10	-0.08
0.400		-0.11	-0.12	-0.13	-0.13	-0.11	-0.10	-0.09	-0.08	-0.07
0.450		-0.09	-0.10	-0.11	-0.11	-0.09	-0.08	-0.06	-0.06	-0.05
0.500		-0.09	-0.09	-0.10	-0.09	-0.08	-0.08	-0.06	-0.05	-0.04
0.550		-0.07	-0.07	-0.09	-0.08	-0.06	-0.06	-0.04	-0.04	-0.02
0.600		-0.05	-0.06	-0.07	-0.06	-0.05	-0.04	-0.03	-0.03	-0.01
0.650		-0.04	-0.06	-0.05	-0.05	-0.04	-0.03	-0.02	-0.02	0.00
0.700		-0.03	-0.04	-0.04	-0.03	-0.02	-0.02	-0.01	-0.01	0.01
0.750		-0.01	-0.03	-0.03	-0.02	-0.02	-0.01	0.01	0.01	0.02
0.800		0.00	-0.02	-0.02	-0.01	-0.01	0.00	0.02	0.02	0.03
0.850		0.01	-0.01	-0.01	0.00	0.00	0.02	0.02	0.03	0.04
0.900		0.03	0.00	-0.01	0.01	0.02	0.03	0.03	0.04	0.05
0.950		0.04	0.02	0.00	0.02	0.03	0.04	0.05	0.05	0.06

9% RAE 101. Values of  $C_p$  for  $R = 3.9 \times 10^6$  and  $\alpha = 2.08^\circ$

$x/c$	$\eta$	0.195	0.383	0.556	0.707	0.831	0.882	0.924	0.957	0.981
0.001		0.12	0.07	0.04	0.01	-0.04	-0.05	-0.07	-0.09	-0.11
0.003		0.04	-0.01	-0.04	-0.06	-0.07	-0.09	-0.09	-0.10	-0.10
0.006		-0.01	-0.07	-0.12	-0.11	-0.12	-0.12	-0.12	-0.12	-0.12
0.010		-0.08	-0.15	-0.17	-0.17	-0.15	-0.15	-0.14	-0.13	-0.12
0.015		-0.12	-0.18	-0.22	-0.22	-0.17	-0.18	-0.16	-0.15	-0.13
0.025		-0.15	-0.21	-0.24	-0.22	-0.20	-0.20	-0.18	-0.17	-0.14
0.035		-0.17	-0.23	-0.25	-0.24	-0.20	-0.22	-0.19	-0.19	-0.16
0.050		-0.19	-0.24	-0.26	-0.26	-0.23	-0.23	-0.20	-0.20	-0.17
0.075		-0.21	-0.23	-0.25	-0.26	-0.24	-0.24	-0.23	-0.21	-0.18
0.100		-0.21	-0.23	-0.25	-0.25	-0.24	-0.23	-0.22	-0.21	-0.20
0.125		-0.21	-0.24	-0.25	-0.25	-0.24	-0.22	-0.22	-0.22	-0.21
0.150		-0.21	-0.23	-0.24	-0.24	-0.23	-0.22	-0.22	-0.22	-0.21
0.200		-0.21	-0.23	-0.24	-0.24	-0.23	-0.23	-0.22	-0.21	-0.22
0.250		-0.21	-0.22	-0.24	-0.23	-0.22	-0.21	-0.20	-0.21	-0.21
0.300		-0.21	-0.21	-0.23	-0.22	-0.21	-0.20	-0.19	-0.20	-0.20
0.350		-0.18	-0.19	-0.20	-0.19	-0.18	-0.19	-0.17	-0.18	-0.19
0.400		-0.15	-0.16	-0.17	-0.16	-0.16	-0.16	-0.16	-0.16	-0.19
0.450		-0.12	-0.13	-0.14	-0.14	-0.12	-0.12	-0.10	-0.10	-0.18
0.500		-0.12	-0.12	-0.13	-0.11	-0.10	-0.12	-0.09	-0.08	-0.08
0.550		-0.09	-0.10	-0.11	-0.10	-0.08	-0.11	-0.07	-0.07	-0.06
0.600		-0.07	-0.08	-0.09	-0.08	-0.07	-0.07	-0.06	-0.06	-0.05
0.650		-0.06	-0.07	-0.07	-0.06	-0.05	-0.05	-0.04	-0.04	-0.03
0.700		-0.05	-0.05	-0.06	-0.05	-0.04	-0.03	-0.02	-0.02	-0.02
0.750		-0.02	-0.04	-0.04	-0.03	-0.03	-0.02	-0.01	-0.01	-0.01
0.800		-0.01	-0.02	-0.02	-0.02	-0.01	-0.01	0.01	0.01	0.01
0.850		0.01	-0.02	-0.01	-0.01	0.00	0.01	0.01	0.02	0.02
0.900		0.02	0.00	-0.01	0.01	0.01	0.02	0.02	0.03	0.03
0.950		0.04	0.01	0.01	0.02	0.03	0.04	0.04	0.04	0.04

TABLE 9—continued

9% RAE 101. Values of  $C_p$  for  $R = 3.9 \times 10^6$  and  $\alpha = 8.32^\circ$ 

$x/c$ $\eta$	0.195	0.383	0.556	0.707	0.831	0.882	0.924	0.957	0.981
0.001	-0.83	-1.22	-1.38	-1.30	-1.28	-1.14	-1.04	-0.87	-0.46
0.003	-0.95	-1.32	-1.46	-1.34	-1.27	-1.22	-1.09	-0.88	-0.42
0.006	-0.97	-1.32	-1.46	-1.34	-1.26	-1.23	-1.14	-0.91	-0.40
0.010	-0.98	-1.27	-1.40	-1.37	-1.22	-1.22	-1.13	-0.90	-0.37
0.015	-0.96	-1.21	-1.30	-1.32	-1.22	-1.19	-1.08	-0.89	-0.34
0.025	-0.85	-1.08	-1.17	-1.11	-1.08	-1.08	-1.01	-0.86	-0.28
0.035	-0.78	-0.95	-1.00	-0.99	-1.01	-0.99	-0.94	-0.83	-0.23
0.050	-0.71	-0.85	-0.92	-0.90	-0.89	-0.91	-0.88	-0.73	-0.19
0.075	-0.63	-0.71	-0.78	-0.77	-0.77	-0.77	-0.80	-0.57	-0.17
0.100	-0.57	-0.64	-0.68	-0.68	-0.68	-0.68	-0.67	-0.42	-0.16
0.125	-0.52	-0.59	-0.61	-0.61	-0.61	-0.60	-0.60	-0.32	-0.15
0.150	-0.50	-0.54	-0.56	-0.54	-0.56	-0.56	-0.50	-0.27	-0.15
0.200	-0.44	-0.46	-0.48	-0.48	-0.47	-0.45	-0.36	-0.24	-0.15
0.250	-0.40	-0.42	-0.43	-0.46	-0.39	-0.36	-0.26	-0.23	-0.16
0.300	-0.36	-0.38	-0.36	-0.35	-0.32	-0.27	-0.23	-0.22	-0.16
0.350	-0.30	-0.31	-0.30	-0.29	-0.24	-0.21	-0.24	-9.22	-0.16
0.400	-0.26	-0.26	-0.24	-0.23	-0.19	-0.20	-0.25	-0.22	-0.15
0.450	-0.22	-0.21	-0.19	-0.18	-0.16	-0.20	-0.27	-0.24	-0.12
0.500	-0.19	-0.18	-0.16	-0.14	-0.15	-0.21	-0.29	-0.26	-0.09
0.550	-0.15	-0.14	-0.13	-0.12	-0.15	-0.22	-0.33	-0.25	-0.06
0.600	-0.12	-0.12	-0.11	-0.11	-0.15	-0.25	-0.38	-0.22	-0.06
0.650	-0.10	-0.11	-0.09	-0.10	-0.16	-0.29	-0.45	-0.18	-0.06
0.700	-0.08	-0.09	-0.08	-0.09	-0.16	-0.33	-0.53	-0.16	-0.06
0.750	-0.06	-0.08	-0.07	-0.09	-0.17	-0.37	-0.62	-0.20	-0.06
0.800	-0.04	-0.07	-0.07	-0.09	-0.17	-0.40	-0.68	-0.32	-0.09
0.850	-0.02	-0.07	-0.07	-0.09	-0.16	-0.36	-0.64	-0.37	-0.13
0.900	-0.01	-0.06	-0.07	-0.09	-0.14	-0.27	-0.42	-0.39	-0.28
0.950	0.00	-0.05	-0.07	-0.08	-0.11	-0.12	-0.19	-0.41	-0.40

9% RAE 101. Values of  $C_p$  for  $R = 3.9 \times 10^6$  and  $\alpha = 10.40^\circ$ 

$x/c$ $\eta$	0.195	0.383	0.556	0.707	0.831	0.882	0.924	0.957	0.981
0.001	-1.38	-1.97	-2.19	-2.00	-1.87	-1.57	-1.17	-0.44	-0.21
0.003	-1.47	-2.01	-2.22	-1.99	-1.83	-1.65	-1.19	-0.39	-0.18
0.006	-1.44	-1.96	-2.15	-1.95	-1.76	-1.63	-1.19	-0.35	-0.15
0.010	-1.42	-1.83	-2.01	-1.93	-1.68	-1.58	-1.15	-0.30	-0.14
0.015	-1.35	-1.71	-1.89	-1.81	-1.59	-1.50	-1.04	-0.24	-0.12
0.025	-1.16	-1.44	-1.55	-1.48	-1.39	-1.30	-0.89	-0.18	-0.11
0.035	-1.03	-1.28	-1.32	-1.29	-1.29	-1.14	-0.74	-0.17	-0.11
0.050	-0.92	-1.12	-1.18	-1.15	-1.09	-1.00	-0.57	-0.16	-0.10
0.075	-0.79	-0.93	-0.98	-0.95	-0.90	-0.78	-0.36	-0.15	-0.10
0.100	-0.71	-0.80	-0.84	-0.82	-0.76	-0.61	-0.31	-0.15	-0.09
0.125	-0.64	-0.71	-0.74	-0.76	-0.65	-0.47	-0.30	-0.15	-0.09
0.150	-0.60	-0.65	-0.66	-0.63	-0.55	-0.36	-0.29	-0.15	-0.09
0.200	-0.52	-0.55	-0.54	-0.51	-0.39	-0.30	-0.24	-0.15	-0.08
0.250	-0.47	-0.48	-0.47	-0.41	-0.30	-0.29	-0.27	-0.15	-0.06
0.300	-0.42	-0.42	-0.38	-0.31	-0.28	-0.29	-0.26	-0.16	-0.05
0.350	-0.35	-0.34	-0.30	-0.24	-0.28	-0.30	-0.26	-0.17	-0.04
0.400	-0.30	-0.28	-0.24	-0.21	-0.29	-0.31	-0.25	-0.16	-0.03
0.450	-0.25	-0.23	-0.21	-0.19	-0.31	-0.33	-0.23	-0.12	-0.02
0.500	-0.22	-0.20	-0.19	-0.20	-0.33	-0.36	-0.23	-0.10	-0.02
0.550	-0.18	-0.17	-0.19	-0.20	-0.34	-0.40	-0.22	-0.07	-0.02
0.600	-0.15	-0.16	-0.18	-0.21	-0.36	-0.47	-0.23	-0.07	-0.03
0.650	-0.12	-0.16	-0.18	-0.22	-0.39	-0.53	-0.26	-0.07	-0.03
0.700	-0.10	-0.15	-0.19	-0.24	-0.39	-0.55	-0.29	-0.07	-0.04
0.750	-0.08	-0.14	-0.20	-0.26	-0.39	-0.56	-0.33	-0.09	-0.05
0.800	-0.05	-0.14	-0.22	-0.28	-0.41	-0.54	-0.32	-0.11	-0.06
0.850	-0.04	-0.14	-0.23	-0.30	-0.36	-0.45	-0.30	-0.14	-0.08
0.900	-0.02	-0.12	-0.23	-0.28	-0.38	-0.33	-0.26	-0.17	-0.10
0.950	-0.01	-0.10	-0.17	-0.20	-0.19	-0.23	-0.28	-0.21	-0.11

TABLE 9—continued

9% RAE 101. Values of  $C_p$  for  $R = 3.9 \times 10^6$  and  $\alpha = 12.48^\circ$ 

$x/c$	$\eta$	0.195	0.383	0.556	0.707	0.831	0.882	0.924	0.957	0.981
0.001		-2.04	-2.87	-3.17	-2.89	-2.51	-1.66	-0.49	-0.29	-0.08
0.003		-2.09	-2.85	-3.14	-2.80	-2.40	-1.68	-0.40	-0.24	-0.07
0.006		-2.01	-2.71	-2.97	-2.69	-2.27	-1.59	-0.31	-0.20	-0.06
0.010		-2.03	-2.51	-2.76	-2.60	-2.10	-1.46	-0.26	-0.17	-0.06
0.015		-1.81	-2.32	-2.55	-2.43	-1.95	-1.31	-0.22	-0.15	-0.06
0.025		-1.48	-1.87	-1.98	-1.86	-1.61	-0.91	-0.21	-0.14	-0.05
0.035		-1.32	-1.64	-1.69	-1.62	-1.44	-0.64	-0.21	-0.14	-0.05
0.050		-1.16	-1.41	-1.48	-1.40	-1.12	-0.47	-0.20	-0.14	-0.05
0.075		-1.02	-1.15	-1.18	-1.11	-0.79	-0.41	-0.19	-0.13	-0.05
0.100		-0.86	-0.98	-1.00	-0.91	-0.57	-0.39	-0.19	-0.13	-0.06
0.125		-0.77	-0.87	-0.86	-0.76	-0.49	-0.39	-0.19	-0.13	-0.06
0.150		-0.70	-0.78	-0.75	-0.62	-0.47	-0.38	-0.19	-0.12	-0.06
0.200		-0.61	-0.63	-0.58	-0.46	-0.47	-0.36	-0.21	-0.12	-0.06
0.250		-0.54	-0.53	-0.46	-0.39	-0.51	-0.37	-0.22	-0.10	-0.06
0.300		-0.47	-0.45	-0.38	-0.38	-0.57	-0.37	-0.21	-0.10	-0.07
0.350		-0.40	-0.37	-0.35	-0.38	-0.63	-0.35	-0.19	-0.09	-0.07
0.400		-0.34	-0.32	-0.34	-0.38	-0.63	-0.35	-0.17	-0.08	-0.08
0.450		-0.29	-0.29	-0.34	-0.39	-0.59	-0.35	-0.15	-0.08	-0.09
0.500		-0.25	-0.31	-0.35	-0.40	-0.58	-0.38	-0.15	-0.09	-0.10
0.550		-0.22	-0.28	-0.38	-0.44	-0.58	-0.42	-0.15	-0.09	-0.11
0.600		-0.19	-0.29	-0.41	-0.49	-0.63	-0.48	-0.18	-0.11	-0.12
0.650		-0.16	-0.31	-0.47	-0.56	-0.69	-0.50	-0.20	-0.12	-0.13
0.700		-0.14	-0.30	-0.52	-0.62	-0.67	-0.47	-0.22	-0.15	-0.14
0.750		-0.11	-0.28	-0.55	-0.67	-0.61	-0.37	-0.24	-0.17	-0.15
0.800		-0.08	-0.23	-0.53	-0.68	-0.54	-0.32	-0.24	-0.19	-0.15
0.850		-0.06	-0.18	-0.44	-0.62	-0.39	-0.33	-0.29	-0.21	-0.14
0.900		-0.03	-0.11	-0.30	-0.41	-0.38	-0.41	-0.36	-0.22	-0.14
0.950		-0.01	-0.05	-0.10	-0.38	-0.68	-0.57	-0.39	-0.20	-0.12



TABLE 10

*Corrected Forces and Moments on 5% Wing from Integrated Normal Pressures*

$R \times 10^{-6}$	$\alpha$	$C_L$	$C_D$	$C_m$	$-C_m/C_L$	$\bar{\eta}$	$\frac{C_D - C_{D0}}{C_L^2}$
1.3	0	0	0.001	0	—	—	—
1.3	2.08	0.084	0.002	-0.002	0.027	0.478	0.12
1.3	5.20	0.209	0.010	-0.014	0.065	0.486	0.20
2.2	0	0	0.001	0	—	—	—
2.2	2.08	0.083	0.001	-0.001	0.017	0.475	0.12
2.2	4.16	0.168	0.007	-0.005	0.029	0.477	0.24
2.2	5.20	0.210	0.008	-0.011	0.054	0.483	0.18
2.2	5.73	0.236	0.012	-0.017	0.072	0.487	0.21
2.2	6.25	0.264	0.017	-0.020	0.077	0.488	0.24
2.2	8.37	0.382	0.045	-0.016	0.043	0.467	0.31
2.8	8.35	0.362	0.038	-0.030	0.084	0.482	0.28
3.3	8.34	0.352	0.029	-0.030	0.085	0.485	0.23
3.9	0	0	0.000	0	—	—	—
3.9	0.52	0.021	0.000	0.000	-0.007	0.469	—
3.9	1.04	0.042	0.001	0.000	0.010	0.474	0.14
3.9	2.08	0.084	0.001	-0.002	0.026	0.477	0.12
3.9	4.16	0.170	0.004	-0.012	0.069	0.480	0.13
3.9	5.20	0.210	0.007	-0.007	0.035	0.478	0.14
3.9	6.25	0.256	0.016	-0.016	0.063	0.483	0.24
3.9	7.29	0.298	0.020	-0.020	0.068	0.484	0.22
3.9	8.33	0.340	0.021	-0.019	0.055	0.481	0.18

TABLE 11

*Corrected Forces and Moments on 9% Wing from Integrated Normal Pressures*

$R \times 10^{-6}$	$\alpha$	$C_L$	$C_D$	$C_m$	$-C_m/C_L$	$\bar{\eta}$	$\frac{C_D - C_{D0}}{C_L^2}$
1.3	0	0	0.001	0	—	—	—
1.3	2.08	0.082	0.002	-0.003	0.036	0.482	0.10
1.3	8.31	0.318	0.015	0.004	-0.014	0.461	0.13
2.2	0	0	0.001	0	—	—	—
2.2	1.04	0.042	0.001	-0.001	0.032	0.481	0.14
2.2	2.08	0.084	0.002	-0.003	0.038	0.481	0.10
2.2	4.16	0.171	0.003	-0.006	0.034	0.480	0.09
2.2	6.24	0.246	0.007	-0.006	0.026	0.477	0.10
2.2	8.31	0.326	0.015	-0.001	0.003	0.464	0.13
3.9	0	0	0.001	0	—	—	—
3.9	2.08	0.087	0.002	-0.004	0.044	0.484	0.09
3.9	8.32	0.336	0.016	-0.014	0.043	0.475	0.13

TABLE 12

*Magnitude and Spanwise Location of Maximum Increment  $\delta(-C_p)$  due to Main Vortex (Section 4.5)*

Wing	$R \times 10^{-6}$	$\alpha$	Estimated $\delta(-C_p)$	Estimated $\eta$	Eqn. (8) $\delta(-C_p)$
5%	2.2	5.73	0.2 <sub>5</sub>	0.9	0.21
5%	2.2	6.25	0.3	0.8	0.31
5%	2.2	8.37	0.4 <sub>5</sub>	0.6	0.63
5%	3.9	8.33	0.4	0.8 <sub>5</sub>	0.36
5%	3.9	9.36	0.5 <sub>5</sub>	0.7	0.58
5%	3.9	10.40	0.8	0.6	0.78
5%	3.9	11.44	0.9	0.5	1.00
9%	2.2	8.31	0.3 <sub>5</sub>	0.9	0.31
9%	2.2	9.36	0.3 <sub>5</sub>	0.9	0.35
9%	2.2	10.40	0.3 <sub>5</sub>	0.8	0.52
9%	2.2	11.44	0.5	0.7	0.71
9%	2.2	12.48	0.8	0.7	0.78
9%	2.2	13.52	1.0	0.6 <sub>5</sub>	0.93
9%	2.2	14.56	1.1	0.6	1.09
9%	2.2	15.60	1.2	0.5 <sub>5</sub>	1.27
9%	2.2	16.64	1.2	0.5 <sub>5</sub>	1.35
9%	3.9	10.40	0.5	0.8 <sub>5</sub>	0.46
9%	3.9	12.48	0.6 <sub>5</sub>	0.8	0.62

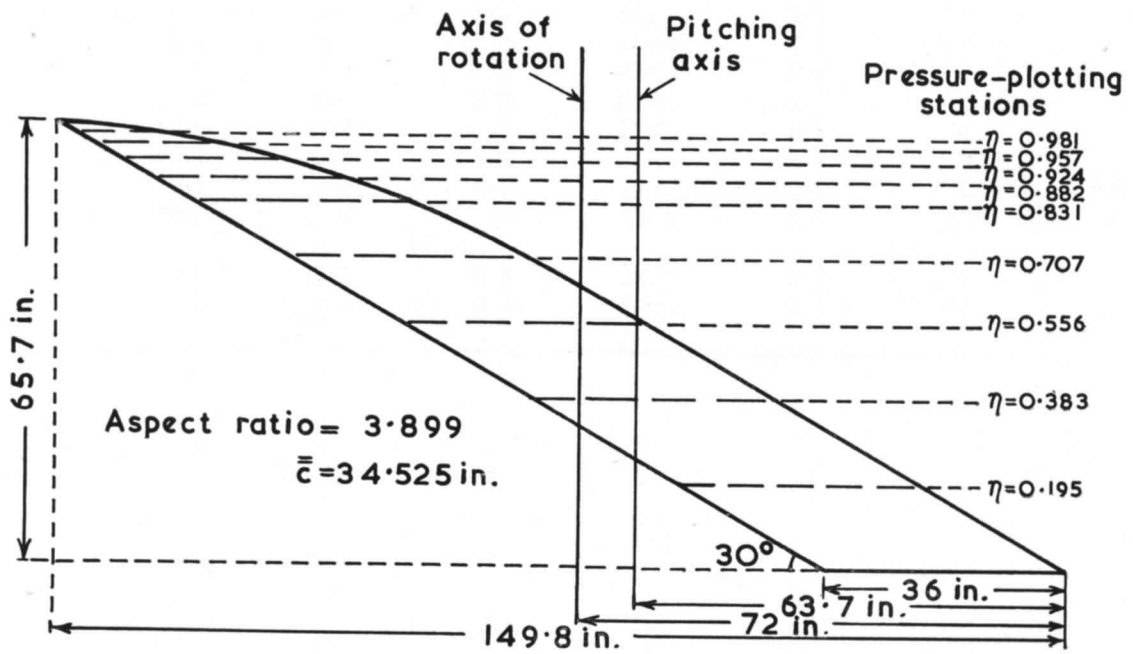
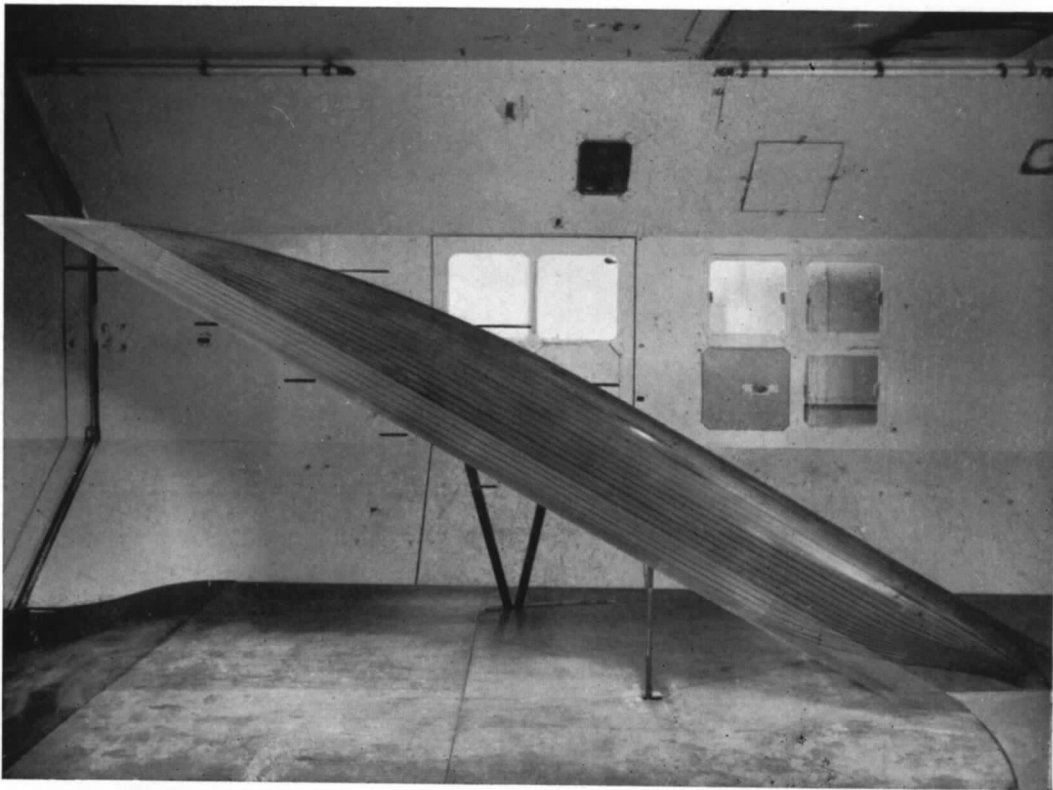


FIG. 1. Arrangement and details of curved-tip wing in N.P.L. 13 ft.  $\times$  9 ft. Wind Tunnel.

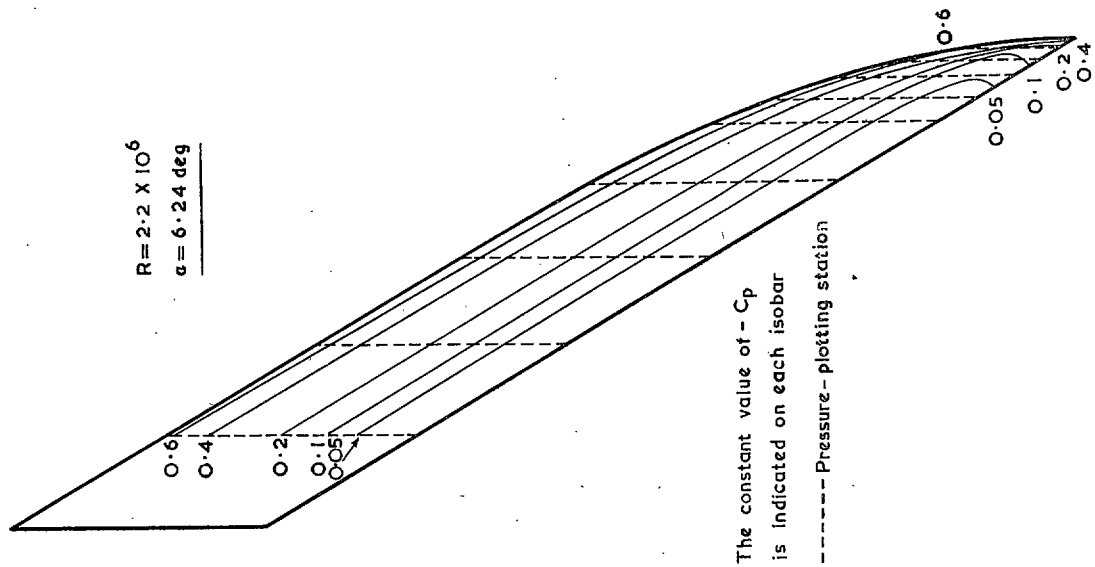
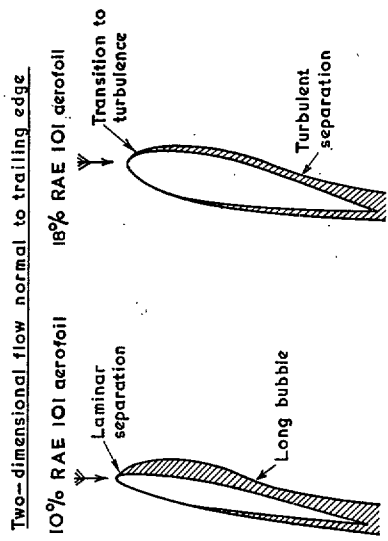


FIG. 2. Surface isobars on 9% RAE 101 curved-tip wing.

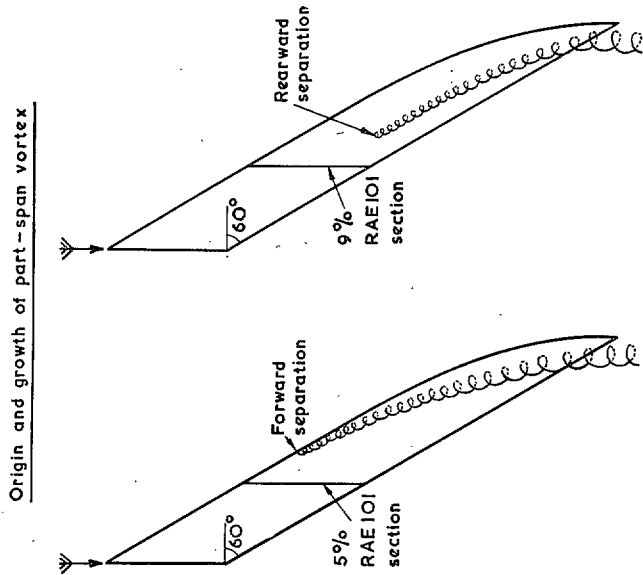


FIG. 3. Sketch of separated flow over wings of 60° sweepback.

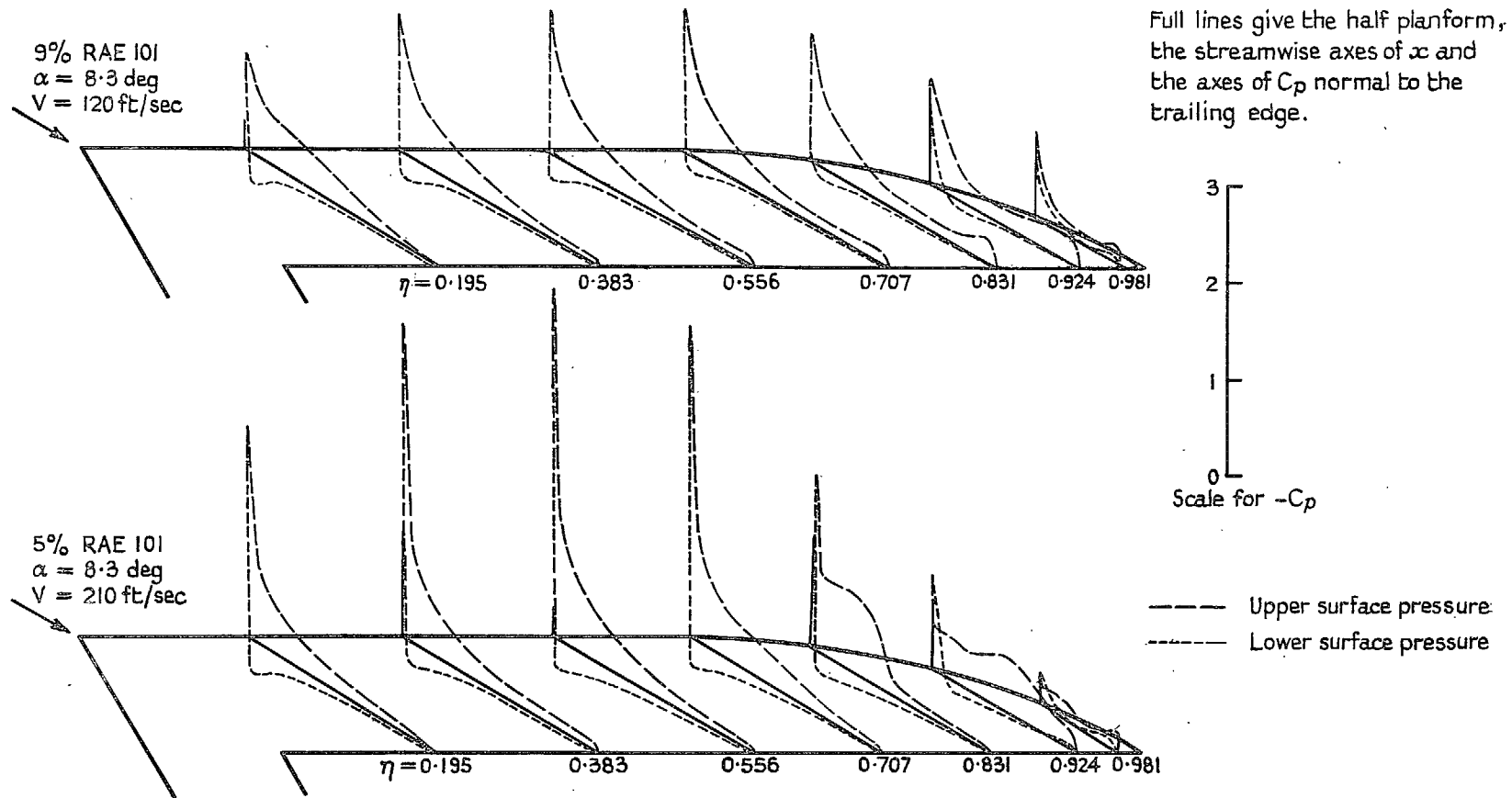


FIG. 4. Pressure distributions over curved-tip wings at  $\alpha = 8.3^\circ$

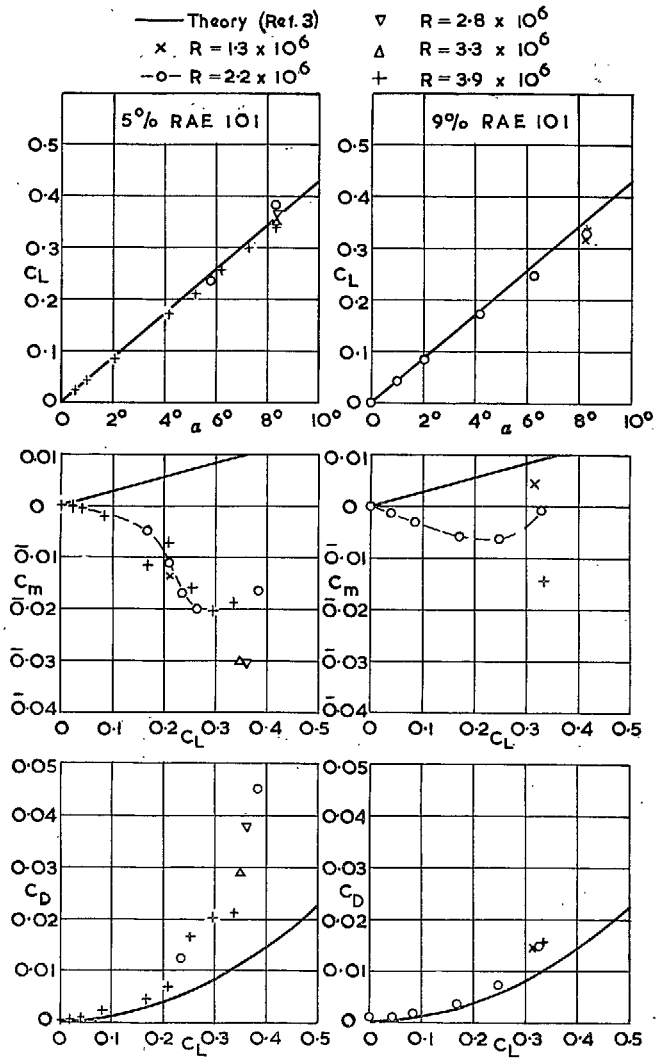


FIG. 5. Characteristics of curved-tip wings from integrated normal pressures.

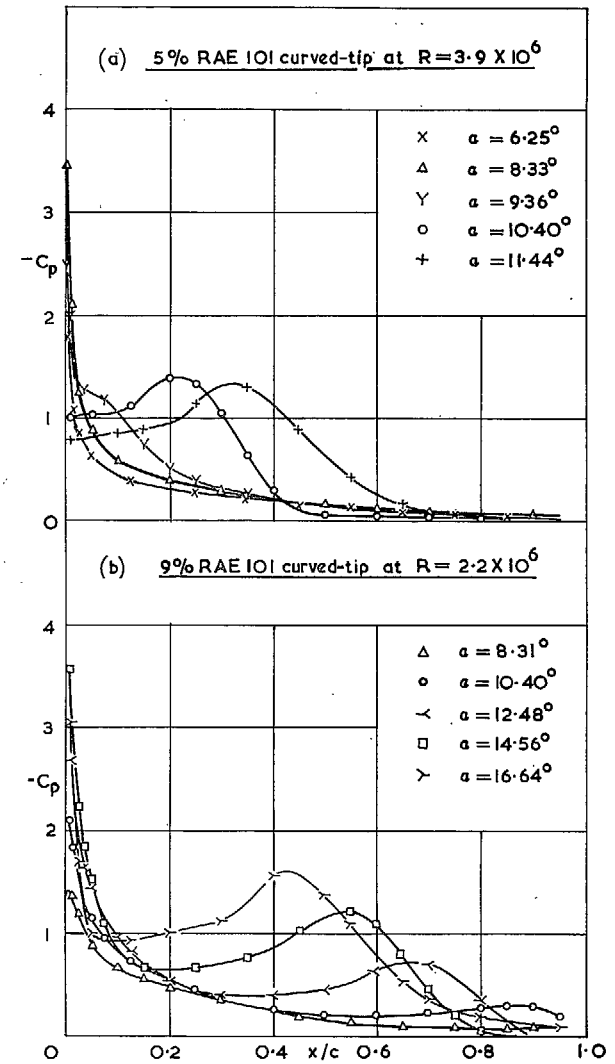


FIG. 6. Chordwise pressure distributions on the upper surface at  $\eta = 0.556$ .

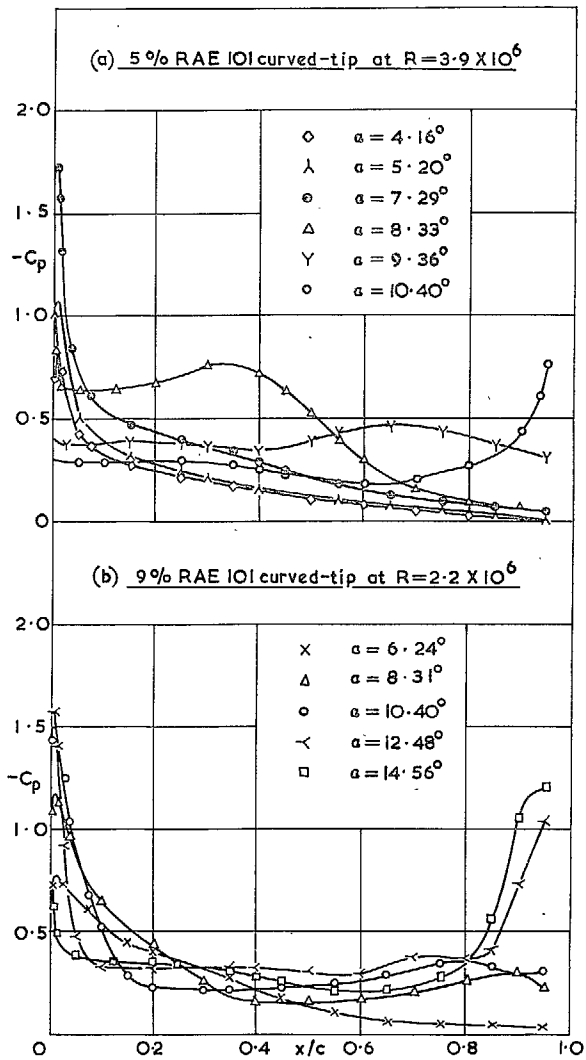


FIG. 7. Chordwise pressure distributions on the upper surface at  $\eta = 0.882$ .

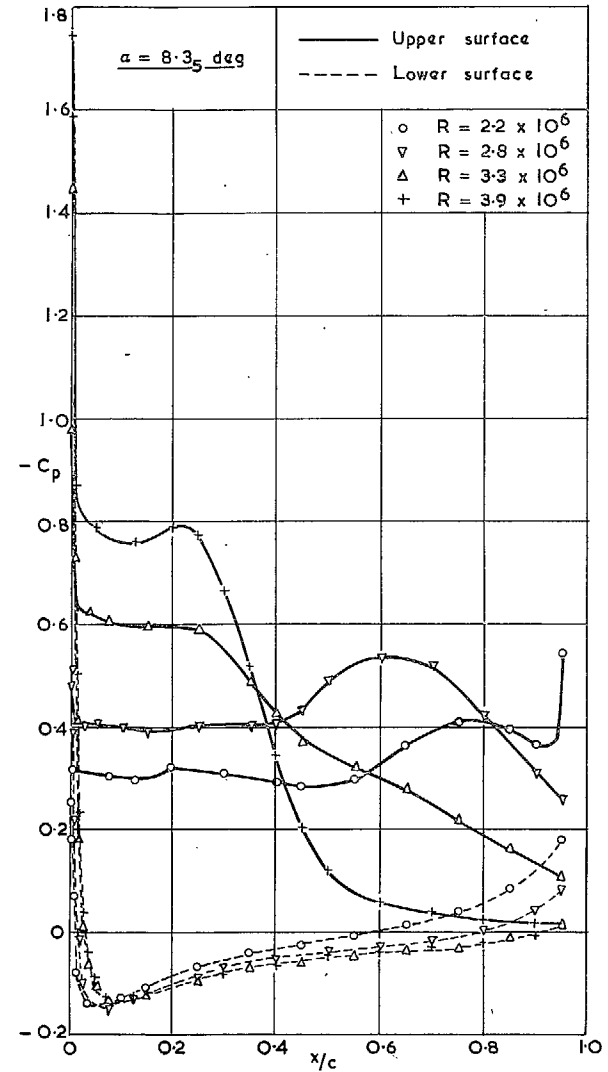


FIG. 8. Scale effect on pressure distribution of 5% wing at  $\eta = 0.831$ .

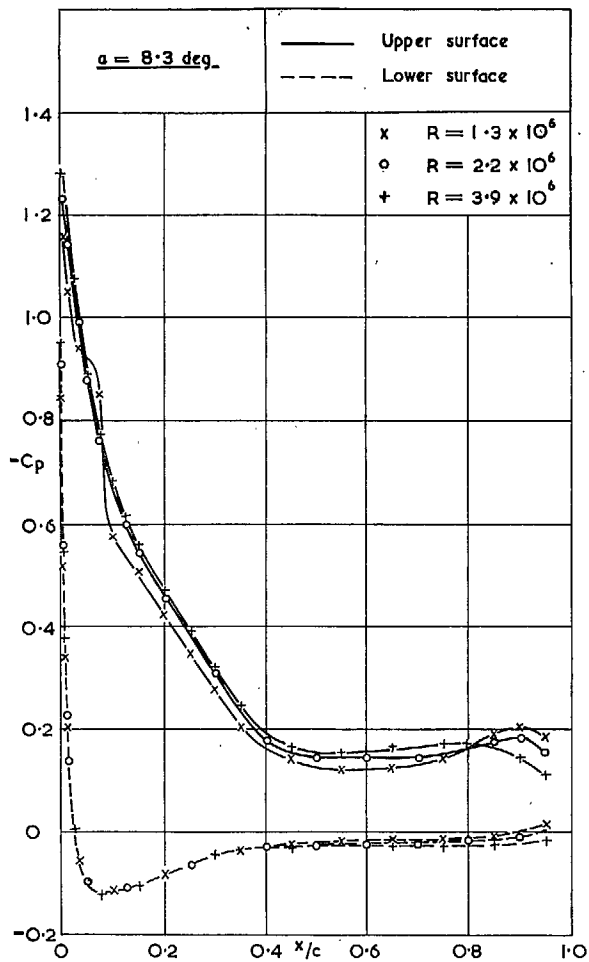


FIG. 9A. Scale effect on pressure distribution of 9% wing at  $\eta = 0.831$ .

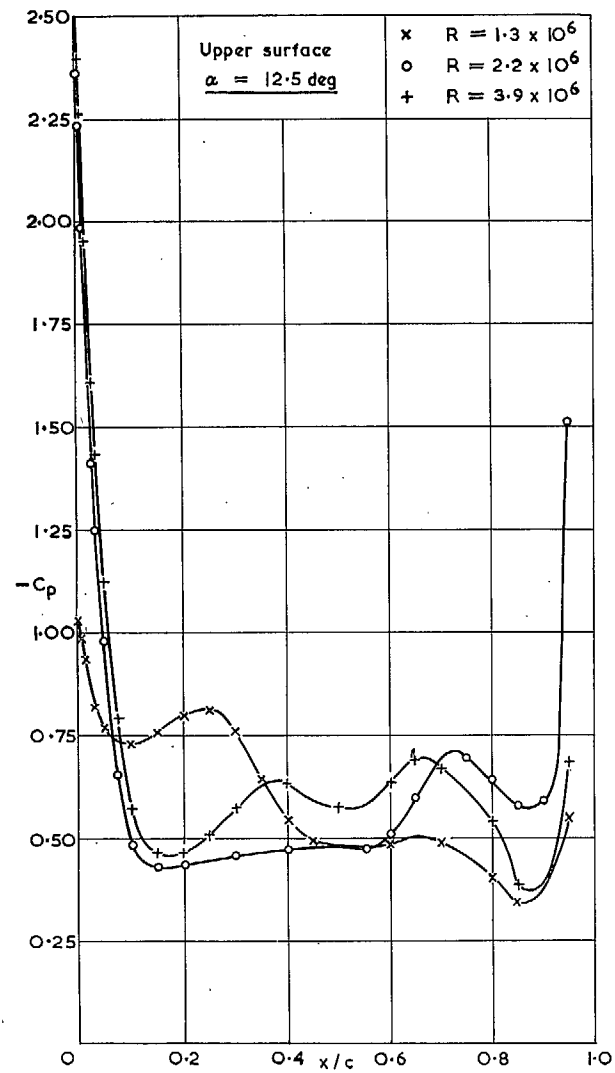


FIG. 9B. Scale effect on pressure distribution of 9% wing at  $\eta = 0.831$ .



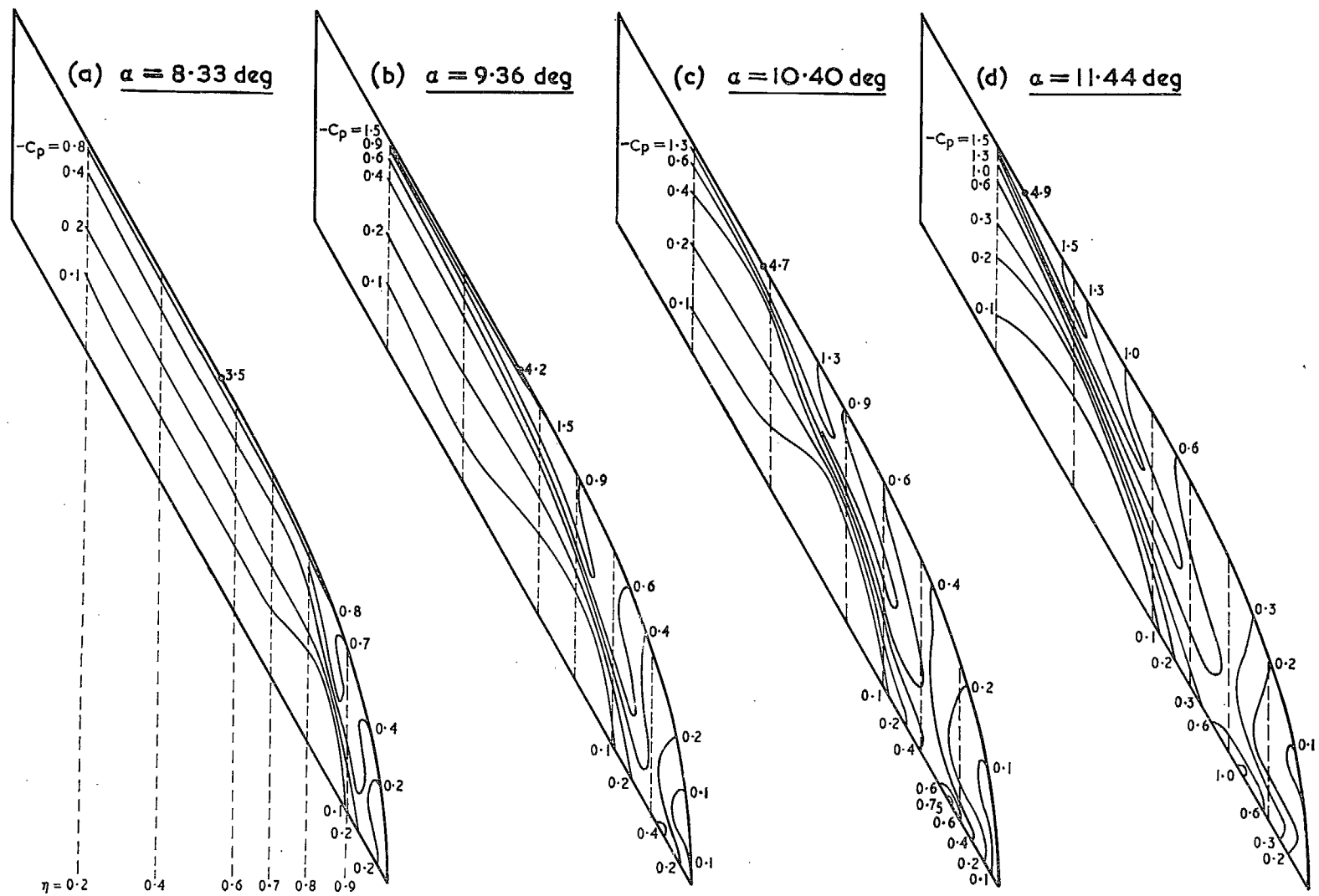


FIG. 10. Effect of incidence on surface isobars of 5% wing at  $R = 3.9 \times 10^6$ .

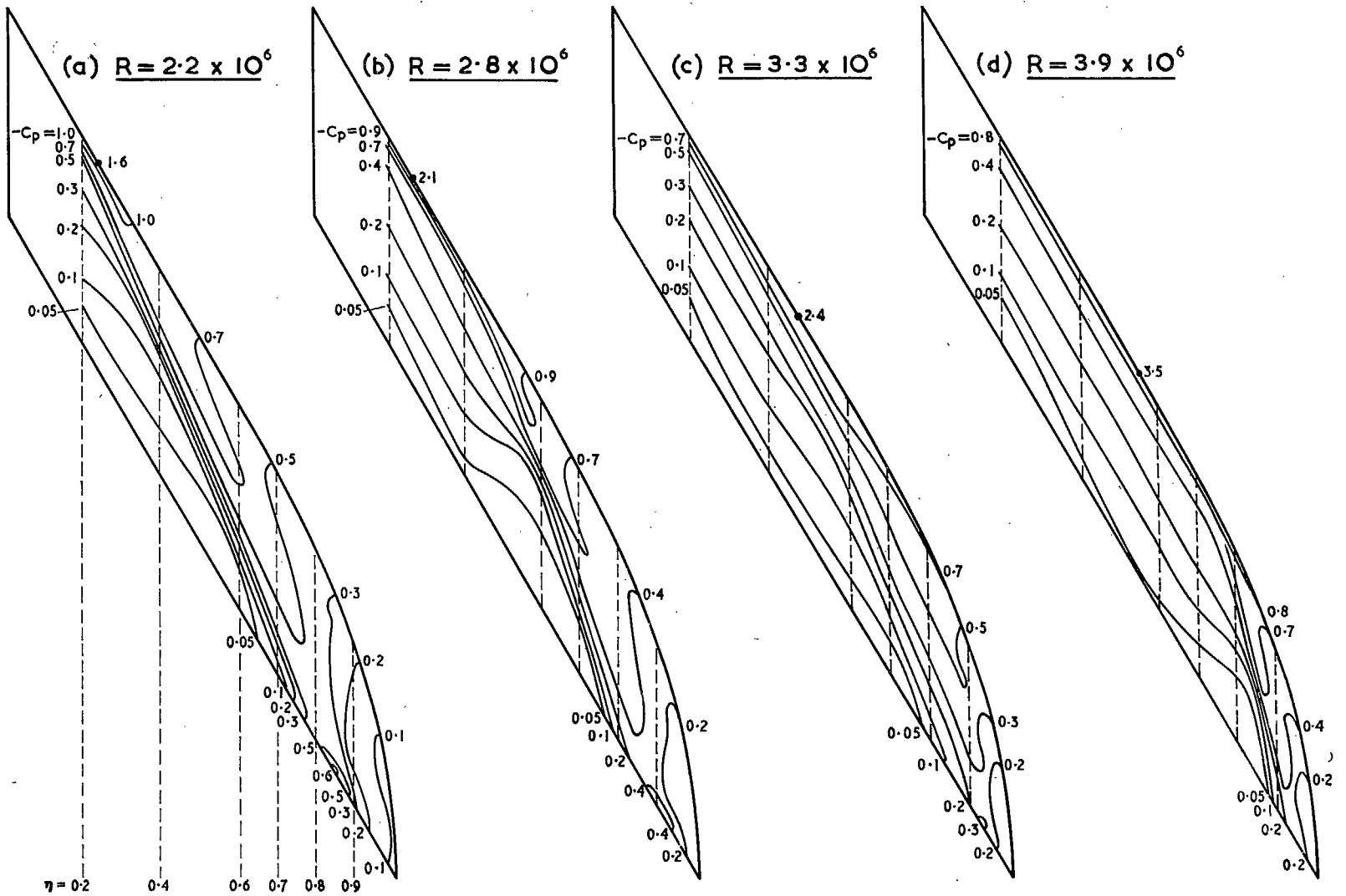


FIG. 11. Effect of Reynolds number on surface isobars of 5% wing at  $\alpha = 8.35^\circ$ .

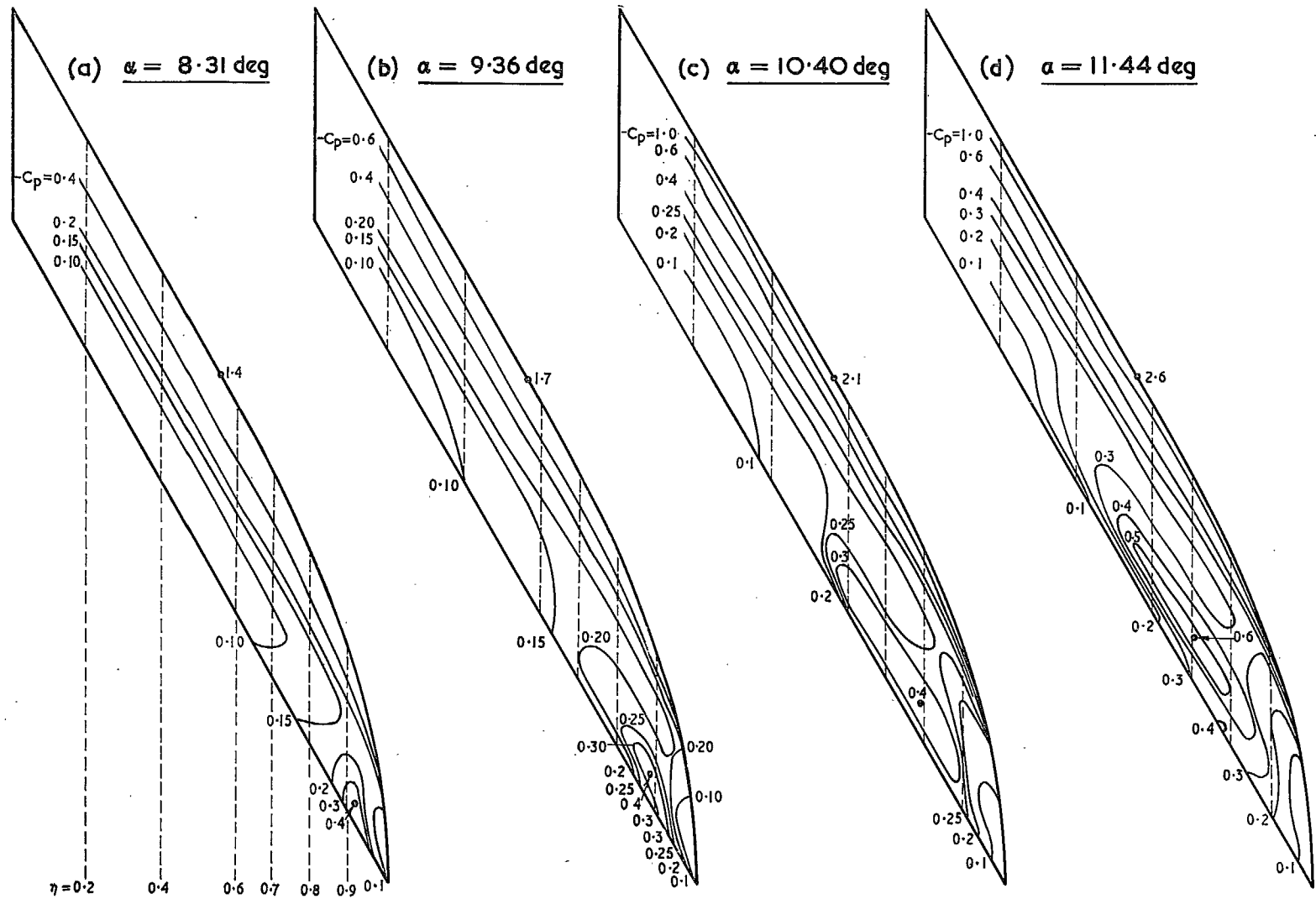


FIG. 12. Effect of incidence on surface isobars of 9% wing at  $R = 2.2 \times 10^6$ .

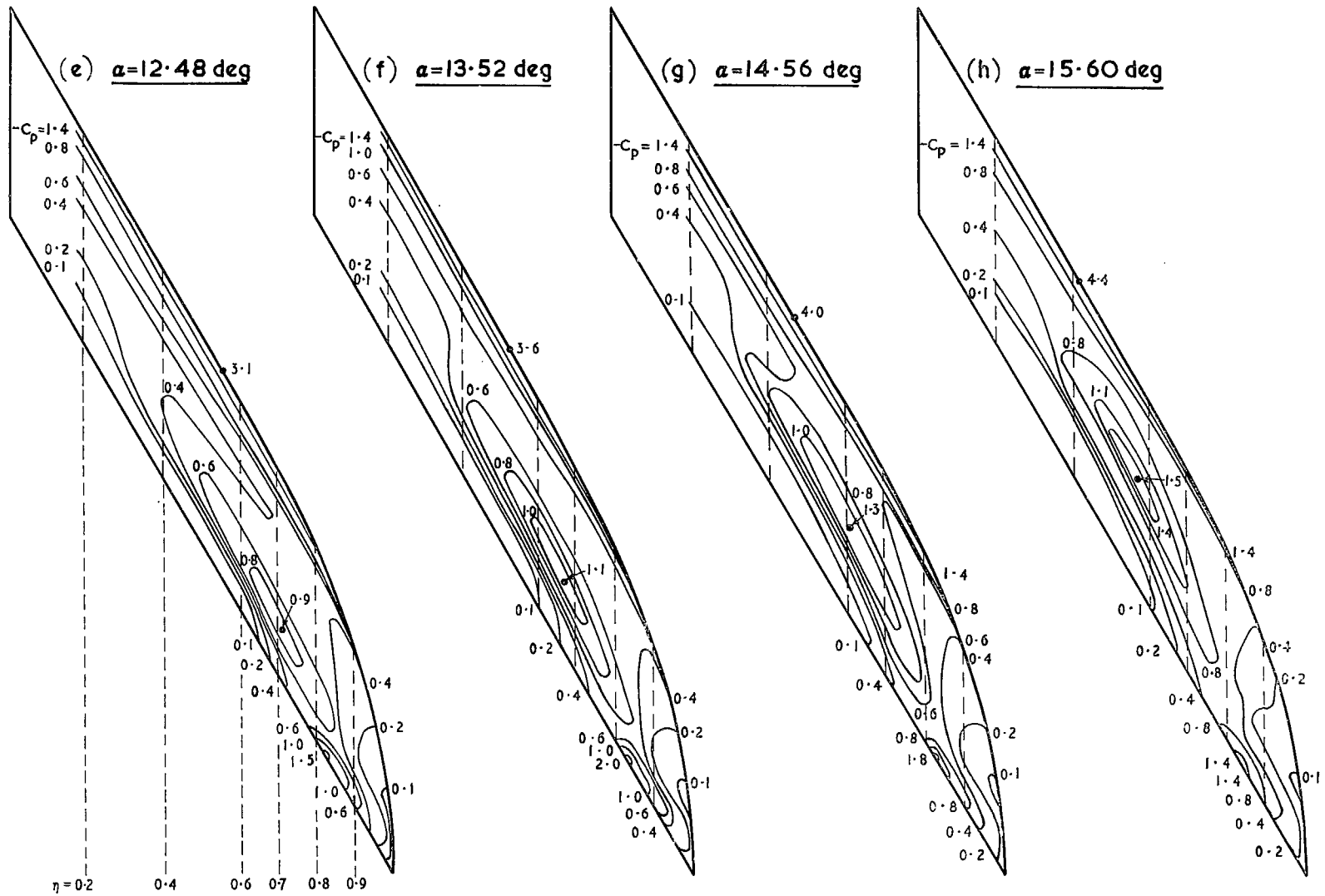


FIG. 12 (continued). Effect of incidence on surface isobars of 9% wing at  $R = 2.2 \times 10^6$ .

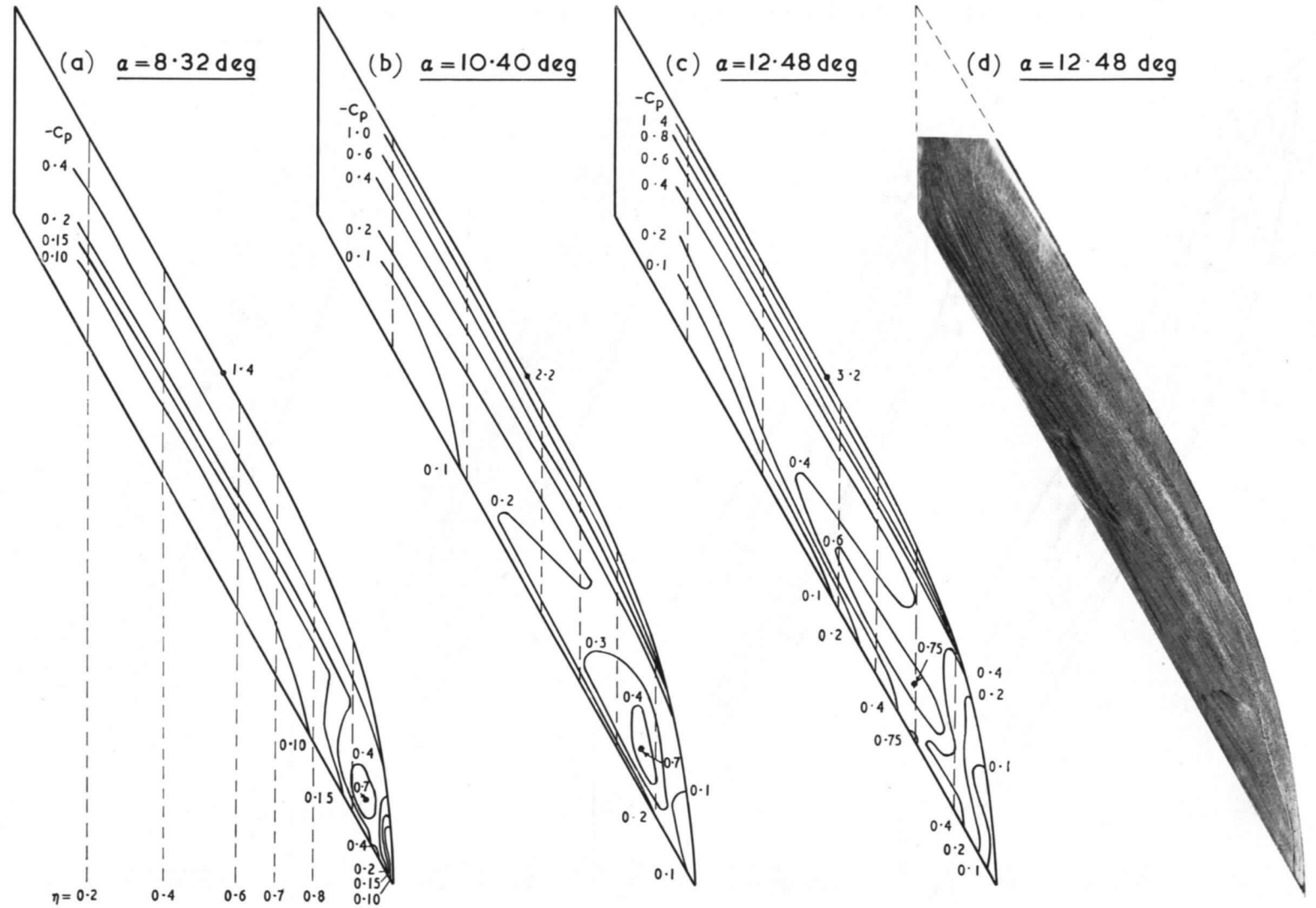


FIG. 13. Surface isobars and oil pattern of 9% wing at  $R = 3.9 \times 10^6$ .

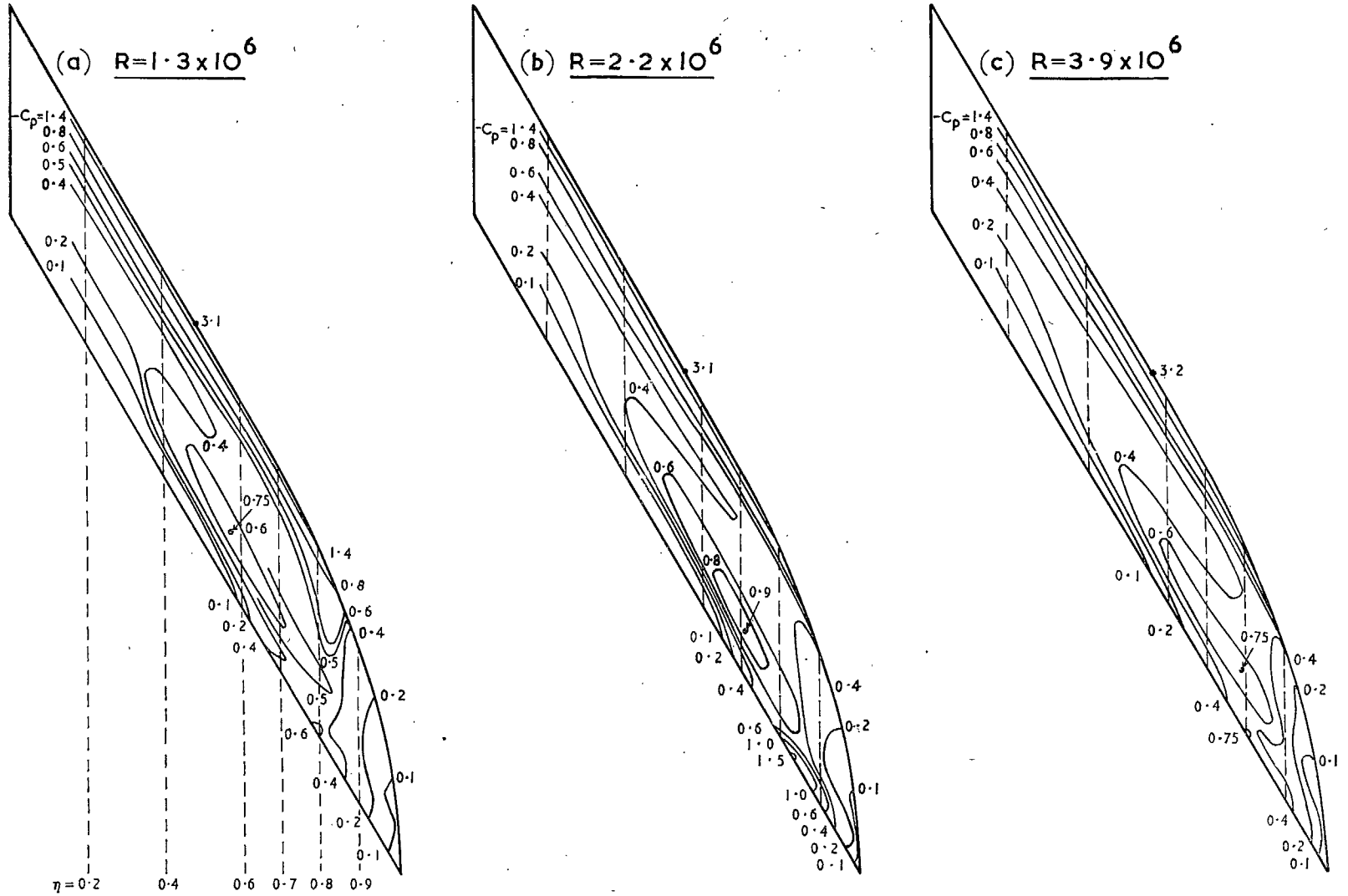


FIG. 14. Effect of Reynolds number on surface isobars of 9% wing at  $\alpha = 12.5^\circ$ .

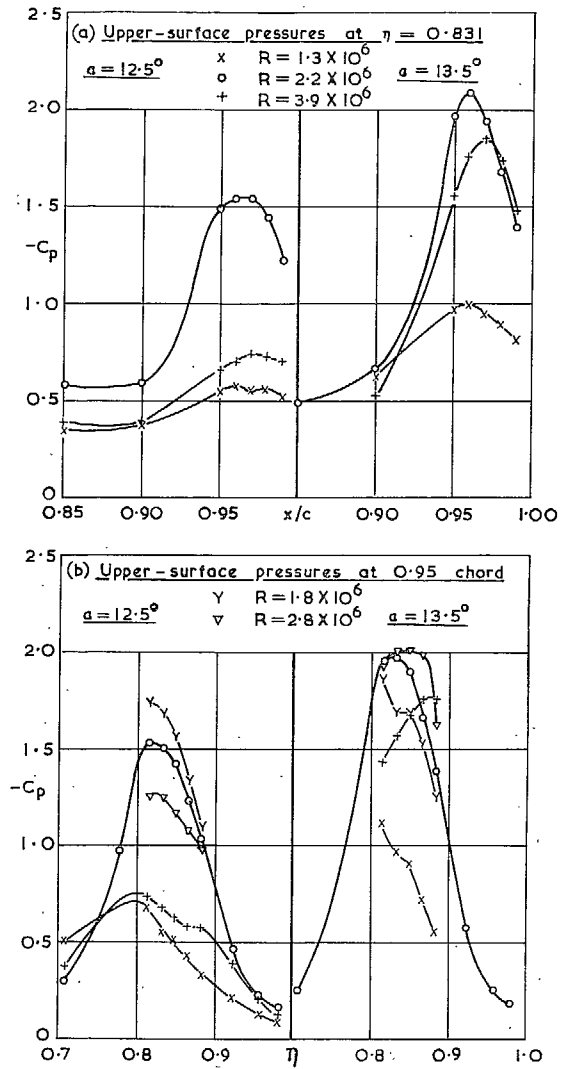


FIG. 15. Pressures near trailing-edge vortex on 9% wing.

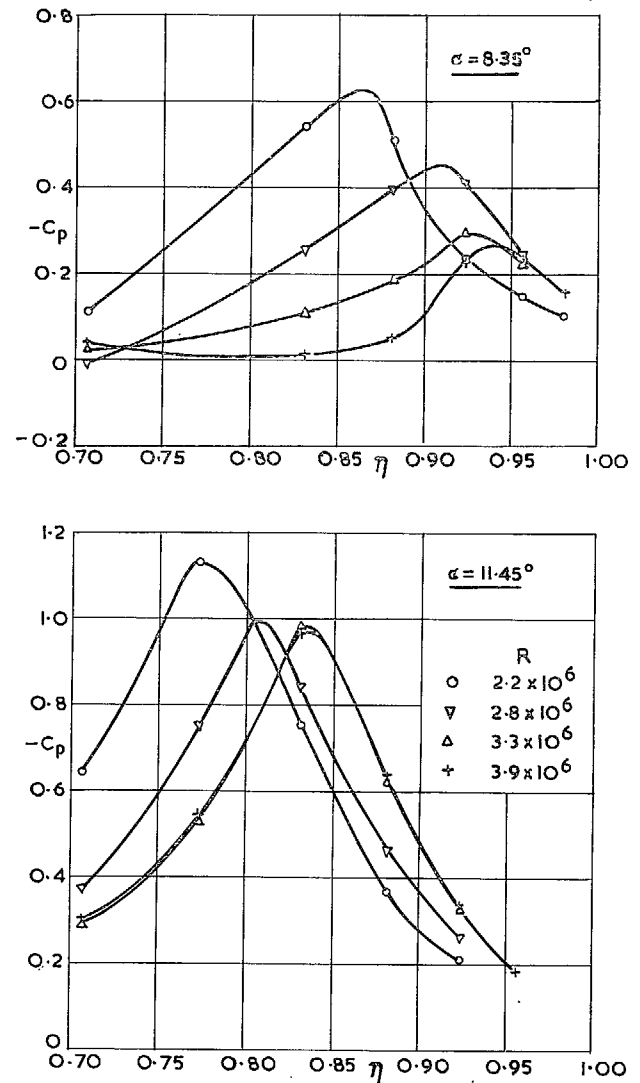


FIG. 16. Scale effect on pressure variation at 0.95 chord of 5% wing.

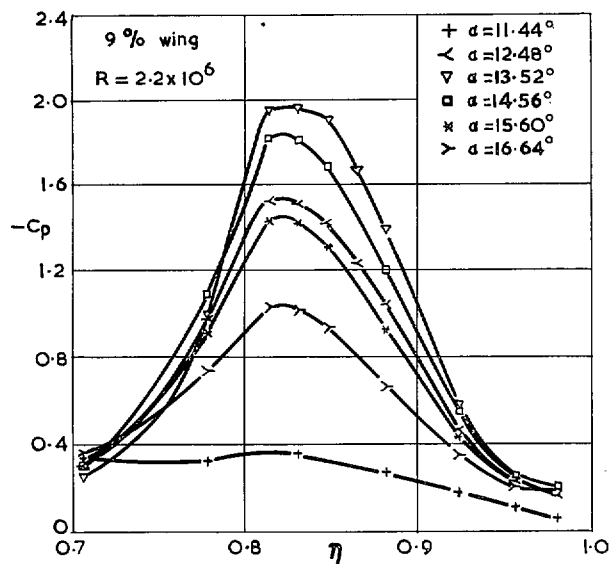
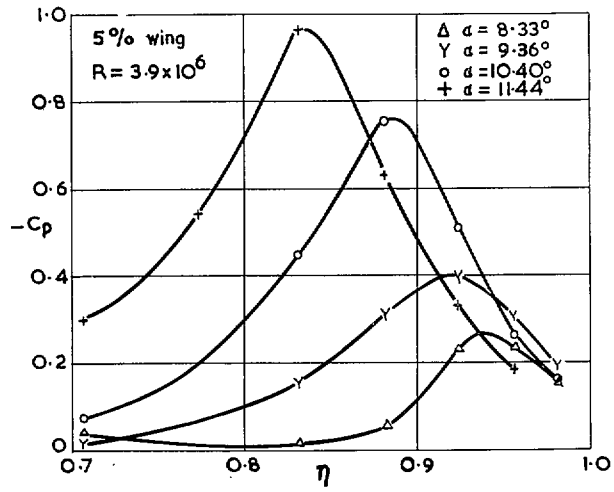


FIG. 17. Effect of incidence on pressure variation at 0.95 chord.



Main vortex



Secondary vortex

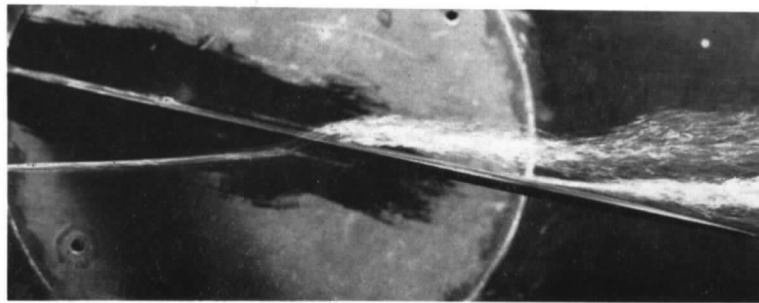
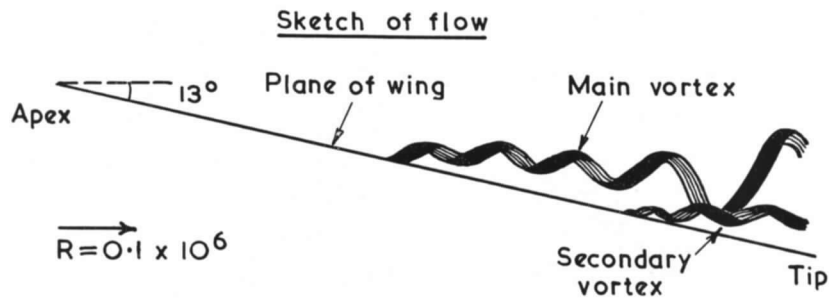


FIG. 18. Vortices observed on 9% wing at  $\alpha = 13^\circ$  in water.

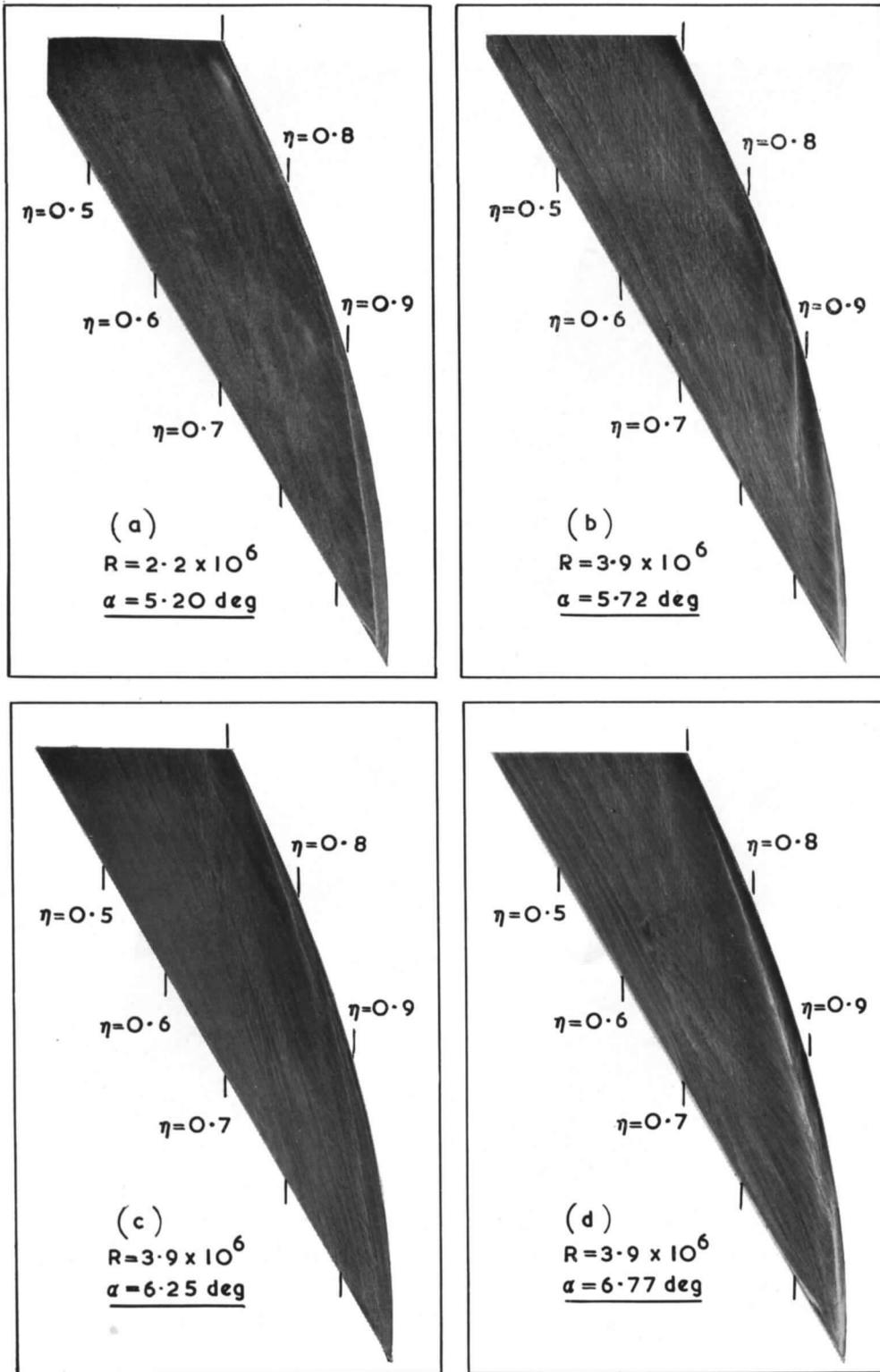


FIG. 19. Effect of incidence on oil patterns of 5% curved tip.

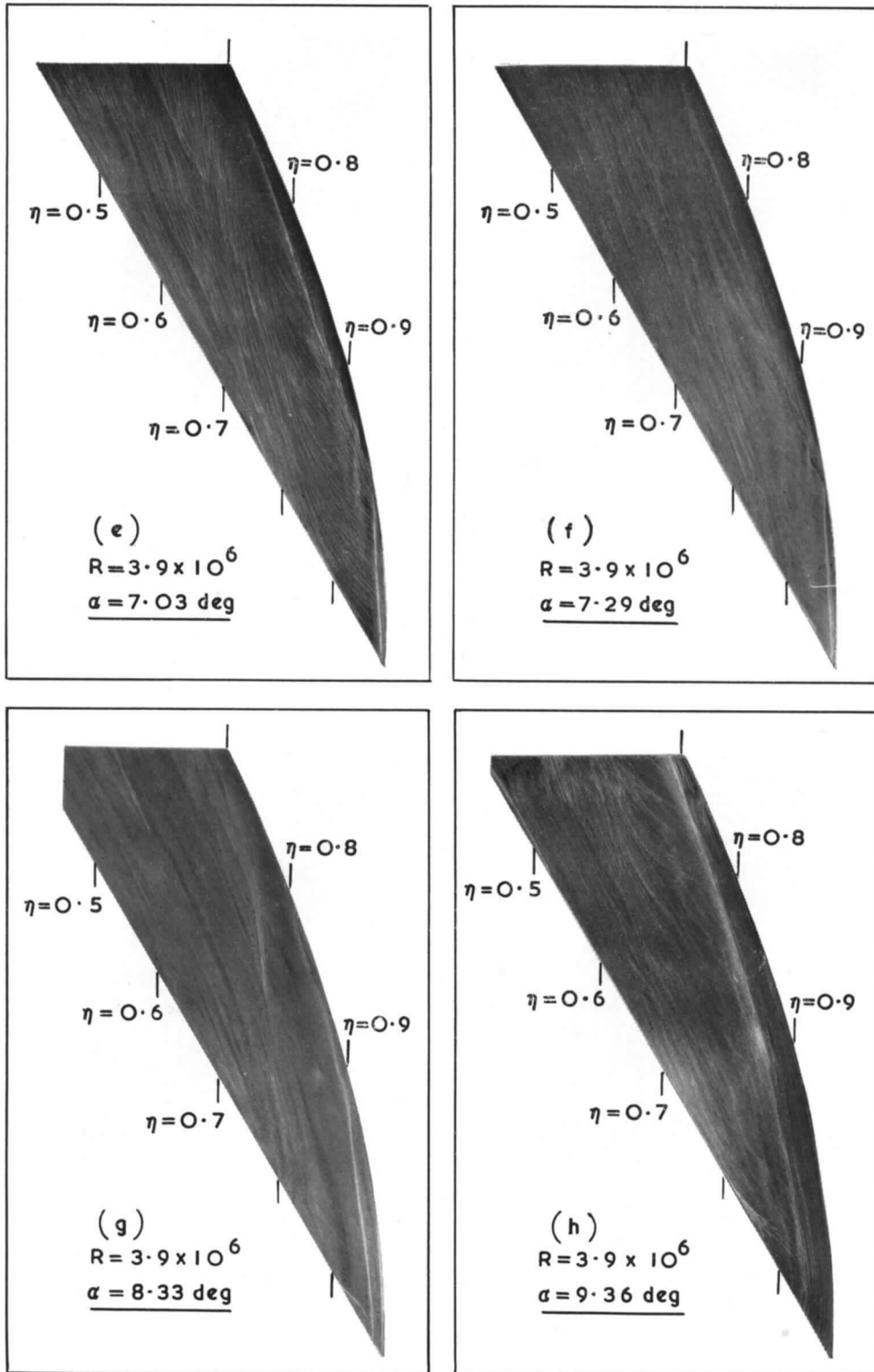


FIG. 19 (continued). Effect of incidence on oil patterns of 5% curved tip.

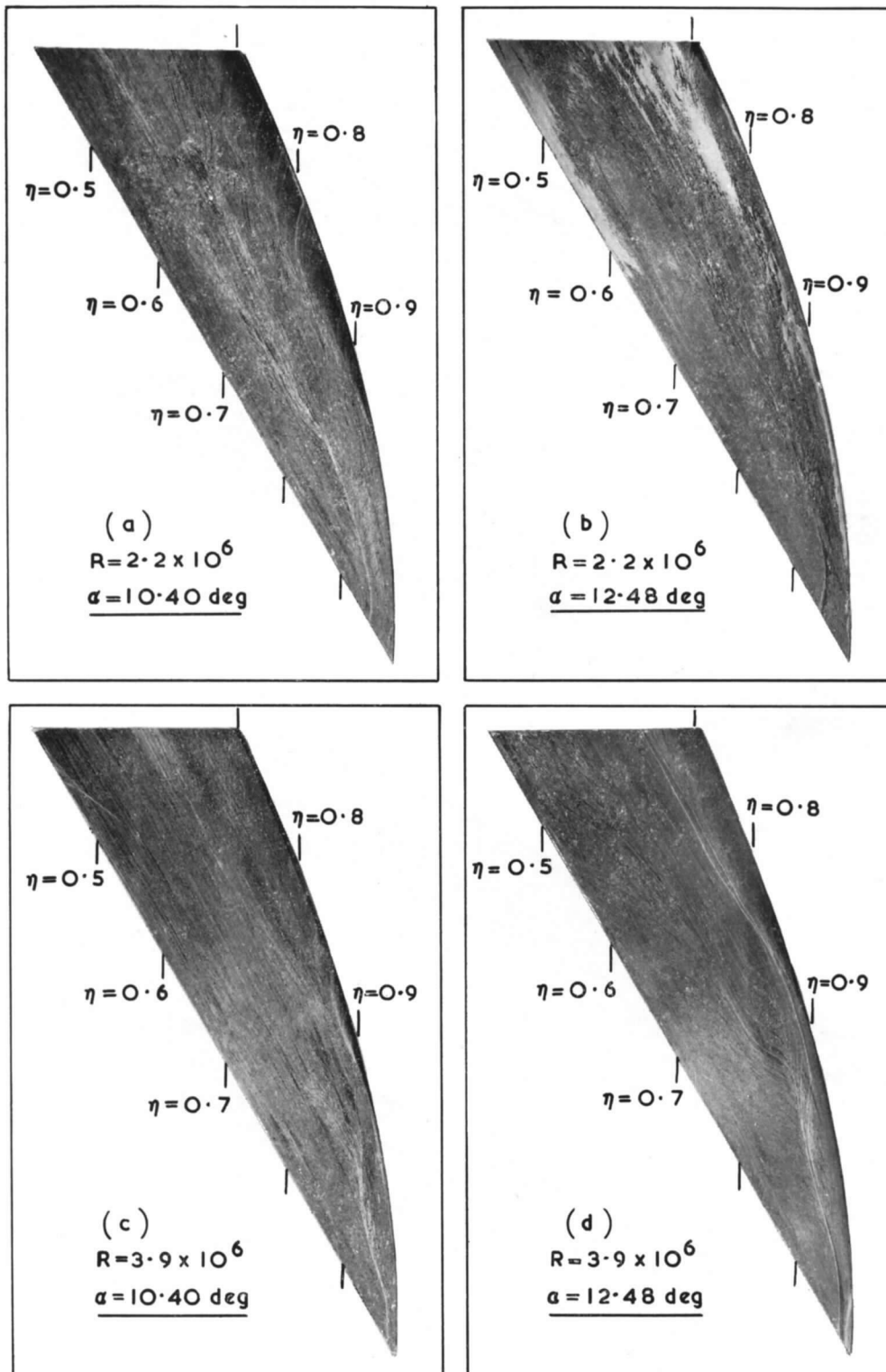


FIG. 20. Oil patterns of 9% curved tip at two incidences and Reynolds numbers.

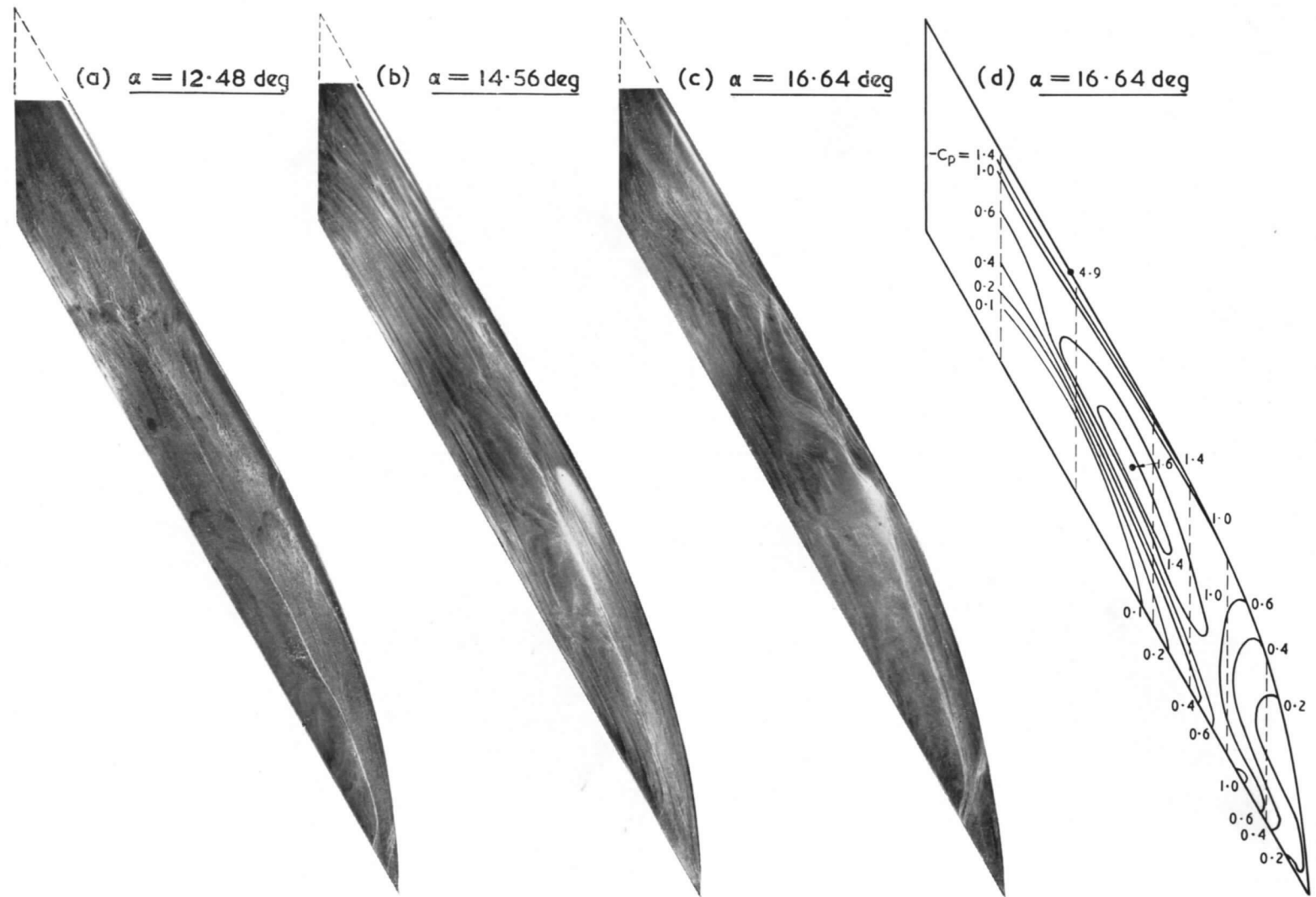


FIG. 21. Oil patterns and surface isobars of 9% wing at high incidences and  $R = 2.2 \times 10^6$ .

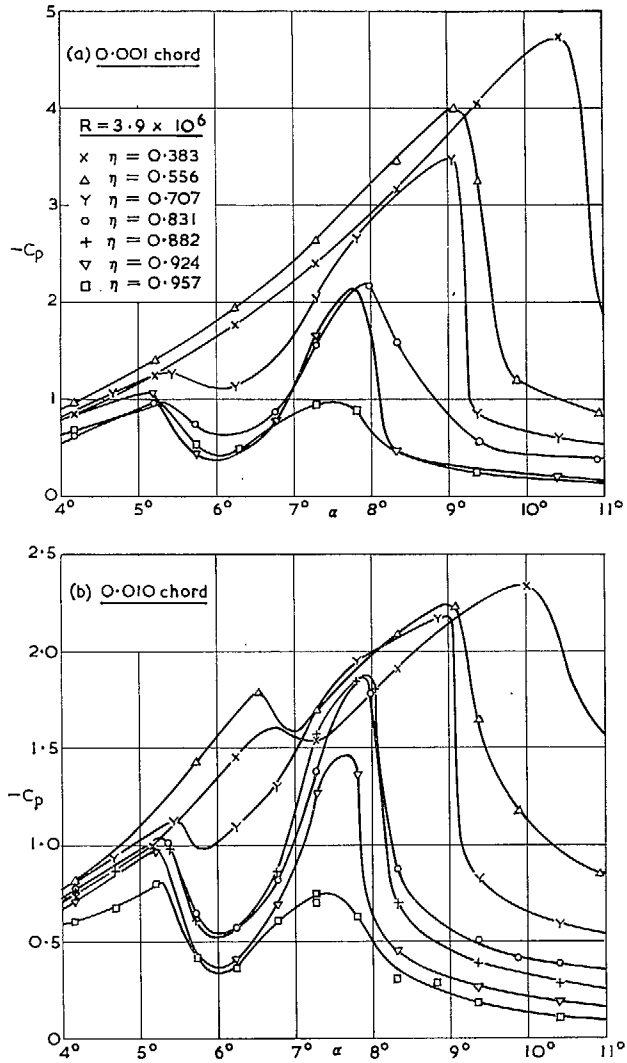


FIG. 22. Pressure coefficients against incidence at selected points of 5% wing.

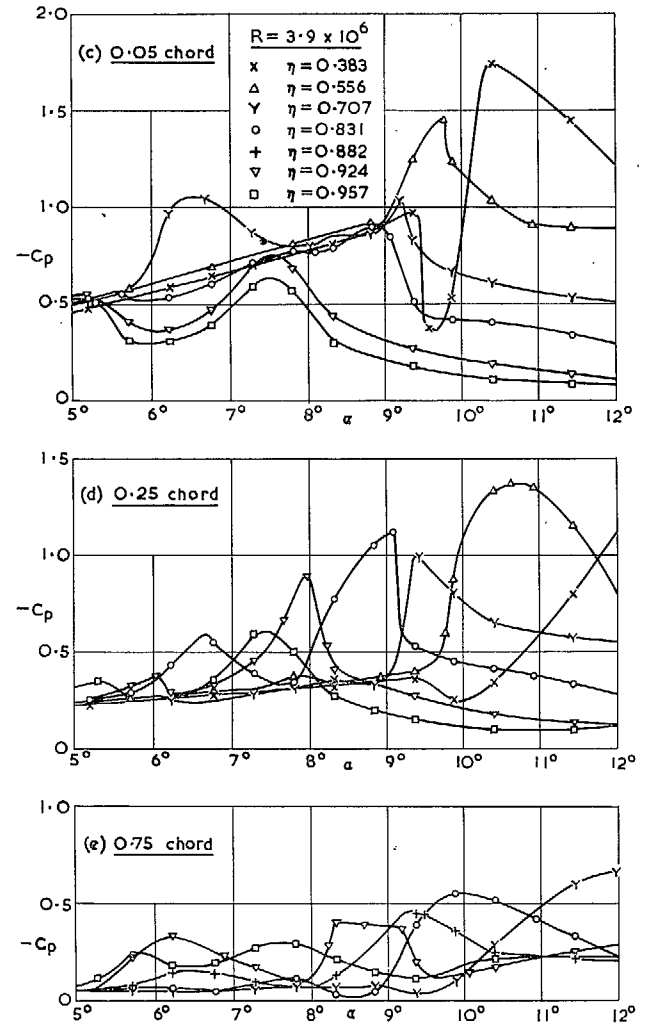


FIG. 22 (continued). Pressure coefficients against incidence at selected points of 5% wing.

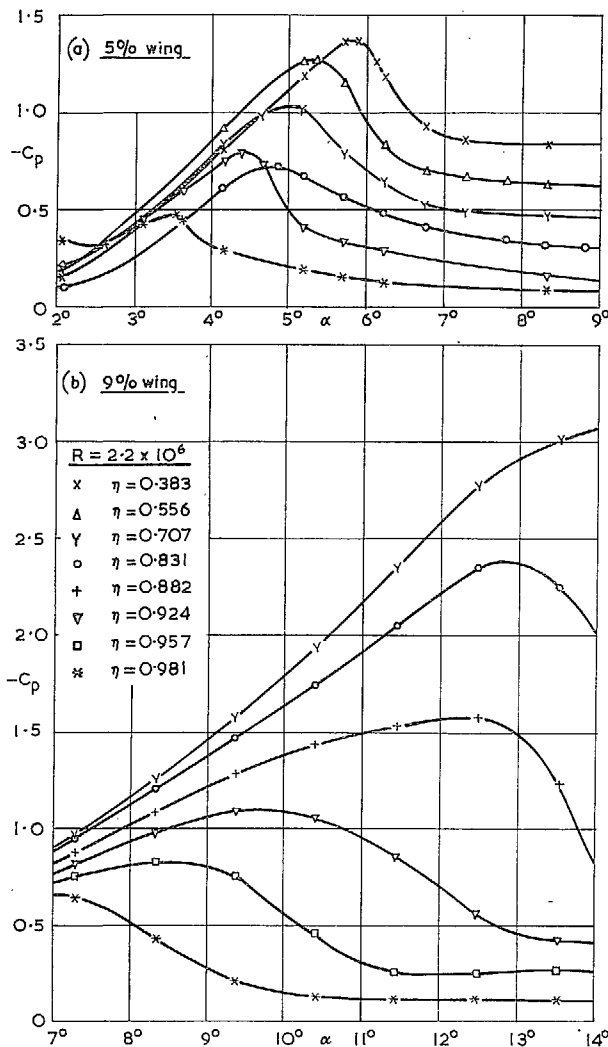


FIG. 23. Pressure coefficients against incidence at 0.001 chord.

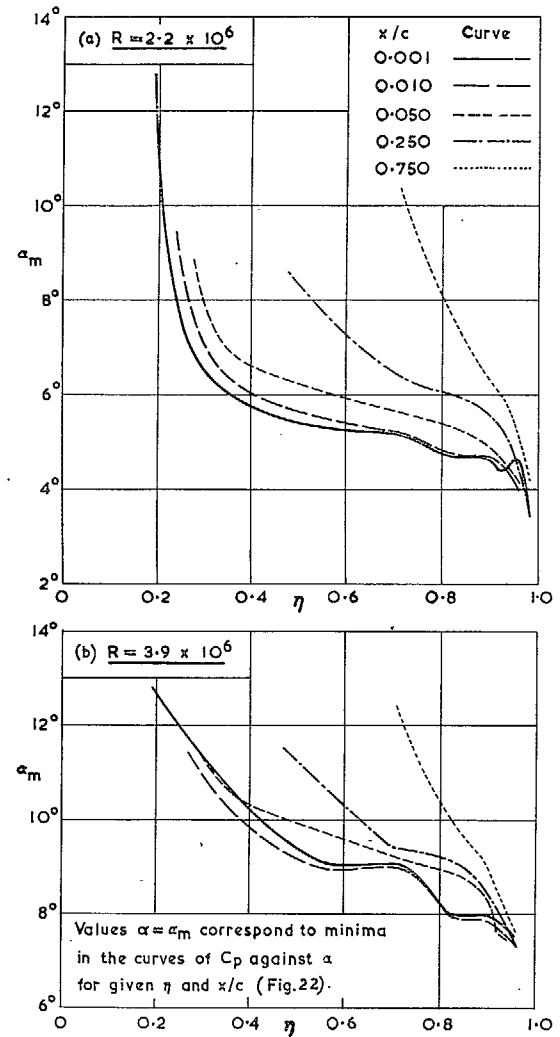


FIG. 24. Spanwise location of part-span vortex from pressures on 5% wing.

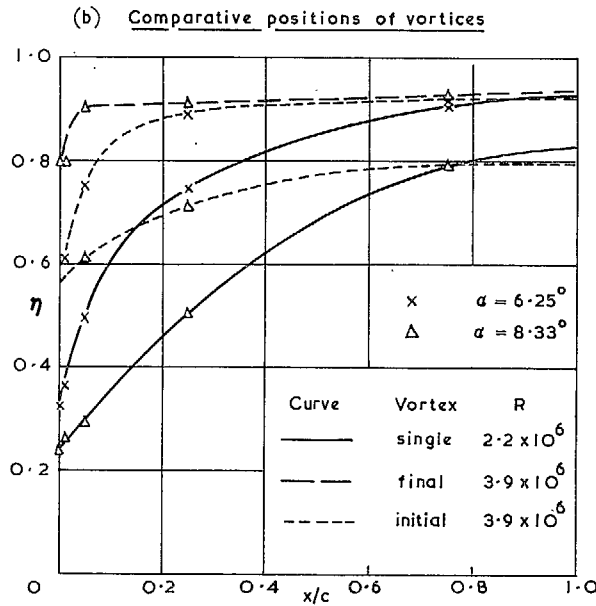
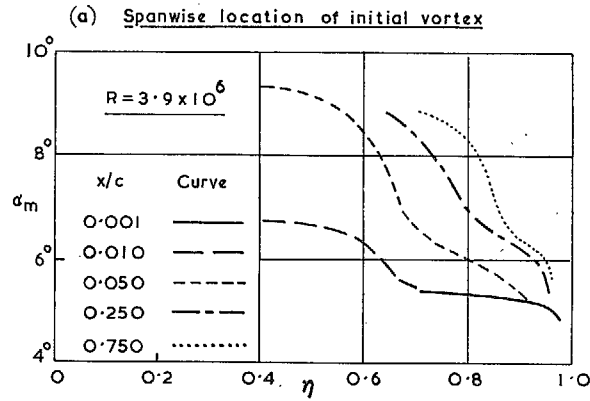


FIG. 25. Initial and final part-span vortices on 5% wing.

The full curves represent the plan view of the part-span vortex, as deduced from Fig. 24.

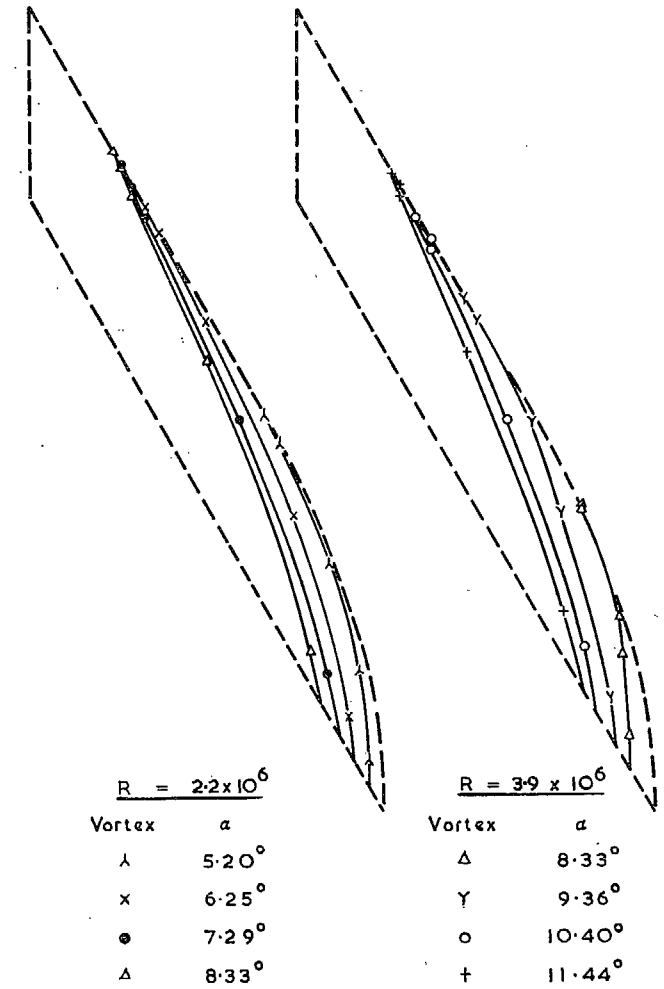


FIG. 26. Estimated movement of vortex on 5% wing with increasing incidence.



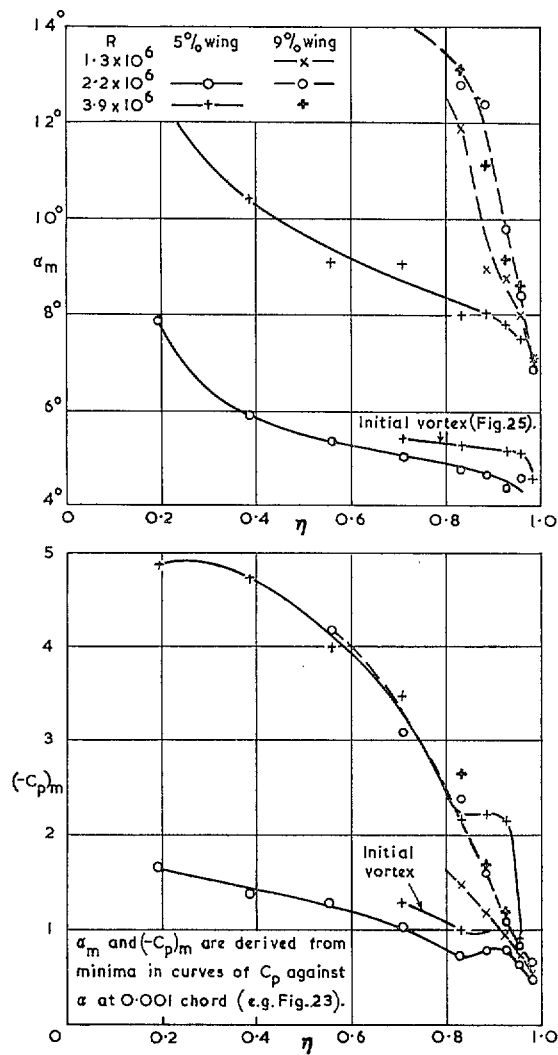


FIG. 27. Scale effect on leading-edge stall of 5% and 9% wings.

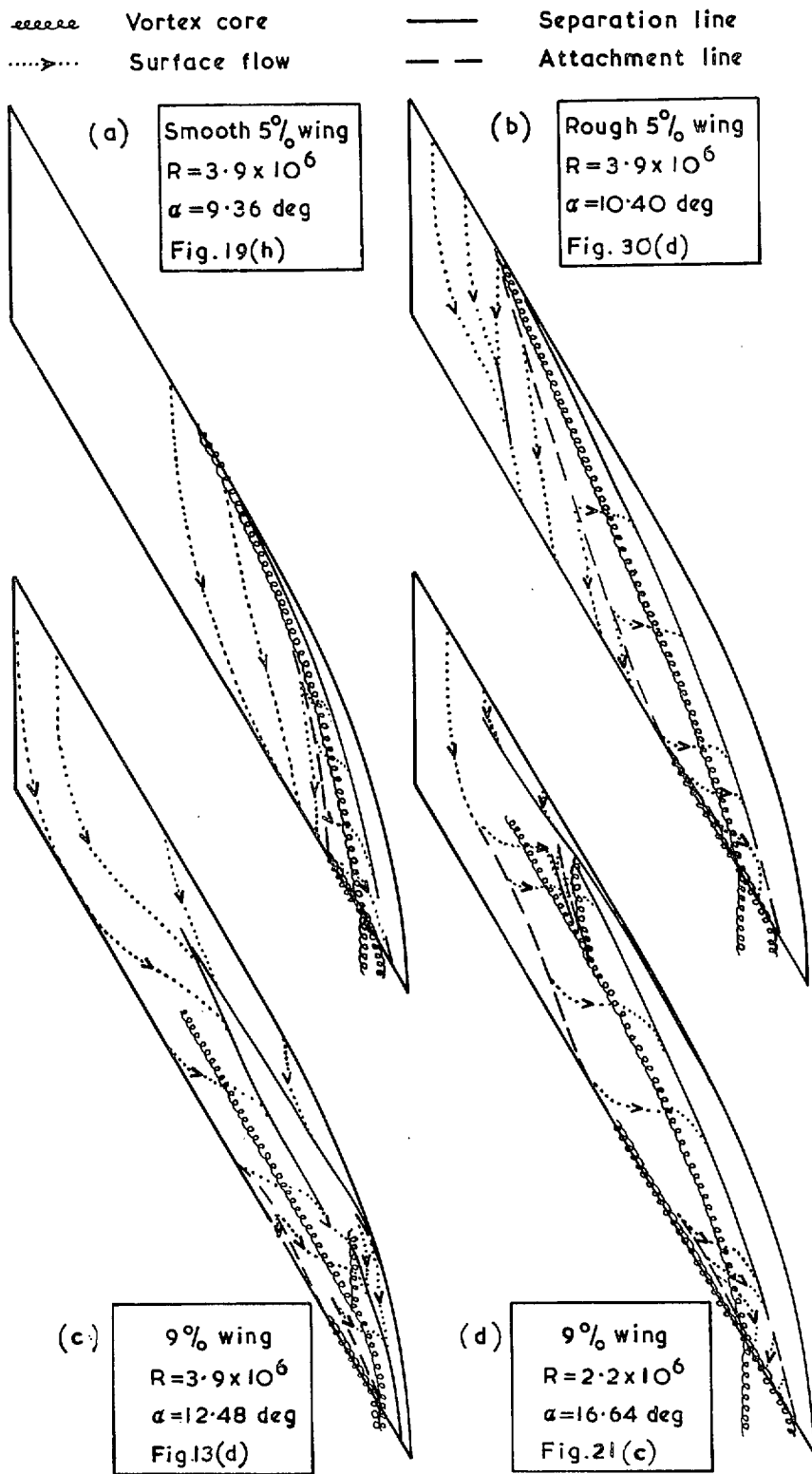


FIG. 28. Superposed vortex location and flow lines on curved-tip wings.

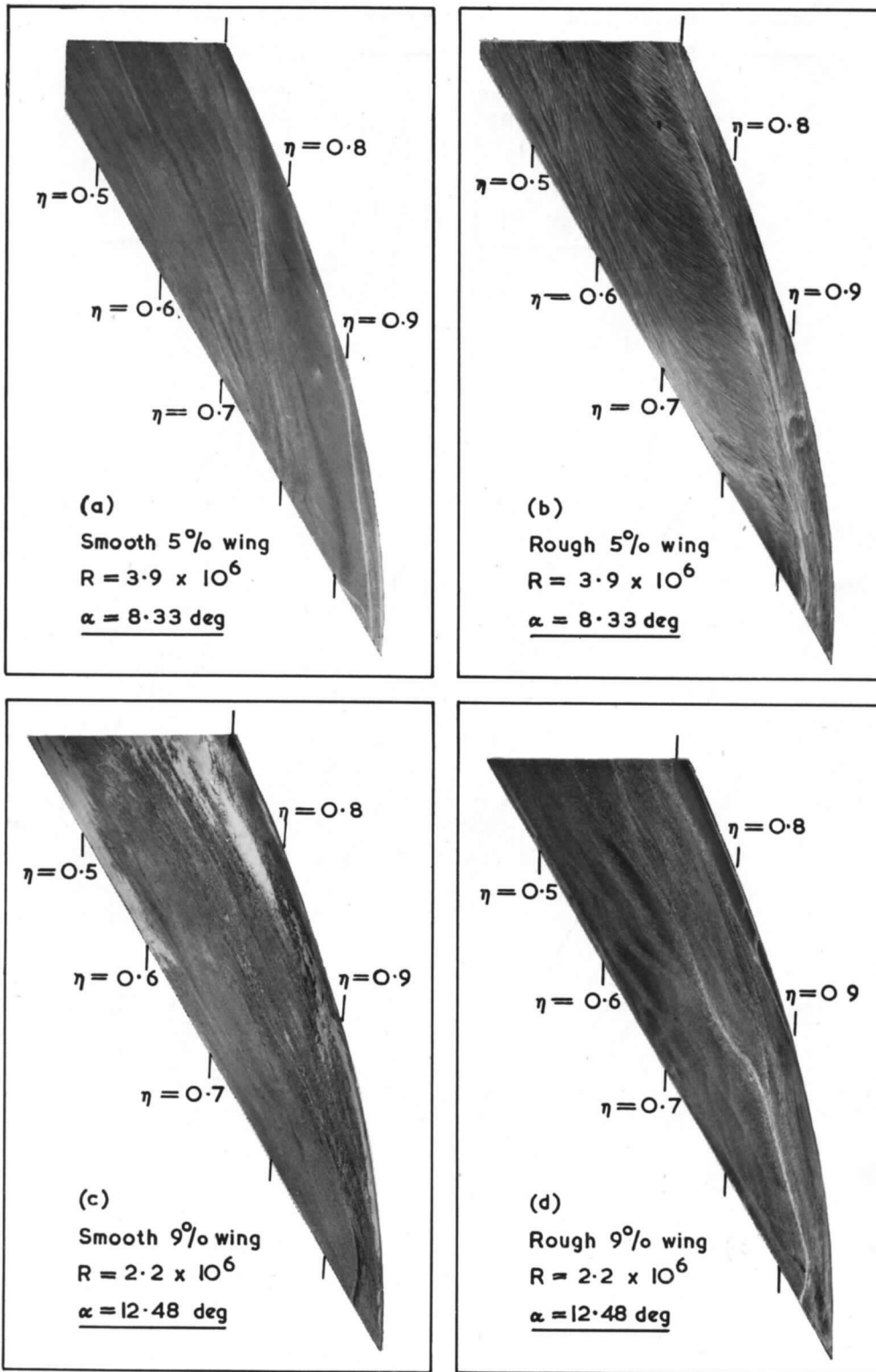


FIG. 29. Oil patterns of curved-tip wings with and without roughness.

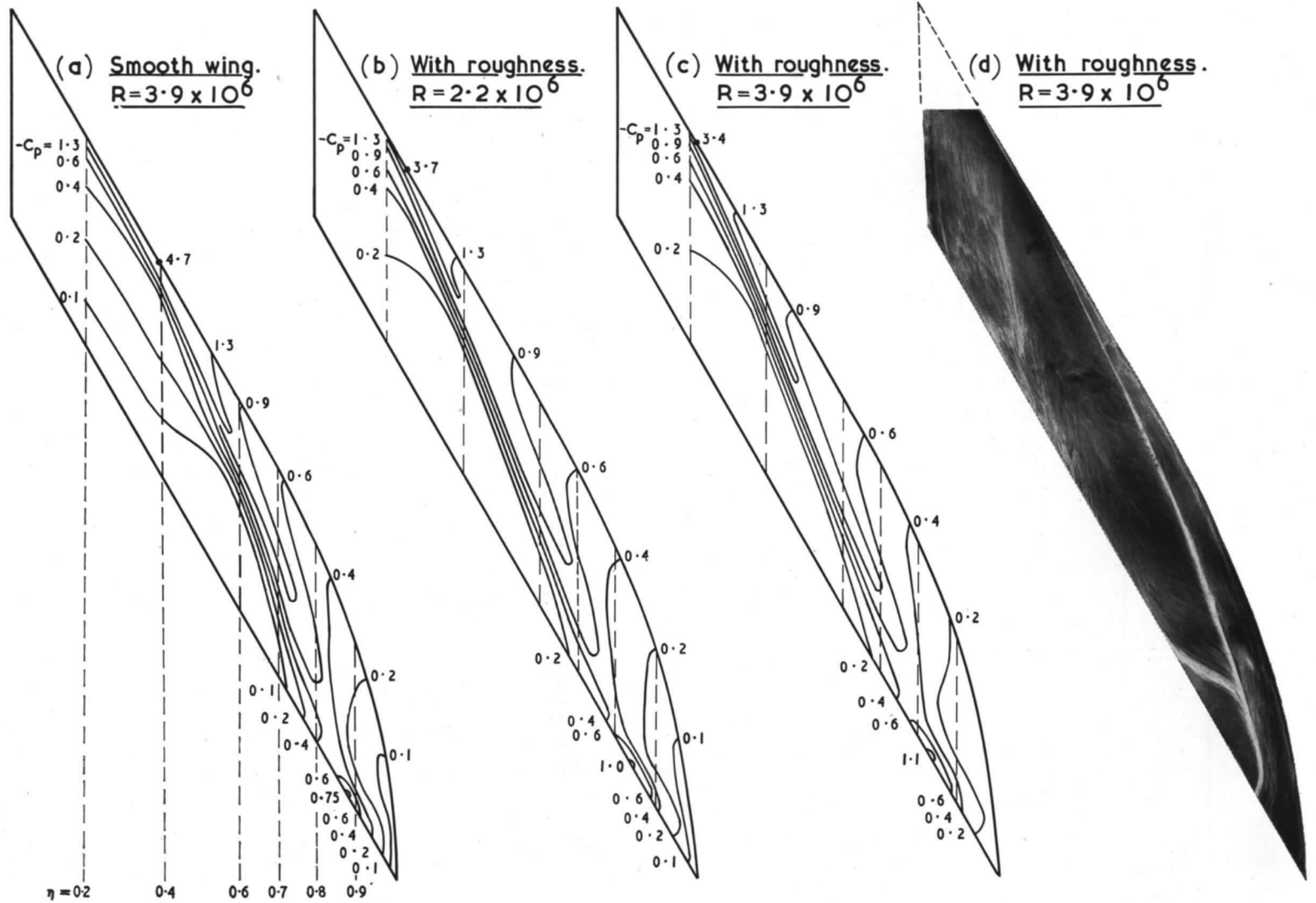


FIG. 30. Effect of leading-edge roughness on 5% wing at  $\alpha = 10.4$  deg.

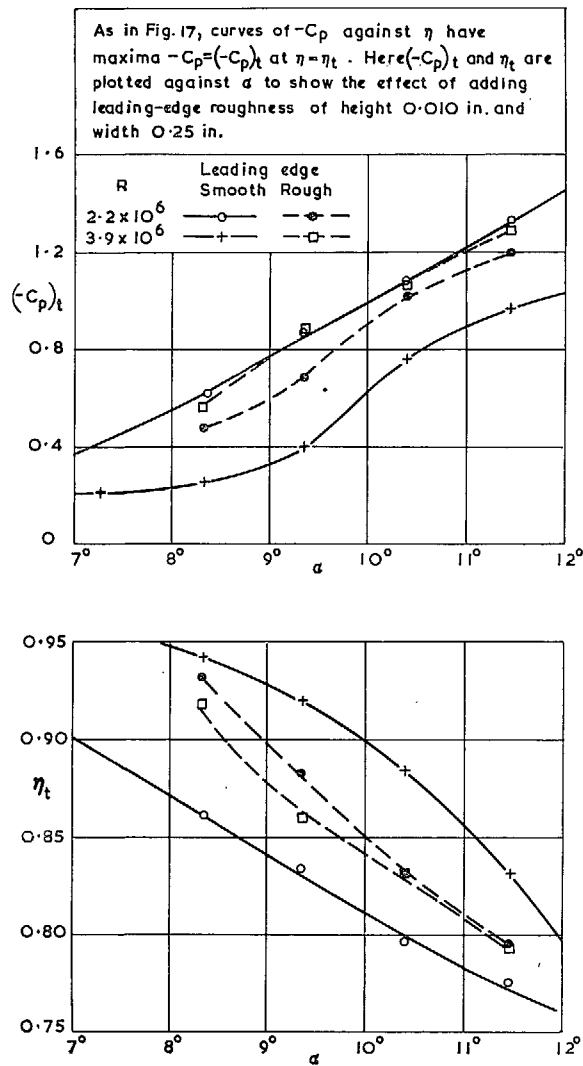


FIG. 31. Effect of roughness and incidence on lowest  $C_p$  at 0.95 chord of 5% wing.

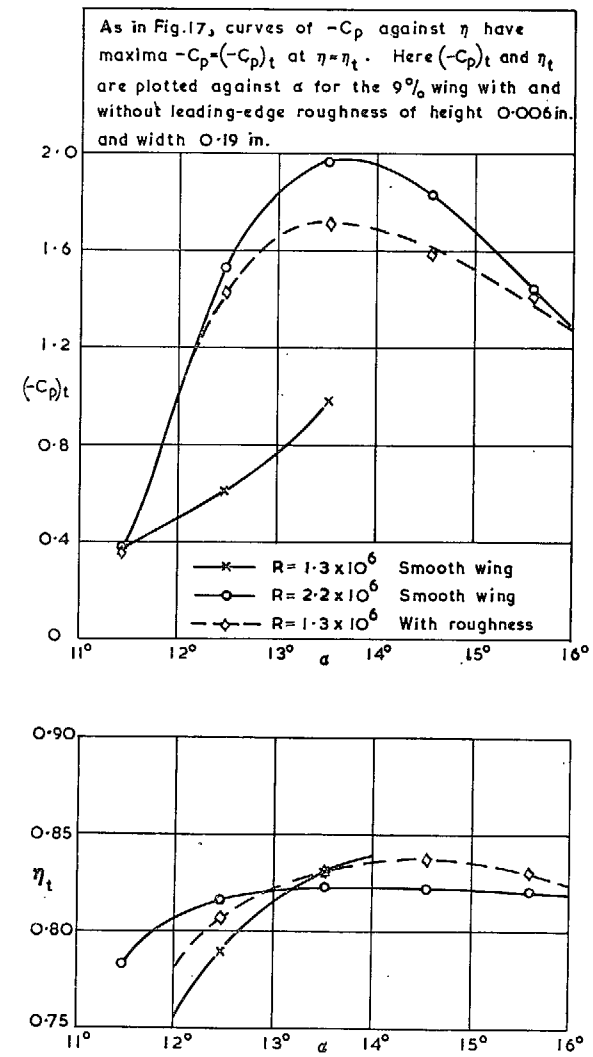


FIG. 32. Effect of roughness and incidence on lowest  $C_p$  at 0.95 chord at 9% wing.

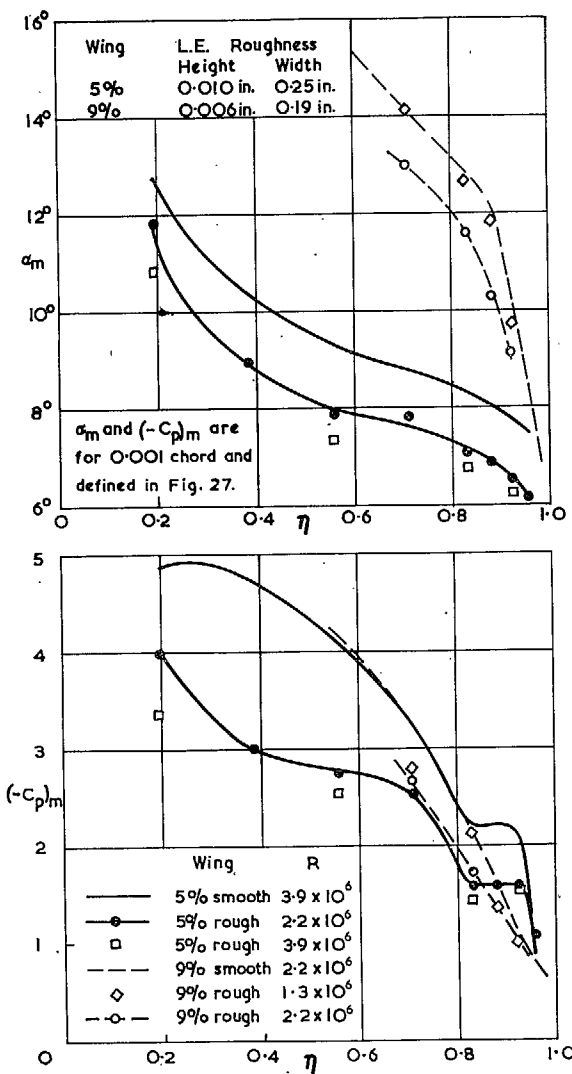


FIG. 33. Effect of roughness on leading-edge stall of 5% and 9% wings.

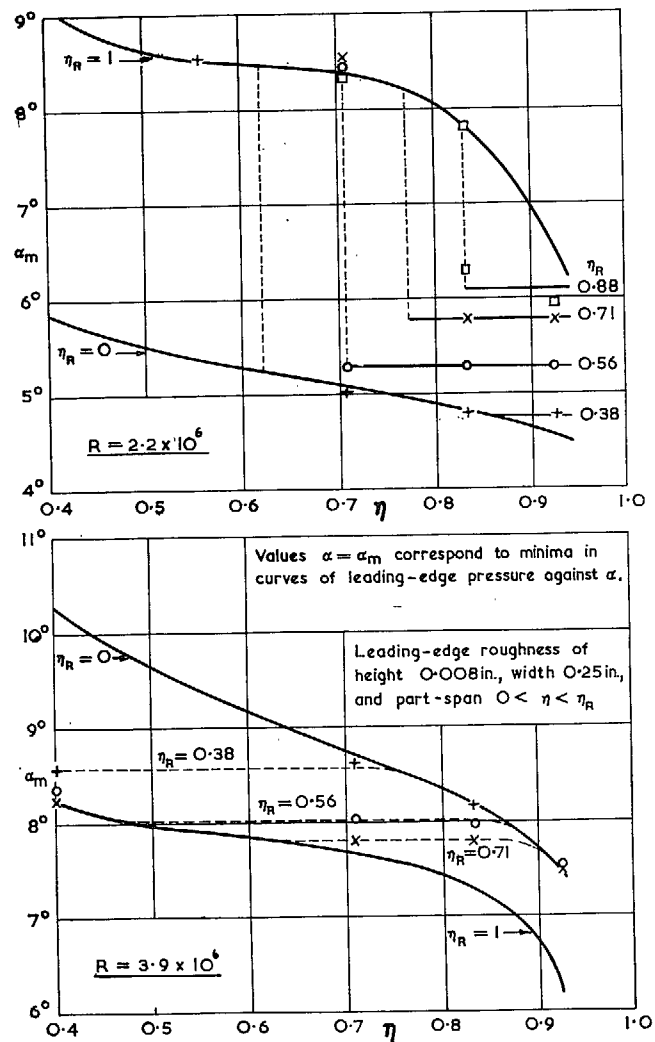


FIG. 34. Effect of part-span roughness on leading-edge stall of 5% wing.



# Publications of the Aeronautical Research Council

## ANNUAL TECHNICAL REPORTS OF THE AERONAUTICAL RESEARCH COUNCIL (BOUND VOLUMES)

- 1941 Aero and Hydrodynamics, Aerofoils, Airscrews, Engines, Flutter, Stability and Control, Structures. 63s. (post 2s. 3d.)
- 1942 Vol. I. Aero and Hydrodynamics, Aerofoils, Airscrews, Engines. 75s. (post 2s. 3d.)  
Vol. II. Noise, Parachutes, Stability and Control, Structures, Vibration, Wind Tunnels. 47s. 6d. (post 1s. 9d.)
- 1943 Vol. I. Aerodynamics, Aerofoils, Airscrews. 80s. (post 2s.)  
Vol. II. Engines, Flutter, Materials, Parachutes, Performance, Stability and Control, Structures. 90s. (post 2s. 3d.)
- 1944 Vol. I. Aero and Hydrodynamics, Aerofoils, Aircraft, Airscrews, Controls. 84s. (post 2s. 6d.)  
Vol. II. Flutter and Vibration, Materials, Miscellaneous, Navigation, Parachutes, Performance, Plates and Panels, Stability, Structures, Test Equipment, Wind Tunnels. 84s. (post 2s. 6d.)
- 1945 Vol. I. Aero and Hydrodynamics, Aerofoils. 130s. (post 3s.)  
Vol. II. Aircraft, Airscrews, Controls. 130s. (post 3s.)  
Vol. III. Flutter and Vibration, Instruments, Miscellaneous, Parachutes, Plates and Panels, Propulsion. 130s. (post 2s. 9d.)  
Vol. IV. Stability, Structures, Wind Tunnels, Wind Tunnel Technique. 130s. (post 2s. 9d.)
- 1946 Vol. I. Accidents, Aerodynamics, Aerofoils and Hydrofoils. 168s. (post 3s. 3d.)  
Vol. II. Airscrews, Cabin Cooling, Chemical Hazards, Controls, Flames, Flutter, Helicopters, Instruments and Instrumentation, Interference, Jets, Miscellaneous, Parachutes. 168s. (post 2s. 9d.)  
Vol. III. Performance, Propulsion, Seaplanes, Stability, Structures, Wind Tunnels. 168s. (post 3s.)
- 1947 Vol. I. Aerodynamics, Aerofoils, Aircraft. 168s. (post 3s. 3d.)  
Vol. II. Airscrews and Rotors, Controls, Flutter, Materials, Miscellaneous, Parachutes, Propulsion, Seaplanes, Stability, Structures, Take-off and Landing. 168s. (post 3s. 3d.)

### Special Volumes

- Vol. I. Aero and Hydrodynamics, Aerofoils, Controls, Flutter, Kites, Parachutes, Performance, Propulsion, Stability. 126s. (post 2s. 6d.)
- Vol. II. Aero and Hydrodynamics, Aerofoils, Airscrews, Controls, Flutter, Materials, Miscellaneous, Parachutes, Propulsion, Stability, Structures. 147s. (post 2s. 6d.)
- Vol. III. Aero and Hydrodynamics, Aerofoils, Airscrews, Controls, Flutter, Kites, Miscellaneous, Parachutes, Propulsion, Seaplanes, Stability, Structures, Test Equipment. 189s. (post 3s. 3d.)

### Reviews of the Aeronautical Research Council

- 1939-48 3s. (post 5d.)      1949-54 5s. (post 5d.)

### Index to all Reports and Memoranda published in the Annual Technical Reports

- 1909-1947      R. & M. 2600 6s. (post 2d.)

### Indexes to the Reports and Memoranda of the Aeronautical Research Council

- |                        |                                     |
|------------------------|-------------------------------------|
| Between Nos. 2351-2449 | R. & M. No. 2450 2s. (post 2d.)     |
| Between Nos. 2451-2549 | R. & M. No. 2550 2s. 6d. (post 2d.) |
| Between Nos. 2551-2649 | R. & M. No. 2650 2s. 6d. (post 2d.) |
| Between Nos. 2651-2749 | R. & M. No. 2750 2s. 6d. (post 2d.) |
| Between Nos. 2751-2849 | R. & M. No. 2850 2s. 6d. (post 2d.) |
| Between Nos. 2851-2949 | R. & M. No. 2950 3s. (post 2d.)     |
| Between Nos. 2951-3049 | R. & M. No. 3050 3s. 6d. (post 2d.) |

HER MAJESTY'S STATIONERY OFFICE

*from the addresses overleaf*



© *Crown copyright* 1962

Printed and published by  
HER MAJESTY'S STATIONERY OFFICE

To be purchased from  
York House, Kingsway, London W.C.2  
423 Oxford Street, London W.1  
13A Castle Street, Edinburgh 2  
109 St. Mary Street, Cardiff  
39 King Street, Manchester 2  
50 Fairfax Street, Bristol 1  
35 Smallbrook, Ringway, Birmingham 5  
80 Chichester Street, Belfast 1  
or through any bookseller

*Printed in England*